



VADOSE FLOW SYNTHESIS FOR THE NORTHERN GUAM LENS AQUIFER

By

**Nathan C. Habana
Leroy F. Heitz
Arne E. Olsen
John W. Jenson**



WERI

**WATER AND ENVIRONMENTAL RESEARCH INSTITUTE
OF THE WESTERN PACIFIC
UNIVERSITY OF GUAM**

**Technical Report No. 127
October 2009**

VADOSE FLOW SYNTHESIS FOR THE NORTHERN GUAM LENS AQUIFER

By

**Nathan C. Habana
Leroy F. Heitz
Arne E. Olsen
John W. Jenson**

Water and Environmental Research Institute of the Western Pacific
University of Guam, UOG Station Mangilao, Guam 96923

**Technical Report No. 127
October 2009**

This project was funded by the Guam Hydrologic Survey (GHS), a water resources research program funded exclusively by a local appropriation awarded to the University of Guam (UOG) under the Public Law No. 24-247 and administered through the Water and Environmental Research Institute of the Western Pacific (WERI). The content of this report does not necessarily reflect the views and policies of the Government of Guam, nor does the mention of trade names or commercial products constitute their endorsement by the Government of Guam.

ACKNOWLEDGEMENTS

I would like to thank Dr. Leroy F. Heitz for giving me the opportunity to work with him on this project. This project was truly his idea and my understanding and diligent effort to bring it to life. We were able to take hydraulic modeling of the Northern Guam Lens Aquifer into a new frontier. I am forever indebted to his full support of all my endeavors in making this happen. His belief in me was everything I needed to succeed. He is a true teacher and I am fortunate to have learned from the best.

I can't forget to mention everyone who has contributed to the research as well - some in funny ways. Thanks to Dr. John Jenson for making the project more challenging, Mr. Arne Olsen for revealing the secrets of groundwater modeling, Dr. Henry Taijeron for checking the math, Mr. John Jocson for releasing the data, Dr. Dinshaw Contractor for pioneering hydraulic modeling on Guam, Dr. Gary Denton for the motivation and perspective, Dr. Mark Lander for the sunshine and rain, Dr. Wen Yuming for the advanced lessons in GIS, and Dr. Shahram Khosrowpahah for witnessing it all. I also can't forget how a day without Norma Blas was literally like a day without coffee. Thanks to my Mom and Dad, Brothers and Sisters, for the times of my life. And the rest of the WERI family, Cris, Melissa, Gwen, Kennedy, Mike, Ryan, Maria, Tomo, Jen, and whoever I failed to mention, thank you all for giving me a break.

ABSTRACT

As Guam moves into the future, development demands will require increased sources of high quality water. A possible source of this increased water supply is the Northern Guam Lens Aquifer (NGLA). Eighty percent of the supply of water for the island's residents and businesses depend on this water source for their daily water needs (Contractor et al., 1999). In 2005, Guam Visitor's Bureau recorded a record high tourist arrival of over 1.2 million visitors (GVB, 2006). Guam is expecting more expansion in tourism in the future. In the next three years, the U.S. military plans to relocate approximately 8,000 Marines (Guam PDN, 2009) and 3,000 from the Air Force (Guam PDN, 2007) along with their dependents to Guam. These impacts along with other growth in the islands population will clearly have an effect on Guam's demand for fresh water supply resources. Possible impacts could include exceeding pumping rate limits of sustainable yield to meet the increase population demands. This in turn could threaten the fresh water quality through salt water intrusion.

An accurate estimate of the NGLA's sustainable yield is vital for water resource managers from Guam Waterworks Authority and Guam Environmental Protection Agency in order for them to plan and make confident decisions in managing and protecting the NGLA. Knowing the inflows or recharge to the aquifer is one important factor in regulating pumping so as not to exceed the limits of sustainable yield.

Attempts to estimate the NGLA recharge have been carried out since the late 1940s. Early estimates have been refined using increasingly sophisticated approaches. With modern computer technologies, more in-depth analyses are available to improve previous recharge estimates. These improvements are required as Guam's water demands approaches the safe yield of the aquifer. The approach described in this thesis is an improvement over recent work accomplished at WERI (Contractor et al., 1999). In this new approach, we will be examining how soil moisture properties affect evapotranspiration (ET) and ultimately recharge estimates. Recharge from vadose flow synthesis is used as the water that arrives to the water table. The resulting recharge values are applied to a finite element ground water model. A computer program called AQUA CHARGE is developed to integrate the spatially distributed properties of the aquifer and the recharge model with the time variable inputs of rainfall and pan evaporation.

The *Vadose Flow Synthesis Conceptual Model* was designed for the NGLA to synthesize recharge to the aquifer. The model development begins with an area over a node and is the size of that node's *cell*, of a two-dimensional groundwater model *finite element mesh*, from the water table, elevated to the soil surface as a vertical geologic column of shaft. This vertical shaft is termed *node-shed* and describes the vadose hydrologic watershed supplying each node. This node-shed is divided into two stages: the soil layer and the unsaturated limestone bedrock. The soil layer in the node-shed is composed of sub polygons with unique attributes we termed *zones*. These zones employ a mass balance equation referred to as the *soil moisture model* to account for the moisture input, the proportioning to recharge and evapotranspiration (ET), and the remaining soil moisture computed in a daily cycle. The proportioning of recharge and ET is determined by a soil moisture curve relationship for the two hydrologic processes. For a day's computation of recharge for each zone in the node-shed, the soil stage ends with the calculation of the node-shed's area weighted average recharge. This area weighted average recharge is split to account for the bedrock stage's fast and slow flows to recharge. The time arrival of recharge to the lens, lagged and attenuated, is determined using a transfer function called *the modified*

pulse routing technique. This conceptual model is derived from the US Army Corps of Engineer's *Streamflow Synthesis and Reservoir Regulation* (SSARR) model (1987). It is an alternative route around the NGLA's complex hydrogeology producing realistic estimates of the volume and time arrival of recharge to the lens. The project construction required ESRI® Geographic Information System Arc Editor and MICROSOFT® Excel 2003 and Visual Basic 6.0 Professional. The synthesized recharge serves as flux into a simple two dimensional, transient, saturated-flow, finite element groundwater model for history matching as a means of calibration. The ultimate purpose of AQUA CHARGE is to serve as a modeling tool to help water distribution and protection agencies on Guam to optimize the groundwater resource exploitation and development, to manage the population's increased water needs and set limits to the aquifer's yield capacity, and to maintain abundant quality water.

TABLE OF CONTENTS

ACKNOWLEDGEMENTS	ii
ABSTRACT	iii
LIST OF TABLES	vii
LIST OF FIGURES	vii
INTRODUCTION	1
Objectives	2
Increased Demands on Groundwater Sources	2
Improving Groundwater Modeling of the NGLA.....	3
VADOSE FLOW SYNTHESIS CONCEPTUAL MODEL	9
The Physical Properties of the Domain	9
The Domain	9
Hydrologic Cycle of the NGLA.....	12
The Surface Environment and Soils	12
The Bedrock Media.....	13
The Conceptual Model Components	15
Node-Shed and Zone Design	18
Stages of the Conceptual Model	20
Streamflow Synthesis Basis.....	21
SSARR to AQUA CHARGE Flow Diagram	27
Soil Moisture Split Curves.....	29
Area Weighted Average Recharge.....	35
Modified Pulse Routing Technique	35
The Vadose Flow Synthesis Conceptual Model of AQUA CHARGE.....	40
CALIBRATION THROUGH HYDRAULIC MODELING	41
Developing the Finite Element Code.....	42
Boundary Conditions	42
Finite Element Equations.....	43
Computer Programming Flow Diagram	45
Calibrating Results to Observed Data.....	46
DATA COMPILATION	48
Spatial Data – Development of the Polygon Attribute Table	48
Background Map Setup.....	48
Finite Element Mesh Design.....	49
Node-Sheds	50
Thiessen Polygons for Rain and Pan Evaporation Gages.....	56
PAT Data File	59

Vadose Flow Synthesis for the Northern Guam Lens Aquifer
Table of Contents

All-In-One Input Data.....	61
Temporal Data (Rain and Pan Evaporation).....	61
Soils Data.....	64
PAT Data.....	65
Synthesized Recharge Data.....	66
Finite Element Method Data (FEMData).....	68
COMALL.....	68
Node X-Y Coordinates.....	69
Element Nodes.....	69
Boundary Conditions.....	71
Initial Head.....	71
Semi-Bandwidth.....	72
METHODS, USER INTERFACE DESIGN, AND CODE DEVELOPMENT.....	74
Development of AQUA CHARGE, via MS VB 6.0.....	74
Input Data.....	75
Zone Recharge.....	78
Area Weighted Average Recharge.....	80
Routing Recharge.....	82
AQUA CHART Display of Recharge at M-11.....	83
Recharge Synthesis Well Guide.....	85
Hydraulic Model.....	88
Interface Forms, Data, and Chart Connection Flow Diagram.....	89
AQUA CHARGE USER MANUAL.....	91
Installation.....	91
Stage 1 – Area Weighted Average Recharge.....	92
Input Data.....	94
Array Variables.....	103
Computational Interval and Recharge Calculation.....	104
Stage 2 – Routing.....	111
AQUA CHART Output Monitor.....	114
Text File Recharge Output for Hydraulic Models.....	119
AQUA CHARGE Finite Element Method Program.....	119
RESULTS AND DISCUSSIONS.....	132
Soil Model Conditions.....	132
Soil Model Condition 1.....	132
Soil Model Condition 2.....	134
Soil Model Condition 3.....	135
Routing.....	139
Spatial Variations.....	153
Hydraulic Model Results.....	158
History Matching.....	158
GW Simulations of M-11 and M-10a.....	175
Comparisons with Earlier Models.....	200

Discussion	201
Major Contributors to Errors	201
Hydraulic Model Improvement.....	203
RECOMMENDATIONS AND CONCLUSION	204
Recommendations.....	204
Management Practice.....	204
Sustainable Yield and Optimum Development.....	206
Advanced GW Modeling.....	206
Conclusion	209
REFERENCES.....	210
APPENDIX.....	213
TERMINOLOGIES, ABBREVIATIONS, ACRONYMS, AND BLENDS.....	219

LIST OF TABLES

1. Soil Model Condition 1 calculated records.....	133
2. Soil Model Condition 2 calculated record	135
3. Soil Model Condition 3 calculated records.....	136
4. Soil Model 1 overall monthly summary	138
5. Soil Model 1 area weighted average recharge for each node-shed.....	139
6. Spatial variation of recharge for selected nodes	156
7. Sum of Squared Error comparisons to previous models.....	201

LIST OF FIGURES

1. Groundwater modeling improvements in the 1990s.....	5
2. AQUA CHARGE's alternative approach	7
3. Contractor and Joeson's mesh domain of the Finegayan and Yigo-Tumon Trough	10
4. The new linear quadrilateral finite element mesh design	11
5. Node-sheds and mesh aligned.....	11
6. Satellite image of the surface environment.....	12
7. Soil map over the satellite image.....	13
8. Barrigada and Mariana Limestones, bedrock	15
9. A virtual 3D model of the domain	14
10. Node-shed vadose column of node 59 and Observation Well M-11	17

11. Allogenic recharge node-shed and boundary flux set up.....	18
12. Surface area node-sheds with sub-node-shed polygons called zones.....	19
13. Node-shed zone's unique polygon attributes.....	19
14. The two stages of the conceptual model.....	21
15. Contractor's UNSAT1D vadose model recharge.....	22
16. Observation wells data resembles surface hydrology behavior.....	23
17. Hydrograph of streamflow synthesis.....	24
18. SSARR was used to model the streamflow in Dworshak, Idaho.....	25
19. Conceptual model of watersheds feeding into a lake.....	26
20. Conceptual model of node-shed tributary columns feeding the lens.....	26
21. The SSARR User Manual and Depletion-Curve Watershed Model.....	27
22. Stage 1-a, the SM model for zone recharge.....	28
23. The soil moisture splitter curve concept.....	29
24. Soils with multiple layers used to compute FC.....	30
25. Soil moisture vs. recharge split flow diagram.....	31
26. Soil moisture vs ET split flow diagram.....	32
27. ET SM models to examine ET effectiveness.....	33
28. Three soil model conditions, project objective investigation.....	34
29. Node-shed zone areas and recharge to zones for computing AWA recharge.....	35
30. Stage 2, router flow diagram.....	36
31. Cascading reservoirs, routing model, producing flow lag time and attenuation.....	37
32. Recharge synthesis sample in AQUA CHART.....	39
33. The Vadose Flow Synthesis Conceptual Model.....	40
34. Hydraulic model's boundary conditions.....	43
35. 2-D transient, saturated flow, programming flow diagram.....	46
36. The background map.....	49
37. Finite element mesh design.....	50
38. Applying Euclidean allocation function in GIS for building node-sheds.....	51
39. Extending the node-shed for boundary flux conditions.....	52
40. A completed node-shed.....	52
41. Soils polygon shape file.....	53
42. The GIS Union tool.....	54
43. Soil and node-shed shape files.....	54
44. Union of soils and node-shed.....	55
45. PAT for the union of node-shed and soil.....	55
46. Rain Thiessen polygons.....	57
47. Pan evaporation station Thiessen polygons.....	58
48. Union of rain and pan evaporation Thiessen polygons.....	58
49. PAT of the union of rain and pan evaporation gages.....	59
50. Final union of rain, pan evaporation, soils, and node-sheds.....	59
51. The PAT database file of the final union.....	60
52. Node-shed 59, of node 59 and Observation Well M-11.....	60
53. The node-sheds superimposed over the finite element mesh.....	61
54. All-in-one data recordset setup for the rain tab.....	63
55. All-in-one Excel file data recordset setup for pan evaporation tab.....	64
56. All-in-one data recordset setup for soils.....	65

57. All-in-one data recordset setup for PAT	66
58. Sample of text file recharge synthesis output	67
59. FEMData Excel file recordset setup for COMALL tab	68
60. FEMData recordset setup for NODEXY tab	69
61. FEMData recordset setup for ELMNTNODES tab	70
62. Element nodes numbering order	70
63. FEMData recordset setup for BNDRY tab	71
64. FEMData recordset setup for INITIAL tab	72
65. SBW size solutions tab	73
66. MICROSOFT® Visual Basic 6.0 programming environment	74
67. Input data programming flow diagram	75
68. AQUA CHARGE Daily Rain and Pan Evaporation tab	76
69. AQUA CHARGE Soil Index tab	76
70. AQUA CHARGE PAT tab	77
71. Programming flow diagram of zone recharge	79
72. Programming flow diagram of area weighted average recharge	80
73. AQUA CHARGE Arrays and Groundwater Recharge tab	81
74. AQUA CHARGE Calculated Records tab	81
75. Programming flow diagram of the router	82
76. AQUA CHART	84
77. Properties of groundwater in a porous media	85
78. Sample of the Well Guide in AQUA CHART	87
79. Finite Element Method program graphical user interface	89
80. AQUA CHARGE program flow diagram connectivity	90
81. The program setup files	91
82. Windows installer Setup Wizard and the installed shortcut icon	92
83. AQUA CHARGE Splash screen startup	93
84. AQUA CHARGE program title cover tab	93
85. AQUA CHARGE file menu	94
86. Data input common dialog box	95
87. PAT tab data extraction instructions message box	96
88. Zone field identifier text box and field name selection	96
89. Extract and sort required field data from PAT file button	97
90. Daily rain and pan (evaporation) tab	98
91. Soil Index tab	99
92. Switching focus on charts	99
93. The x-axis options	100
94. The Percent Yield Variable and Field Capacity frame	100
95. Changing the field capacity for a specific soil type	101
96. Save the ET curve settings with the save option	101
97. Loading saved curve settings	102
98. A loaded curve setting for recharge	102
99. Create Arrays button	103
100. Arrays and GWR tab showing array values prepared	104
101. Ready for Groundwater Recharge Calculation button	105
102. Computational Interval Form	105

103.	Monthly groundwater recharge to node-sheds list box	106
104.	Verifications tab	107
105.	Calculated Records tab	108
106.	Exporting the calculated records to an Excel file	108
107.	Overall Monthly and Yearly average spreadsheet	109
108.	Averages by Month spreadsheet	109
109.	Monthly Averages spreadsheet	110
110.	Node-shed Average Recharge spreadsheet	110
111.	The Routing tab	111
112.	Open AQUA CHART command button	112
113.	Percent Fast/Slow curve adjustment	113
114.	The ROUTE IT and Output to AQUA CHART command buttons	114
115.	Field names setting	115
116.	Insert, Name, and Define from the menu bar	115
117.	Defining names for recharge output to AQUA CHART	115
118.	Field Names and Node numbers for SIMOUT	116
119.	Define name for SIMOUT	117
120.	Save the file name	117
121.	AQUA CHART interface	118
122.	Saving the routed recharge to a text file	119
123.	AQUA CHARGE GWModel tab	120
124.	Finite element program interface	120
125.	Opening FEMData	121
126.	Opening the recharge text file	122
127.	NODES option button	123
128.	ELEMENT N MATERIALS option button	123
129.	MATERIALS PROPERTIES option button	124
130.	Changing the materials property data	124
131.	TIME STEP Options	125
132.	COMALL Options	125
133.	GW3 (Istok) Transient, Saturated groundwater flow button	126
134.	Output to AQUA CHART and Simulated Output (30) button	127
135.	Select AQUA CHART if not opened, common dialog box pop up	127
136.	Simulation charted (orange)	128
137.	SIM OUTPUT spreadsheet in AQUA CHART	129
138.	X12 animation frame	130
139.	X29 animation frame	131
140.	Model 1 soil conditions	133
141.	Model 2 soil conditions	134
142.	Model 3 soil conditions	135
143.	Monthly model comparison bar chart	137
144.	Monthly and yearly ET and GW recharge model comparison bar chart	137
145.	Synthesized recharge model comparison graph	140
146.	Router parameters and curve settings	141
147 to 169.	<i>Synthesized recharge results</i>	142 - 153
170 to 173.	<i>Spatial variation of recharge results</i>	154 - 155

174. Results of changing fast flow parameters	157
175 to 190. <i>Synthesized recharge and GW model simulation results</i>	159 - 174
191. Final materials properties setting for GW model.....	175
192 to 206. <i>Final synthesis and simulation results for M-11</i>	176 - 190
207 to 215. <i>Final synthesis and simulation results for M-10a</i>	191 - 199
216. Monthly average simulation chart	200
217. Thiessen polygons, gages, and well location	202
218. GIS Darcian Function flow direction for initial conditions	207
219. GIS Darcy Velocity Function; starting conditions, flow direction and velocities	207
220. GIS Darcy Velocity Function, flow direction and magnitude	208

INTRODUCTION

The modeling of the *Northern Guam Lens Aquifer* (NGLA) has dramatically improved over the last three decades, incorporating increasingly sophisticated numerical modeling techniques and more precise data on the meteoric and hydrologic factors affecting the flows into the aquifer. Today's advanced computer technology with improved software applications has contributed to the development of a program called AQUA CHARGE. AQUA CHARGE integrates the meteoric, hydrologic, and hydrogeologic components of the *vadose* (aerated rock media layer) and *phreatic* (saturated rock media zone) system into a numerical/computer program to synthesize *recharge*. The recharge produced from the vadose flow synthesis model is defined here as the volume of water that gets to the water table. Obtaining a refined recharge estimate means an accurate determination of *evapotranspiration* (ET) since recharge is rainfall loss to ET. We achieved these approximations through the development of *soil moisture* (SM) *model*. Then, the estimated dual recharge flows through the thick bedrock plateau to the water table were synthesized using a router type *transfer function*. The SM model and the router are the two main guiding components necessary to build the vadose flow synthesis model. With improved estimates of vadose flow, *groundwater* (GW) modeling's reliance on accurate recharge can be met. Ultimately, this project aims to take GW modeling done in the previous two decades, 1980s and 90s, to new and improved levels of simulation accuracy through the synthesis of a realistic GW recharge calculation.

AQUA CHARGE was designed with the endeavor to resolve the shortfalls of past GW modeling attempts that the modelers themselves announced as errors. Three major problems addressed and accounted for were the spatial variability of soils, complex geologic material properties, and the temporal variations of meteoric events (Contractor, 1981). The spatial variability issue was resolved with clever topologic configurations of the study domain with respect to the meteoric, hydrologic, and hydrogeologic aspects using *Geographic Information System* (GIS) techniques to design and assign boundary conditions and polygon properties or attributes. The temporal meteoric data includes daily rainfall and pan evaporation. The time steps were refined to daily and transient (unsteady state). Unlike the former models that were limited by computer processing capability and capacity at that time, the models were forced to run monthly time steps. Now, the processing of the entire model is in a matter of minutes, rather than which previously took hours or even days. This allows the modeler to develop and examine many simulation scenarios in a very short time.

The hydrologic portion of AQUA CHARGE incorporated soils properties that determine the amounts of moisture that yield to recharge and ET and the lag time and attenuation of water moving down through the vadose zone to the water table. After the moisture moves through the soil layer, a transfer function called the *modified pulse routing technique* is used to mimic the fast and slow time arrival flow of moisture to the water table. This routing method was an alternative to the finite element method Contractor used to simulate vadose flow (Contractor et al. 1999). It was taken piecewise from the moisture flow diagrams and numerical code found in the U.S. Army Corps of Engineers' *Streamflow Synthesis and Reservoir Regulation* (SSARR) User Manual (USACE, 1987). This method is independent of deciding spatially varied hydraulic conductivities for a complex karst system. Instead, it focused on sampling time arrivals and attenuation of flows amounts. SSARR allowed us to design the Vadose Flow Conceptual Model

that guided the construction of AQUA CHARGE. The program calculated realistic account and control of moisture flow through a deep composite island karst vadose.

Numerous calibration simulations were processed in order to adjust the various curves and parameters to fine tune the model to the observed well data. This new model not only provides better estimates of recharge volume accounting with respect to spatial and temporal variations, but can provide a basis for future GW studies in the NGLA as well as other similar aquifers in the Marianas islands and throughout the world.

Objectives

The objectives of this project were to: (a) improve the existing AQUA CHARGE program to simulate the temporal hydrologic processes that influence GW recharge, (b) apply 3 sets of soil curves to explore the effects of soil properties on evapotranspiration (ET) and eventual GW recharge, (c) use surface water routing techniques to model the effect of vadose zone storage and hydraulics on aquifer recharge, (d) modify AQUA CHARGE to include a two-dimensional, transient, saturated GW-flow, finite element model, and (e) make recommendations concerning which modeling parameter values lead to the most realistic recharge estimates.

Increased Demands on GW Resources

The NGLA is a fresh GW aquifer system that is crucial to the economic growth of Guam. It is without a doubt one of Guam's most precious renewable resources. Currently, about eighty percent of Guam's water supply comes from the NGLA (Contractor and Jenson, 1999). Managing this resource means that Guam Waterworks Authority (GWA) and the Guam Environmental Protection Agency (GEPA) must obtain reliable estimates of the aquifer's sustainable yield. A lack of accurate sustainable yield estimates can lead to over pumping and deterioration of the quality of the water pumped from the aquifer.

In the past decades, well site selection was rather simple. Most of the wells pumped high quality water in high quantities. Increased development today and in the future has changed this situation. As new development occurs, increased water demands will require new well expansions. The amount of water that can be pumped and the placement of these wells is crucial in preventing development that exceeds the capacity of the aquifer's quality water content.

Guam's water system development is expected to increase to accommodate for the island's future growth. The tourism industry has had fluctuations of visitors in the recent years. In 2005, the island reached a record high of over 1.2 million visitors, mostly Japanese tourists (GVB, 2006). This number is expected to increase in the near future when the Chinese and Russian tourist visas are approved, expecting an addition of more than 50,000 visitors per year (Guam PDN, Jan., 2009). The population increase includes the island's anticipation of the United States Marines realignment from Okinawa to Guam, bringing an additional 8,000 service members plus 9,000 dependents (Guam PDN, Feb., 2009). The Air Force is also expecting an increase of an additional 3,000 personnel and their dependents; the WWII historic Northwest Field near Ritidian Point has already begun reconstruction (Guam PDN, 2007). In order to facilitate these population increases, additional supplies of quality water will be vital.

Sound management of the GW system requires an enhanced understanding of the relationship between rainfall and soil properties that results in recharge to the aquifer. Aquifer recharge is the starting point for calculating the sustainable yield for the aquifer. This recharge estimate coupled with accurate hydraulic models such as the finite element method for GW modeling will help to define how much water can be safely extracted and where these extractions should occur in order to safeguard the quality of the supply. The research described here focuses on acquiring an improved understanding of the spatial and temporal distribution of the rain falling on Northern Guam that finally recharges the aquifer system and the role of soil properties and time lag and attenuation of infiltration through the limestone bedrock in determining these recharge estimates.

Improving Groundwater Modeling of the NGLA

In the past several years, researchers at the University of Guam *Water and Environmental Research Institute* (WERI) of the Western Pacific have been working diligently to develop advanced hydraulic models of the NGLA. These models provided enhanced knowledge including estimates of sustainable yields which provided water management agencies information to determine optimized pumping scenarios and to implement regulations that protect the water supply system's quality and integrity. These models also gave agencies insight on establishing strategic well site selection and development. Another benefit from these models was an improved comprehension of contaminant conveyance in the ground water system.

Accurate recharge estimates played a role in determining the water balance and set limits to GW exploitation. To protect the GW quality, a simple rule was not to exceed pumping rates that will upset the long term water inflow and outflow balance. In the past, recharge rates were estimated based on data from elsewhere rather than the Northern Guam area (Ayers, 1981). Many estimates were based on Southern Guam's surface flow data to estimate the Northern Guam's daily average recharge value. Only Austin Smith and Associates Inc. in 1970 matched recent estimates in the 1990s and 2000s of recharge averages above 1 million gallons per day per square kilometer (mgd/km²). These estimates were contained in a report for Public Utilities Agency of Guam, using rainfall runoff data from 1959-1966 with the assumption that the runoff coefficient for Southern Guam surface flows could be used to estimate Northern Guam's recharge. The following lists daily averaged recharge estimates that were over 1 mgd/km²:

1970, Austin, Smith and Associates, Inc. (Ayers, 1981):	1.04 mgd/km ²
1991, Mink (Mink, 1991), his "most probable estimate":	1.07 mgd/km ²
1999, Jocson, Jenson, and Contractor (Jocson et al., 1999):	1.19 mgd/km ²
2008, Habana and Heitz – AQUA CHARGE:	1.23 mgd/km ² .

The results we used were from the calculated records generated from AQUA CHARGE recharge model, using linear and Thornthwaite soil models for recharge and ET respectively. We also used the same rainfall and pan evaporation data as Jocson, except the rainfall data were corrected using the *Normal Ratio Method* (Linsley et al., 1982), historic archives (JTWC, 1982 - 1995), and advice from Dr. Mark Lander, Meteorologist. In an early stage of recharge modeling, using Jocson's area coverage of Yigo-Tumon and Finegayan sub-basins, and minimum adjustment to the rainfall data, AQUA CHARGE calculated 1.12 mgd/km².

A major contributor to the success of the development of the AQUA CHARGE program is attributed to GW modeling attempts and the reports produced by Dinshaw Contractor and his team. Contractor pioneered GW modeling of the NGLA from 1980 and continued his research for 20 years. Contractor with Srivastava developed a GW model called Salt Water Intrusion/Groundwater Flow — Two Dimensional (SWIG2D) that John Jenson's research assistant John Jocson would later use in the 1990s as a basis for his Masters Thesis titled *Hydrologic Model for the Yigo-Tumon and Finegayan Sub-basin of the Northern Guam Lens Aquifer, Guam*, (Jocson, 1998). Jocson applied an "instantaneous recharge" (Contractor et al., 1999; see Figure 1), using Northern Guam rainfall and pan evaporation data from 1982 to 1995 (NCDC, 1995), and calculating recharge as monthly totals of daily rainfall minus pan evaporation as input to the SWIG2D model. His best simulation match to the observation wells used a regional hydraulic conductivity value of 5.8 km/day. Soon after, Contractor, in his last GW model efforts for Guam and technical report for WERI, reduced the errors compared to Jocson's results by installing a 1-dimensional (1-D) vertically positioned unsaturated finite element model, UNSAT1D, to simulate vadose flow to the 2-D mesh elements for SWIG2D together called VADOSWIG (Contractor, et al., 1999). Contractor continued work over the same mesh area domain Jocson used in his thesis. All of Contractor's technical reports of GW modeling over the NGLA made important conclusions that addressed the significant sources of errors as well as discoveries and suggestions that helped us pursue and build a better model. An important observation Contractor made, also recognized by hydrologist Dr. Leroy Heitz, were the shapes of the hydrographs produced by the UNSAT1D that resembled streamflow hydrographs in surface hydrology (Contractor et al., 1999, Heitz, personal communication). They also saw that same suspiciously familiar behavior of the GW response to rain pulses in the observation well data. These observations helped us better understand the nature of the aquifer and led to the use of streamflow synthesis to produce the recharge.

MODELING IMPROVEMENTS, 1990s

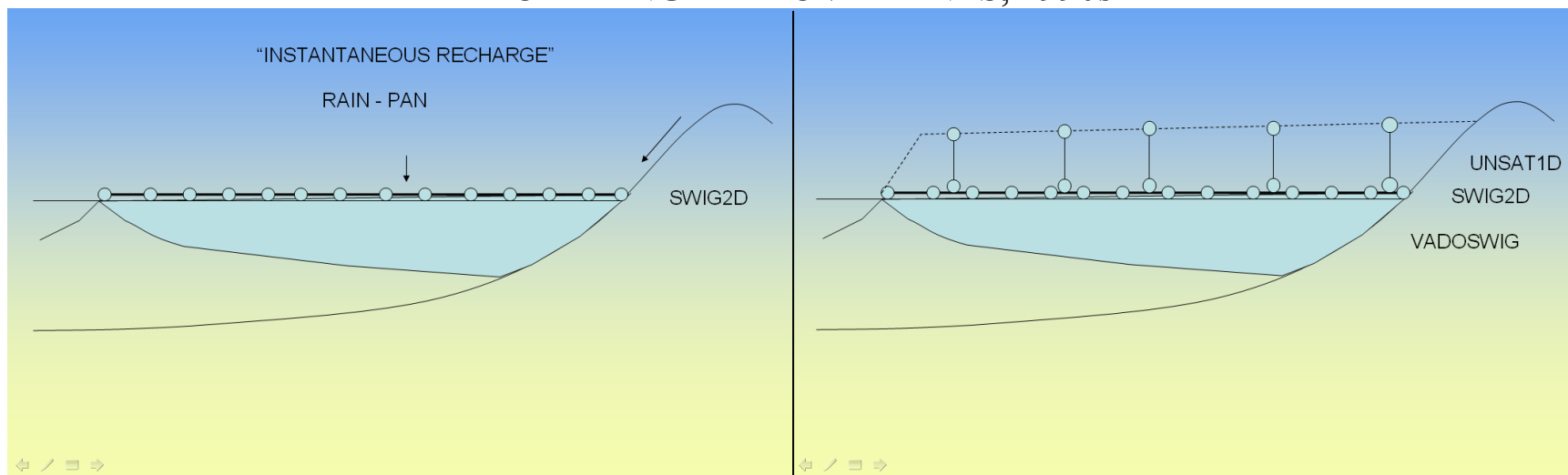


Figure 1. Groundwater modeling improvements in the 1990s. Left picture shows Jocson’s “instantaneous recharge”, without a vadose to the SWIG2D model’s elements. Right picture is Contractor’s vadose model with UNSAT1D into SWIG2D, together called VADOSWIG (Contractor and Jenson, 1999).

One significant element in understanding the aquifer system is to comprehend the spatial and temporal distribution of the aquifer recharge. GW recharge in the NGLA is the rainfall reduced by losses due to ET. In order to calculate this recharge value, accurate estimates of ET rates and their temporal and spatial distribution over the study area are necessary.

In previous undergraduate research assistance work done back in 1998-99, Habana developed a working computer program application titled "AQUA CHARGE". Simply stated, the AQUA CHARGE program allowed us to examine the effects of spatial and time variability of soil properties and ET over Jocson's study area. Using this program, we explored and evaluated various relationships between ET, pan evaporation, and soil moisture. At that time, the soil layer hydrology model, AQUA CHARGE, produced a monthly total area weighted average recharge for the mesh elements and was supposed to be applied to Contractor's VADOSWIG model (See Figure 1.2). The planned study was interrupted, and AQUA CHARGE was secured and stored for six years. In 2006, returning as a graduate student research assistant this time, it was decided to again run the AQUA CHARGE model. It was found that the SWIG2D software was inoperable and the program file was corrupt and unreadable. As a result, two additional processes were added to AQUA CHARGE; the routing and the finite element method for hydraulic modeling of flow through the aquifer. These additions, as part of its upgrade, led to the renaming of the program to AQUA CHARGE Deluxe. We will often still refer to it as AQUA CHARGE.

AQUA CHARGE'S NEW APPROACH

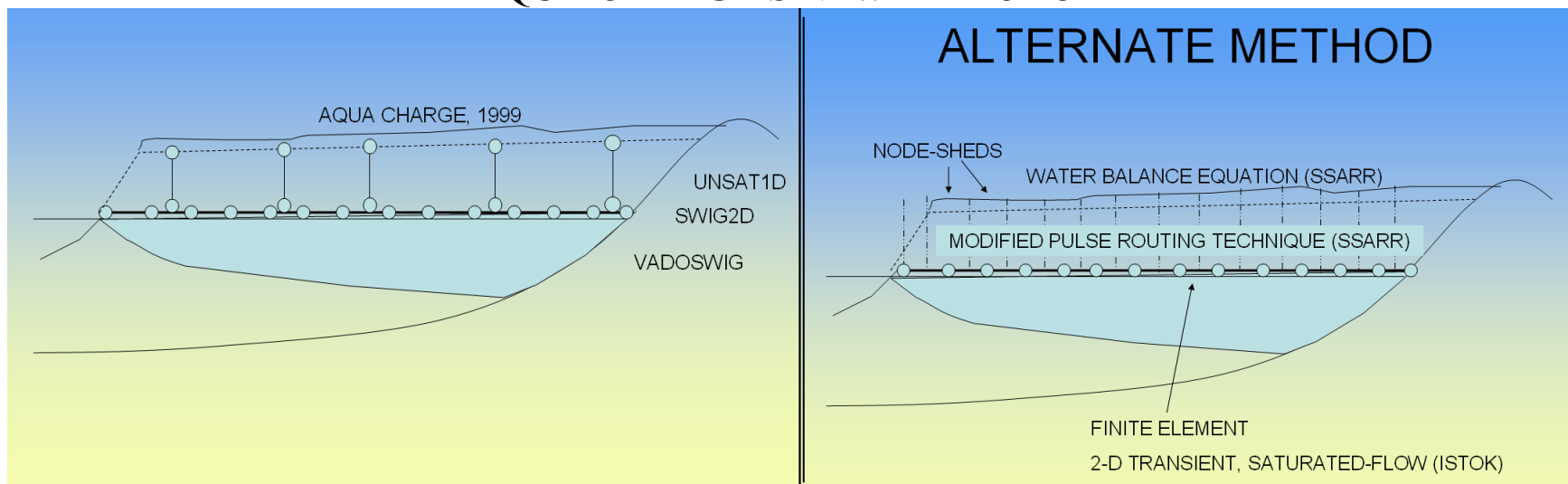


Figure 2. AQUA CHARGE's alternative approach. Left, plan to improve the VADOSWIG model using AQUA CHARGE to handle the soil layer hydrologic modeling. Right is new model design for AQUA CHARGE Deluxe. The details to the alternate method are in Chapters 2 and 3.

This project resulted in an improved understanding of the ET process and also yields a better understanding of how recharge changes with location and time. One important aspect of this project is the analysis of determining the recharge hydrograph shapes that contribute to simulate aquifer responses. This interesting technique guides the modeler in adjusting the routing parameters for fast and slow flow recharge.

The method for employing spatial and temporal variability data for generating ET and recharge in this study may also be applicable to the Saipan's (one of the Commonwealth of the Northern Marianas Islands), GW systems and other similar karst type systems throughout the world. The lack of basic field spatial and temporal parameters in the Marianas and other high islands of the Western Pacific impede them in determining their aquifer's yield potentials and limitations. Saipan's aquifer system has already experienced salt water intrusion due to over development from lack of good data for strategic optimization of GW exploitation, and also geologic structural issues that classifies Saipan as a *complex island aquifer system* (Wexel et al., 2001). This project's improved techniques for estimating ET and recharge on Guam can help in estimating safe yields and making better plans for future aquifer development and restoration on Saipan.

VADOSE FLOW SYNTHESIS CONCEPTUAL MODEL

This chapter describes the theoretical approach for synthesizing vadose flow or recharge. The process begins with a general description of the conceptual model for a hydrologic node watershed (node-shed). A node-shed is a *Euclidean allocated* area contributing water flows to a node in the finite element mesh. The conceptual model design takes a single node-shed and attempts to capture relevant characteristics of the Northern Guam Lens Aquifer (NGLA). The node-shed is made up of sub-polygons called zones that identify the zone number, node-shed number, soil type, rain gage, pan evaporation gage, area of the zone, and area of the zone's node-shed. The *soil moisture* (SM) balance accounting through each zone's soil layer is based on the Streamflow Synthesis and Reservoir Regulation (SSARR) model. This model includes the explanation of the streamflow synthesis model to determine recharge. The model is separated into two stages; the water accounted for in the soil, and the water traveling through the bedrock. The soil layer moisture allocated between recharge and SM, and between SM and evapotranspiration (ET) is interpolated through a SM relation split curve. The recharge to a node-shed is calculated using an area weighted average (AWA) recharge of all the zones in the node-shed. Stage 2 splits the results of Stage 1, to percent of AWA recharge that moves into fast and slow flows through the bedrock to the water table. The fast and slow flow moisture quantities are then routed using a transfer function to simulate the time lagged and attenuated flows of recharge. Finally, the conceptual model is applied to calculate all the node-sheds in the finite element mesh domain on a daily transient time step. Some basic and special design concepts of the node-shed top surface are discussed and considered to account for *autogenic* and *allogenic* recharge that is important for connecting the AQUA CHARGE recharge model to meet the modeler's finite element mesh boundary conditions.

The Physical Properties of the Domain

This section describes how the physical attributes of the aquifer and hydrologic data are incorporated into the model. With the available data, some assumptions about reality must be made for the limitations in order to maintain a reasonable and acceptable conceptual vadose flow model. Recognizing the complexities of the aquifer requires alternative solutions. A close examination of the domain's physical properties and the understanding of its waterflow mechanism have guided the assembly and development of a virtual model computer program for synthesizing recharge.

The Domain

The model domain started with Jocson's two-dimensional (2-D) triangular finite element mesh over the *Finegayan* and *Yigo-Tumon sub-basins* designed with the ARGUS® ONE (Open Numerical Environment) program (Jocson et al., 2002; Figure 3). Contractor et al. (1999) used the same domain boundaries with increased node and element resolution for the purpose of improving results. They had completed a program called VADOSWIG (SWIG2D and UNSAT1D model combination, Chapter 1) that combined the hydraulic modeling of the limestone bedrock's unsaturated and saturated portion of the aquifer. One-dimensional

vertically-positioned node and element lines were placed on top of the 2-D phreatic mesh posted as high as the nearest surface contour. As mentioned earlier, the objective for this thesis was to develop a hydrologic program to model the soil layer's effect on recharge and ET. AQUA CHARGE calculates monthly recharge for each element in the Jocson/Contractor mesh.

The coding of a new groundwater (GW) model requires that recharge flux be input at the junctions or node points in the finite element mesh. The areas contributing to each node point were determined using a Geographic Information System (GIS) technique called Euclidian allocation (ESRI, 2007) which is similar to the Thiessen Polygon (Linsley, 1982) technique used in traditional hydrology investigations. Euclidean Allocation identifies the *cells* to be allocated to a source based on closest proximity. The Euclidian allocation technique assigns the areas closest to a node.. The AQUA CHARGE program uses the Euclidian allocated polygons assigned to each node to calculate recharge. The use of available software tools along with GIS projection selection (*Universal Transverse Mercatum*, UTM, *World Geographic System 1984*, WGS 84, Zone 55 North) and new basement volcanic map (Vann, unpublished) led to the development of new model boundary construction as shown in Figures 4 and 5. The finite element mesh in Figure 4 is a linear quadrilateral design having four nodes and element lines around each element area. The numbering of the nodes was specifically configured to produce the smallest maximum *semi-bandwidth* (SBW) value (for the entire mesh) used in the matrix compilation, speeding up processing, and the node-sheds are numbered the same as the node they bound (Istok, 1989).

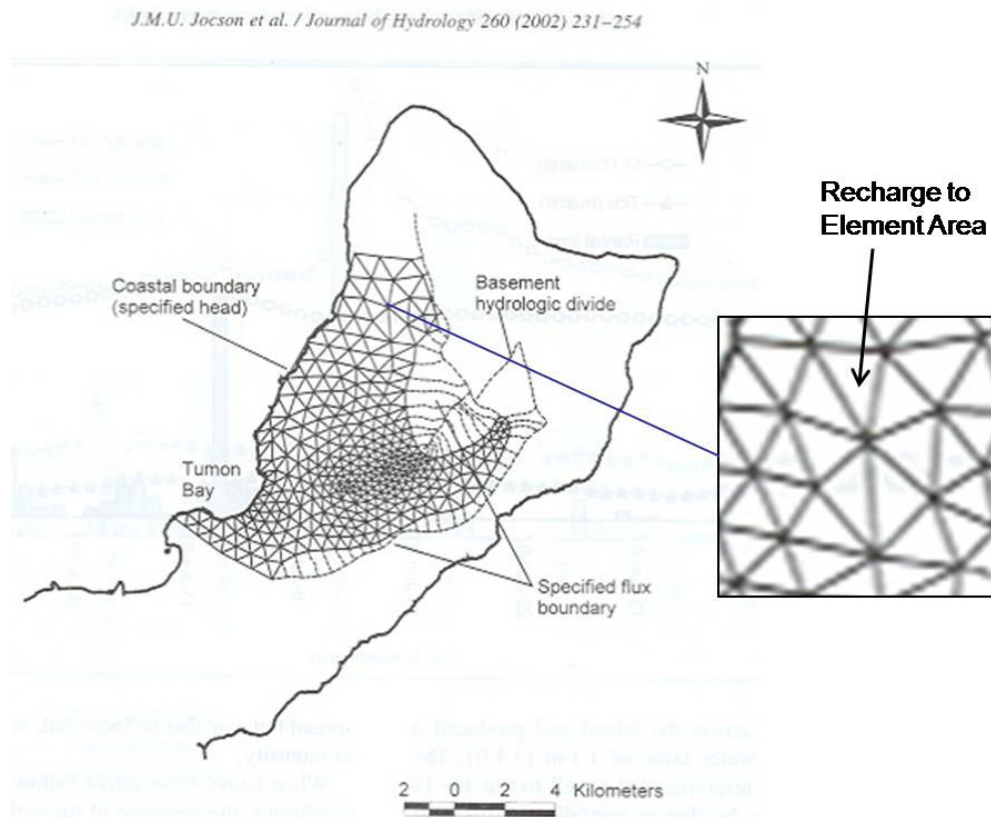


Figure 3. Contractor and Jocson's mesh domain of the Finegayan and Yigo-Tumon Trough. SWIG2D code required the recharge to flux into the mesh elements.

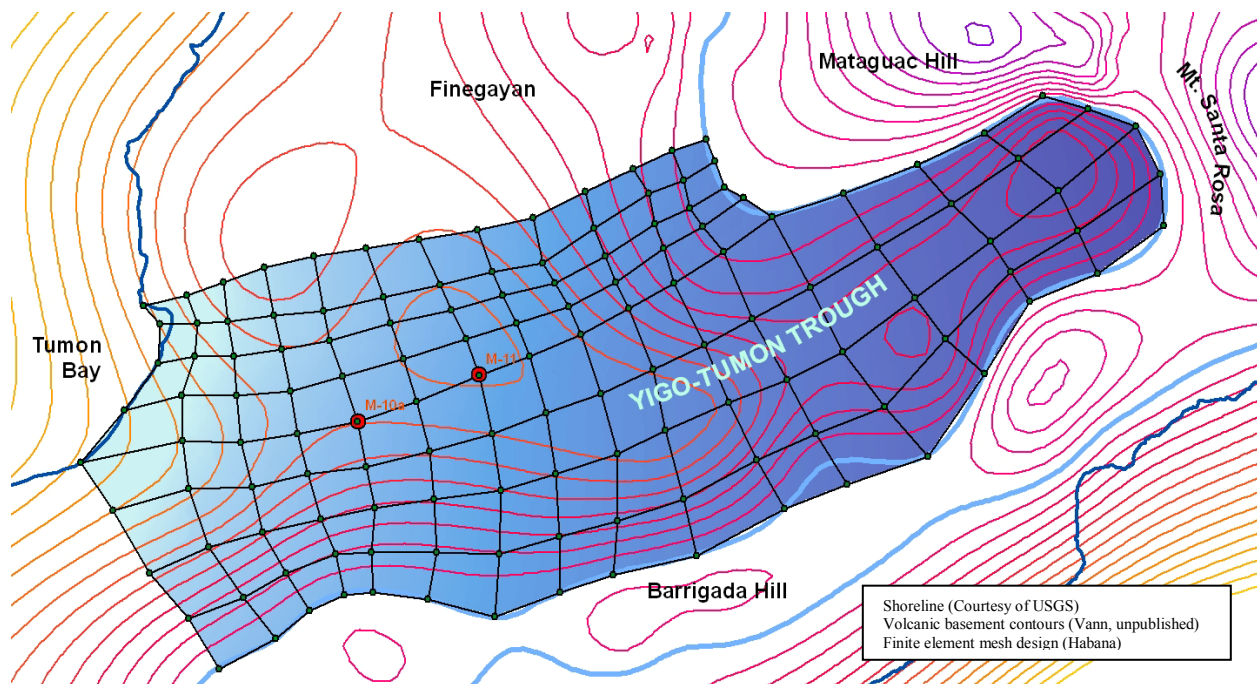


Figure 4. The new linear quadrilateral finite element mesh. Designed using GIS of the Yigo-Tumon Trough with two observation wells M-10a and M-11 marked in red points.

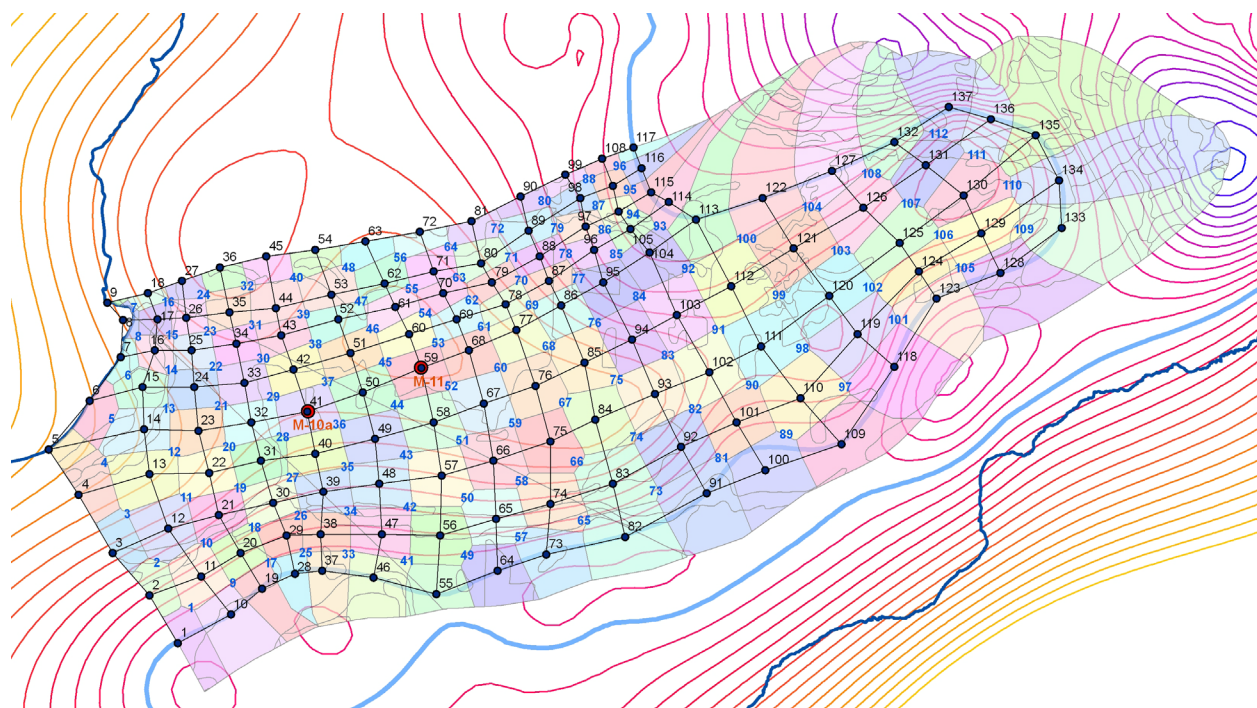


Figure 5. Node-shed and mesh aligned. Each colored areas around a node are defined as a node-shed. The nodes are numbered to produce the smallest maximum semi-bandwidth, and the node-sheds are numbered the same as the node it bounds.

The Hydrologic Cycle of the NGLA

The Northern Guam Lens Aquifer (NGLA) is typical of island karst aquifers (Myroie and Carew, 1995). A major part of accurately estimating recharge is following and understanding the relevant hydrologic mechanism and incorporating them into the conceptual model. The hydrologic cycle over the NGLA begins the overall concept and study for designing and understanding the model. The NGLA's high hydraulic conductivity results in short distance runoffs. The brief and short runoff is due to the thin to no soil layer and high permeable limestone bedrock. Once rain water infiltrates the soil surface, SM has two paths; some portion continues flowing down through the limestone bedrock as recharge, some is returned to the atmosphere through vegetation as transpiration, and un-infiltrated moisture evaporates. The water moving past the soil layer travels through the vadose zone and makes its way through about 200 – 500 ft (60-150m; Contractor, 1999) of limestone. When the water reaches the saturated zone, or phreatic zone, it then moves horizontally or into the lens, and then eventually discharges along the coast line.

The Surface Environment and Soils

The surface environment is complex and affects the infiltration of rainfall. Figure 6 shows a DIGITAL GLOBE® QuickBird Satellite Image of Northern Guam (2006) sub-watershed boundary (red line) and the water lens toe boundary (blue line). The picture shows high urban development with the greatest concentration of human population of the entire island living above this main water source. The urban development today continues to increase, and the entire natural landscape has changed, increasing the urban complex soil area. Some of these developments are impervious structures that intercept and divert rainfall to a storm drain system or ponding basins, or surface depression.

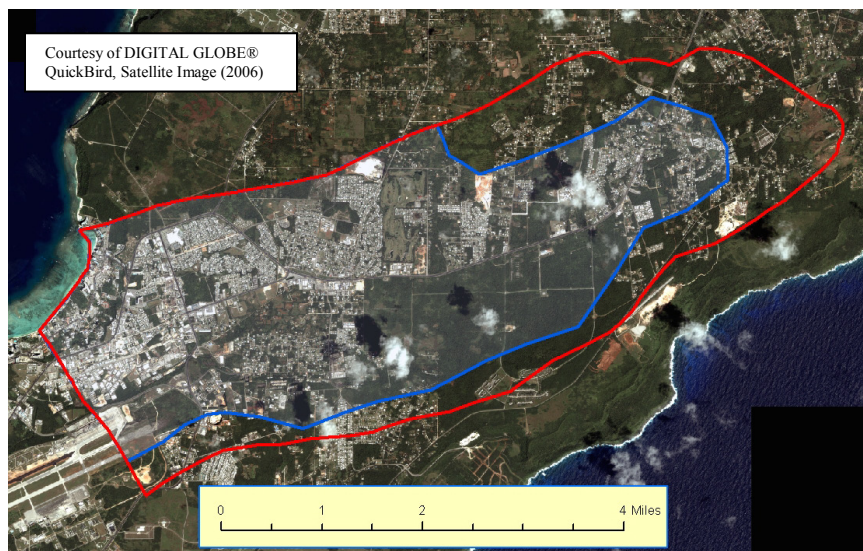


Figure 6. Satellite image of the surface environment. It is the most developed area having impervious surfaces (buildings, parking lots, etc.) that continue to increase yearly within and around the red boundary. Other obstructions or hindrances to direct infiltration are the vegetation canopies and surface slopes.

Soil layers vary in depth. Soil pipes can have strong local effects on soil field capacity (FC), and thus can vary the SM vs. recharge/ET relationship throughout the domain. The island's growing urban development through the 1980s to present time had removed soil layers, exposed the limestone bedrock, and replaced natural soils and vegetation (as on golf courses and landscaping). The soils map inventory has not been updated since the 1980s to meet those changes (see Figure 7). The soils have a variety of vegetation covers, including urban vegetation, forest on elevated limestone, pastures, savannah complex, coconut plantations, and ravine forest (Mueller-Dombois and Fosberg, 1998). The study area has varied vegetation types that transpire differently. The vegetation as a canopy cover varies as well, affecting spatially direct infiltration due to interception. Jocson, for the estimation of recharge for his model, assumed rainfall measuring less than 0.6 cm (0.24 inches) was lost through interception and evaporation (Jocson et al., 2002).

A digital vegetation map was still in development at the time of the construction of the AQUA CHARGE program and thus is not included in this model. Now ET is based on the soil properties for the type of soil laid out in the soils map (Habana, 2008, APPENDIX D).



Figure 7. Soil map over the satellite image. New development show outdated areas. Urban development has increased the urban complex soil type area.

The Bedrock Media

The NGLA is probably one of the most uniquely complex aquifers in the world. This complexity poses a real challenge to accurately modeling the system. A special hydrologic approach applying a streamflow synthesis technique was used to deal with many of the problems. The development of a computer program to apply this technique is discussed next after examining the physical complexities of the aquifer.

The terrain features are typical of island karst aquifers, in which sink holes, fissures, conduits, and fractures can redirect vertical percolation. The NGLA occupies a thick, 200 to 500 feet amsl (above mean sea level) (60-150m), uplifted carbonate island karst aquifer plateau. Recharge to the lens arrives in different quantities at different times because it travels the vadose zones large vertical distance through different pathways: connective pores, fractures, and shafts to get to the lens. Karst aquifers in general exhibit triple porosity, having matrix, fractures, and conduits (Worthington, 2003). The fractures and conduits are large openings in the limestone that allow water to infiltrate the bedrock easily. Waters flowing through these openings move quickly through the vadose zone. A large volume of water may thus accumulate at a surface depression and find a rapid path of flow downward during heavy storms. The matrix porosity is generally composed of granulated or spongiform rock that is still permeable enough for water to weave its way around small rock particles and through tiny, even microscopic, connective pores. Recharge percolates slowly through the matrix of the vadose zone. The limestone rock can thus store some percolating water and slowly release it into the lens. Water moving through these different pathways thus reaches the saturated zone at different times and in different amounts across the phreatic interface. The triple porosity of the vadose zone is impossible to capture in fine resolution, so models must assume representative composite properties.

Autogenic and allogenic are two types of recharge found in the aquifer. The autogenic recharge is the vertical flow of water through the aquifer's vadose zone. This is the case when no impervious material exists beneath the point of infiltration vertically through the vadose zone down to the lens. Allogenic recharge is found where the sloping impervious volcanic basement is in contact with the unsaturated limestone and has large voids between the contact surfaces of the two materials. This allogenic recharge occurs around Mount Santa Rosa and probably also in Mataguac and the flanks of Barrigada Hills. Mass amounts of water are known to travel through the voids between these two surfaces and bring large volumes of flux into the lens toe. This feature is important to consider in the boundary conditions at the lens toes in the mesh and node-shed domain design since their flows are recognized as significant in rate and volume.

The geologic map of Guam (Tracey et al. 1964) reveals two limestone components of the aquifer, *Mariana Limestone* and *Barrigada Limestone* (Figure 8). The younger Mariana Limestone lies on top of the Barrigada Limestone. Most of the lens water lies in the Barrigada Limestone. The Mariana Limestone is detrital with large voids while the older Barrigada Limestone is mostly granular and facilitates matrix flows. In some cases, the points of contact amid two different rock materials have large voids between the two. If not accounted for, these voids could be a significant flow path that can cause problems in accurate modeling. The difficulty in modeling these two in the same domain are their contact points in the aquifer and the transition of extreme spatial variation of porosity, specific storage, and hydraulic conductivity. This complicates the decision of assigning hydraulic conductivity and specific storage values to the nodes in the hydraulic model. Nodes should be positioned where the two rocks meet (Istok, 1989), but at mean sea level (msl) in the aquifer, we do not have spatial data of where they meet.

Sea level changes may have also affected the vadose zone. Relict flank margin caves are visible evidence of former sea-level highstands seen throughout the limestone plateau sides. It is at the water table where the limestone dissolution process is highly active (Moore and Sullivan, 1997). This means that during a time when the water table was high above its current position, caves were formed at the interfaces of former lens position. Water traveling downward may thus be redirected horizontally when it intercepts zones of high lateral conductivity.

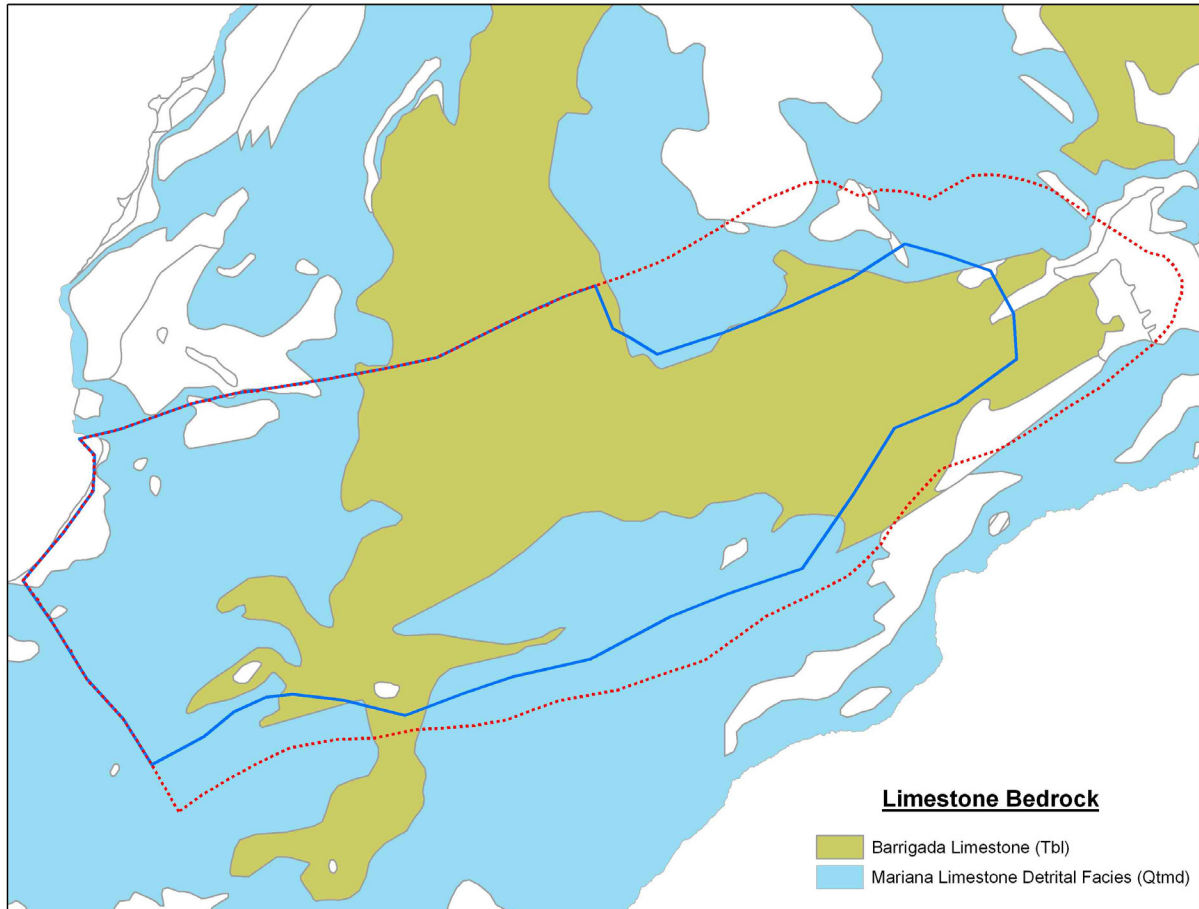


Figure 8. Barrigada and Mariana Limestones, bedrock. They are the major bedrock materials of the aquifer. The Barrigada Limestone is granular having matrix porosity where most of the water lens resides. The Marianas Limestone is detrital and has greater porosity.

The Conceptual Model Components

The conceptual model was designed to account for movement of moisture in and out of a Euclidean allocated node-shed. The model for a single node-shed calculates the recharge for that node in the GW hydraulic model. This section explains the modeling design approach in synthesizing recharge through a single node-shed and then later throughout the domain. To start, a virtual 3-Dimensional model (Figure 9) with the cross section of the domain reveals the geo material components in the study area. This virtual model shows the placement of the finite element mesh design at mean sea level. The vadose zone is composed mostly of limestone bedrock, and the plateau surface shows surface hydrologic polygons. Figure 10 shows the surface detail of a node-shed piece of the virtual model. The surface satellite image is in scale, while the bedrock is exaggerated for visual emphasis. The light blue layer is the freshwater phreatic component, and beneath bottom of the lens is the salt water portion. From this node-shed piece, the conceptual model design for AQUA CHARGE begins to take form as a vertical column of surface and sub-surface material that will sit over a node cell in the finite element mesh. The conceptual model was then constructed from available GIS data in attempt to capture all of reality's physically important hydrologic attributes.

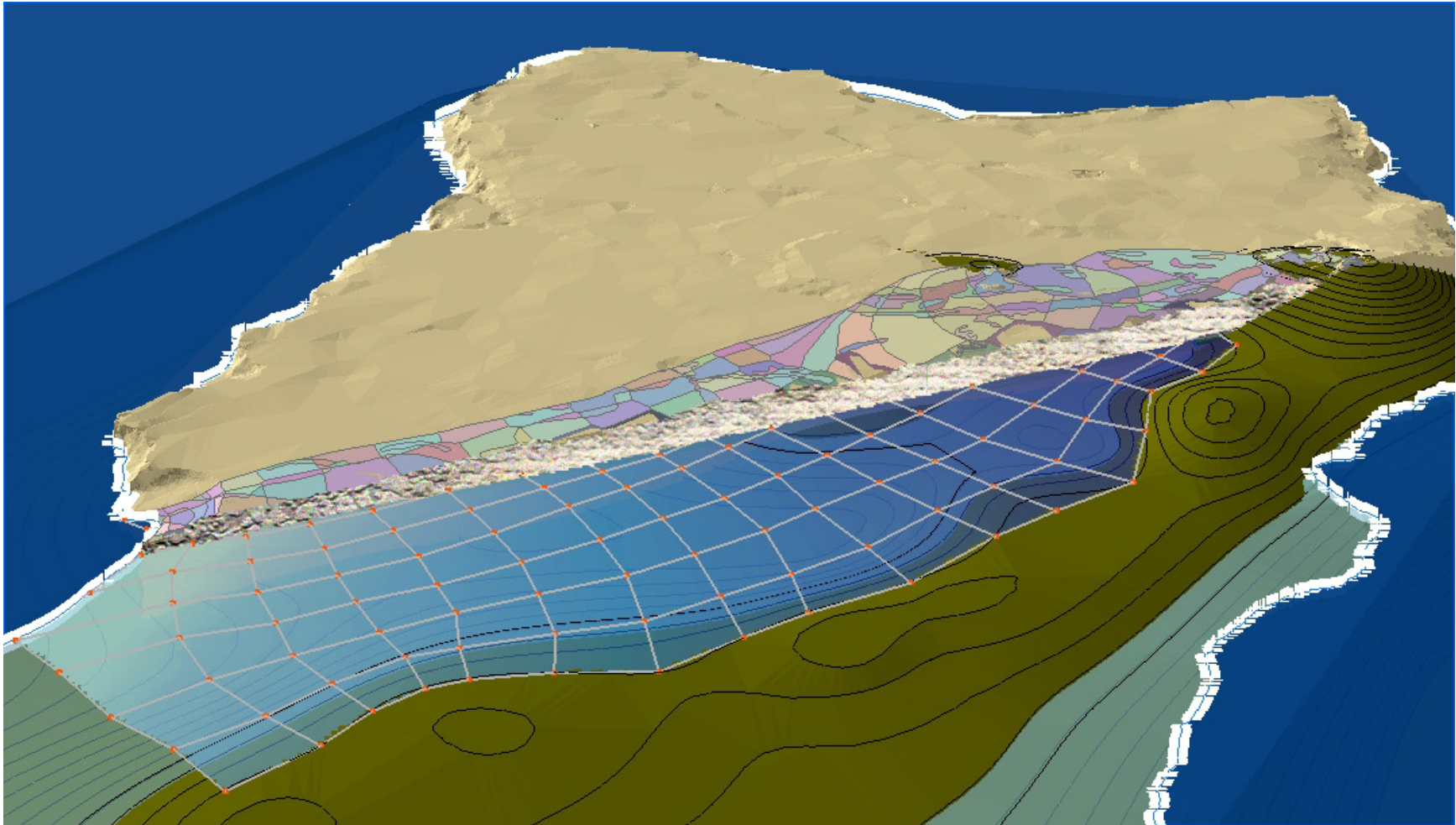


Figure 9. A Virtual 3D model of the domain. This domain has the surface hydrologic polygons, two limestone materials, finite element mesh at the water table, and the extension of hydrologic surface polygons to account for the allogenic recharge seen at Mt. Santa Rosa.

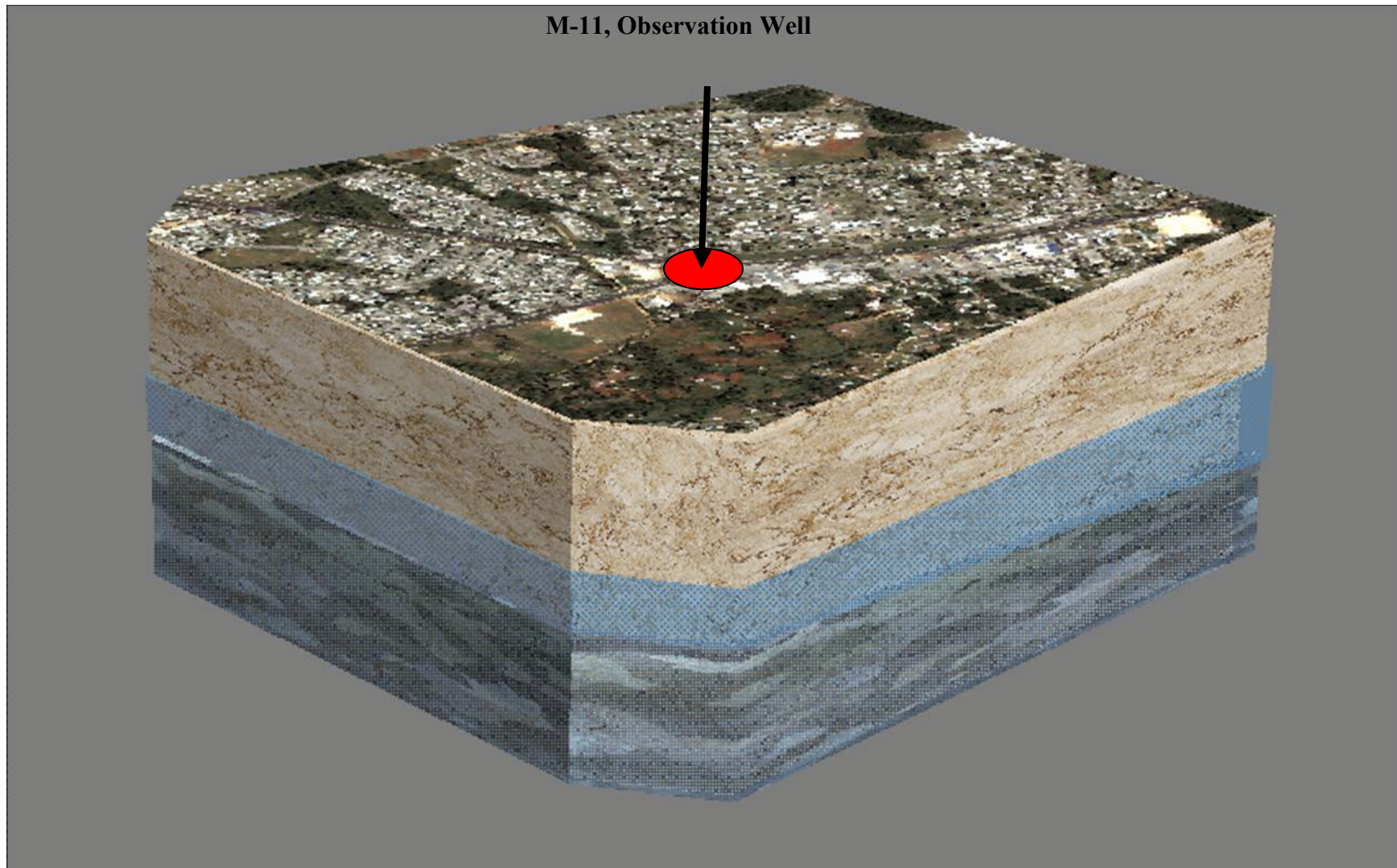


Figure 10. Node-shed vadose column of node 59 and Observation Well M-11. This piece was used to build the conceptual model.

Node-Shed and Zones Design

The spatial attributes requires the combination of layers unionized (combined) via GIS. The details to GIS tool *Union* are explained in Chapter 4. Since this project aimed to improve hydraulic modeling for the NGLA, the layers associated with this model were developed around the boundary of the finite element mesh of Jocson's project during the early phase. The addition of finite element code into AQUA CHARGE led to the reconstruction of the finite element mesh using GIS. As mentioned earlier, the new code moved the concentration recharge shed from the element to the nodes. Another addition was boundary flux shed design extending the area of influence beyond the lens toe. This takes into consideration the recharge that flows over the impermeable rock and flux as allogenic recharge to the lens toe shown in Figure 11.

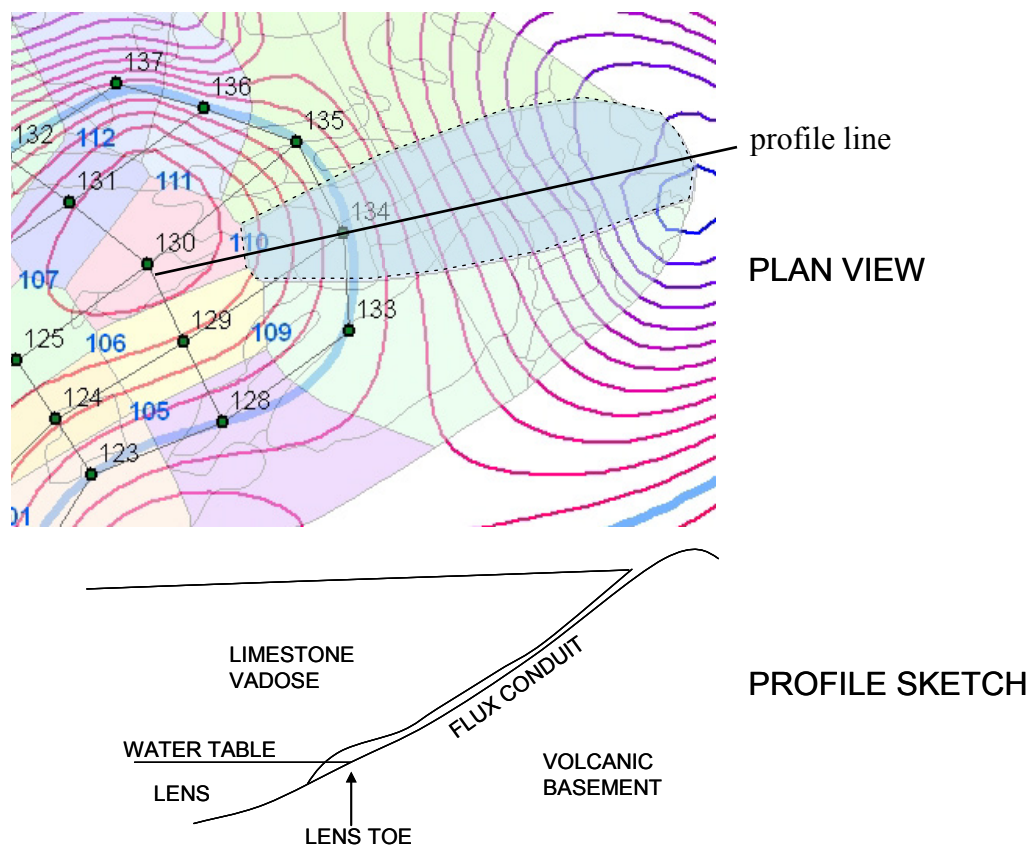


Figure 11. Allogenic recharge node-shed and boundary flux setup. The node-shed is edited from the lens' toe to reach the elevated volcanic ridge and perpendicular to the volcanic contours.

The layers unionized in the GIS are polygons for rainfall and pan evaporation Thiessen polygons, soils, and Euclidean allocated nodes. The Euclidean allocated nodes are referred to as *cells* in finite element terminology. The node-shed is made up of the AQUA CHARGE conceptual model of vertical columns that sits on top of these cells that feeds recharge to the nodes. The final unionization of the spatial data (Figure 12) and the details to the hydrologic construction of the spatial data are explained in Chapter 4.



Figure 12. Surface area node-sheds with sub-node-shed polygons called zones.

Inside a node shed may be composed of smaller polygons of sub-watersheds called zones (see Figure 13). These zones have a unique attribute assignment of Node-Shed ID (Number), Zone ID, Node-Shed Area, Zone Area, Rain Gage ID, Pan Evaporation Gage ID, and Soil Type ID.

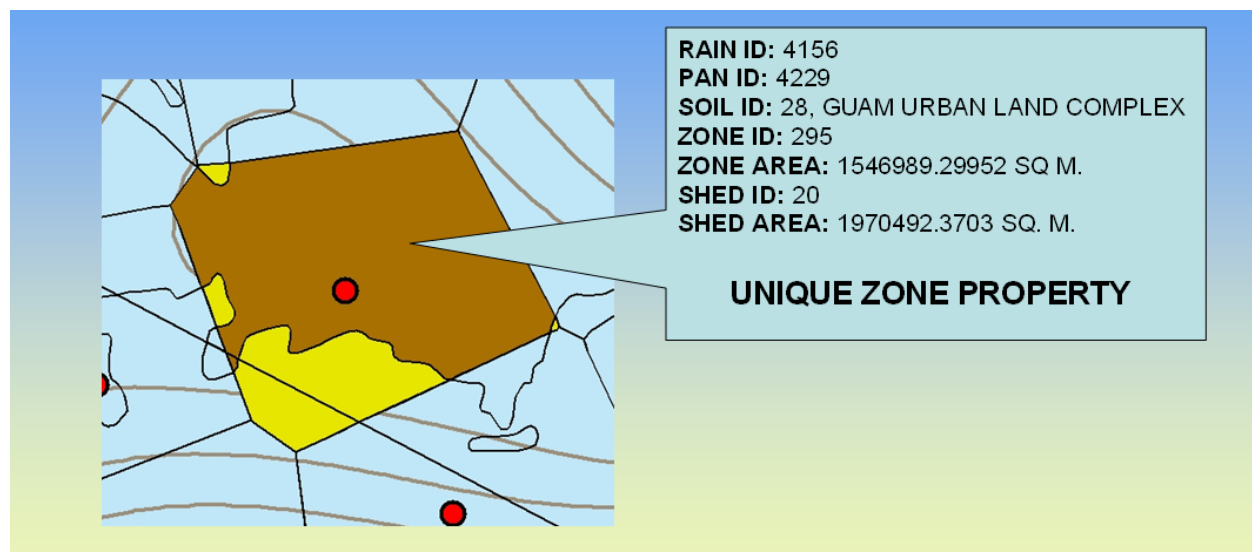


Figure 13. Node-shed zone's unique polygon attributes.

The unionized layer of node-sheds has a database file that can be extracted from the GIS file collection. This file is referred to as a polygon attribute table (PAT) file. The AQUA CHARGE program uses the PAT file to apply the water balance and routing equations with reference to all the attributes associated within the zone and node-sheds as it sweeps the study area on a daily basis.

Stages of the Conceptual Model

The AQUA CHARGE conceptual model has two stages. The first stage is water accounting in the soil layer and the second stage is the water transfer past the soil layer through the unsaturated bedrock. The conceptual model with details to the stages is shown in Figure 14.

Stage 1 is separated into two sub-stages, 1-a zone recharge and 1-b AWA recharge. The best data available for the surface is the soils map (Habana, 2008, APPENDIX D). The buildings and impervious areas are not specifically included. Instead they are assigned to the soil type urban complex. Each soil type in a zone has a certain thickness, which in this conceptual model can be described as the soil's FC. The node-shed assumes all the rainfall for a single day goes into SM and that no surface runoffs occur. The model also shows each zone producing different amounts of recharge for a day's infiltration as a result of differing soil properties. The soils properties will also handle the amount of moisture that will go into ET. Then, Stage 1-b, all the zone recharge for the day, in a node-shed is area weighted average recharge past the soil layer.

In Stage 2, the AWA amount of moisture was assumed to travel down vertically through 200 to 500 feet of limestone bedrock. As it travels down, it may take days to deliver portions of the recharge water that was estimated from the AWA recharge in Stage 1-b to the aquifer. As mentioned earlier, the limestone bedrock is complex, and spatially it can greatly vary in porosity and hydraulic conductivity. Currently, there is no really good and accurate data on the spatial variations of the hydraulic conductivities, porosities, and thickness of the vadose layer for every place in the domain where changes may be significant. These variations of vadose flow were accounted for by using a modified pulse routing technique that applies the concept of cascading reservoirs (USACE, 1987). This method disregards the thickness of the vadose zone in the calculation and uses a time in reservoir storage and numbers of reservoirs in a series to produce the attenuated and lag time recharge simulation.

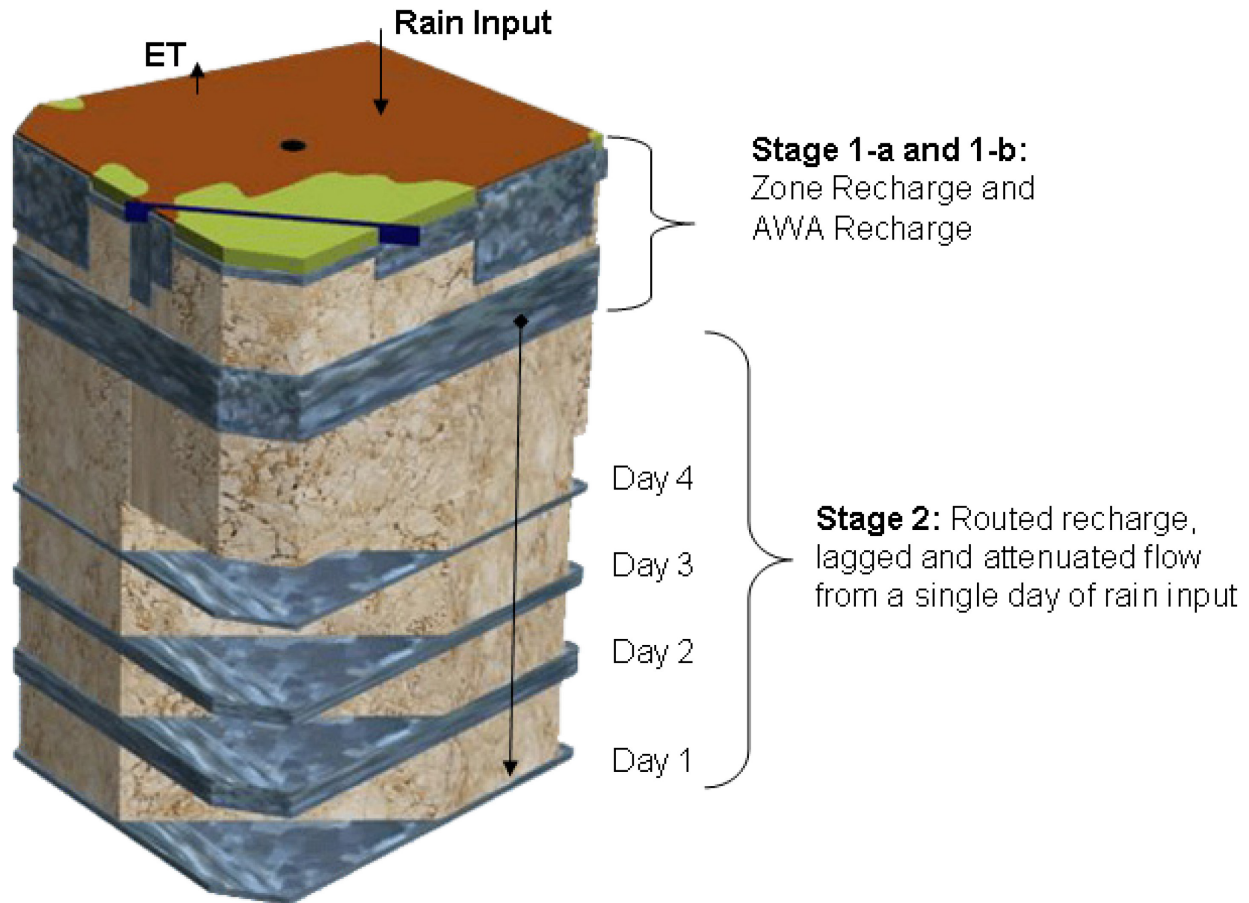


Figure 14. The two stages of the conceptual model. The first stage shows zone recharge for the sub-polygons in the node-shed and then the AWA of all the zone recharge. In stage two, the AWA for the node-shed is routed to produce the attenuation and lag time arrival of water to the water table.

Streamflow Synthesis Basis

The idea of applying streamflow synthesis method to estimate recharge was realized through the shape of the curves seen in the observation well data. Heitz and Contractor, who in their careers studied and observed many streams and reservoirs throughout the Northwest and other regions of the United States, recognized that the shapes of the observation wells were similar to charted streamflow measurements. Contractor, using UNSAT1D modeled the recharge having the shape of a skewed bell curve; rising quickly and decreasing with a tail (see Figure 15). Typhoon Omar, in 1982 (Figure 16) is a classic representation of the resemblance that show the well level response at M-11 to rainfall events were similar to streamflow levels response to rainfall. This led to the realization that the well levels underground are behaving just like stream levels on the surface which meant the practicability of applying streamflow synthesis to the NGLA (Contractor, 1999; Heitz, personal communication). Figure 17 shows an actual streamflow hydrograph produced with streamflow synthesis methods that qualified to represent how recharge might arrive to the lens in the same flow quantity distribution through time from a pulse of rainfall.

Contractor & Jenson
WERI Technical Report #90
November 1, 1999

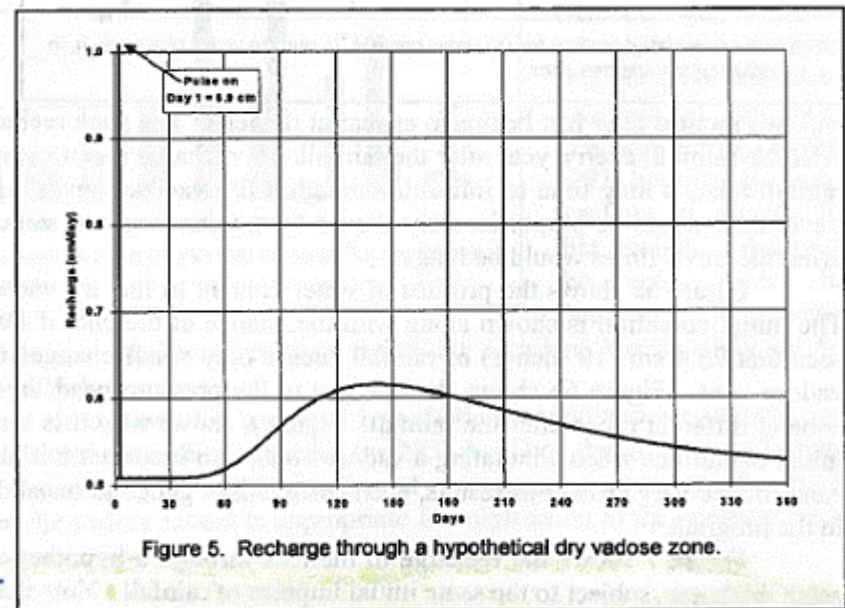
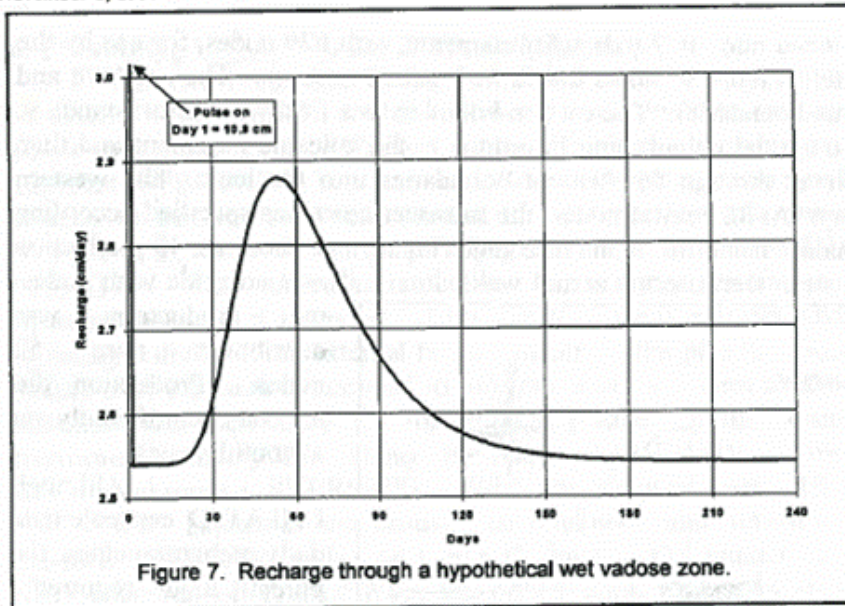


Figure 15. Contractor's UNSAT1D vadose model recharge.

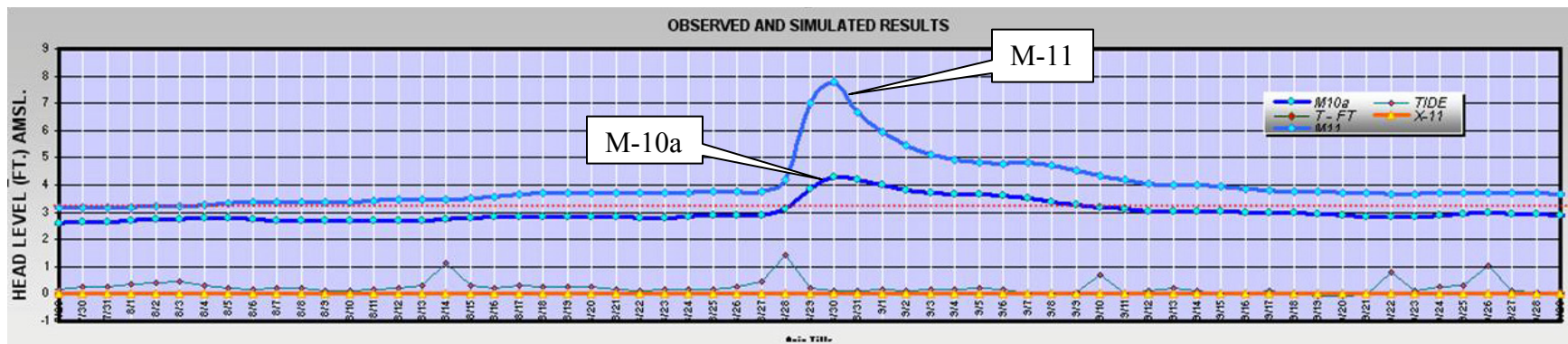


Figure 16. Observation wells data resembles surface hydrology behavior. Above, observation wells M-10a (dark blue) and M-11 (light blue) responding to approximately 12 to 18 inches of rainfall during Typhoon Omar (Lander, personal communication).

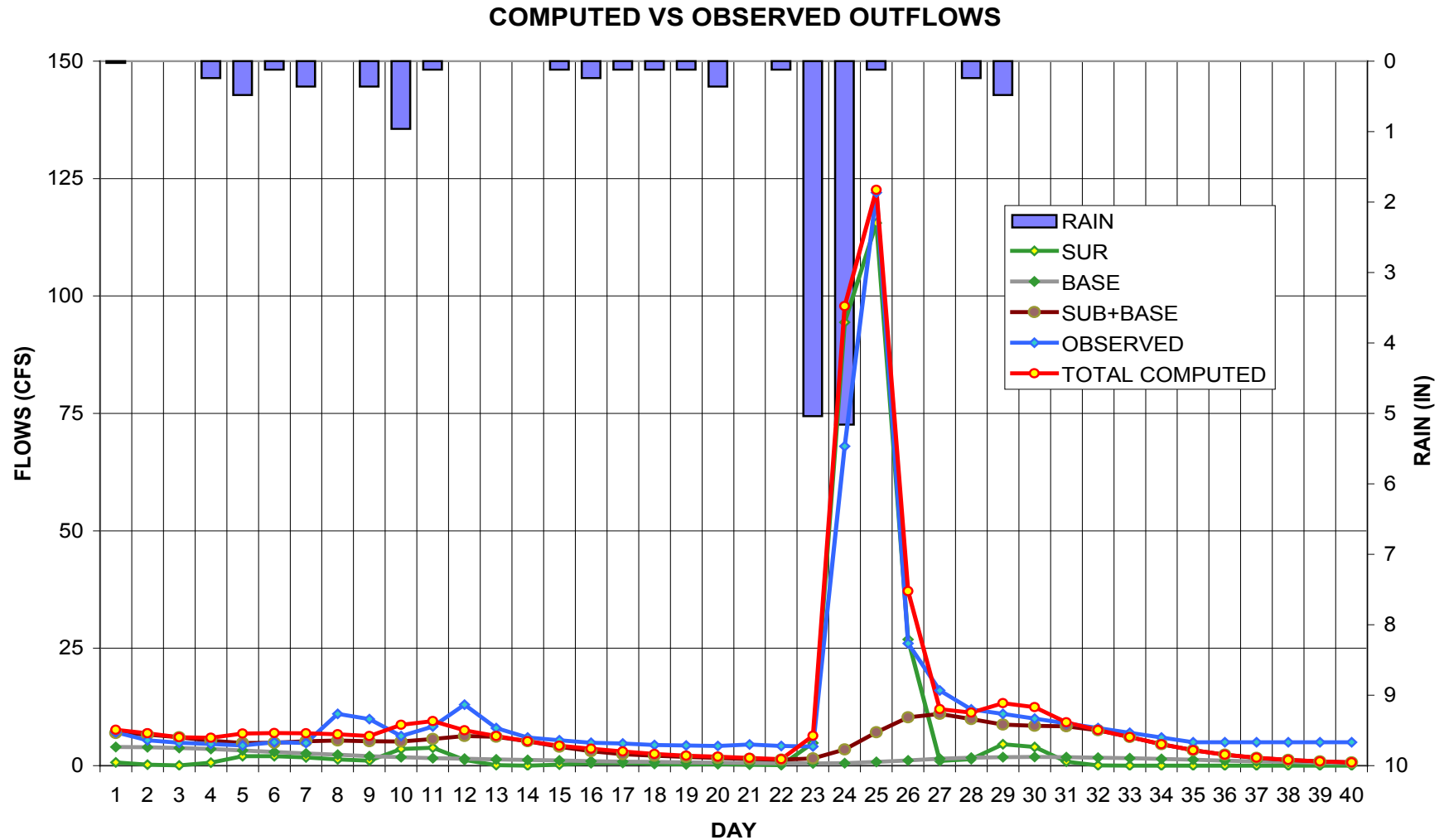


Figure 17. Hydrograph of streamflow synthesis. The attenuated and lag time arrival of streamflow could possibly be similar to the delivery of recharge to the lens. This hydrograph has three flow routes; surface, subsurface, and baseflow.

A graphical illustration reveals the applicability of streamflow synthesis to the NGLA. Figure 18 shows Dworshak Reservoir, Idaho with a number of streams feeding into it. Figure 19 is an example of four watersheds with tributaries connecting into a reservoir. Each watershed may be modeled using SSARR to predict the flow into the reservoir. Figure 20 is the schematic profile of the NGLA showing vertical columns of node-sheds with vertical flow channels as matrix, faults, and conduits. Water moving down through the vadose zone of the NGLA was treated like vertical streams and sub-surface flow feeding the lens in the same fashion as streams in a river system runoff into a reservoir.

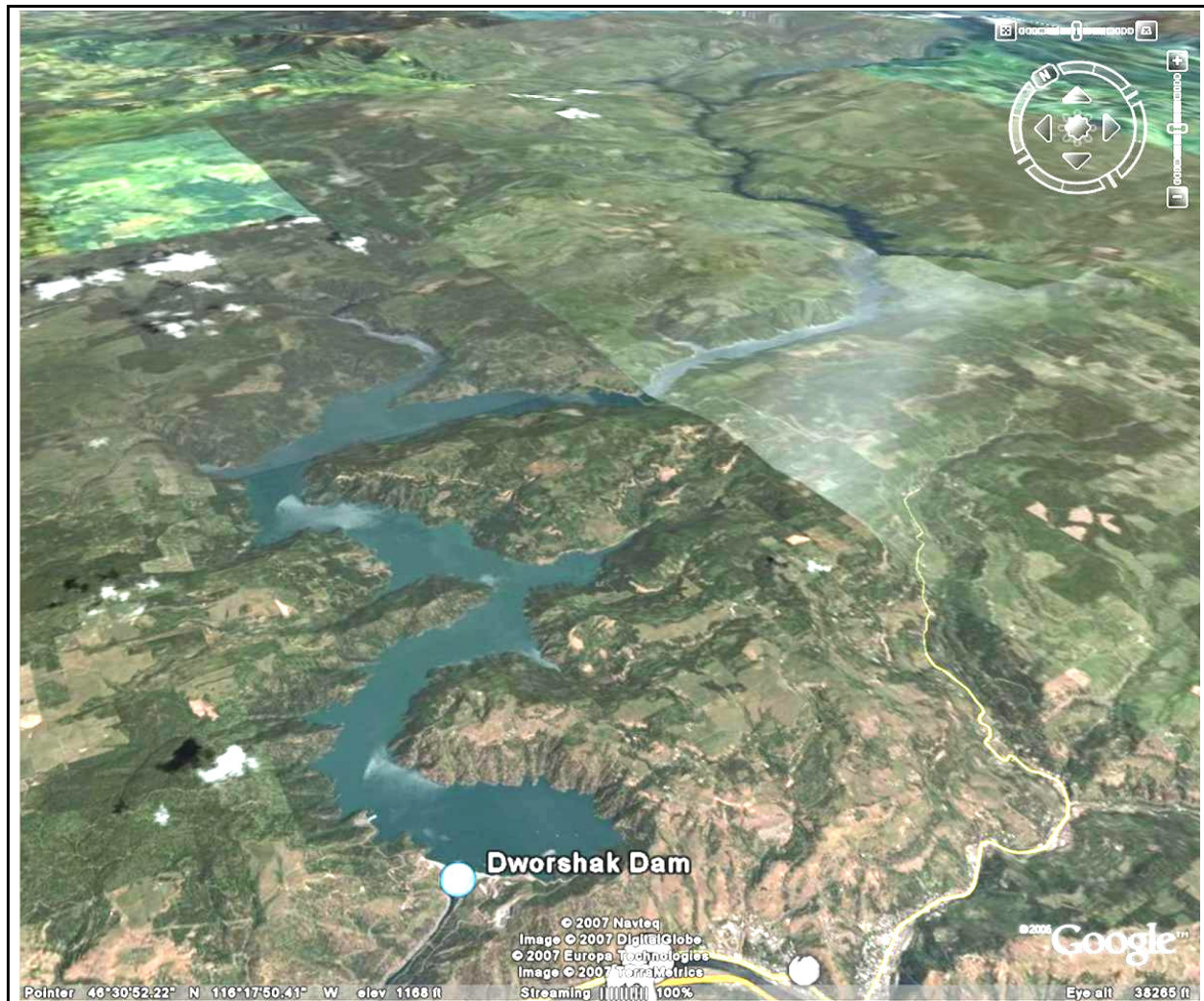


Figure 18. SSARR was used to model the streamflows in Dworshak, Idaho (Heitz, personal communication). These stream tributaries were modeled using SSARR to predict the water flow into the reservoir.

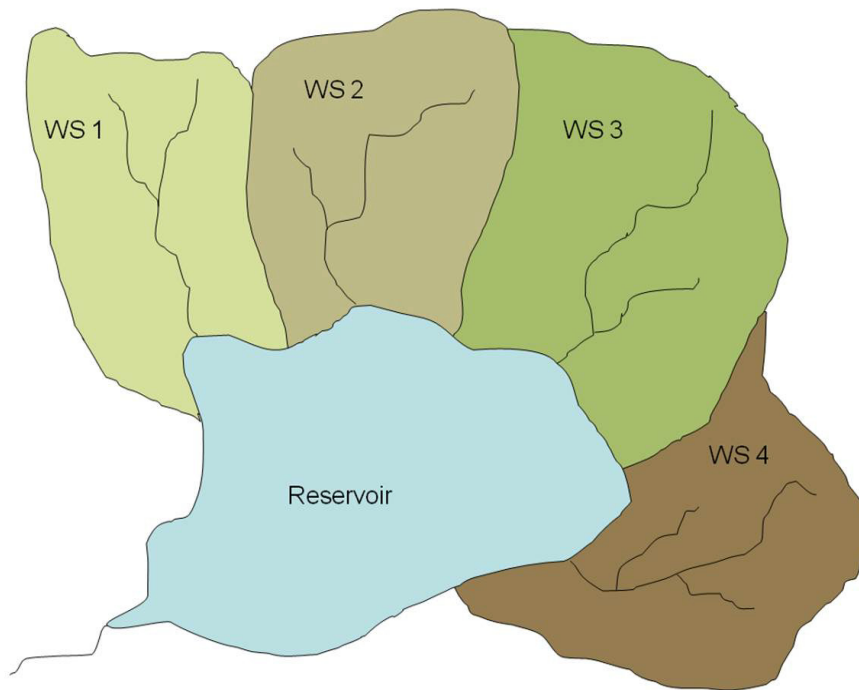


Figure 19. Conceptual model of watersheds feeding into a lake. Four delineated watersheds with tributaries feeding into a reservoir.

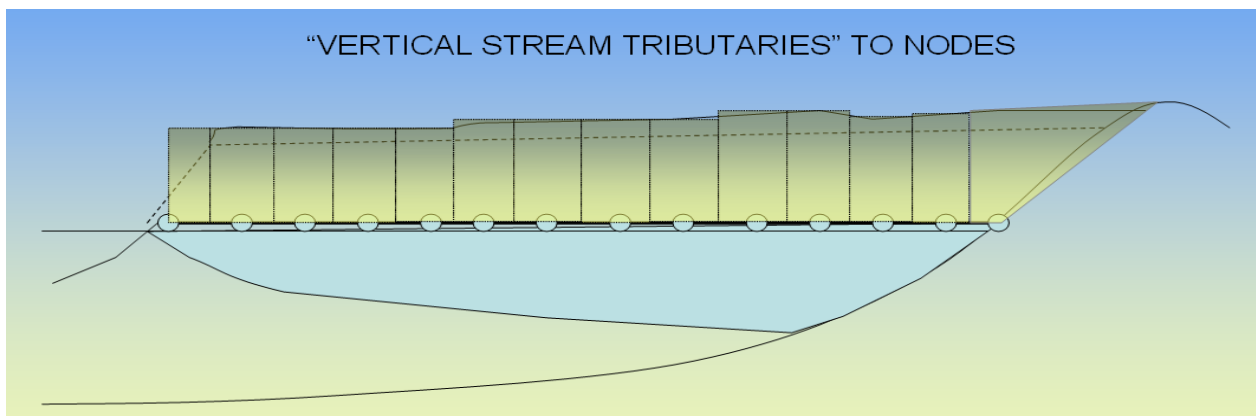


Figure 20. Conceptual model of node-shed tributary columns feeding the lens. The columns extend down to the lens surface and sits on top of node cells treated as having vertical flow channels that contribute to fast flow (conduits and faults) like surface runoff and slow flow (matrix) similar to sub-surface runoff.

An existing streamflow synthesis program called SSARR is the basis for developing AQUA CHARGE. SSARR was developed by the US Army Corps of Engineers and the program has been applied to predict streamflow throughout the Columbia River system and other rivers and reservoir systems in the Northwestern parts of the United States as well as in Vietnam and other places in the world (Heitz, personal communication). In this project, the basis of SSARR's computer program is extracted and used to account for soil and bedrock media flow.

SSARR to AQUA CHARGE Flow Diagram

The programming logical flow diagram model that shows how SSARR operates is shown in Figure 21. This model is called the Depletion-Curve Watershed Model and was designed to account for snow precipitation as well as rainfall. The portion of the model that is applied to this project is boxed in red since precipitation data for Guam is currently rainfall.

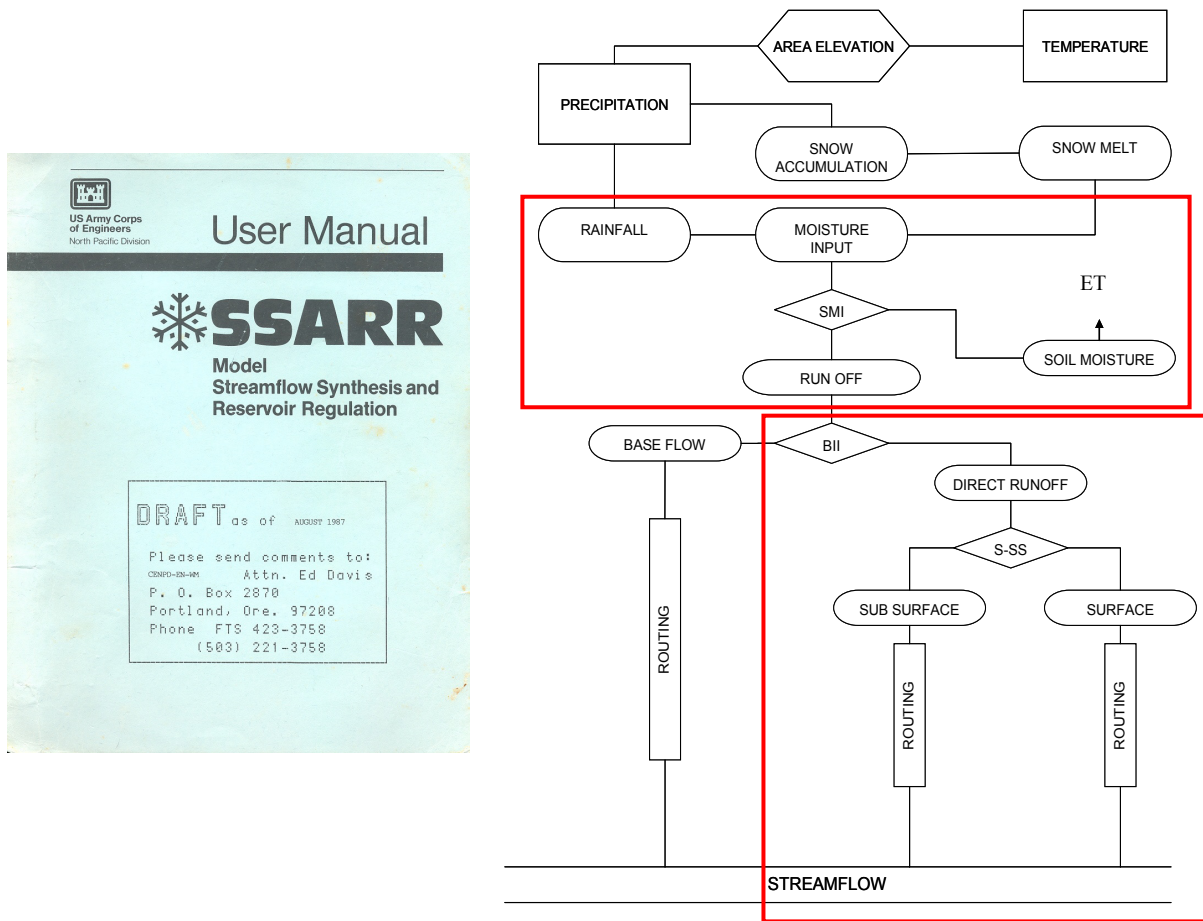


Figure 21. The SSARR User Manual and Depletion-Curve Watershed Model.

A split junction called the Soil Moisture Index (SMI) shows some of the moisture input moving into runoff and some remaining as SM. The SM is then further reduced through ET. The runoff is split between baseflow and direct runoff. The baseflow is routed to reach the streamflow and the direct runoff is split to surface and sub-surface (S-SS) flow. Then, the S-SS components are routed to account for the effect of channel storage and time of travel as the water travels to the main streamflow.

The AQUA CHARGE prelude built in 1998-99 began with a portion of the flow diagram from SSARR converted to calculate recharge instead of surface runoff. This portion of the flow diagram calculates the daily net recharge quantity that passes the soil layer. Figure 22 shows

rainfall input absorbed into a zone with a specific soil type as SM input. This model assumes that all of the rainfall goes into SM disregarding surface runoff. The SM is further reduced with an ET effect to account for the return of moisture back to the atmosphere.

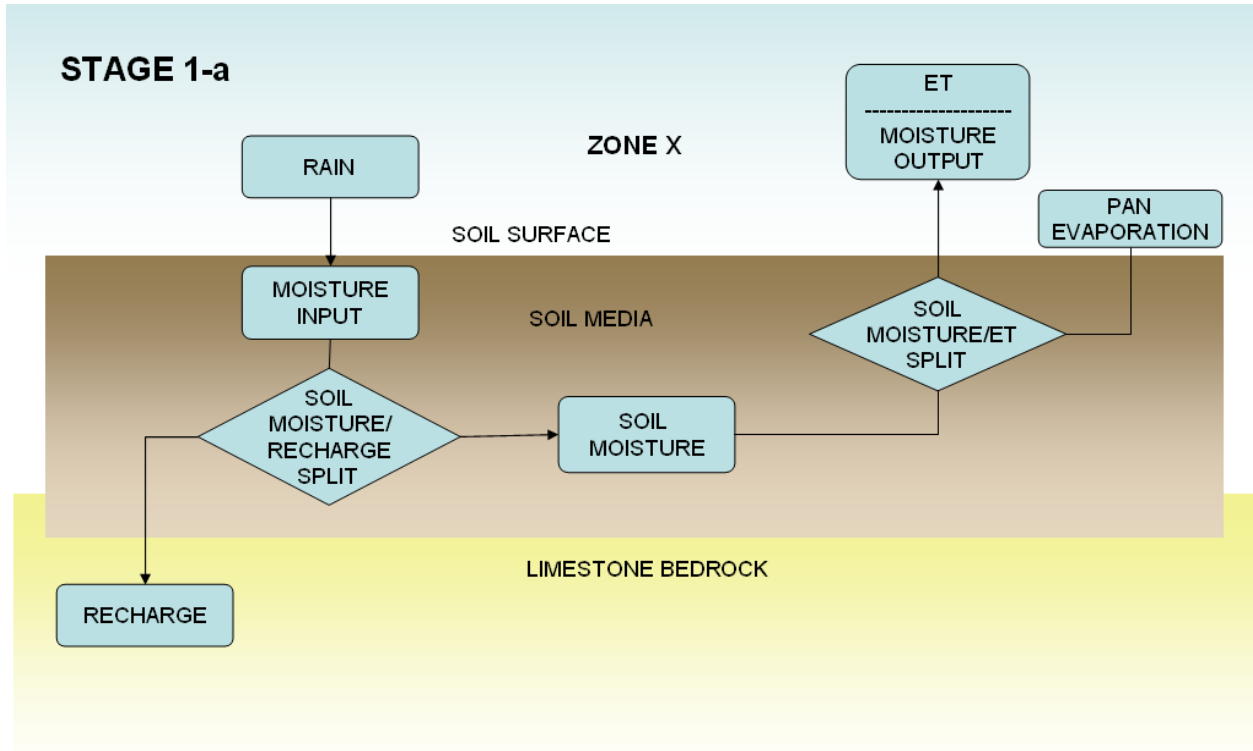


Figure 22. Stage 1-a, the SM model for zone recharge.

In figure 22, the SM model is converted into a moisture balance equation and considers time in the accounting of the moisture change. The equation applied is the mass continuity equation which is simply an input minus output equals change in storage balance equation. The SM model, equation E1, considering “*t*” as a given day of evaluation, i.e. today, is

$$SM_t = SM_{t-1} + P_t(1 - R\%_{(t-1)}) - PAN_t(ET\%_{(t)}) \quad (E1)$$

where

SM_t is soil moisture for today,

SM_{t-1} is soil moisture from previous day,

P_t is measured rain precipitation for today,

$R\%_{(t-1)}$ is the percent factor of precipitation that is accounted for recharge dependent on previous day's soil moisture,

PAN_t is the measured pan evaporation value for today,

$ET\%_{(t)}$ is the percent factor of PAN reduced from the soil moisture dependent the remaining soil moisture.

The $R\%$ and $ET\%$ are percent splitters that are obtained from SM split curves and a linear interpolation sub-routine. The $R\%$ splits the percent of precipitation as moisture input that goes into recharge and the $ET\%$ is the percent of pan evaporation value that is reduced from the left over SM. Both percent splitters are dependent on a SM calculation. The split curve component is discussed next.

Soil Moisture Split Curves

The soil media properties affect the way soil moisture (SM) quantity is proportioned between recharge and ET as well as remaining as SM. A relationship curve for splitting recharge/ET vs. SM is shown in Figure 23. SSARR, again, also uses this curve method for splitting SM between runoff and ET for a streamflow model. In this case, the x-axis is set from the plant available water (PAW) determined from the available water content (AWC) and soil depth that is obtained from the *Soil Survey of Territory of Guam, 1988*, in a physical properties table. The value in inches, 0 inches set as wilting point (WP) and the PAW value as the FC. The hydrologic process percent yield is for either recharge or ET, depending on SM or % of soil field capacity (FC), where a curve is set specifically for each. With the FC determined for each soil type, hydrologic process percent yield is dependent on the percent of or inches of FC for which the curve is shaped. A linear interpolation function sub-routine code handles this determination (Habana, 2008, APPENDIX C).

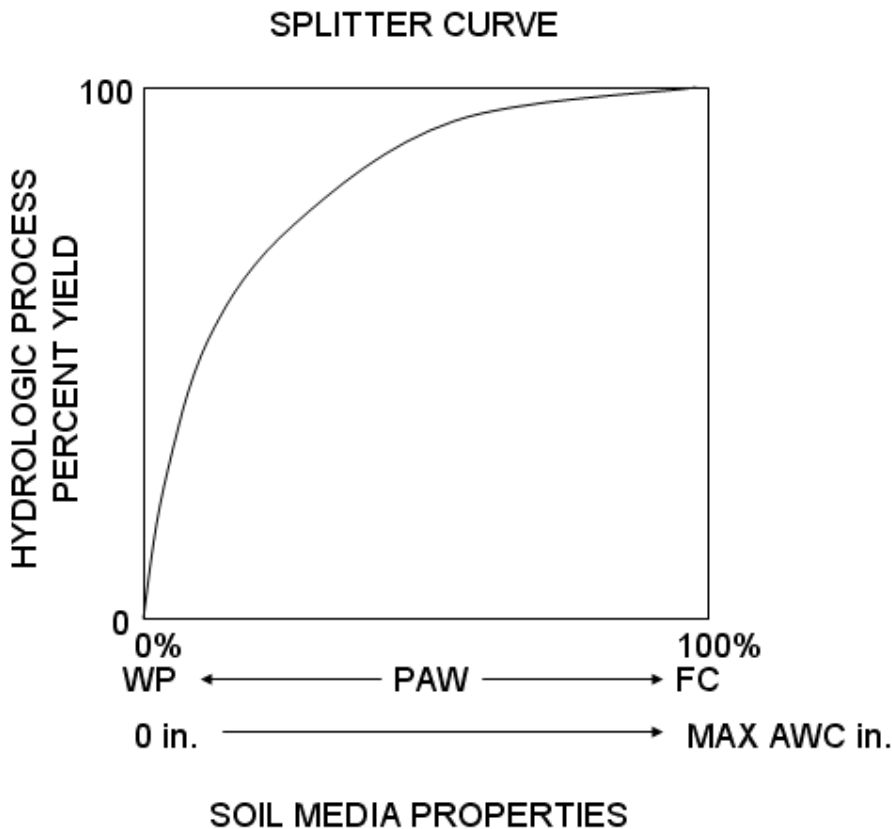


Figure 23. The soil moisture splitter curve concept.

The FC is determined from a simple summation formula and average values of soil depth and AWC listed in the physical properties table in the soil survey. The summation equation E2 used to determine FC for each soil type in the domain is

$$FC \approx \sum_{i=1}^n D_i \times AWC_i, \quad (E2)$$

where

D_i is the depth of i-th soil

AWC_i is the available water content of the i-th soil.

The soil's depth for every layer is an average of its difference range and the AWC is the average of just the range. See Habana, 2008, APPENDIX D, for the soil's physical properties data and the calculated FC for each soil in the domain. An example of soils with more than one layer is shown in Figure 24.

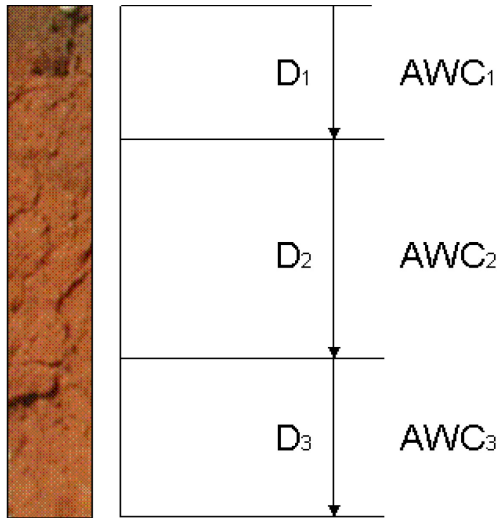


Figure 24. Soils with multiple layers used to compute FC.

The SM split curves determines the percent portion that moves into recharge from the SM and the portion that goes back to the atmosphere as ET. The curves apply when the available SM are less than or equal to the FC.

This is an example of a day's event of soil moisture, recharge, and ET process in the Stage 1-a of the SM model. Figure 25 shows the soil chart's role for the curve set relationship of the recharge/SM split when moisture input is less than or equal to FC. Let a soil zone have a FC equal to 1 inch. And previous day's SM (SM_{t-1}) equals 0.2 in, and rainfall measured 0.5 in, the sum of rainfall and SM_{t-1} is the starting SM (SSM) which is 0.7 in. The percent amount of rainfall that will go into recharge is solved by equation E3, which is a portion of the soil moisture equation E1.

$$R_t = P_t(R\%_{(t-1)}) \quad (E3)$$

Interpolating R% from the chart is dependent on SM_{t-1} , which is 20% of FC, resulting in 55% (0.55 as a decimal percent). The amount that goes into recharge is rain times R% (0.5 in x 0.55), which is 0.275 in. Reduce the SSM with the recharge (0.7 in – 0.275 in), which is 0.425 in and we will now refer to the value as the recharge reduced soil moisture (RRSM). The remaining RRSM will be the soil moisture dependent value for the interpolation of ET%. For the soil's FC at 1in, 0.425 in is 42.5% of the FC. The RRSM can now be further reduced by the ET reduction portion of the SM equation. Looking at the ET Effectiveness chart displayed in Figure 26, 42.5% of FC yields ET% of 93%. If the pan evaporation value was 0.2 in, and using equation E4 to solve for ET (0.93 x 0.2 in), which means 0.186 in of the RRSM will go into evapotranspiration.

$$ET_t = PAN_t(ET\%_{(t)}) \quad (E4)$$

The final soil moisture for the day is now solved by equation E5 (0.425 in – 0.186), which is 0.239 in. That SM will be used in the next day's computation as SM_{t-1} .

$$SM_t = RRSM - ET_t \quad (E5)$$

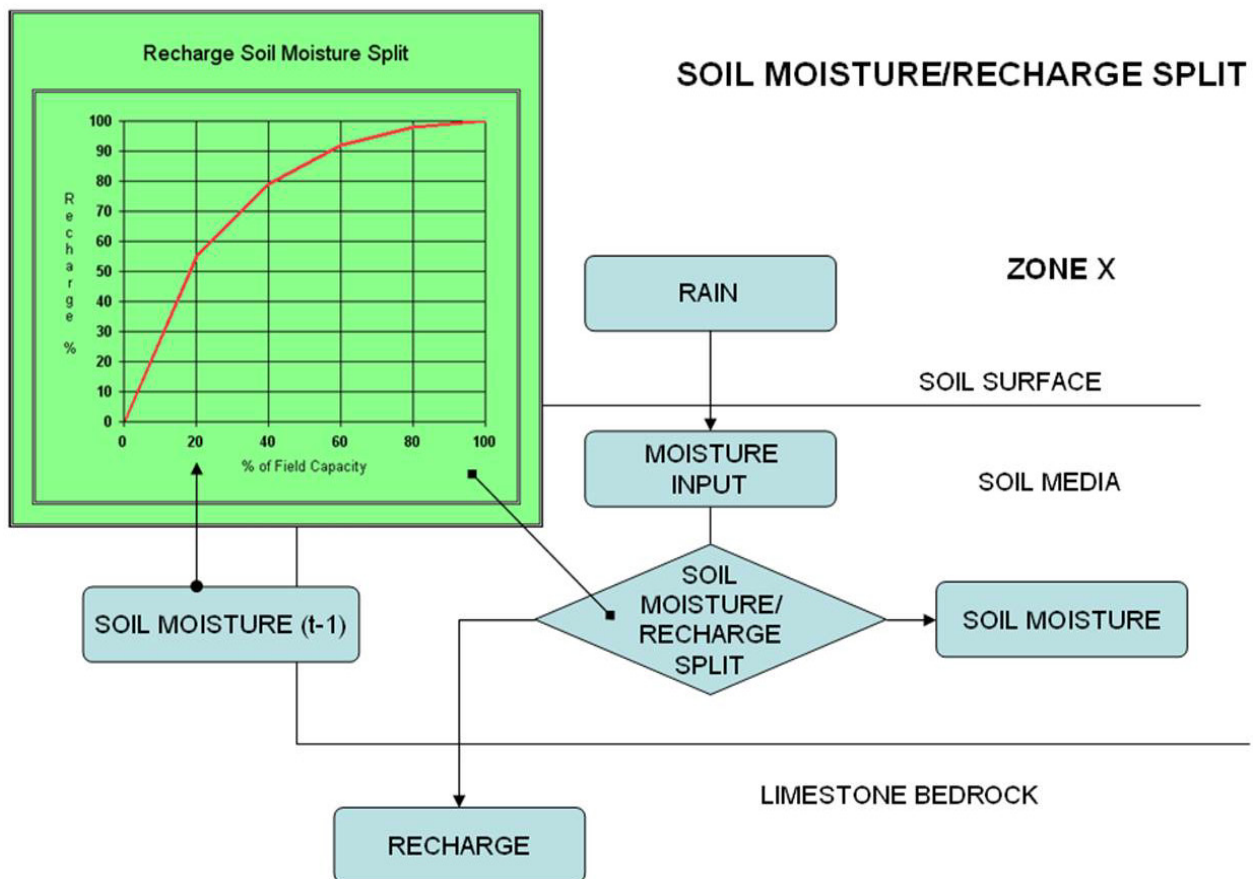


Figure 25. Soil moisture vs. recharge split flow diagram. The SM remaining in the split is further reduced with ET effect process.

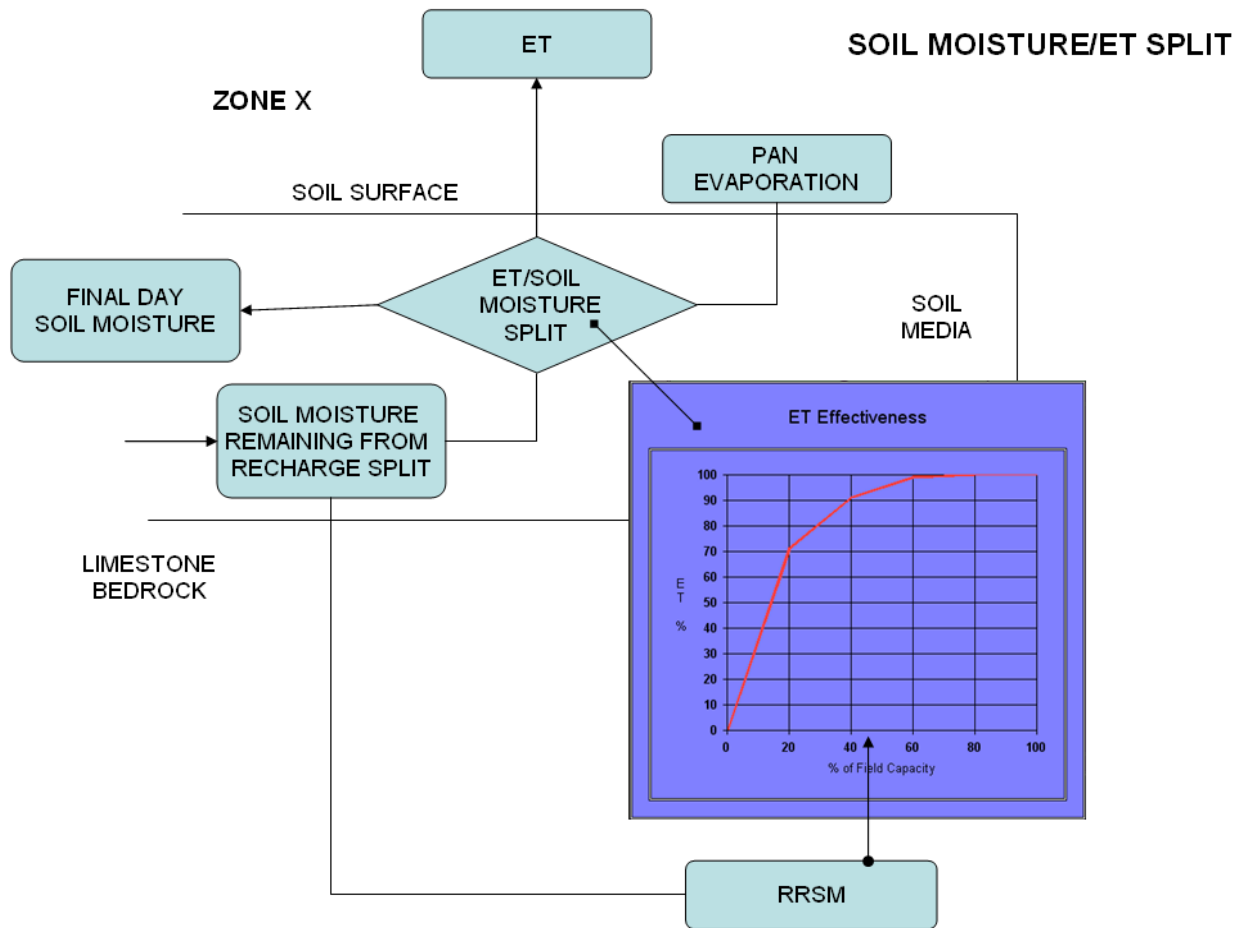


Figure 26. Soil moisture vs. ET split flow diagram. The remaining SM is the SM calculated for the day.

The SM equation and the flow diagrams must consider special conditions with respect to the soils FC characteristics. The soil's FC is the maximum amount of moisture the soil can hold, if ever it is supersaturated, the excess is assumed to go into recharge and none to surface runoff in this model. The SM equation can be separated associatively, so to separate the recharge conditions on the SM from the ET condition, and so, the order of calculation may follow the programming flow diagrams as well. So, for the day, the soil gets moisture which is the previous day's moisture or initial set SM and the rain for the day as starting soil moisture (SSM). If the SSM is greater than the soils FC, then recharge is SSM minus FC and the recharge reduced soil moisture (RRSM) is set equal to the FC. This is to say that the soil exceeded FC, and the excess has gone to recharge leaving the soil saturated. If the SSM is less than the FC, then the linear interpolator for the SM curve for recharge uses the SM from the previous day to determine the percent of the rainfall that will go into recharge. In either case, the RRSM will not exceed FC considering the "If" conditions. Now, for the ET portion, with the RRSM less than or equal to FC, the ET needs to be determined. The RRSM is used as the SM dependent value for the SM ET effectiveness chart interpolation for ET percent. Then the ET percent times the pan evaporation for the day is the ET. So the conditions follow that if the RRSM is less than ET,

then ET is set equal to the RRSM since all that can be evapotranspired is the available SM. The final SM equals RRSM minus ET. In the end, the final SM will be positive and will be used in the next day as the previous day's SM. For each zone and day this numerical code solves the Stage 1-a of the conceptual model. The APPENDIX, shows the generalized Visual Basic (VB) code to model the Stage 1-a, zone recharge, of the soil moisture model.

As an objective of this research, a relationship curve model is applied to produce the splitting effect of recharge and ET from SM. For ET, the relationship between SM and potential ET is taken from studies of three models. ET vs. SM models (Figure 27) show three different curve shape relationships of Thornthwaite, Pierce, and Viemeyer models (Ward and Trimble, 2004). The PAW is the soil's moisture FC minus the wilting point.

ET is taken from studies of three models. ET vs. SM models (Figure 27) show three different curve shape relationships of Thornthwaite, Pierce, and Viemeyer models (Ward and Trimble, 2004). The PAW is the soil's moisture FC minus the wilting point.

Although there is no particular study model of SM relationship for recharge, a similar method as in ET is used for splitting recharge and SM. This is where adjustments are made finding the right relationship curve that works to produce recharge. A few scenarios are examined, using a direct linear relationship and then to a somewhat curved relationship. In either case, linear or curved, each one is examined with the three ET models until a close simulation is produced. This is the first variability control portion for calibration. Figure 28 shows the three soil model curve relationship that satisfies our objective for exploring the effects of soil properties on ET and eventual GW recharge. The details to the results are on Chapter 7.

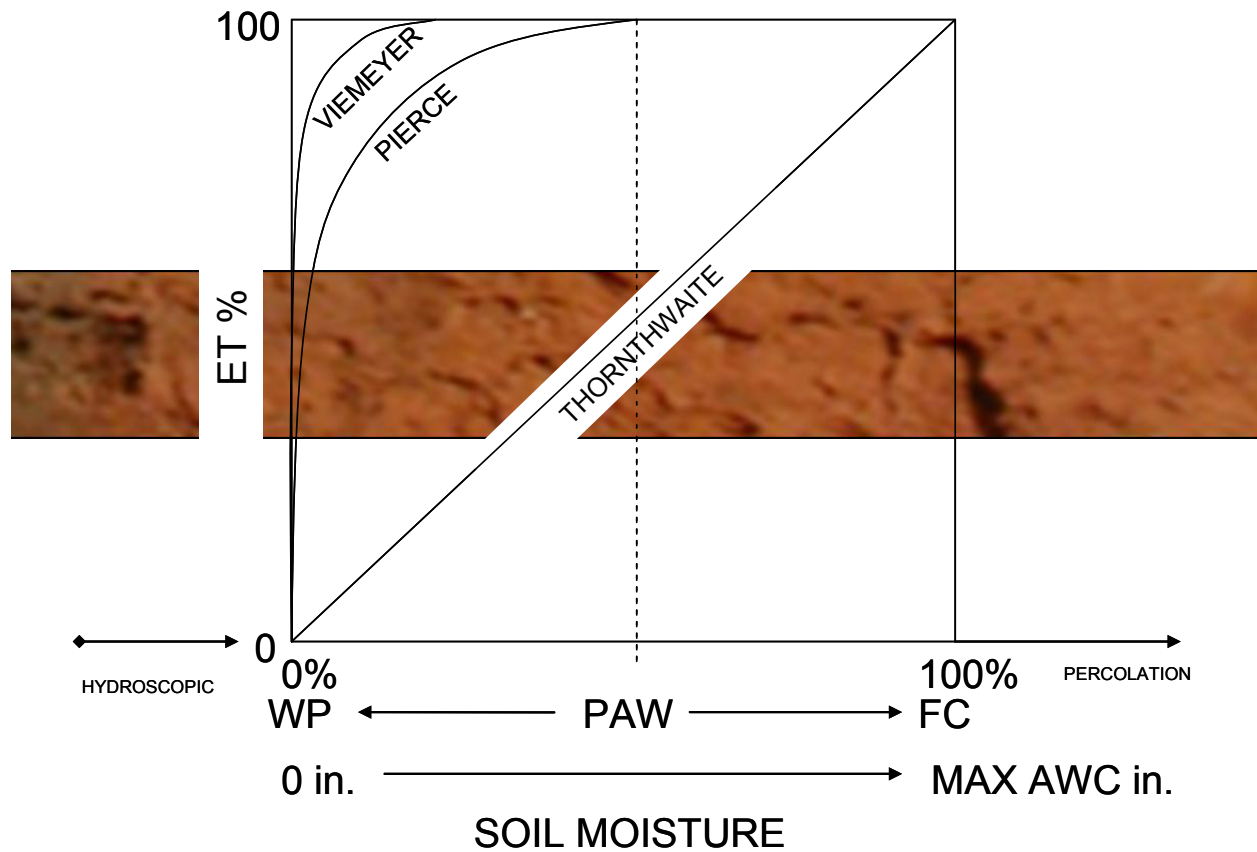


Figure 27. ET SM models to examine ET effectiveness (Ward, et al, 2004).

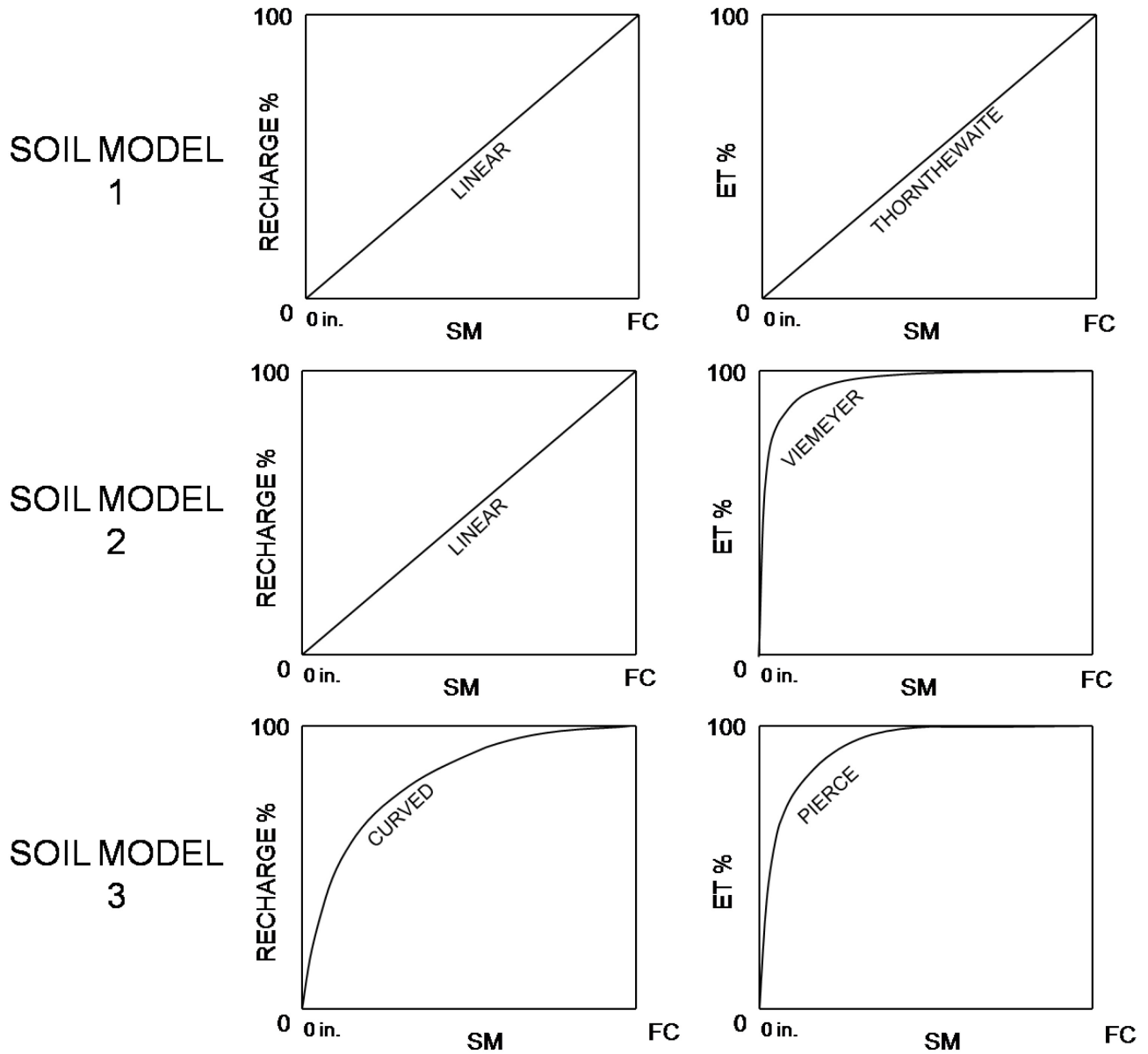


Figure 28. Three soil model conditions, project objective investigation.

The soil media in the study area plays an important role in determining recharge and ET as it was the crux of this research project in the starting phase. The need to compare the results with observation well records and improved knowledge of hydrology had widened the focus and expanded the capabilities of AQUA CHARGE. Next, we will discuss how the lag and attenuated arrival of recharge is computed in Stage 2 of the conceptual model.

Area Weighted Average Recharge

The area weighted average (AWA) recharge is calculated in Stage 1-b of the node-shed recharge conceptual model. The area of each zone in the node-shed and the area of the node-shed were determined through the GIS calculator in the attributes table. The recharge results for each zone were used to calculate the AWA recharge (see Figure 29).

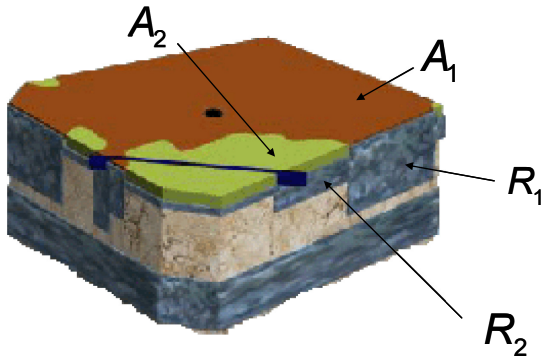


Figure 29. Node-shed zone areas and recharge to zones for computing AWA recharge.

The formula for determining AWA recharge is given in the summation equation E5:

$$R_{NODE-SHED} = \sum_{j=1}^n \frac{A_j \times zR_j}{A_{NODE-SHED}}, \tag{E5}$$

where

$R_{NODE-SHED}$ is recharge to the node-shed,
 A_j is the area of node-shed zone j,
 zR_j is zone recharge j, of the node-shed,
 and $A_{NODE-SHED}$ is the area of the node-shed.

Modified Pulse Routing Technique

The final vadose flow synthesis or recharge simulation process (Stage 2) specifically chosen for this project is a type of transfer function called *modified pulse routing* technique used in the SSARR model. In routing, the daily AWA recharge value past the soil layer goes through a hydrologic routing code to synthesize the probable attenuation and lag arrival of recharge. The code process is similar to the routing code used in SSARR, just modified to handle an array of node-shed AWA recharges that are fast and slow separated. The routing code receives two flow rates determined by a fast/slow splitter curve. This user adjustable curve lets the modeler set the percent of the daily AWA recharge that will move into the fast flow routing. The remaining portion of the recharge will move into the slow routing process. Each routing handler, for fast or slow, uses two input attenuation settings that give the lag time effect. “T_s” is a modeler

assignable constant that signifies the *time in storage*. The *number of phases* (nps) is also assignable and is the number of imaginable weirs in a series referred in SSARR as cascading reservoirs. Imagining again that the entire node shed and the bedrock beneath as a vertical stream explains the feasibility of streamflow routing in this model. The VB codes for the routing process are in the APPENDIX.

First, the AWA recharge for a node-shed must be split into fast and slow amounts. A percent fast split curve was used to handle this and it is designed similar to the SM splitters for recharge and ET (See Figure 30). The fast flow percent splitter determines the percent of the AWA recharge for the day that goes into fast routing and the remainder goes into the slow routing. The curve uses a bedrock capacity value in inches and the percent of that value is the previous day's recharge plus the AWA recharge minus the sum of the fast and slow routed recharge. The routers both fast and slow flow uses the preset T_s and number of phases into the routing calculation and the output of the two are added to get the final synthesized recharge.

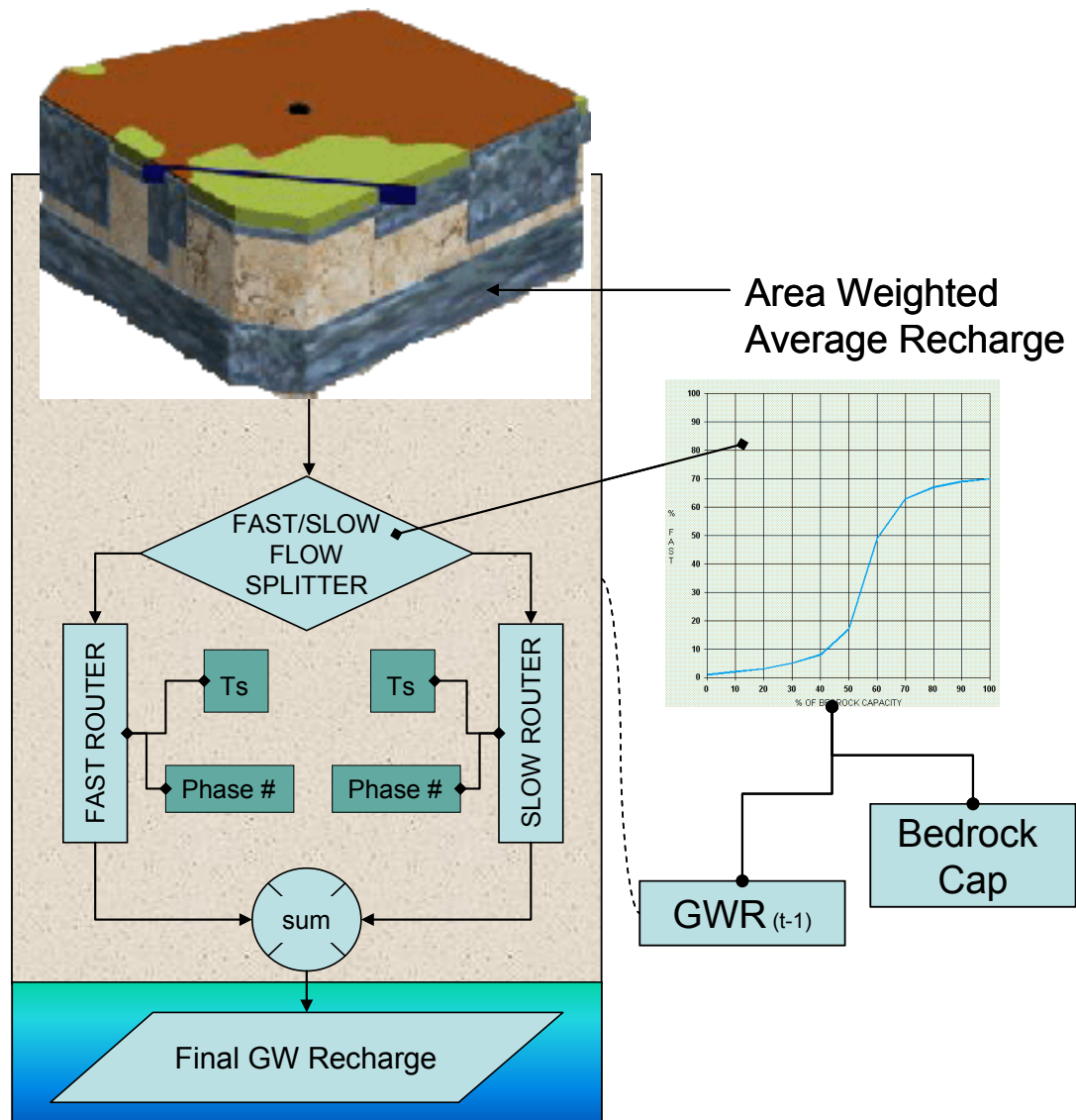


Figure 30. Stage 2, router flow diagram.

The routing equation is an algebraically manipulated function of the change in storage equation. The mean input minus the mean output equals the change in storage. The output for reservoir 2 can be expressed as (next page)

$$O_2 = O_1 + (\bar{I} - O_1)t \times \left[\frac{t}{T_s + \frac{t}{2}} \right] \quad (E6)$$

where

- O_1 is Output at reservoir 1,
- O_2 is Output at reservoir 2,
- \bar{I} is the mean input, $(\frac{I_2 - I_1}{2})$,
- t is the time increment (24 hrs.),
- T_s is the time in storage.

This equation can be seen working in a cascading reservoir setup shown in Figure 31. Whether fast or slow, each goes through the same router algorithm to get the synthesized recharge to lens flow quantity arrival in daily time steps. The input for the first reservoir is an AWA recharge, either fast or slow. The output of reservoir 1 is shown in the figure as O_1^t which will be used in the equation I_2^t as input to the second reservoir. The output of reservoir 2 is equation E6 above. The router was coded to handle multiple number of cascading weir phases depending on the modeler's need to increase or decrease the lag time for each fast or slow flows. An increase in T_s results in a wider bell curve shape output referred to as the attenuation. The router can distribute a day's worth of fast flow or slow flow over several days, having an appearance of a Gaussian distribution curve, as it arrives down to the water table.

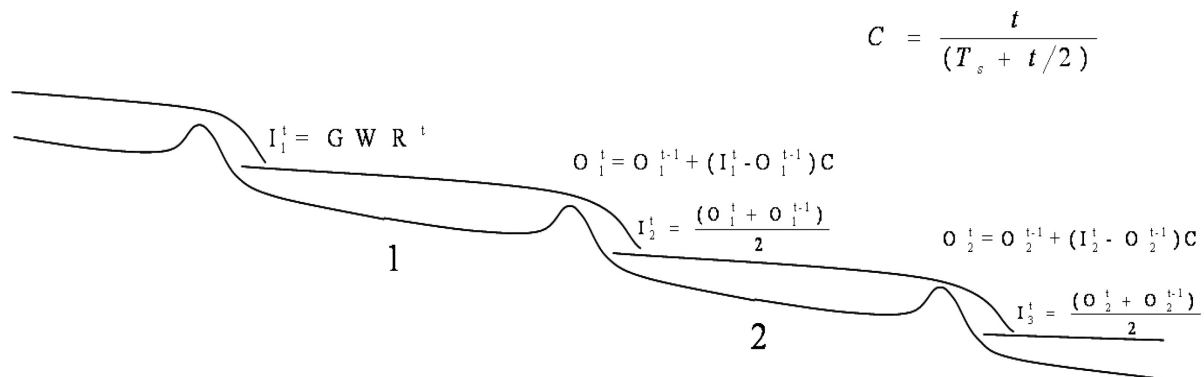


Figure 31. Cascading reservoirs, routing model, producing flow lag time and attenuation. The "Is" and "Os" are inputs and outputs with respect to the reservoir numbers it accounts for. The superscript t is a day's time period while T_s is the time in storage. Increasing the number of reservoirs increases time delay while increasing T_s spreads out the discrete amounts of recharge pulse input. The t in the variable C is set to 24 hrs.

A chart is generated for visual evaluation of the probable shape of the synthesized recharge. A special chart called AQUA CHART was designed in Excel to allow the modeler to scan through the entire data and analyze the output using the Well Guide technique (Chapter 5) before putting it through the hydraulic model. Figure 32 shows the recharge synthesis displayed in AQUA CHART.

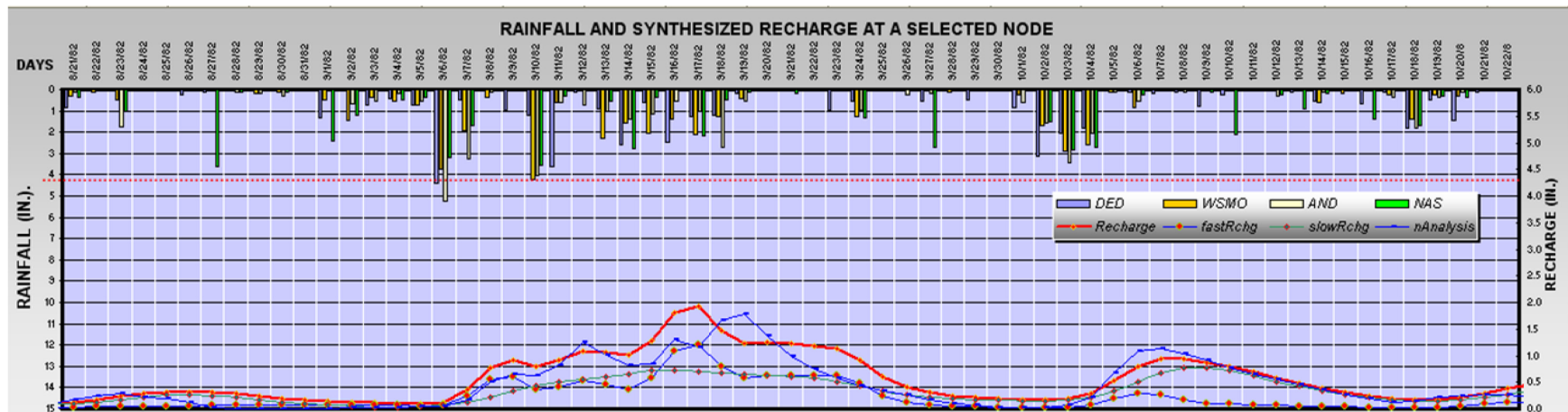


Figure 32. Recharge synthesis sample in AQUA CHART (red curve). This is a sample recharge synthesis at Observation Well M-11 receiving Dededo (DED) gage rainfall.

The final synthesized recharge for the day is the sum of the fast and slow routed recharge. The synthesized recharge output (inches, converted to meters) is multiplied by the node shed area (square meters) and converted to get the recharge volume (cubic meters) as flux for all the nodes in daily time step. This output is a text file that can be used in a GW modeling program.

The Vadose Flow Synthesis Conceptual Model of AQUA CHARGE

A computer program can account for only so much of the complexities of the real world, but a general and simplified conceptual model can be developed to guide the computer modeling process. Figure 33 shows the Vadose Flow Synthesis Conceptual Model for a single node-shed. Notice that Stage 2 is made of two funnels that collect moisture into two tubes to represent the fast (bigger tube) and slow (thinner tube) flow. The tubes have bulbs that represent the water time in storage reservoir and the number of bulbs represents the number of phases to produce the attenuation and the lag time respectively. The routing alternative approach has its advantage of disregarding the complexities of the vadose zone that may be near impossible to account for accurately concerning distance from the surface to phreatic zone and the hydraulic conductivities and triple porosity spatial variations. This method focuses on the time delivery portions of water to the lens. This satisfies our objective to improve the existing AQUA CHARGE program that can now transfer volumes of water with realistic results.

The next step is to use this synthesized recharge into a hydraulic model to simulate the hydraulic heads at each node. An aerial 2-D saturated transient finite element model code was designed specifically for this and is discussed in the next chapter.

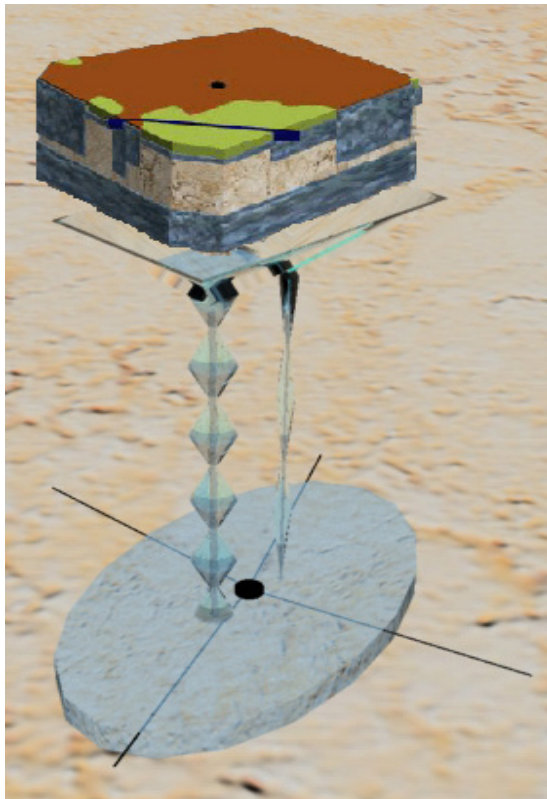


Figure 33. The Vadose Flow Synthesis Conceptual Model.

CALIBRATION THROUGH HYDRAULIC MODELING

Synthesizing recharge has its difficulties as it requires sampling, adjusting, and setting of many parameters. The recharge results are then applied to a hydraulic model or groundwater (GW) model to match historical data. The varied complexity of nature found in the Northern Guam Lens Aquifer (NGLA), both spatially and geologically, makes every detail difficult to nearly impossible to account for, even with a powerful desktop computer. Whether the synthesis represents the actual recharge is not known because there is no comparable field measurement of the recharge to the lens at any place in the study domain. At the same time, there is really no way to test the validity of the hydraulic model as well, as the two complete each other in the modeling process. Jocson, Jenson, and Contractor, in their technical report stated that estimating water loss from rainfall on Guam remains the central challenge in making accurate estimates of aquifer recharge (Jocson, et al., 1999). Without accurate estimates of recharge, it is difficult to connect any realism to the modeling simulations in determining aquifer response.

Previous studies and efforts were done in the late 1990s to model the vadose flow. Contractor used one-dimensional vertically aligned element nodes setup attached to the elements of a 2-dimensional (2-D), plan view, GW mesh (Contractor and Jenson, 1999). Jocson, as mentioned earlier, computed recharge by subtracting the pan evaporation as maximum potential ET from rainfall that fell on to his mesh elements for recharge (Jocson, 1998). The need to produce a good recharge input for any aquifer hydraulic model led to the pursuit of the development of a computer program that can accurately estimate recharge through the thick vadose zone. The goal of this project, as mentioned in Chapter 2, was to develop recharge using a method similar to that used in surface water hydrologic models.

Since there are no direct measurements of recharge for the NGLA, the recharge estimates that were developed were applied to a hydraulic model of the study area. The resulting GW simulations were checked against the actual well levels of observation wells M-11 and M-10a. Of the many hydraulics modeling techniques, i.e. *Finite Difference Method*, *Finite Element Method* (FEM), we chose Istok's code (Istok, 1989) of the FEM for a 2-D transient, saturated-flow model coded for a rectangular mesh. The FEM for a 2-D transient code receives the synthesized recharge into the nodes and mathematically computes the ground water levels (hydraulic heads). The hydraulic heads are simulated and extracted for the observed sites and compared with actual measurements to verify the calibration of the synthesized recharge just as Jocson and Contractor did with their results.

This Chapter will describe the development of the Finite Element Code to help determine the quality of the recharge simulation. It will look into previous works that employed recharge and vadose flow simulations. Then, we will look at the equations Istok used to construct the FEM for transient saturated flow. We will also explain the setting of the boundary conditions for the model. For the finite element programming, a logical program flow diagram will elucidate the algorithms and the connectivity of the subroutines. The actual code used was not included in the APPENDIX, but the program flow diagram describes each subroutine process and can be found in Istok's book coded in *FORTRAN* (Istok, 1989). Last, this chapter will also touch on the methods for calibrating the simulation results with observation data.

Developing the Finite Element Code

Of the available literature on FEM, we chose to use the technique and code found in Jonathan Istok's book titled *Groundwater Modeling by the Finite Element Method*. Our goal was to develop a 2-D daily transient, saturated GW-flow, FEM modeling program that can receive the daily simulated recharge output from the AQUA CHARGE model. Contractor and Srivastava's codes and software (SWIG2D, VADOSWIG, SINK, SCE-UA Method; Contractor and Jenson, 1999) specifically designed for the NGLA were retired and unavailable for WERI's access, and the computer software program compatibilities has changed since 1999. The GW modeling group at WERI was using SUTRA, but was doing steady state cross sections at the time. Argus ONE, another program that could run finite element code, had its limitations and again could not perform the modeling required for this project. There were no off the shelf models ready or available to perform the required transient saturated GW modeling, therefore it was determined that a new code would be written.

A special course on *FEM for Groundwater Modeling* (2007) was taught by Dr. John Jenson and Mr. Arne Olsen at WERI. Mr. Olsen helped in the understanding of the differential equations involved and the compiling of the code for various finite element models. This course also investigated the finite element mathematics involved in producing the programs that were covered in the literature described in Istok's book. Mr. Olsen also helped in advising the boundary conditions, providing GW modeling insight, and debugging the program. The literature in Istok's book included codes written in FORTRAN language that can solve multi dimensional mesh configuration. The FORTRAN codes in his book that were for quadrilateral mesh design, 2-D transient, and saturated GW flow, were extracted and rewritten in BASIC language and added to AQUA CHARGE's program and interface.

In this project, the hydraulic model is not as sophisticated as what Contractor and Srivastava coded since it lacks the inclusion of the salt water interface and tide effect. This hydraulic model is simple and holds steady the solved head through out the domain from the *Dupuit-Ghyben Herzberg* formula (E7) for coastal aquifers (Fetter, 2001). It also uses that solution as its initial condition, in the dark blue to light blue color gradient as hydraulic head, in Figure 32. The GW model solves the hydraulic head response to any recharge flow to the nodes.

Dupuit-Ghyben Herzberg

$$h = \sqrt{\frac{2q'x}{GK}} \quad (E7)$$

Boundary Conditions

The boundary conditions are determined in the finite element mesh design over the study area. With the details discussed in Chapter 4, the finite element mesh is configured so that it is at sea level inside the aquifer on through the lens. Figure 34 shows the designated boundary conditions for the no flow lines, the time variable *Dirichlet boundary*, and the *Neumann boundaries* (Olsen, personal communication; Istok, 1989). At the toe of the lens is also a Neumann boundary where allogenic recharge or boundary flux occurs. The flank of the volcanic basement ridge, where it is overlain by vadose limestone has many large voids and water flows

like a fast underground stream through these openings and into the toe of the lens. A special node shed producing this boundary flux is designed in GIS and is also explained earlier in Chapter 2.

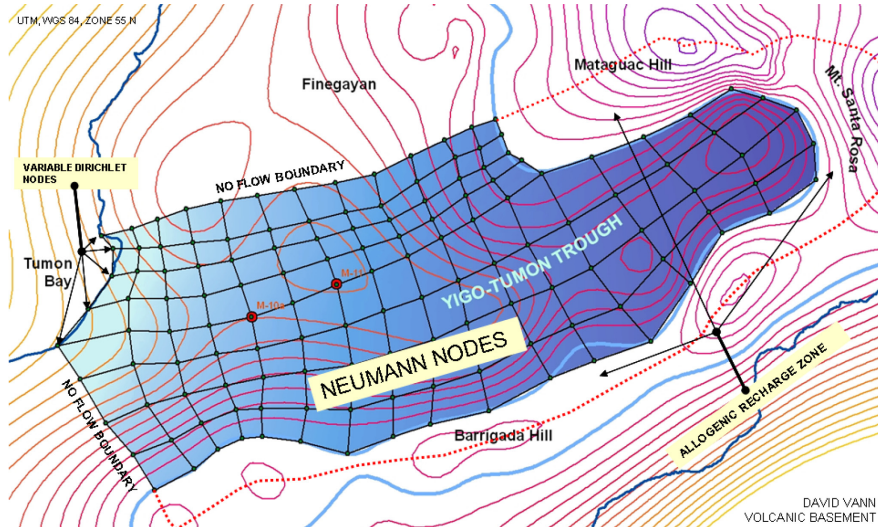


Figure 34. Hydraulic model's boundary conditions.

Finite Element Equations

For the transient 2-D saturated flow, the equation is derived from the inflow-outflow balance equation, where:

Net rate of inflow = inflow – outflow = rate of change in storage.

The basic unit control area model of inflow (ρv) and outflow (*Taylor series* approximation) as differential equations in the x and y directions for 2-D, is substituted into the general formula above. The solution results in the *net rate of inflow* formulation (E8).

$$\text{Net rate of inflow} = -\frac{\partial}{\partial x}(\rho v_x) - \frac{\partial}{\partial y}(\rho v_y) = \frac{\partial}{\partial t}(\rho n) \quad (\text{E8})$$

The right hand side of the equation is solved resulting in the derivation of *Specific Storage* (S_s) and the equation for a *2-D Transient Saturated Flow Equation* (E9) has *Darcy's Law* substituted for the velocity and the densities divide out. The details of its derivation are found in APPENDIX II of Istok's literature.

2-D Transient Saturated Flow Equation,

$$\frac{\partial}{\partial x} \left(K_x \frac{\partial h}{\partial x} \right) + \frac{\partial}{\partial y} \left(K_y \frac{\partial h}{\partial y} \right) = S_s \frac{\partial h}{\partial t}. \quad (\text{E9})$$

The *Method of Weighted Residuals* substitutes an interpolating function $N_i^{(e)}$ for the weighting function with the 2-D Transient Saturated Flow equation inserted to form the *Galerkin Method* equation (E10). The equation is expanded in the form E11.

Galerkin Method,

$$R_i^{(e)} = - \iint_{A^{(e)}} N_i^{(e)} \left[\frac{\partial}{\partial x} \left(K_x^{(e)} \frac{\partial \hat{h}^{(e)}}{\partial x} \right) + \frac{\partial}{\partial y} \left(K_y^{(e)} \frac{\partial \hat{h}^{(e)}}{\partial y} \right) - S_s^{(e)} \frac{\partial \hat{h}^{(e)}}{\partial t} \right] dx dy \quad (E10)$$

$$= - \iint_{A^{(e)}} N_i^{(e)} \left[K_x^{(e)} \frac{\partial^2 \hat{h}^{(e)}}{\partial^2 x} + K_y^{(e)} \frac{\partial^2 \hat{h}^{(e)}}{\partial^2 y} \right] dx dy + \iint_{A^{(e)}} N_i^{(e)} S_s^{(e)} \frac{\partial \hat{h}^{(e)}}{\partial t} dx dy \quad (E11)$$

Equation E10, the left integral is simplified with *Integration by Parts*, and the right hand side of the equation is solved with the *Lumped Element Formulation*. The equations for both solutions are converted to their *Global Matrix* forms and simplified to a *System of Ordinary Differential Equation* (E12).

System of Ordinary Differential Equation

$$\underset{global}{[C]} \overset{o}{\{h\}} + \underset{global}{[K]} \{h\} = \underset{global}{\{F\}} \quad (E12)$$

Equation E12 can be solved with the *Mean Value Theorem* to produce the *Finite Difference Formulation for a transient, saturated-flow* equation (E13).

Finite Difference Formulation for Transient, Saturated Flow Equation

$$\left([C] + \omega \Delta t [K] \right) \{h\}_{t+\Delta t} = \left([C] - (1-\omega) \Delta t [K] \right) \{h\}_t + \Delta t \left((1-\omega) \{F\}_t + \omega \{F\}_{t+\Delta t} \right) \quad (E13)$$

Equation E13 parts can be setup as $[M]\{X\} = \{B\}$ in the following equations (E14 and E15).

$$[M] = [C] + \omega \Delta t [K]$$

$$\{X\} = \{h\}_{t+\Delta t} \quad (E14)$$

$$\{B\} = \left([C] - (1-\omega) \Delta t [K] \right) \{h\}_t + \Delta t \left((1-\omega) \{F\}_t + \omega \{F\}_{t+\Delta t} \right)$$

$$[M]\{X\} = \{B\} \quad (E15)$$

Equation E15 can be solved using *Choleski's Method* (decomposed or factored). Finally, *Backward Substitution* solves for $\{X\}$ (E16).

$$x_{n+1-i} = z_{n+1-i} - \sum_{k=1}^{i-1} u_{n+1-i, n+1-k} x_{n+1-k}, \quad i = 1 \text{ to } n. \quad (\text{E16})$$

The numerical solution and coding that employs material conductivity and capacitance assemblage, decomposition matrix solutions, approximating equations, and solution is complex and can be a literary entity on its own. In this thesis, we will summarize Istok's code via its actual programming flow diagram reconfigured to work into AQUA CHARGE's interface design.

Computer Program Flow Diagram

The development of the FEM code, as mentioned earlier, was extracted from Istok's text. As mentioned earlier, Istok's program code can solve many forms of finite element configuration. The entire code was dissected and the necessary pieces were put together to complete a 2-D transient GW model. The computer programming flow diagram summarizes the coding process (Figure 35). The mesh information and the synthesized recharge input data text files are loaded first. The recharge data is obtained as a saved output file after the recharge routing process in the AQUA CHARGE model. The daily simulated recharge is transferred into an array organization. The input data is an Excel file and is configured by the modeler according to the boundary conditions of the mesh, the node's x-y coordinates, material properties, node sequence around an element, and other parameters that are transferred into variables and arrays. Each data set is defined for access by the program. A table of the input data is in APPENDIX H, FEM Input Data called FEMData also explained in detail in Chapter 4. Finally, with the arrays and variables prepared and set accessible as variable type's public and global, the modeler runs the FEM algorithm. The algorithm uses a daily time step in the computational loop. In the loop, first the global conductance and capacitance matrix is prepared through the Assembly of the global conductance and capacitance matrix (ASMBKC) code. The DECOMP does the decomposition of the matrix, RHS solves the $\{B\}$ portion, and SOLVE solves matrix equation $[M]\{X\} = \{B\}$ for $\{X\}$ as hydraulic head. The loop continues on to the next day and the process in the loop is run again. The loop ends at the final day and the data for a specific node is extracted into the AQUA CHART.

FINITE ELEMENT METHOD
PROGRAM FLOW DIAGRAM

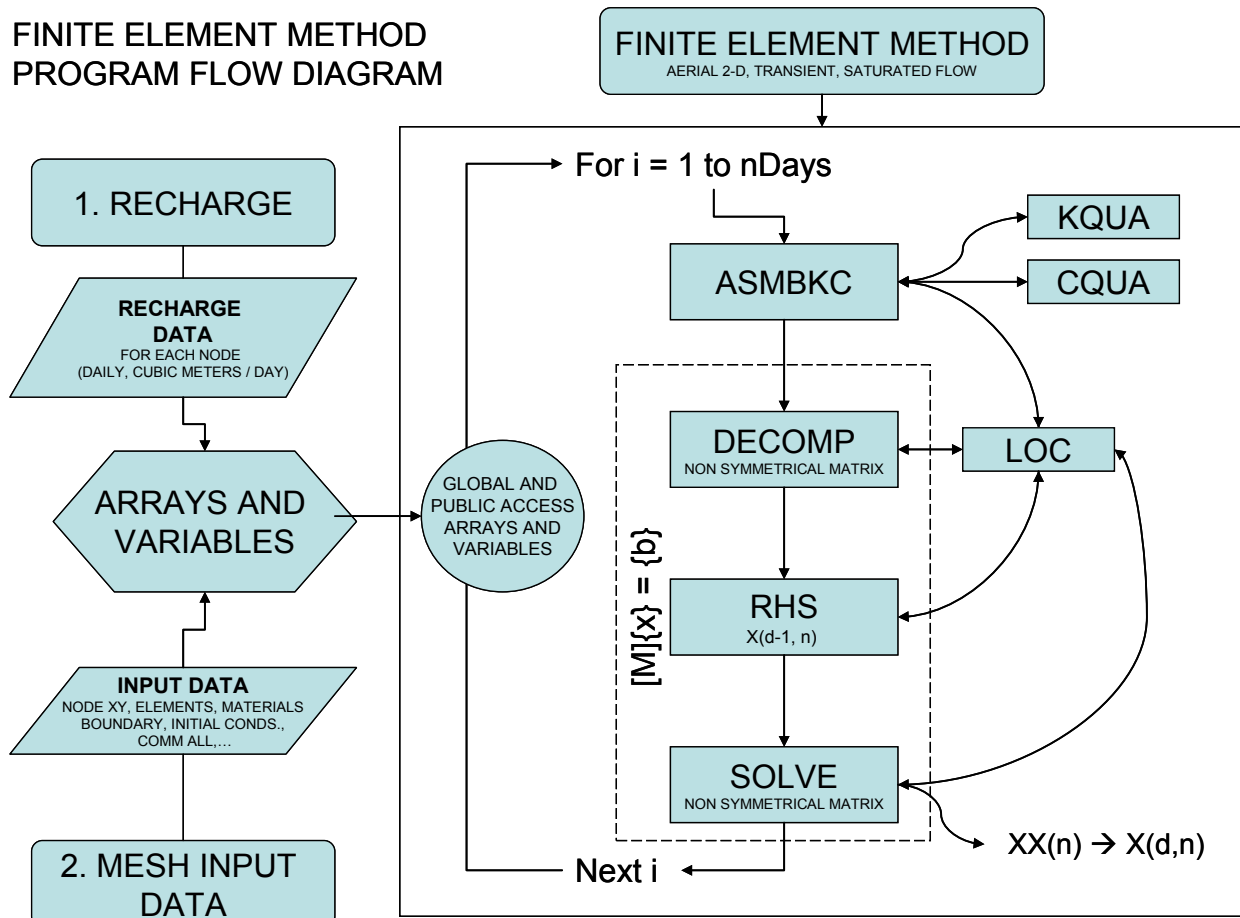


Figure 35. 2-D transient, saturated flow, programming flow diagram.

Calibrating Results to Observed Data

The results were calibrated by way of history matching and curve fitting. The simulated transient hydraulic heads at wells M-11 (Node 59) and M-10a (Node 41) are extracted from the solution of the FEM. The solutions are charted and compared with the observed results. Next modeling parameters were adjusted to obtain the best fit to the observed values. When an acceptable match was made between the simulated and the observed values, the recharge simulation was deemed successful.

In the practice and testing of both simulating recharge and the verification/calibration process, many factors were discovered concerning modeling the NGLA. The understanding of the hydrogeological nature of this aquifer proved to be very difficult and affected our ability to accurately match simulated and observed hydraulic head values. This aquifer, having triple porosity properties laid throughout its limestone media, revealed the complexity of making accurate simulations where one node shed can produce different recharge values than the next. The variability in the hydraulics could possibly be so significant from one node-shed to another that more observation wells were required to approve its calibration. The observation well results alone revealed how well M-11 has a rapid and flashy response to recharge while well

*Vadose Flow Synthesis for the Northern Guam Lens Aquifer
Calibration Through Hydraulic Modeling*

M-10a's response is much more sluggish. The AQUA CHART makes it possible to see this behavior that helped us adjust the modeling parameters and percent yield curve shapes. Although only two observation wells were used for comparison with hydraulic modeling simulation, the real focus was producing realistic spatially different recharge for each node-shed. The GW model hydraulic conductivities were also spatially variable for each node. In the end, the *Sum of Squared Errors* (SSE) between simulation and observation wells were reduced compared to the VADOSWIG (Contractor and Jenson, 1999). The details to the history matching are revealed in Chapter 7

DATA COMPILATION

This chapter covers the details of preparing the spatial, temporal, and output data file and recordsource that are necessary and accessible to the AQUA CHARGE program. The spatial data is built around a ground water modeler's finite element mesh plan to create hydrologic node-sheds. The Geographic Information Systems (GIS) tool Euclidean allocation builds these node-sheds over the mesh nodes. The node-shed, soils, rain and pan evaporation Thiessen as polygon shapefiles are combined with the GIS *Union* tool to produce the polygon attribute table (PAT) database file that contains the spatial information. The temporal data, rainfall and pan evaporation are extracted from the records stored in the *National Climatic Data Center* (1995/2005) compact disk. The field capacities of the soils are solved using the physical properties table in the Soil Survey of the Territory of Guam. Each data, whether used as input or output files in AQUA CHARGE, require a special formatting setup and configuration in order for the program to read or write to. This was accomplished using ESRI® Arc Map GIS and MICROSOFT® Excel for data analysis, extraction, programmed solving techniques, and creating program accessible data recordsource. The soils curve and the recharge synthesis output were specially programmed in AQUA CHARGE as savable/loadable text files.

Spatial Data – Development of the Polygon Attribute Table (PAT)

The spatial data is prepared with GIS software where a database file (*.dbf) containing polygon attribute table (PAT) can be extracted or exported. This database has values for each spatial zone polygon such as rain gage, pan evaporation gage, soil id, and so on. The spatial data is a 2-Dimensional (2-D) aerial or plan view of the study area in Northern Guam's *Yigo-Tumon Trough* sub-basin. The geographic projection used in the GIS is Universal Transverse Mercator (UTM), World Grid System 1984 (WGS 84), zone 55 North. The coordinate system is set to meters for all spatial development. The setup begins with the development of the finite element mesh domain over the selected study area. Next, a node-shed is generated and is spatially combined with the soils polygons. The areas assigned to the rainfall and pan evaporation gages are also spatially combined with the previously combined soils and node-shed polygons. The combination of each shape file overlay is done by a GIS tool called Union. The database table of the 4 piece polygon shape files combination described above is copied with some minor editing and will serve as a spatial PAT file for AQUA CHARGE's recharge synthesis. Each of these processes will be described in detail next.

Background Map Setup

Again, all of the data for the spatial information used in AQUA CHARGE were developed using the ArcMap. The starting base map consisted of shape files for the Guam shoreline (USGS), the Northern Guam volcanic basement contours (David Vann, unpublished), and observation wells M-11 and M-10a. The observation wells were pin-point located (Jocson, personal communication) with QuickBird®, satellite image over the domain, and identified using point shape files. This background map (Figure 36) is used to help determine boundaries and node placement when building the finite element mesh. The sub-basin is visually edited using

the volcanic basements contours to delineate the boundaries as a mesh boundary and node-shed boundary setting guide. The observation wells M-11 and M-10a are points of interest and a finite element computational node was placed at each location. A sketch of the mesh was made on a background map printout and was used to develop the digital mesh discussed next.

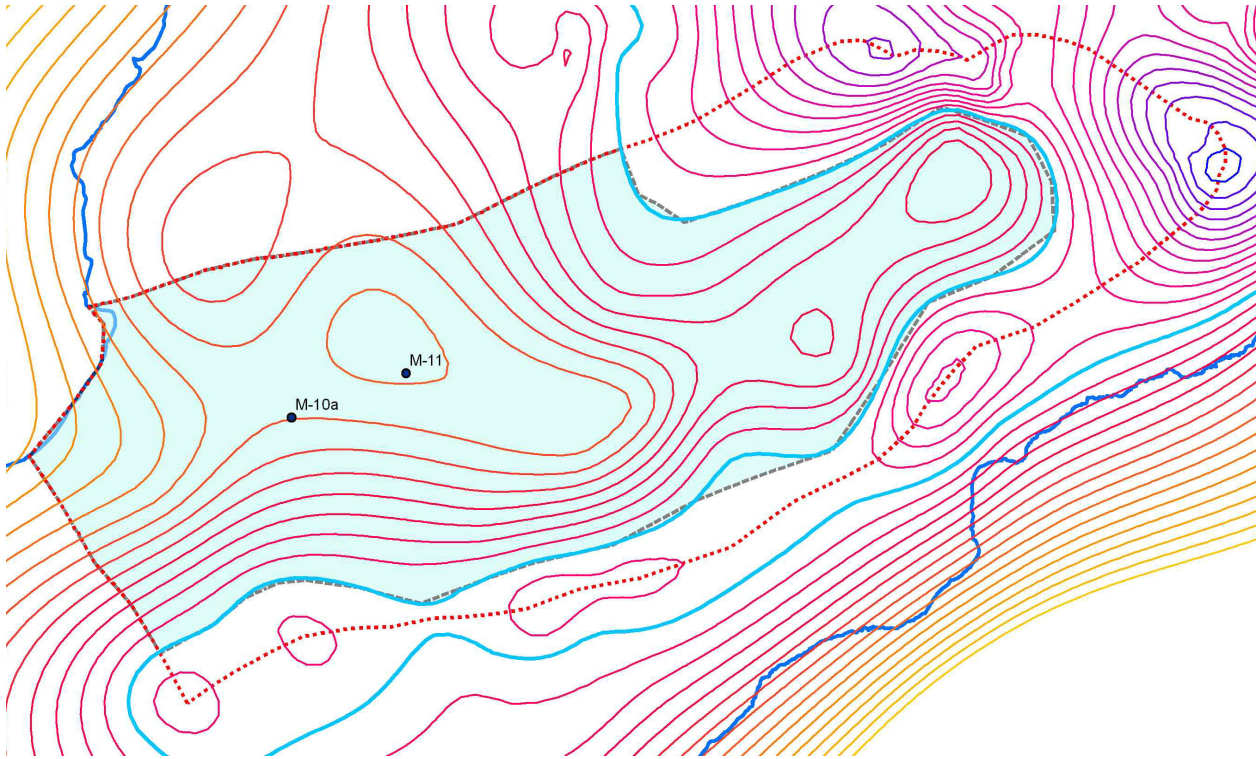


Figure 36. The background map. It consists of volcanic basement contours (light blue contour is 0 elevation, mean sea level, contour interval is 20m), shoreline, and observation wells M-10a and M-11. The light blue transparent area is the lens plan view area where the hydraulic model was placed and the dotted red line is the area boundary of the node-shed extending beyond the lens toe line for the allogenic recharge effect.

Finite Element Mesh Design

The finite element mesh is the hydraulic analysis framework for the sampling of the study area. The finite element method code written in AQUA CHARGE works for an aerial 2-D quadrilateral mesh network. The mesh was constructed manually in the GIS (see Figure 37). The method and rules for developing finite element meshes are in *Groundwater Modeling by the Finite Element Method* (Istok, 1989). From a paper sketch with the background and boundaries, new shapefiles were edited with GIS for nodes (points) and elements (polygons).

Node placement was done along and within the mesh boundary. Two nodes were specifically placed on the two selected observation wells. The nodes were placed as sketched to form rectangles where element lines are connected. The node numbering is shown on Figure 35 and is numbered specifically to provide the smallest maximum semi-bandwidth (SBW) numbering scheme as possible to optimize the matrix arrangement (Istok, 1989).

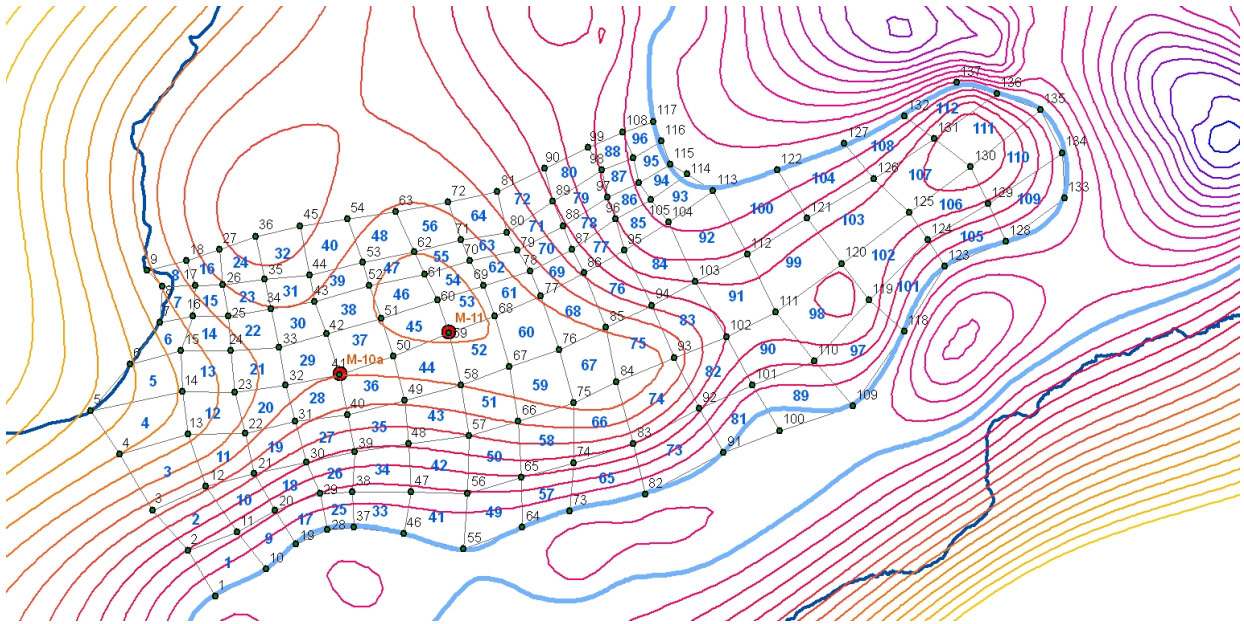


Figure 37. Finite element mesh design. Quadrilateral mesh numbering configured to produce the smallest maximum semi-bandwidth. The perimeter nodes and element lines serves as the mesh-boundary.

Polygons connect the nodes to make an element. These polygons are necessary for the topology of node and element arrangement. The polygon development starts from node 1 and the rectangles are formed by connecting neighboring nodes in a counter clockwise direction. An Excel VB program was written to automatically extract the element and counter clockwise node arrangement sequence into a spreadsheet. This is due to the finite element method code designed to read the nodes of an element, from lowest to highest, in a counter clockwise fashion. The rectangles are built from one node to the next in increasing node number order. When the mesh was finalized, the node-sheds were created next.

Node-Sheds

A GIS tool called Euclidean Allocation is used to develop what we have termed “node-sheds”. These node-sheds are polygons of area that supply recharge to each of the nodes that sit on top of a node cell. Euclidean allocation is similar to the Thiessen polygon technique used in traditional hydrologic analysis. The Euclidian technique assigns the closest proximity area around each node to that node. These areas are referred to as *cells* in finite element method. We assumed that these closest areas constituted the node-sheds for each node. The Euclidean allocation assigns the individual node number attribute to each node-shed for that node. The Euclidean allocation tool produces a raster or grid type map of the node-sheds (Figure 38). This raster map is then converted to polygon shape files for compatibility with the rest of the polygon shape files.

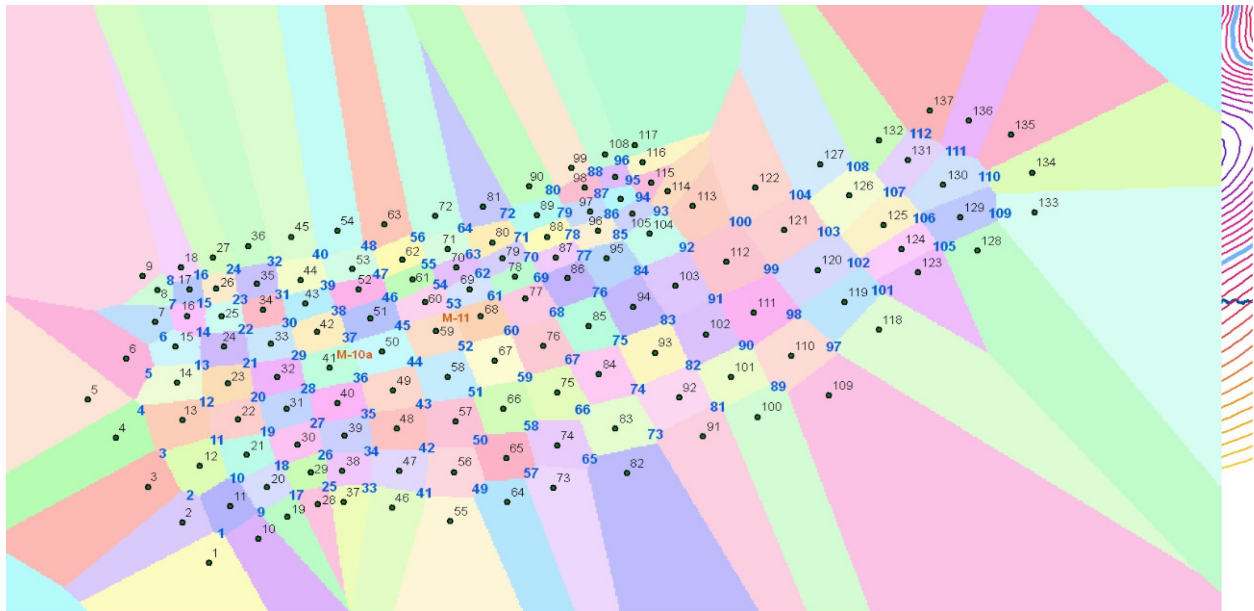


Figure 38. Applying Euclidean allocation function in GIS for building node-sheds. Euclidean allocation creates area boundaries between nodes and is a raster file. The raster file was then converted to a polygon shape file and clipped with the mesh boundary.

Allogenic recharge and boundary flux requires the extension beyond the finite element mesh boundary at the toe of the lens. Chapter 2 discusses boundary flux and allogenic recharge determination. The polygons may be edited to extend the node-shed at the lens toe boundary, where allogenic recharge flux is presumed to occur, to the extent of the basement volcanic ridge. The boundaries are edited so that the side lines, dividing the edge node-sheds next to the other, are perpendicular to the volcanic basement topography (see Figure 39). The no flow boundaries assume flow to the coast is parallel to this boundary and its node-sheds are not edited as at the toe, instead terminate at the node to node connection. The new area extent is now termed shed-boundary to differentiate from the mesh-boundary. All polygon shape files are inspected for slivers or gaps and edited as necessary. The final edit of the node-sheds is shown in Figure 40.

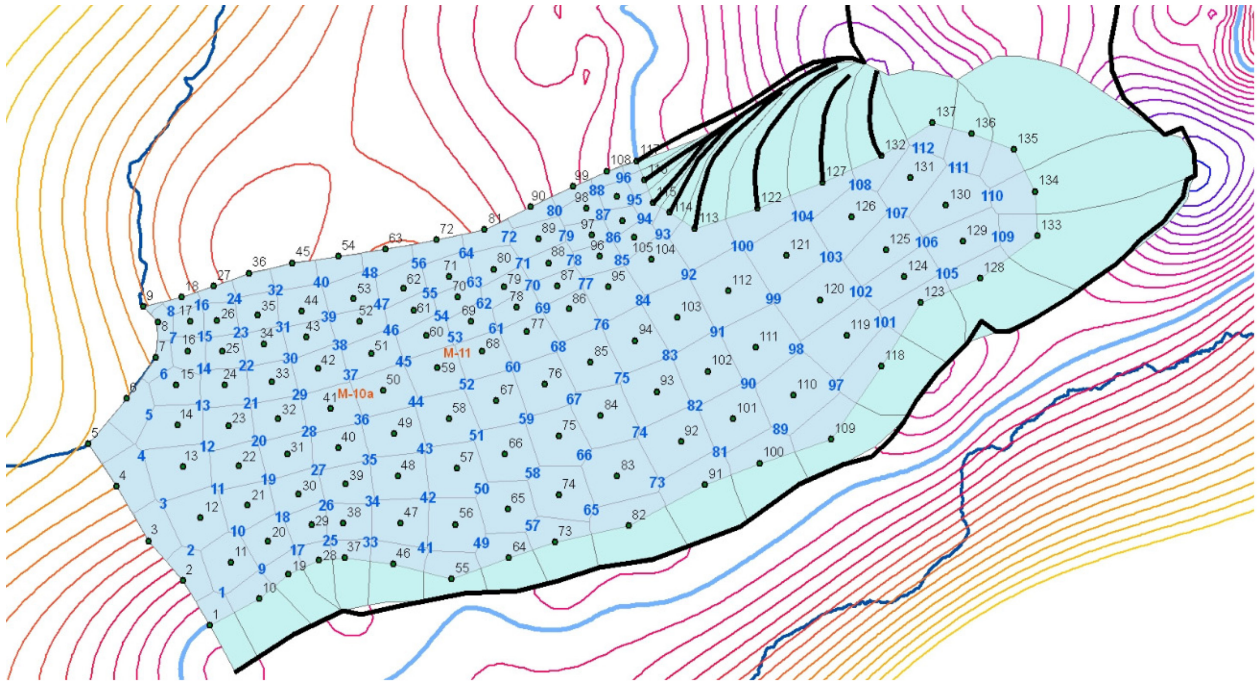


Figure 39. Extending the node-shed for boundary flux conditions. The thick black lines are sketch guidelines of the volcanic basement contour ridge and perpendicular to contour guides around Mataguac Hill. The guidelines help make good extension of the node-shed where allogenic recharges are supposed to occur.

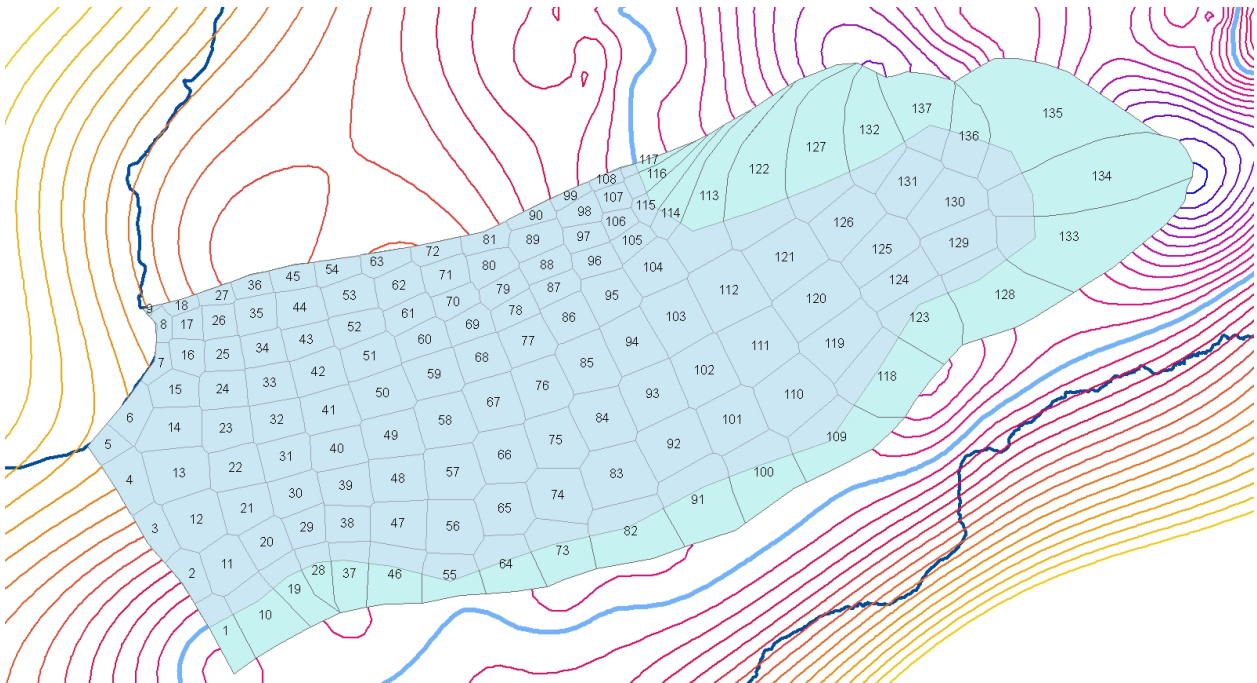


Figure 40. A completed node-shed. Node-sheds, each polygon number is associated with the node it overlays. Node-sheds with boundary flux or allogenic recharge are edited to extend to the ridge of the volcanic contours which make up the shed-boundary.

Each node-shed area is now included in the node-shed attribute table. A node-shed area field (column and column name) is first added. The calculate function is used to determine each node-shed polygon's area and this value is included in the newly added shed area field of the attribute table. The attribute table for the node-shed should have field names and values of node-shed id (number same as the node number it covers), and a node-shed area in meters.

Soils polygons: The soils shapefile is used to characterize the spatially variable soils characteristics throughout the study area. This shapefile was digitized from the detailed soil maps in Soil Survey of the Territory of Guam. Details to the soils in the domain are in Habana, 2008, APPENDIX D. The attribute table for this map has the following fields: soil id, soil name/type, and stratum. The Guam soil shapefile is clipped by the shed-boundary (see Figure 41). The polygons were then *simplified*, a GIS tool function.

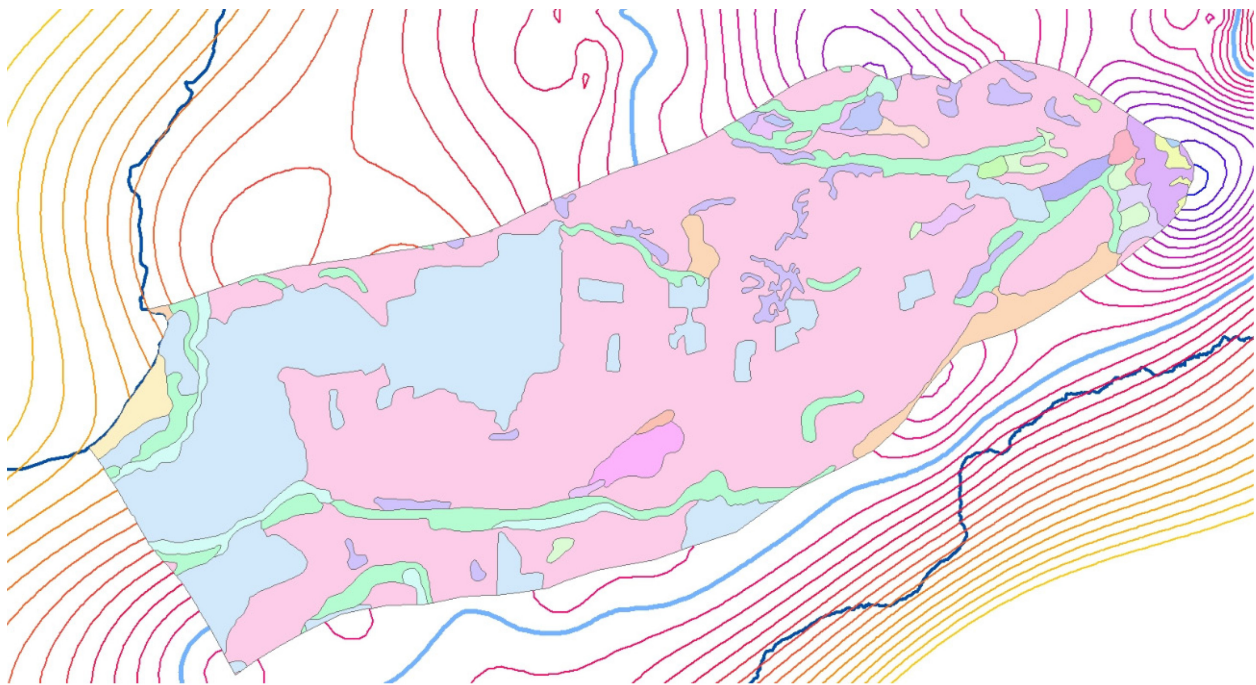


Figure 41. Soils polygon shape file.

Union of Node-Sheds and Soils: The node-sheds and the soil are joined with the *union* tool. *Union*, as defined in GIS, computes a geometric intersection of the input features. In the union process, all features will be written to the output feature class with the attributes from the input features, which it overlaps (see Figure 42; GIS Help). Figure 43 shows the soils and node-shed layers ready for the union process. Figure 44 shows the union of the two node-shed and soils and the resulting attribute table (Figure 45). If the shape files were digitized properly with no gaps between polygons, then the soils id values will have no zero values. If, on the other hand, gaps exist meaning polygon edges are contiguous, then a zero value can be found in the soil id. This can be identified simply by sorting the soil id field in ascending order. The entire row of soil id with a zero value is then deleted in the attributes table while in edit mode. Usually, these excess and not easily identifiable polygons are small and insignificant and may be ignored.

But if the area of one of these zero id elements is significant, the modeler may zoom in the gaps and join the polygon edges in edit mode. A careful inspection before the union of the two shapefiles could prevent this problem.

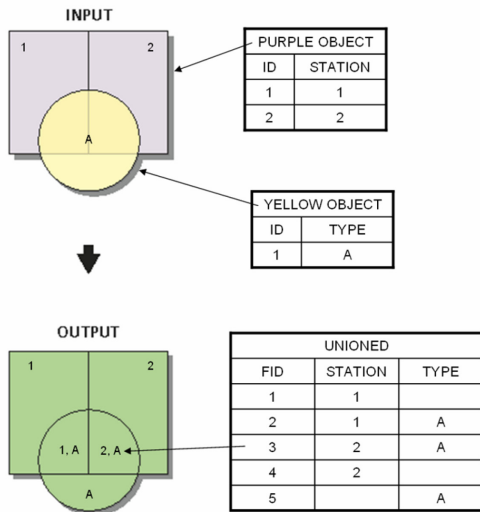


Figure 42. The GIS Union tool. The tool creates a new polygon shape file where intersecting polygons include field values of the input polygons (ESRI GIS Help).

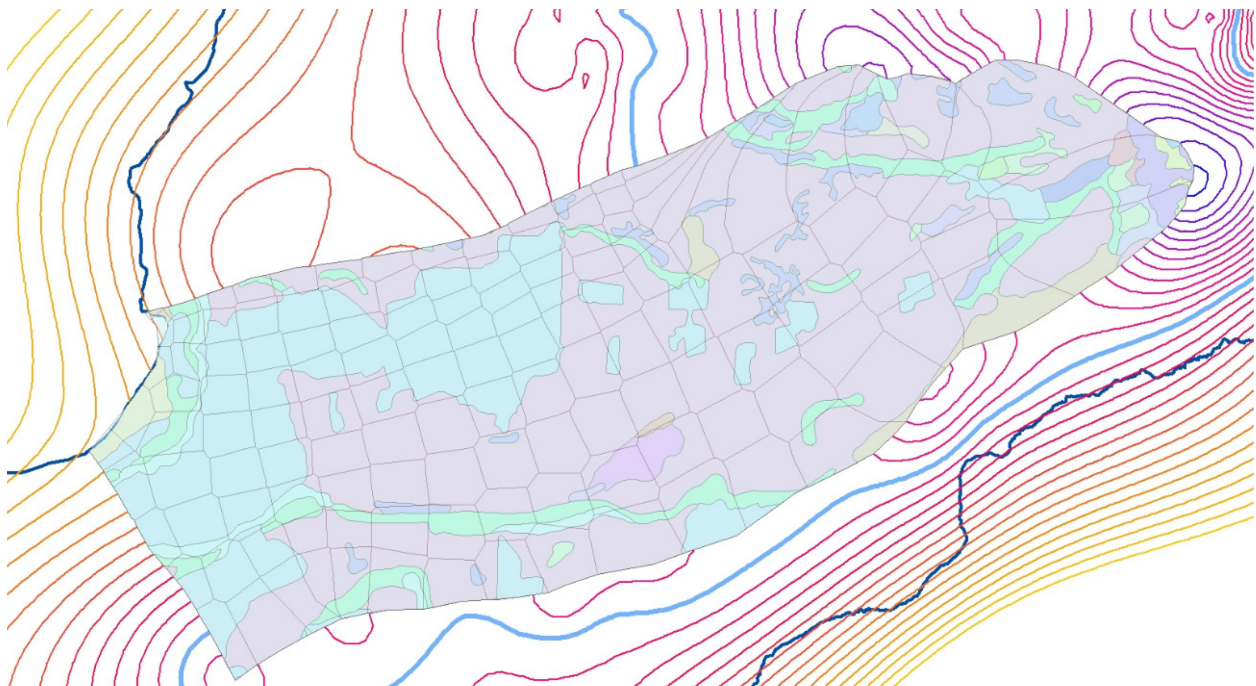


Figure 43. Soil and node-shed shape files.

Vadose Flow Synthesis for the Northern Guam Lens Aquifer
Data Compilation

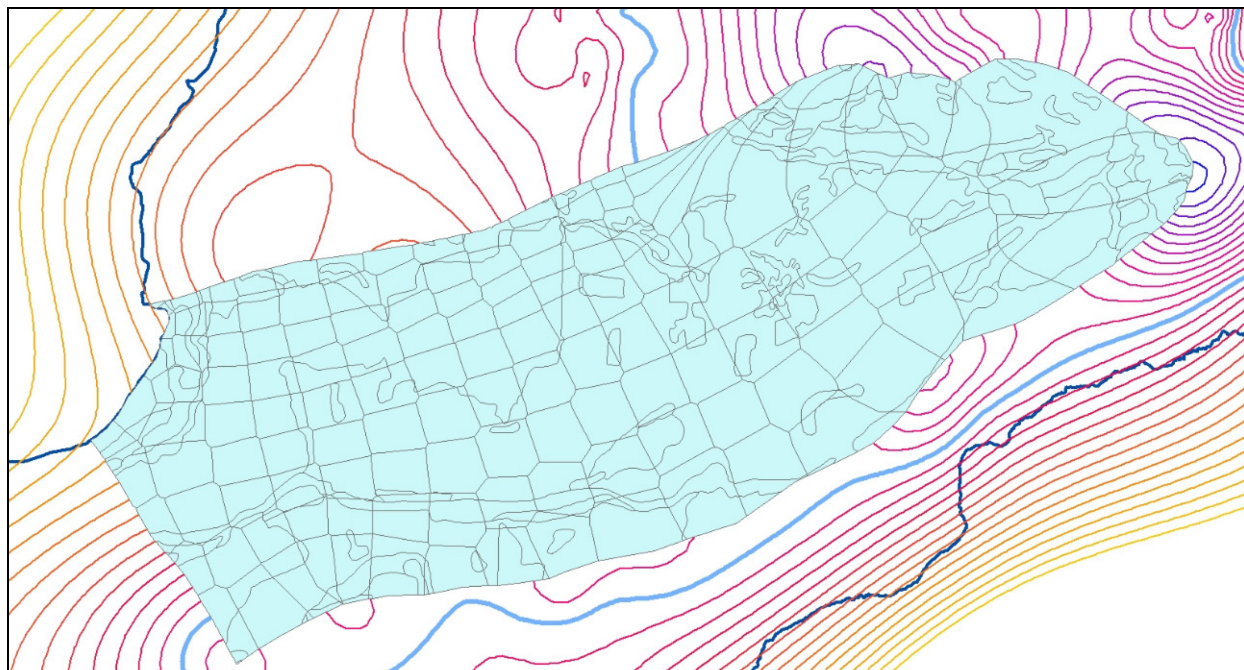


Figure 44. Union of node-sheds and soils.

Attributes of SOILSHED_UNION1

FID	Shape'	SHED_ID	SHED_AREA	SOIL_ID	STRATUM	SOIL_TYPE
0	Polygon	137	622309.442503	20	Volcanic	AKINA-BADLAND COMPLEX
1	Polygon	137	622309.442503	29	Limestone	GUAM-YIGO COMPLEX
2	Polygon	137	622309.442503	38	Limestone	PULANTAT-CHACHA CLAYS
3	Polygon	137	622309.442503	26	Limestone	GUAM COBBLY CLAY LOAM
4	Polygon	137	622309.442503	25	Limestone	GUAM COBBLY CLAY LOAM
5	Polygon	117	72389.54123	25	Limestone	GUAM COBBLY CLAY LOAM
6	Polygon	136	390601.766478	29	Limestone	GUAM-YIGO COMPLEX
7	Polygon	136	390601.766478	26	Limestone	GUAM COBBLY CLAY LOAM
8	Polygon	136	390601.766478	23	Limestone	CHACHA CLAY
9	Polygon	136	390601.766478	28	Urban	GUAM-URBAN LAND COMPLEX
10	Polygon	136	390601.766478	25	Limestone	GUAM COBBLY CLAY LOAM
11	Polygon	135	1752876.26296	29	Limestone	GUAM-YIGO COMPLEX
12	Polygon	135	1752876.26296	23	Limestone	CHACHA CLAY
13	Polygon	135	1752876.26296	29	Limestone	GUAM-YIGO COMPLEX
14	Polygon	135	1752876.26296	29	Limestone	GUAM-YIGO COMPLEX
15	Polygon	135	1752876.26296	18	Volcanic	AKINA-BADLAND COMPLEX
16	Polygon	135	1752876.26296	27	Limestone	GUAM-Saipan COMPLEX
17	Polygon	135	1752876.26296	26	Limestone	GUAM COBBLY CLAY LOAM
18	Polygon	135	1752876.26296	23	Limestone	CHACHA CLAY
19	Polygon	135	1752876.26296	9	Volcanic	AKINA SILTY CLAY
20	Polygon	135	1752876.26296	28	Urban	GUAM-URBAN LAND COMPLEX
21	Polygon	135	1752876.26296	19	Volcanic	AKINA-BADLAND COMPLEX
22	Polygon	135	1752876.26296	25	Limestone	GUAM COBBLY CLAY LOAM
23	Polygon	108	58021.850586	25	Limestone	GUAM COBBLY CLAY LOAM
24	Polygon	132	691256.074778	20	Volcanic	AKINA-BADLAND COMPLEX
25	Polygon	132	691256.074778	46	Volcanic	SASALAGUAN CLAY
26	Polygon	132	691256.074778	39	Limestone	PULANTAT-KAGMAN CLAYS
27	Polygon	132	691256.074778	38	Limestone	PULANTAT-CHACHA CLAYS
28	Polygon	132	691256.074778	26	Limestone	GUAM COBBLY CLAY LOAM
29	Polygon	132	691256.074778	26	Limestone	GUAM COBBLY CLAY LOAM
30	Polygon	132	691256.074778	29	Limestone	GUAM-YIGO COMPLEX
31	Polygon	132	691256.074778	25	Limestone	GUAM COBBLY CLAY LOAM
32	Polygon	116	166891.870086	25	Limestone	GUAM COBBLY CLAY LOAM
33	Polygon	99	70413.828807	29	Limestone	GUAM-YIGO COMPLEX

Record: 1 | Show: All Selected | Records (0 out of 427 Selected) | Options

Figure 45. PAT for the union of node-shed and soil.

Thiessen Polygons for Rain and Pan Evaporation Gages

The input and output spatial distribution range of moisture is bounded and determined using the traditional hydrologic analysis called the Thiessen method which allocates closest areas to point locations such as rain gage locations. The Thiessen method is easily implemented in GIS using the *Euclidean Allocation* tool. Two shapefiles, one rain and the other pan evaporation gage points, are added in the GIS. The Euclidian allocation produces a raster or grid file of closest areas. The resulting raster file is then converted to polygons as done with the node-shed development mentioned previously. The rainfall and pan evaporation polygon shapefiles are then clipped with the shed-boundary. The details for developing each Thiessen polygons for the rain gages and pan evaporation gages are explained next.

Rain Thiessen Polygons: The best data for rain gages located in the NGLA was obtained from climatological data stored in a CD obtained from the US Weather Service National Climatic Data Center (NCDC, 1995 or 2005; also see Habana, 2008, APPENDIX B). The rain gages used are identified as station location and gage number identification: Andersen (AND, 4025), Weather Service Meteorological Observatory (WSMO, 4229), Dededo (DED, 4156), and Naval Air Station (NAS, 4226). The shapefile show their locations in Figure 46.

Again, ArcMap was used to perform the Thiessen closest area allocation method using the Euclidean allocation tool. In order to insure a complete allocation, the point map to be allocated was first edited by adding two points at opposite corners of the study area. The Euclidean allocation tool produced a raster file of the Thiessen polygons. This raster was converted into a polygon shapefile and clipped with the node-shed perimeter boundary. The attribute table for this shapefile contains a field called the "GAGE_ID" which identifies which gage is assigned to that particular area. Another possible and maybe simpler method is to use the shed-boundary as a mask which does not require clipping later.

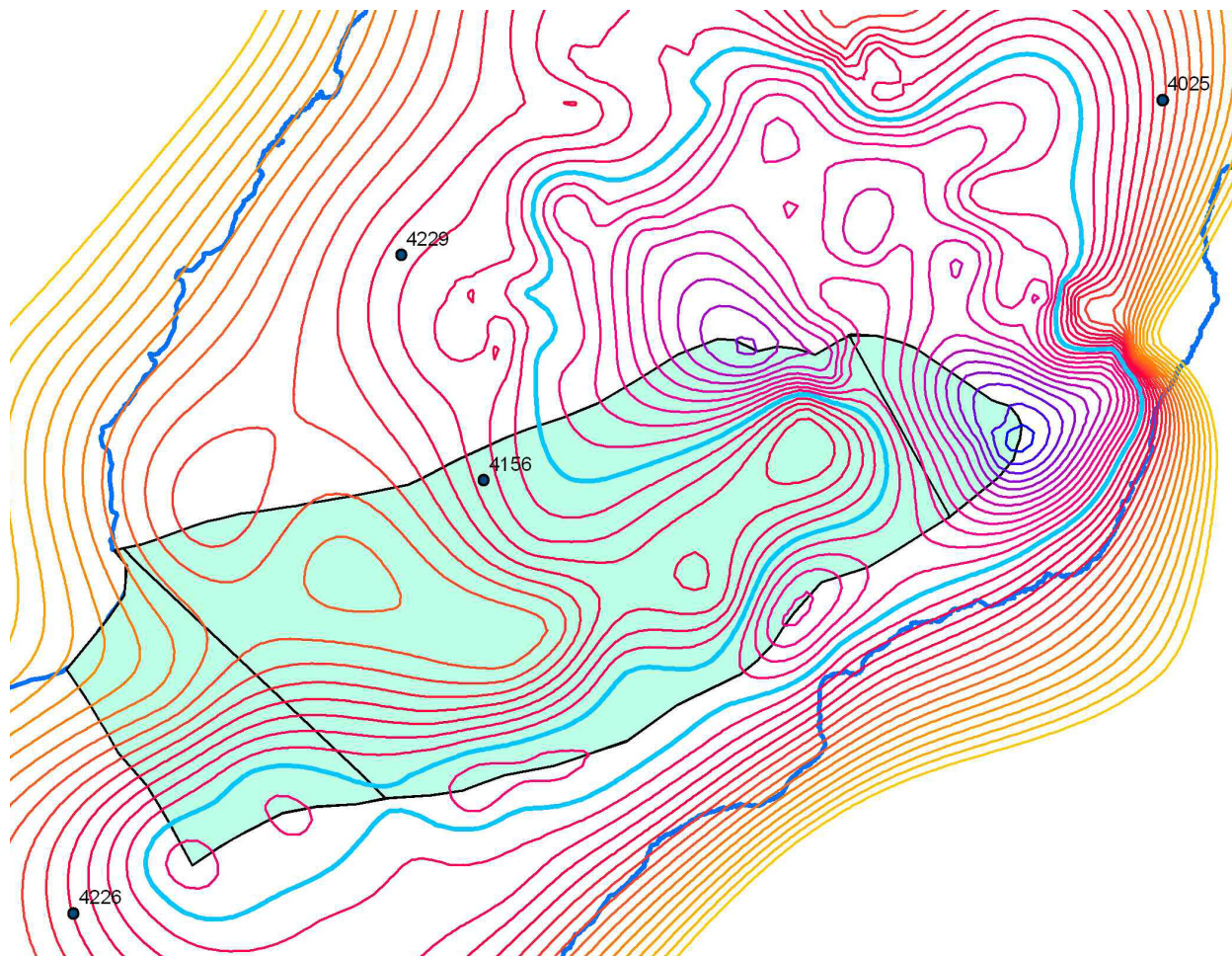


Figure 46. Rain Thiessen polygons. Notice that WSMO's (4229) area of influence does not reach the node-shed boundary, therefore will have no contribution of rainfall to the domain.

Pan Evaporation Thiessen Polygons: The best data for pan evaporation is also obtained from the previously mentioned climatological CD (NCDC, 2005). Two stations that measured pan evaporation were WSMO and NAS. These are the two same stations that measured rainfall mentioned in the Rain Thiessen Polygons section. Figure 47 shows the point locations of the pan evaporation recording stations.

The Thiessen method was performed for the pan evaporation in the same manner as was done for the rain gages. Figure 47 shows the Thiessen polygon for the pan evaporation. Finally, for the gages and pans, is the union of rain and pan evaporation polygon shapefiles (Figure 48) with a resulting polygon attribute table (Figure 49).

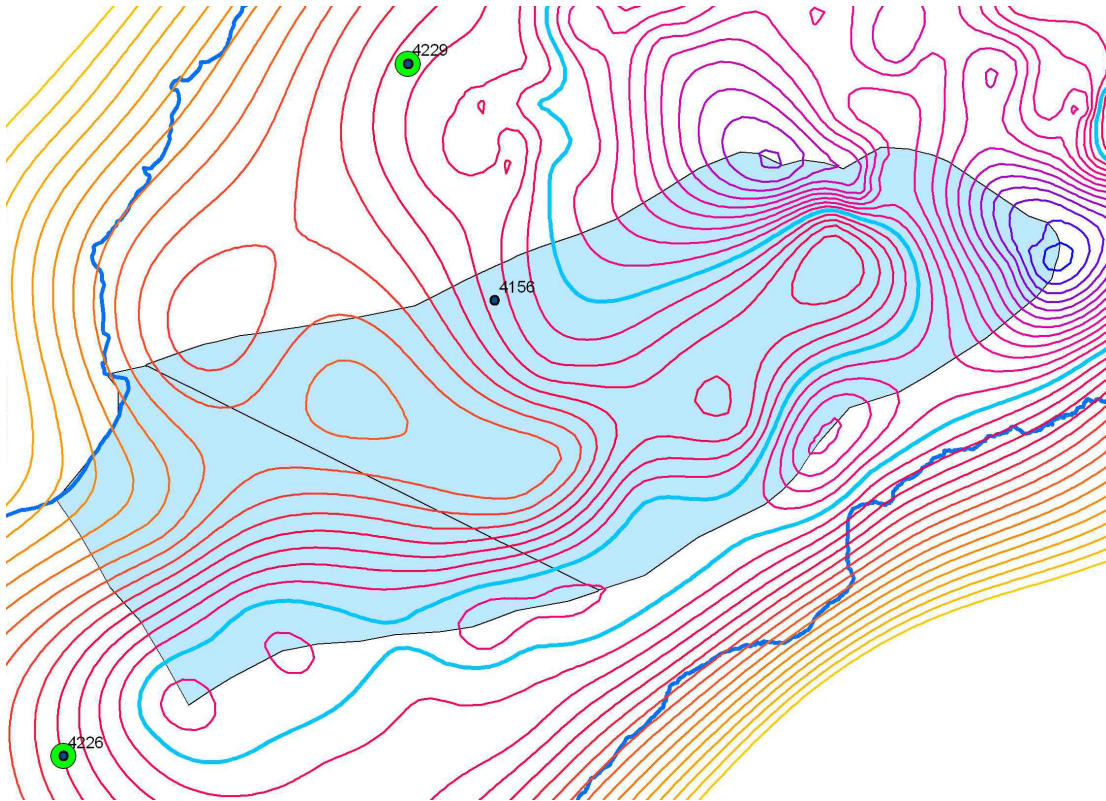


Figure 47. Pan evaporation station (green points) Thiessen polygons.

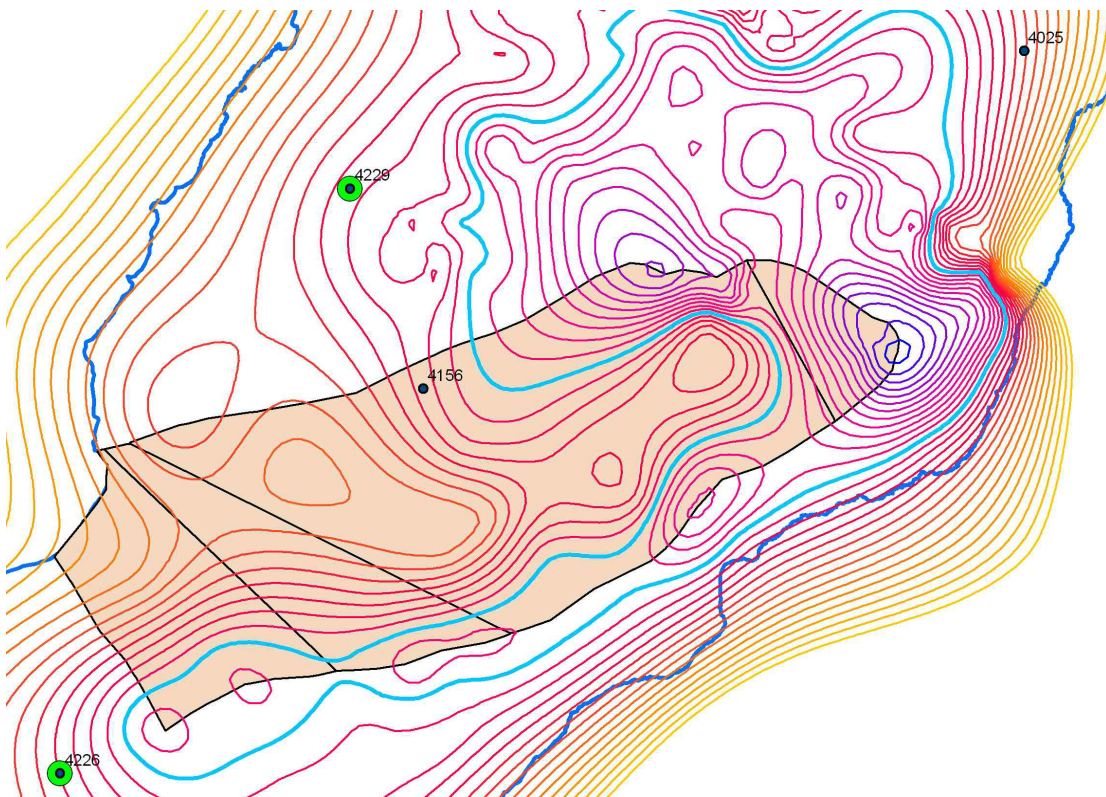
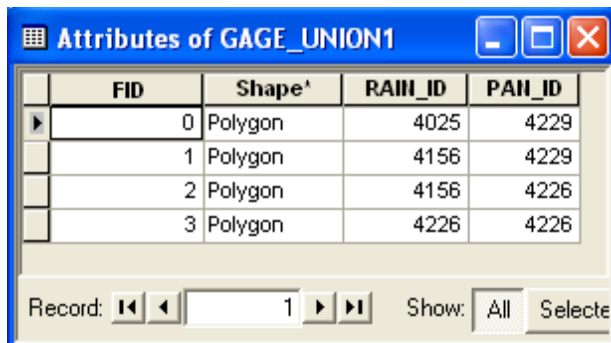


Figure 48. Union of rain and pan evaporation Thiessen Polygons.



FID	Shape*	RAIN_ID	PAN_ID
0	Polygon	4025	4229
1	Polygon	4156	4229
2	Polygon	4156	4226
3	Polygon	4226	4226

Record: 1 Show: All Selecte

Figure 49. PAT of the union of rain and pan evaporation gage

PAT Data File

A final union of all the polygons, union of rain and pan evaporation and union of node-shed and soil is combined (see Figure 50). A zone area field was added and named ZONE_AREA and every polygon's area was calculated under that field name. The attribute table of the final union is edited to contain only the necessary fields (Figure 51). This PAT file extension is recognized as a database file or "dbf" and can be located in the collection of files associated with the final union shapefile. It can also be exported as a database file in GIS. This dbf file was opened in Excel and renamed as "PAT.dbf". Details to the PAT data for every zone are in Habana, 2008, APPENDIX A.



Figure 50. Final union of rain, pan evaporation, soils, and node-sheds. This completes the node-shed model surface construction.

FID	ZONE_ID	SHED_ID	SHED_AREA	SOIL_ID	STRATUM	SOIL_TYPE	RAIN_ID	PAN_ID	ZONE_AREA
0	483	137	622309.442503	20	Volcanic	AKINA-BADLAND COMPLEX	4156	4229	43623.179566
1	484	137	622309.442503	29	Limestone	GUAM-YIGO COMPLEX	4156	4229	75512.607666
2	485	137	622309.442503	38	Limestone	PULANTAT-CHACHA CLAYS	4156	4229	47332.315247
3	486	137	622309.442503	26	Limestone	GUAM COBBLY CLAY LOAM	4156	4229	1760.321839
4	487	137	622309.442503	25	Limestone	GUAM COBBLY CLAY LOAM	4156	4229	454228.00606
5	363	117	72389.54123	25	Limestone	GUAM COBBLY CLAY LOAM	4156	4229	71519.615551
6	478	136	390601.766478	29	Limestone	GUAM-YIGO COMPLEX	4156	4229	11886.348922
7	479	136	390601.766478	26	Limestone	GUAM COBBLY CLAY LOAM	4156	4229	80695.499228
8	480	136	390601.766478	23	Limestone	CHACHA CLAY	4156	4229	5976.134391
9	481	136	390601.766478	28	Urban	GUAM-URBAN LAND COMPLEX	4156	4229	30451.570161
10	482	136	390601.766478	25	Limestone	GUAM COBBLY CLAY LOAM	4156	4229	261844.531819
11	461	135	1752876.26296	29	Limestone	GUAM-YIGO COMPLEX	4025	4229	26179.30283
12	462	135	1752876.26296	29	Limestone	GUAM-YIGO COMPLEX	4156	4229	71993.943172
13	463	135	1752876.26296	23	Limestone	CHACHA CLAY	4025	4229	31759.262085
14	464	135	1752876.26296	29	Limestone	GUAM-YIGO COMPLEX	4025	4229	41911.28206
15	465	135	1752876.26296	29	Limestone	GUAM-YIGO COMPLEX	4156	4229	3271.915293
16	466	135	1752876.26296	29	Limestone	GUAM-YIGO COMPLEX	4025	4229	44073.105213
17	467	135	1752876.26296	18	Volcanic	AKINA-BADLAND COMPLEX	4025	4229	1204.079979
18	468	135	1752876.26296	27	Limestone	GUAM-SaipAN COMPLEX	4025	4229	37977.627838
19	469	135	1752876.26296	27	Limestone	GUAM-SaipAN COMPLEX	4156	4229	67258.308686
20	470	135	1752876.26296	26	Limestone	GUAM COBBLY CLAY LOAM	4025	4229	7157.744866
21	471	135	1752876.26296	26	Limestone	GUAM COBBLY CLAY LOAM	4156	4229	77624.594724
22	472	135	1752876.26296	23	Limestone	CHACHA CLAY	4156	4229	56770.95893
23	473	135	1752876.26296	9	Volcanic	AKINA SILTY CLAY	4025	4229	11692.874072
24	474	135	1752876.26296	28	Urban	GUAM-URBAN LAND COMPLEX	4156	4229	29461.53586
25	475	135	1752876.26296	19	Volcanic	AKINA-BADLAND COMPLEX	4025	4229	43481.400256
26	476	135	1752876.26296	25	Limestone	GUAM COBBLY CLAY LOAM	4025	4229	776981.755255
27	477	135	1752876.26296	25	Limestone	GUAM COBBLY CLAY LOAM	4156	4229	419107.512055

Figure 51. The PAT database file of the final union. This spatial attributes table requires the fields “ZONE_ID”, “SHED_ID”, “SHED_AREA”, “SOIL_ID”, “STRATUM”, “SOIL_TYPE”, “RAIN_ID”, “PAN_ID”, and “ZONE_AREA”.

As mentioned in Chapter 2, the node-shed has unique sub-shed called “zones”. Figure 52 shows another example using node-shed 59 (Observation Well M-11 point), zone id 200, having a unique polygon attribute.

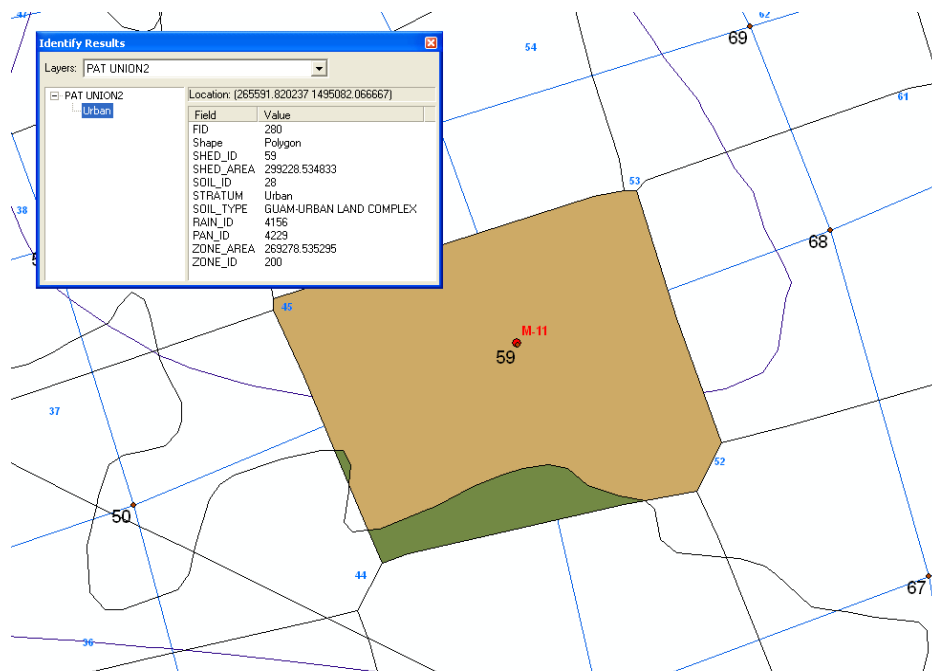


Figure 52. Node-shed 59, of node 59 and Observation Well M-11. Zone id 200 (brown area) has a unique polygon attribute as mentioned in Chapter 2.

The node-shed, spatially, is a 2-D surface map made of polygons with unique attributes referred to here as zones. It combined all the four shape file polygon layers and the information for each polygon area are in the PAT. The complete spatial configuration in GIS with the node-shed superimposing the finite element mesh is shown in Figure 53.

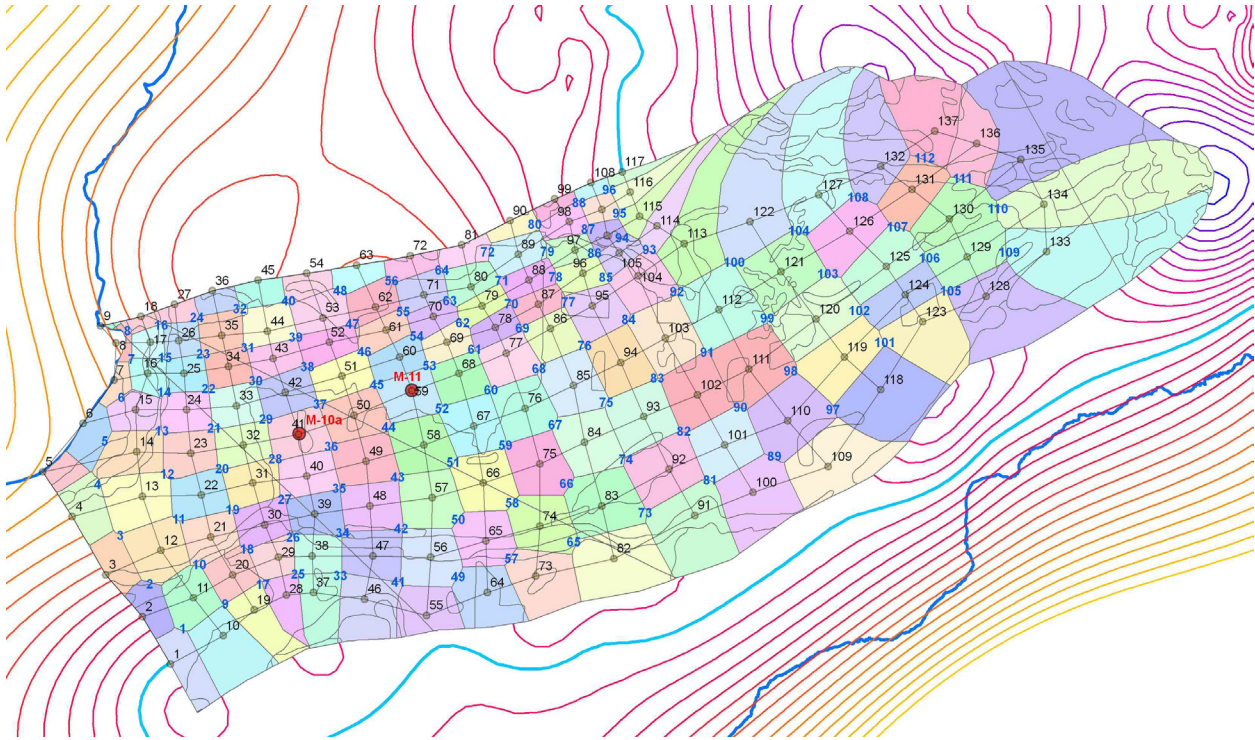


Figure 53. The node-sheds superimposed over the finite element mesh. The final product, for compiling the spatial data, is a surface map of the node-shed conceptual model as described in Chapter 2.

All-In-One Input Data

The early versions of AQUA CHARGE loaded the input data files one at a time. A common dialog box would “pop-up” for modelers to select files to open. The rain, pan evaporation, soils, and PAT files were loaded individually in that order. The AQUA CHARGE program can still do that, but now an “All-In-One” Excel file holds all the four input files (rain, pan evaporation, soils, and PAT) each in a respective data spreadsheet that speeds up the input data loading process with one file selection. The crucial part of the temporal data (rain and pan evaporation) and soil FC table and the spatially varied data (soils and PAT) is the data format set up and the naming and defining of the data sets which are clarified next.

Temporal Data (Rain and Pan Evaporation)

Temporal data of rainfall and pan evaporation were extracted from the NCDC database CD mentioned above. Both rainfall and pan evaporation data are daily measured values from the

gaging stations as located in the rain and pan evaporation spatial data. Fourteen years of data were extracted from the NCDC from 1982 to 1995 as Jocson used for temporal rain and pan data.

Upon development of AQUA CHARGE, the database format and method of extraction depended on the file type. The original programming code for extraction from file to array variables was written for the NCDC text file database format. Since software technology in the late nineties was unpredictable and the outcome of which file type was going to dominate the user preference was undecided at the time (1998). Therefore, three database file types extraction were added and programmed. AQUA CHARGE is able to open a text file from the NCDC, database file format (*.dbf), Microsoft Office's Access 1998 (*.mdb) and Excel (*.xls). Of all database formats, the Excel format was used in the final version of the program. This is due to its popularity and common familiarity among most users. The format for Excel and table set up for both daily rainfall and pan evaporation will be explained next.

The rain data format has five fields (See Figure 54). The first field is the date and its format is "mm/dd/yyyy". The other fields are gage stations AND (Andersen), DED (Dededo), WSM (WSMO), or NAS (Naval Air Station) and the data, which is in inches per day, and the data type is single precision with a two decimal place accuracy. A program was coded to extract the data from the NCDC text file to the proper fields. The pan evaporation data format is similar to the rain with the date and station measured values fields. The data collection ended in 12/31/1995. To end the data, for both rain and pan evaporation, an extra date was added, 1/1/1996, and the values for the gages were their gage ID. Figure 55 shows the pan evaporation data recordset selected and named and defined as PAN as a recordsource. The rain recordset recordsource is named and defined as RAIN. Details to naming and defining recordsets as recordsource are explained in Chapter 6.

The temporal data for both rain and pan evaporation had errors that need to be adjusted or corrected somehow. For each data set, there were missing values. The program was written to read a complete data set for any given time. There could not be any blank cells. To fill those cells, a program was written to use a hydrologic technique called the *normal ratio method* (E17) for missing data (Linsley et al., 1982).

Normal Ratio Method

$$P_x = \frac{1}{3} \left(\frac{N_x}{N_A} P_A + \frac{N_x}{N_B} P_B + \frac{N_x}{N_C} P_C \right) \quad (\text{E17})$$

Another problem with the data is the time when readings were made. The Dededo gage was read and recorded at a different time of the day than the other data. This difference in time alignment was an obvious error recognizable during major storm events. The Dededo temporal data was moved back one day (Mark Lander, personal communication). The last data changes were applied when known powerful typhoons and storm events might have caused gauges to malfunction and erroneous data was recorded as a result and was estimated with historic storm records (JTWC, 1982 - 1995; Mark Lander, personal communication). Again, details to the temporal data for both rain and pan evaporation are shown in Habana, 2008, APPENDIX B.

Vadose Flow Synthesis for the Northern Guam Lens Aquifer Data Compilation

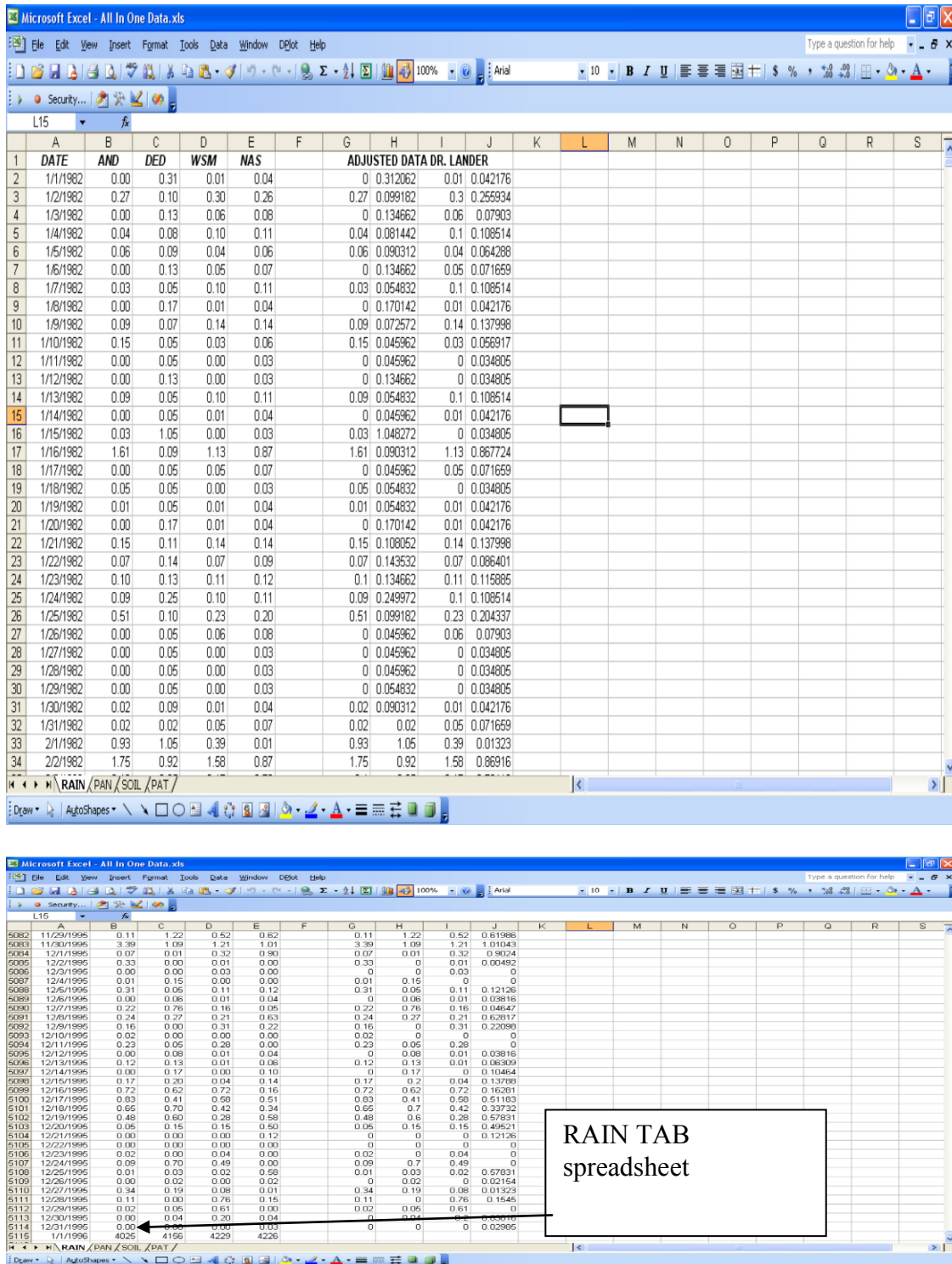


Figure 54. All-in-one data recordset setup for the rain tab. The first column is the date and the rest are gages. To the right of that recordset were adjustments to the rainfall data. Adjustments made were time alignment, normal ratio method for missing data, reference to the Joint Typhoon Warning Center records and consults from Dr. Mark Lander, Meteorologist, for gages that failed during major storms.

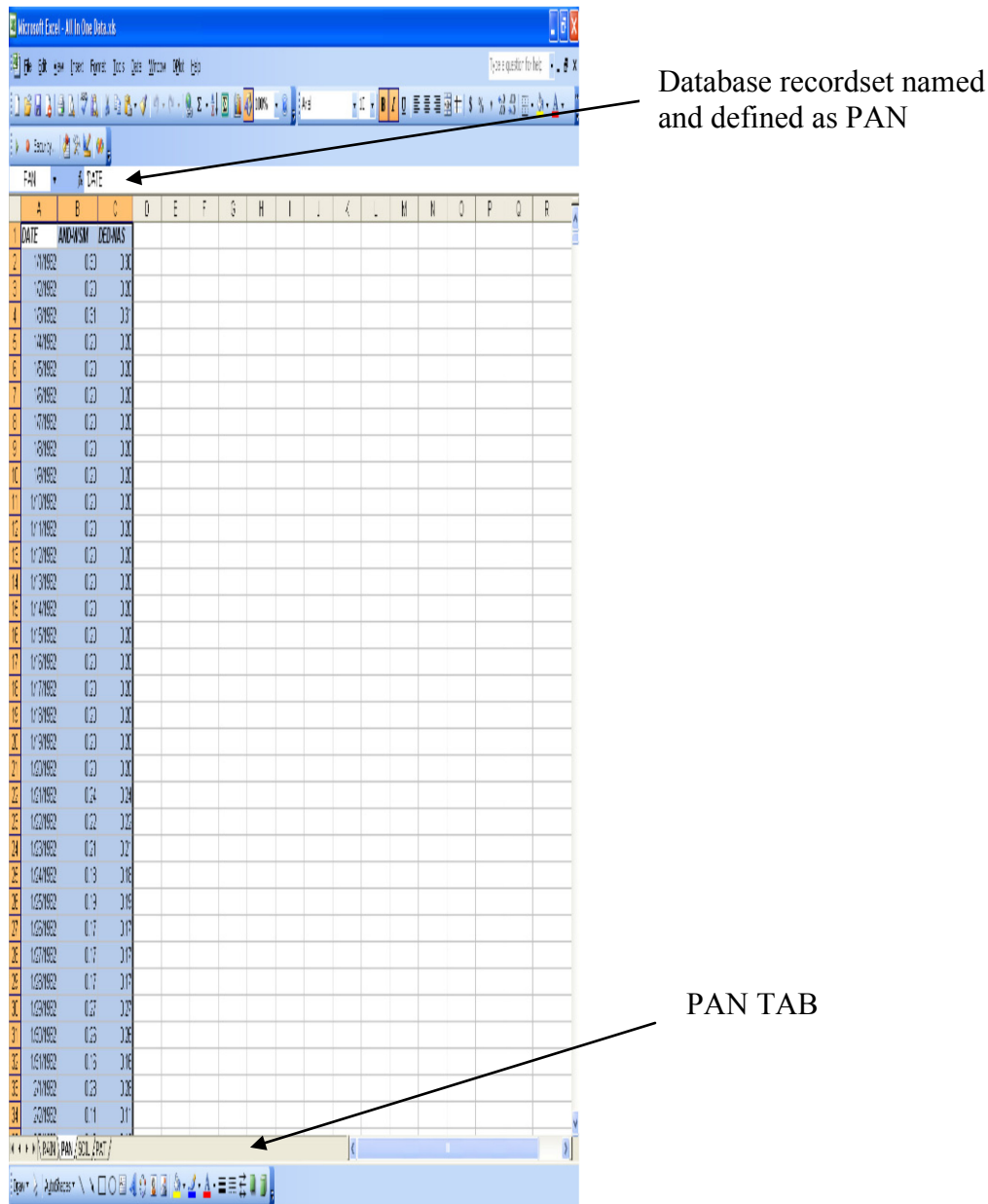


Figure 55. All-in-one Excel file data recordset setup for pan evaporation tab. WSMO and NAS pan evaporation gage records named and defined.

Soils Data

The *Soil Survey of the Territory of Guam* provided data that allowed us to model the soil's effect on moisture input. First, the list and identification of soils in the node-shed domain was obtained and then the FC was determined as described in Chapter 2. Twenty-one different mapped soils were found in the node-shed domain. The field names are given "ID", "SOIL NAME", and "FC" and the database recordsource was defined and named as SOIL (Figure 56). details to the soils in the node-shed domain are in Habana, 2008, APPENDIX D.

Vadose Flow Synthesis for the Northern Guam Lens Aquifer Data Compilation

ID	SOIL NAME	FC
1	1 AGFAYAN CLAY	1.19
9	9 AKINA SILTY CLAY	1.27
18	18 AKINA-BADLAND COMPLEX	1.27
19	19 AKINA-BADLAND COMPLEX	1.27
20	20 AKINA-BADLAND COMPLEX	1.27
23	23 CHACHA CLAY	2.68
25	25 GUAM COBBLY CLAY LOAM	1.01
26	26 GUAM COBBLY CLAY LOAM	1.01
27	27 GUAM-SAIRAN COMPLEX	3.86
28	28 GUAM-URBAN LAND COMPLEX	1.03
29	29 GUAM-YIGO COMPLEX	3.06
30	30 INARAJAN CLAY	3.83
33	33 PULANTAT CLAY	1.25
34	34 PULANTAT CLAY	1.25
38	38 PULANTAT-CHACHA CLAYS	2.92
39	39 PULANTAT-KAGMAN CLAYS	3.93
43	43 RITIDIAN-ROCK OUTCROP COMPLEX	0.32
44	44 RITIDIAN-ROCK OUTCROP COMPLEX	0.32
46	46 SASALAGUAN CLAY	1.91
47	47 SHOYA LOAMY SAND	2.07
48	48 TOGCHA-AKINA SILTY CLAYS	3.19

Figure 56. All-in-one data recordset setup for soils.

PAT Data

The PAT data can be exported from GIS as a database file. It is the last tab in the All-In-One Excel file. The data in the database file is copied and added in the spreadsheet tab named PAT (Figure 57). If any sorting is to be done, the best sort should expand from the ZONE_ID field. This speeds up the special sorter programmed in AQUA CHARGE for the spatial data. This recordsource was defined and named as PAT. The complete PAT recordset is in Habana, 2008, APPENDIX A.

PAT	A	B	C	D	E	F	G	H	I	J	K	L
	FID	ZONE_ID	SHED_ID	SOIL_ID	RAIN_ID	PAN_ID	SOIL_TYPE	STRATUM	ZONE_AREA	SHED_AREA		
1	486	1	1	28	4226	4226	GUAM-URBAN LAND COMPLEX	Urban	177,364.957	268,318.339		
2	487	2	1	25	4226	4226	GUAM COBBLY CLAY LOAM	Limestone	111,134.983	268,318.339		
3	478	3	2	44	4226	4226	RITIDIAN-ROCK OUTCROP COMPLEX	Limestone	6,108.215	190,041.914		
4	479	4	2	26	4226	4226	GUAM COBBLY CLAY LOAM	Limestone	60,674.963	190,041.914		
5	480	5	2	25	4226	4226	GUAM COBBLY CLAY LOAM	Limestone	8,124.632	190,041.914		
6	481	6	2	28	4226	4226	GUAM-URBAN LAND COMPLEX	Urban	114,877.375	190,041.914		
7	442	7	3	28	4226	4226	GUAM-URBAN LAND COMPLEX	Urban	141,540.515	204,083.150		
8	443	8	3	44	4226	4226	RITIDIAN-ROCK OUTCROP COMPLEX	Limestone	46,961.248	204,083.150		
9	444	9	3	26	4226	4226	GUAM COBBLY CLAY LOAM	Limestone	14,243.705	204,083.150		
10	445	10	3	25	4226	4226	GUAM COBBLY CLAY LOAM	Limestone	1,077.328	204,083.150		
11	381	11	4	26	4226	4226	GUAM COBBLY CLAY LOAM	Limestone	8,626.000	268,815.762		
12	382	12	4	26	4226	4226	GUAM COBBLY CLAY LOAM	Limestone	17,838.413	268,815.762		
13	383	13	4	26	4226	4226	GUAM-URBAN LAND COMPLEX	Urban	37,533.060	268,815.762		
14	384	14	4	44	4226	4226	RITIDIAN-ROCK OUTCROP COMPLEX	Limestone	40,945.185	268,815.762		
15	385	15	4	28	4226	4226	GUAM-URBAN LAND COMPLEX	Urban	163,908.179	268,815.762		
16	338	16	5	47	4226	4226	SHIOYA LOAMY SAND	Aluvium/Coastal	65,724.694	129,045.698		
17	339	17	5	28	4226	4226	GUAM-URBAN LAND COMPLEX	Urban	52,426.959	129,045.698		
18	317	18	6	47	4226	4226	SHIOYA LOAMY SAND	Aluvium/Coastal	163,922.198	206,351.241		
19	318	19	6	28	4226	4226	GUAM-URBAN LAND COMPLEX	Urban	32,498.970	206,351.241		
20	268	20	7	28	4226	4226	GUAM-URBAN LAND COMPLEX	Urban	37,440.589	91,083.179		
21	269	21	7	47	4226	4226	SHIOYA LOAMY SAND	Aluvium/Coastal	49,989.484	91,083.179		
22	228	22	8	43	4156	4226	RITIDIAN-ROCK OUTCROP COMPLEX	Limestone	7,873.435	73,890.054		
23	229	23	8	43	4226	4226	RITIDIAN-ROCK OUTCROP COMPLEX	Limestone	760.925	73,890.054		
24	230	24	8	28	4156	4226	GUAM-URBAN LAND COMPLEX	Urban	4,744.330	73,890.054		
25	231	25	8	28	4226	4226	GUAM-URBAN LAND COMPLEX	Urban	23,583.521	73,890.054		
26	185	26	9	43	4156	4226	RITIDIAN-ROCK OUTCROP COMPLEX	Limestone	3,002.478	12,547.880		
27	186	27	9	43	4226	4226	RITIDIAN-ROCK OUTCROP COMPLEX	Limestone	4,372.579	12,547.880		
28	482	28	10	28	4226	4226	GUAM-URBAN LAND COMPLEX	Urban	4,742.402	497,844.839		
29	483	29	10	26	4226	4226	GUAM COBBLY CLAY LOAM	Limestone	3,346.827	497,844.839		
30	484	30	10	28	4226	4226	GUAM-URBAN LAND COMPLEX	Urban	107,370.396	497,844.839		
31	485	31	10	25	4226	4226	GUAM COBBLY CLAY LOAM	Limestone	362,307.507	497,844.839		
32	475	32	11	44	4226	4226	RITIDIAN-ROCK OUTCROP COMPLEX	Limestone	23,427.962	307,553.302		
33	476	33	11	26	4226	4226	GUAM COBBLY CLAY LOAM	Limestone	24,346.286	307,553.302		

Figure 57. All-in-one data recordset setup for PAT. This contains polygon attributes of the node-shed spatial data extracted from GIS and sorted in increasing ZONE_ID order.

The format of and recordset naming and defining is very important to follow because AQUA CHARGE was specifically programmed to read the required data and set it into variables and arrays for use by the program. Failure to follow the data setup will lead to errors when running the program and the data will not load.

Synthesized Recharge Data

AQUA CHARGE opens and reads the All-In-One input data, converted into its respective array, for use in the stages of vadose flow or recharge synthesis computation. The second stage, routing, allows the user to send the final synthesized recharge data to the AQUA CHART for visual analysis and making first evaluations of the recharge generated. When the modeler needs to test the recharge synthesis to a finite element model, an output text file of the recharge can be saved and opened for model testing. The output text file may be used by modelers to test the recharge synthesis as an input data for a hydraulic model. Figure 58 shows a portion of an output text file of a final recharge synthesis. This data contains daily recharge values for every node from every node-shed in unit of cubic meter per day (m^3/day).

Vadose Flow Synthesis for the Northern Guam Leas Aquifer Data Compilation

The image shows a Notepad window titled 'Recharge3.txt - Notepad' containing a large table of numerical data. The data is organized into columns, with some values highlighted in blue. The window title is 'Recharge3.txt - Notepad'.

00000	000000	00000	382476	00001	930533	00005	018176	00009	179563	00014	075481	00020	873283	00029	565744	00039	757211	00051	580773	00062	654691	00072	088589		
00081	722780	00012	263795	00016	000000	00015	000000	00014	000000	00015	000000	00015	000000	00015	000000	00015	000000	00015	000000	00015	000000	00015	000000	00015	000000
00194	830249	00208	079422	00216	428538	00219	029662	00221	506957	00224	098597	00225	314717	00223	866348	00316	135949	00774	013696	01302	320516	02368	146535		
00913	463535	00683	960268	00684	585008	00805	093320	01246	384975	01274	476200	00985	891527	00789	417389	00677	222730	00625	579363	01060	969058	01264	755793		
03113	400017	02922	547279	02631	277046	02134	351144	01496	145103	01250	705677	00885	103500	00655	090839	00545	134396	0508	445619	0508	396440	05234	330477		
0511	516177	0477	102470	0442	940886	0436	293211	0414	988564	0444	960716	0441	520283	0414	596344	0438	560838	0371	614421	0438	600838	0371	614421	0438	600838
0344	214672	00326	469675	0342	881669	0361	493699	0327	153340	0350	493699	0327	153340	0350	493699	0327	153340	0350	493699	0327	153340	0350	493699	0327	153340
00136	252981	00121	693842	00108	601774	00096	594849	00085	667341	00075	781231	00066	928043	00059	056891	00052	048584	00045	803360	00040	344316	00035	457418		
00133	090655	00021	487840	00027	755966	00026	212037	00026	212037	00026	212037	00026	212037	00026	212037	00026	212037	00026	212037	00026	212037	00026	212037	00026	212037
00030	843432	00031	352366	00030	348584	00031	121958	00032	326520	00032	393030	00032	812791	00031	955957	00030	491558	00028	599021	00026	446498	00024	160320		
00021	834151	00019	541314	00017	340281	00015	281566	00013	242836	00012	232920	00011	861082	00005	578700	00008	557202	00127	140558	01336	806783	00148	687586		
00078	095505	00225	095031	00333	031227	00470	463051	01009	104572	01868	890567	01030	364178	01427	174676	00980	741929	00748	112775	00970	201972	01074	301695		
0154	382239	01044	281909	00747	903742	00576	274918	00474	322671	00142	946094	00362	272115	00310	619078	00268	466956	00232	087221	00200	604175	00174	523911		
00153	069710	01338	213381	00143	622988	00167	013467	00164	826995	00140	441236	00160	563475	00191	892201	00207	070521	00204	083957	00202	0817980	00205	789316		
0208	634486	0206	791435	0200	125662	0193	104283	0335	287505	03146	978349	07523	600506	07532	245613	04703	283092	02998	669447	01867	880810	01502	800168		
01942	228174	01834	149705	01143	863128	00699	949704	00554	255411	0462	620219	03930	449617	0477	944342	00662	609057	00717	603906	0473	649421	01027	581100		
01740	462757	0146	042846	01276	034822	01157	835566	01099	380354	01082	411004	01094	155951	01710	756748	02900	510075	03256	902812	02639	485160	02103	135482		
01728	779978	01543	752162	01243	853324	00987	797989	00858	297638	08087	981644	00806	284867	00846	086826	01549	485628	02625	634010	02697	091911	02388	698564		
0265	673233	02836	830434	0251	090765	01493	228118	01093	001091	00946	709004	00853	409398	00762	870761	00703	305312	00662	927539	00629	679995	00599	309239		
0059	145778	00522	827692	00495	818124	00506	304771	00585	579413	00657	721229	00996	528986	01540	832448	01482	921482	01002	467799	01954	856356	04018	862193		
04132	036812	02971	042755	01655	285970	03031	237659	06879	721316	08289	497443	06042	046516	03638	867001	04194	623140	07930	352413	09710	010882	07209	338907		
0698	487656	06396	660774	08830	0160315	04729	927430	04728	329667	05479	276876	06031	342425	04979	260381	05399	284297	05399	423637	05313	091653	01905	668238		
01296	994948	00613	481317	00776	566911	01324	978105	01366	700627	02881	850285	01783	108516	0585	943031	03174	612603	01585	453087	01228	439992	03950	946033		
0061	864528	01730	734135	00654	171846	04657	352684	02324	194225	01213	009563	01719	120438	03147	863445	03275	268922	03128	887133	0358	001541	03012	500168		
02411	137903	02605	290936	00421	450327	04354	985657	00202	171403	00882	012266	01819	724239	01011	026216	00605	033511	00420	191844	00337	857174	00295	740637		
0068	247297	0246	110363	00225	198833	00203	428913	00181	931710	00161	303503	00143	942373	00155	835984	00716	051016	01813	674442	02157	101125	01592	258089		
0196	055869	00846	829046	00638	983003	00489	169465	00428	013338	00018	787541	00414	643230	00418	328788	00416	590310	00408	119270	00394	487755	00378	777387		
0037	936930	00461	818238	00237	561052	00737	749394	00242	442069	00265	362187	00265	362187	00265	362187	00265	362187	00265	362187	00265	362187	00265	362187	00265	362187
00795	037652	00816	286647	00712	500891	00612	947388	00557	912983	00528	534537	00510	913730	00493	937016	00476	460827	00458	183524	00431	920379	00401	201465		
0046	802368	00438	702302	00479	604830	00598	299816	00928	005903	0105	631587	00900	349753	00740	532572	00839	857271	01188	788234	01177	941645	00881	338422		
00677	290378	00569	920148	00514	790650	00481	237496	00454	614420	00427	637173	00398	991423	00368	095246	00334	629407	00300	160949	00265	620922	00232	759279		
00202	617470	00175	527047	00131	943101	00131	365844	00113	514088	00098	140505	00084	809353	00073	240605	00063	192981	00054	480606	00047	024672	00043	600299		
0043	600299	00178	299788	00146	334392	00116	042464	00222	703762	00221	525089	00221	525089	00221	525089	00221	525089	00221	525089	00221	525089	00221	525089	00221	525089
00051	974696	00048	853713	00045	255165	00041	522666	00037	923277	00034	576240	00031	473158	00028	562195	00025	802274	00023	137517	00020	692811	00018	175644		
00016	071768	00014	853867	00014	428904	00014	763371	00015	627319	00016	688724	00017	606052	00018	164998	00018	335579	00018	335579	00018	180901	00017	552538		
00016	825294	00016	427733	00013	996540	00015	127913	00017	697048	00014	949218	00119	992206	01242	080519	00806	036638	00446	382422	02622	440072	0194	262042		
00017	652002	00018	299788	00041	073387	00044	926338	00044	926338	00044	926338	00044	926338	00044	926338	00044	926338	00044	926338	00044	926338	00044	926338	00044	926338
00170	644848	00154	481440	00138	060600	00121	927227	00106	638235	00099	206980	00092	368547	00079	351812	00067	679739	00057	368085	00048	378767	00040	630923		
0034	024550	00027	662399	00022	347477	00018	716939	00016	263125	00015	083846	00014	586197	00014	460177	00014	460177	00014	460177	00014	270329	00014	270329	00014	270329
00012	317239	00011	381521	00010	380294	00009	869744	00009	374084	00008	784244	00008	505345	00007	958284	00007	784303	00007	784303	00007	784303	00007	784303	00007	784303
00007	784303	00007	784303	00007	784303	00007	784303	00007	784303	00007	784303	00007	784303	00007	784303	00007	784303	00007	784303	00007	784303	00007	784303	00007	784303
00005	163187	00011	515760	00007	421357	00004	926338																		

Finite Element Method Data (FEMData)

AQUA CHARGE has a simple finite element method program included for calibrating the recharge synthesis results with the observation well data. The finite element method coded in AQUA CHARGE uses an Excel file database called FEMData that is accessed by selecting the file through a common dialog box. This database file holds data extracted from the GIS designed finite element mesh and other parameter settings and information about the model. The database is set up similar to the All-In-One data with spreadsheets that has the mesh domain information on the number of nodes, number of elements, x-y coordinates of nodes, boundary conditions, initial node values, and so on. This section will cover the data setup for all the recordset in the FEMData. Habana, 2008, APPENDIX G and APPENDIX H show details to this FEMData input file.

COMALL

The first spreadsheet, tab named COMALL (Istok, 1989), has variables with values that describe the finite element mesh design and parameter values used for calculation. Finite element mesh values for example are maximum number of nodes, maximum number of elements, number of nodes per element, and so on (see Figure 59). Other parameters include SBW, omega, omomega, number of Dirichlet nodes, just to name a few, that are required during computation. The recordset is named and defined as COMALL.

VARIABLE	VALUE	DESCRIPTION
MAX1	137	MAXIMUM NUMBER OF NODES
MAX2	112	MAXIMUM NUMBER OF ELEMENTS
MAX3	4	MAXIMUM NUMBER OF NODES PER ELEMENT
MAX4	3	MAXIMUM NUMBER OF MATERIAL SETS
MAX5	4	MAXIMUM NUMBER OF MATERIAL PROPERTIES
MAX6	11	MAXIMUM VALUE OF SEMI-BANDWIDTH
MAX7	20	MAXIMUM NUMBER OF DIFFERENT TIME STEP INCREMENTS
MAX8	1000	MAXIMUM SIZE OF MODIFIED GLOBAL CONDUCTANCE MATRIX IN VECTOR STORAGE
SYMM	FALSE	TRUE = SYMMETRICAL, FALSE=NON SYMMETRICAL
DIM	2	FINITE ELEMENT MESH DIMENSION
NUMNOD	137	TOTAL NUMBER OF NODES
NUMELM	112	TOTAL NUMBER OF ELEMENTS
NUMMAT	3	TOTAL NUMBER OF MATERIALS
NUMPROP	3	TOTAL NUMBER OF PROPERTIES
NDN	0	NUMBER OF DIRICHLET NODES
NDN	137	NUMBER OF NEUMANNI NODES
NDOF	137	NUMBER OF DEGREES OF FREEDOM, number of nodes - number of dirichlet nodes
SBW	11	SEMI-BANDWIDTH
OMEGA	0.001	OMEGA
OMOMEGA	0.999	1-OMEGA
MAVSTEP	1	
T	5113	
DT	1	
IST	1	
IGDT	1	

Figure 59. FEMData Excel file recordset setup for COMALL tab.

Node X-Y Coordinates

The node x and y coordinates for the node points can be obtained through GIS. The GIS coordinate system is set to meters rather than latitudinal and longitudinal. The database file is then extracted from GIS and transferred to Excel (Figure 60). The recordset includes material set number for each node and the node-shed area for that node. The recordset is named and defined as NODESHED.

NODES	POINT X	POINT Y	MATERIAL SET NUMBER	SHED AREA
1	263061.556779	1492132.946970	2	288318.3389
2	262751.571194	1492649.588620	1	190041.9145
3	262353.018298	1493107.186390	1	204083.1497
4	261983.987639	1493741.918770	1	268815.7621
5	261659.241035	1494229.038980	1	129045.6977
6	262102.077686	1494760.442840	1	206351.2409
7	262441.585608	1495232.801830	1	91083.17865
8	262463.714555	1495635.966000	1	73890.05432
9	262293.973425	1495823.250560	1	12547.87954
10	263637.244296	1492442.931560	2	497844.8389
11	263312.497492	1492856.245670	1	307553.3017
12	262968.228251	1493372.888320	1	374965.1003
13	262751.571194	1493963.337050	1	405383.8851
14	262692.526320	1494450.457260	1	326879.0704
15	262677.765102	1494908.055020	1	218364.2838
16	262810.616067	1495306.607920	1	152435.5957
17	262840.138504	1495646.115940	1	114160.4523
18	262736.809976	1495926.579090	1	61528.30811
19	263976.752318	1492723.394710	2	326567.3225
20	263740.572624	1493107.186390	1	238891.5296
21	263504.393330	1493520.500500	1	279049.8383
22	263401.064802	1493978.098270	1	288955.1513
23	263282.975055	1494435.688040	1	272080.3696
24	263238.691400	1494908.055020	1	234235.4218
25	263209.168963	1495306.607920	1	168926.6423
26	263150.124090	1495660.877160	1	149726.5888
27	263105.840435	1496059.430060	1	84636.26709
28	264331.021558	1492885.768110	2	214967.294
29	264242.454248	1493299.082220	1	186573.304
30	264094.842065	1493653.351460	1	252723.5889
31	263961.991099	1494110.949230	3	263993.7199
32	263858.662571	1494524.263350	3	258634.9771
33	263784.856479	1494952.338680	3	242593.9041

Figure 60. FEMData recordset setup for NODEXY tab.

Element Nodes

Element nodes have two recordsets in the spreadsheet named ELMNTNODES. The recordset names are ELMNTNODES, left of spreadsheet, and MATPROP at the right (Figure 61). Element nodes describes the nodes connected to an element and the node number, from the bottom left corner, identifying the nodes in a counter clockwise fashion (Figure 62). A special Excel program called *Elements in Nodes* was written that used angles to sweep the order of nodes around the element from a reference point. Type “6” is from Istok’s coding that describes a 2-D, quadrilateral, mesh type design. The “MATERIAL SET NUMBER” field in the ELMNTNODES recordset identifies which “MATERIAL PROPERTIES”. In this project, 3 material properties were made, where each have specified hydraulic conductivities K_x and K_y (in the x and y direction) and its specific storage, S_s .

ELEMENT	TYPE	N1	N2	N3	N4	MATERIAL SET NUMBER	MATERIAL PROPERTIES Kx	Ky	Ss
1	6	1	10	11	2	2	3450	3450	0.0003
2	6	2	11	12	3	3	4500	4400	0.001
3	6	3	12	13	4	3	6500	6500	0.0008
4	6	4	13	14	5	3			
5	6	5	14	15	6	1			
6	6	6	15	16	7	1			
7	6	7	16	17	8	1			
8	6	8	17	18	9	1			
9	6	10	19	20	11	2			
10	6	11	20	21	12	1			
11	6	12	21	22	13	1			
12	6	13	22	23	14	1			
13	6	14	23	24	15	1			
14	6	15	24	25	16	1			
15	6	16	25	26	17	1			
16	6	17	26	27	18	1			
17	6	19	28	29	20	2			
18	6	20	29	30	21	1			
19	6	21	30	31	22	1			
20	6	22	31	32	23	1			
21	6	23	32	33	24	1			
22	6	24	33	34	25	1			
23	6	25	34	35	26	1			
24	6	26	35	36	27	1			
25	6	28	37	38	29	2			
26	6	29	38	39	30	1			
27	6	30	39	40	31	1			
28	6	31	40	41	32	3			
29	6	32	41	42	33	3			
30	6	33	42	43	34	1			
31	6	34	43	44	35	1			
32	6	35	44	45	36	1			
33	6	37	46	47	38	2			
34	6	38	47	48	39	2			

Figure 61. FEMData recordset setup for ELMNTNODES tab.

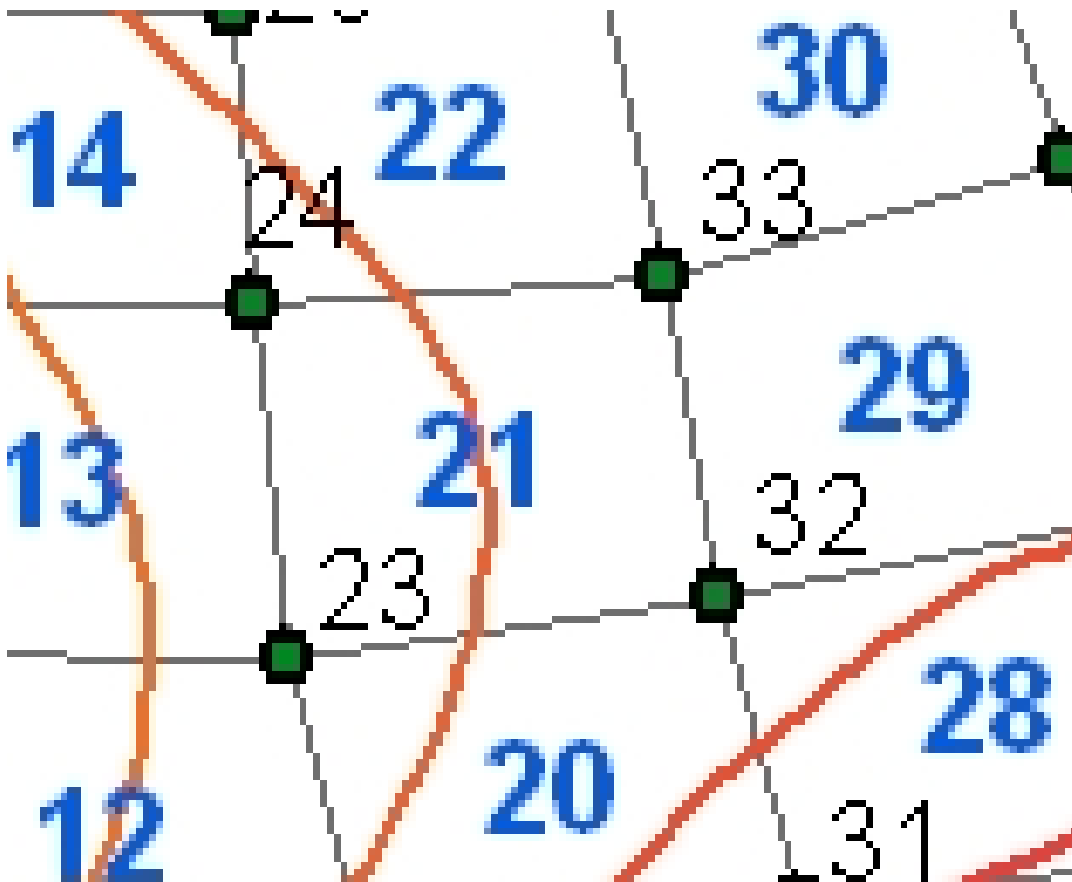
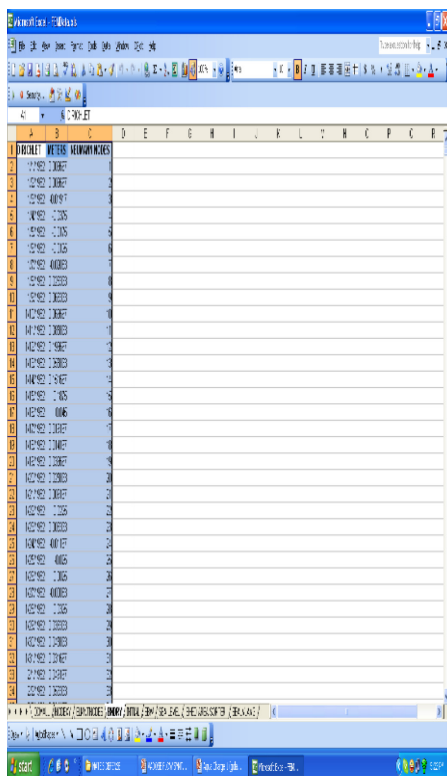


Figure 62. Element nodes numbering order. Element 21, with neighboring nodes, numbering order is from the bottom left counterclockwise, 23, 32, 33, and 24.

Boundary Conditions

The boundary conditions for Dirichlet Nodes were configured within the internal code. The Variable Dirichlet Nodes, shoreline nodes, were hard coded into the finite element codes that are set to receive tidal changes with time. The recordset for Dirichlet nodes are the date and the average sea level in meters for a given day.

The Neumann nodes were set for all the nodes except the shore. The recordset shows that it has all the node values, but the shore nodes were identified within the code to change to Dirichlet Nodes. The spreadsheet tab is named BNDRY (Figure 63) with two recordset names DIRICHLET and NEUMANN. This recordset was left to exist and one day may be used. Since there were only five shoreline nodes, a simple code handled the data for both boundary conditions for use in the computation.



	DIRICHLET	NEUMANN	NEUMANN
1	1/1/92	1.000	1.000
2	1/1/92	1.000	1.000
3	1/1/92	1.000	1.000
4	1/1/92	1.000	1.000
5	1/1/92	1.000	1.000
6	1/1/92	1.000	1.000
7	1/1/92	1.000	1.000
8	1/1/92	1.000	1.000
9	1/1/92	1.000	1.000
10	1/1/92	1.000	1.000
11	1/1/92	1.000	1.000
12	1/1/92	1.000	1.000
13	1/1/92	1.000	1.000
14	1/1/92	1.000	1.000
15	1/1/92	1.000	1.000
16	1/1/92	1.000	1.000
17	1/1/92	1.000	1.000
18	1/1/92	1.000	1.000
19	1/1/92	1.000	1.000
20	1/1/92	1.000	1.000
21	1/1/92	1.000	1.000
22	1/1/92	1.000	1.000
23	1/1/92	1.000	1.000
24	1/1/92	1.000	1.000
25	1/1/92	1.000	1.000
26	1/1/92	1.000	1.000
27	1/1/92	1.000	1.000
28	1/1/92	1.000	1.000
29	1/1/92	1.000	1.000
30	1/1/92	1.000	1.000
31	1/1/92	1.000	1.000
32	1/1/92	1.000	1.000
33	1/1/92	1.000	1.000
34	1/1/92	1.000	1.000
35	1/1/92	1.000	1.000
36	1/1/92	1.000	1.000
37	1/1/92	1.000	1.000
38	1/1/92	1.000	1.000
39	1/1/92	1.000	1.000
40	1/1/92	1.000	1.000
41	1/1/92	1.000	1.000
42	1/1/92	1.000	1.000
43	1/1/92	1.000	1.000
44	1/1/92	1.000	1.000
45	1/1/92	1.000	1.000
46	1/1/92	1.000	1.000
47	1/1/92	1.000	1.000
48	1/1/92	1.000	1.000
49	1/1/92	1.000	1.000
50	1/1/92	1.000	1.000
51	1/1/92	1.000	1.000
52	1/1/92	1.000	1.000
53	1/1/92	1.000	1.000
54	1/1/92	1.000	1.000
55	1/1/92	1.000	1.000
56	1/1/92	1.000	1.000
57	1/1/92	1.000	1.000
58	1/1/92	1.000	1.000
59	1/1/92	1.000	1.000
60	1/1/92	1.000	1.000
61	1/1/92	1.000	1.000
62	1/1/92	1.000	1.000
63	1/1/92	1.000	1.000
64	1/1/92	1.000	1.000
65	1/1/92	1.000	1.000
66	1/1/92	1.000	1.000
67	1/1/92	1.000	1.000
68	1/1/92	1.000	1.000
69	1/1/92	1.000	1.000
70	1/1/92	1.000	1.000
71	1/1/92	1.000	1.000
72	1/1/92	1.000	1.000
73	1/1/92	1.000	1.000
74	1/1/92	1.000	1.000
75	1/1/92	1.000	1.000
76	1/1/92	1.000	1.000
77	1/1/92	1.000	1.000
78	1/1/92	1.000	1.000
79	1/1/92	1.000	1.000
80	1/1/92	1.000	1.000
81	1/1/92	1.000	1.000
82	1/1/92	1.000	1.000
83	1/1/92	1.000	1.000
84	1/1/92	1.000	1.000
85	1/1/92	1.000	1.000
86	1/1/92	1.000	1.000
87	1/1/92	1.000	1.000
88	1/1/92	1.000	1.000
89	1/1/92	1.000	1.000
90	1/1/92	1.000	1.000
91	1/1/92	1.000	1.000
92	1/1/92	1.000	1.000
93	1/1/92	1.000	1.000
94	1/1/92	1.000	1.000
95	1/1/92	1.000	1.000
96	1/1/92	1.000	1.000
97	1/1/92	1.000	1.000
98	1/1/92	1.000	1.000
99	1/1/92	1.000	1.000
100	1/1/92	1.000	1.000

Figure 63. FEMData recordset setup for BNDRY tab.

Initial Head

Initial head was determined using an Excel Visual Basic (VB) written program called *Head Hunter*. The program first uses the modes (through frequency analysis) of the observation wells M-10a and M-11 and the daily average recharge at those observation well nodes. Then, for each well, the hydraulic conductivity was determined, solving for “K” using the Dupuit-Ghyben Herzberg equation. The distance of the well nodes from the shore was determined using the distance formula. The hydraulic conductivities from the two wells were averaged. Then an algorithm employing the Dupuit-Ghyben Herzberg was coded to sweep through all the nodes

with respect to their distance from the shore to determine the hydraulic gradient and the hydraulic heads at each node. The hydraulic head was then converted to feet and meters interchangeably used in the finite element code. The finite element method Istok coded used meters and was converted to feet outside this code for displaying results in AQUA CHART. Spreadsheet tab named INITIAL holds the recordset source for initial heads (Figure 64). The code required other field variables, shown on the sheet, “END”, “DT”, “T”, and “GT” were abandoned since the time step is daily, “one”, and does not change, as it was hard set in the program code. Istok has a special code using the variables for changing time steps which was not necessary for this hydraulic model since the daily time step does not change. The “NODE” and “VALUE”, starts the initial setting of the hydraulic head to zero for every node, then to its specified initial value. See Habana, 2008, APPENDIX G for details to this data.

1	END	DT	T	GT	NODE	VALUE	NODE	HEAD FT	HEAD M	INTERFACE DEPTH
2	1	1		0	1	0	1	2.60	0.79386280	
3			100.1	1	137	0	2	2.27	0.69274407	
4							3	1.88	0.57412886	
5							4	1.25	0.38249242	
6							5	0.02	0.00666667	
7							6	0.02	0.00666667	
8							7	0.02	0.00666667	
9							8	0.02	0.00666667	
10							9	0.02	0.00666667	
11							10	2.68	0.81608436	
12							11	2.40	0.73280556	
13							12	2.05	0.62351889	
14							13	1.74	0.53002658	
15							14	1.69	0.51388284	
16							15	1.26	0.38537754	
17							16	1.01	0.30666837	
18							17	1.01	0.30675883	
19							18	1.11	0.33709880	
20							19	2.73	0.83104003	
21							20	2.52	0.76867387	
22							21	2.31	0.70279662	
23							22	2.18	0.66315048	
24							23	2.10	0.63956047	
25							24	1.76	0.53518258	
26							25	1.44	0.43897676	
27							26	1.36	0.41429921	
28							27	1.51	0.45966581	
29							28	2.84	0.86446572	
30							29	2.72	0.82830607	
31							30	2.59	0.79083340	
32							31	2.49	0.75908097	
33							32	2.44	0.74468492	
34							33	2.13	0.65057274	

Figure 64. FEMData recordset setup for INITIAL tab.

Semi-Bandwidth (SBW)

The SBW is determined in the code to prepare the global conductance and capacitance matrix. The numbering of the nodes and elements was done carefully to produce the smallest SBW. A small SBW configuration speeds up matrix computation. In the early stages of programming, the SBW was determined in the SBW spreadsheet, tab named SBW (Figure 65). the SBW result was entered in the maximum SBW is a variable in the COMALL spread sheet as a set value. To determine SBW for each element, it is the highest node number minus the lowest node number of all the nodes around an element plus one. For example, Element 1 has node neighbors 1, 10, 11, and 2. Node 11 is the highest node number minus 1, the lowest node

Vadose Flow Synthesis for the Northern Guam Lens Aquifer
Data Compilation

number, plus one which results in 11. Therefore, the SBW of Element 1 is 11. Each element's SBW is determined and the maximum SBW solved is the mesh's SBW entered in COMALL.

ELEMENT	TYPE	N1	N2	N3	N4	MAX	MIN	DIFF	SBW	MAXSBW
1	1	6	1	10	11	2	11	1	10	11
2	2	6	2	11	12	3	12	2	10	11
3	3	6	3	12	13	4	13	3	10	11
4	4	6	4	13	14	5	14	4	10	11
5	5	6	5	14	15	6	15	5	10	11
6	6	6	6	15	16	7	16	6	10	11
7	7	6	7	16	17	8	17	7	10	11
8	8	6	8	17	18	9	18	8	10	11
9	9	6	10	19	20	11	20	10	10	11
10	10	6	11	20	21	12	21	11	10	11
11	11	6	12	21	22	13	22	12	10	11
12	12	6	13	22	23	14	23	13	10	11
13	13	6	14	23	24	15	24	14	10	11
14	14	6	15	24	25	16	25	15	10	11
15	15	6	16	25	26	17	26	16	10	11
16	16	6	17	26	27	18	27	17	10	11
17	17	6	19	28	29	20	29	19	10	11
18	18	6	20	29	30	21	30	20	10	11
19	19	6	21	30	31	22	31	21	10	11
20	20	6	22	31	32	23	32	22	10	11
21	21	6	23	32	33	24	33	23	10	11
22	22	6	24	33	34	25	34	24	10	11
23	23	6	25	34	35	26	35	25	10	11
24	24	6	26	35	36	27	36	26	10	11
25	25	6	28	37	38	29	38	28	10	11
26	26	6	29	38	39	30	39	29	10	11
27	27	6	30	39	40	31	40	30	10	11
28	28	6	31	40	41	32	41	31	10	11
29	29	6	32	41	42	33	42	32	10	11
30	30	6	33	42	43	34	43	33	10	11
31	31	6	34	43	44	35	44	34	10	11
32	32	6	35	44	45	36	45	35	10	11
33	33	6	37	46	47	38	47	37	10	11
34	34	6	37	46	47	38	47	37	10	11

Figure 65. SBW size solutions tab.

The rest of the tabs are used for doing special calculations and configurations, to be transferred to the useful recordsets in the database. These extra tab spreadsheets are SEA LEVEL, SHED AREA SORTER, and SEALVLAVG and are not used by the finite element code as a recordsource.

This completes the input data for AQUA CHARGE to run both models. The next chapter discusses methods, coding, and interface design of AQUA CHARGE.

METHODS, USER INTERFACE DESIGN, AND CODE DEVELOPMENT

The programming and code development for AQUA CHARGE is explained through descriptions of the mathematical models used and program logical flow diagrams. The computer program is developed in MICROSOFT® (MS) Visual Basic (VB) 6.0, Professional. The program allows the user to load the input data temporal rainfall and pan evaporation, soils properties, and PAT data. Then the data is extracted and set into array variables. Next, the area weighted average (AWA) recharge is calculated for each node-shed. Finally, a modified pulse routing method simulates the lagged and attenuated flow of recharge to the lens. A special chart for result analysis called AQUA CHART is prepared in MICROSOFT® Excel to view graphically the synthesized recharge for a specified node shed. The user may export the synthesized recharge for a hydraulic groundwater (GW) modeling program.

Development of AQUA CHARGE via MS VB 6.0

AQUA CHARGE was programmed in the *BASIC* language. Microsoft VB 6.0 allows the development of applications with an easy to use Graphical User Interface allowing the building and design of the program with ready made functional forms and controls (GUI, see Figure 66). The programming development of AQUA CHARGE is discussed next.

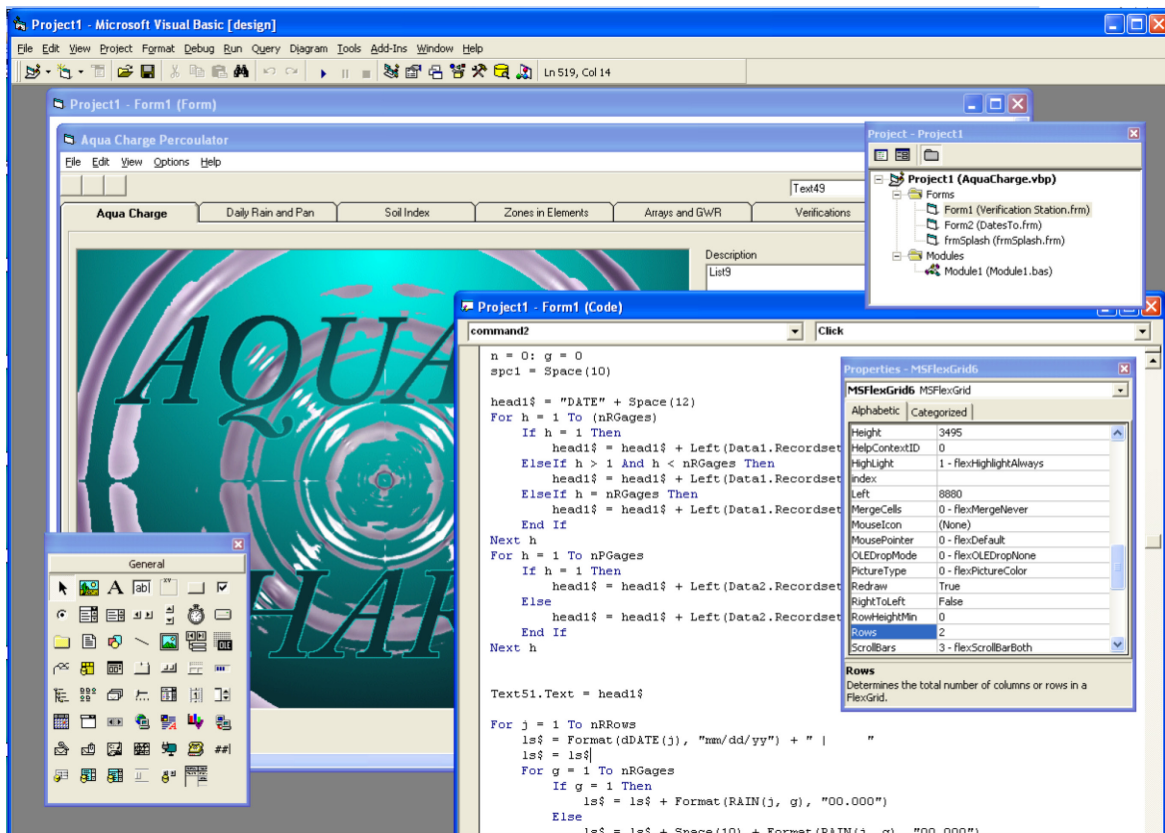


Figure 66. MICROSOFT® Visual Basic 6.0 programming environment.

Input Data

AQUA CHARGE requires four data recordsets as input which can be assembled in an Excel workbook as an “All-In-One” data (see Chapter 4). The logical flow diagram (Figure 67) for data input shows the rainfall data, pan evaporation data, soil properties data, and the polygon attribute table (PAT) data. A common dialog box allows the user to open the All-In-One data recordsets. Each data recordset in the workbook is converted into its respective array variables and displayed in the tabbed user interfaces. The soils characteristics can be adjusted by changing the shape of the curves, using the equalizer like curve adjuster, that affects how recharge and evapotranspiration (ET) are modeled. The PAT data goes through a sorter to optimize the order of execution, in case the sorting was not done prior, and to increase the speed of calculation as it sweeps through the spatial zones.

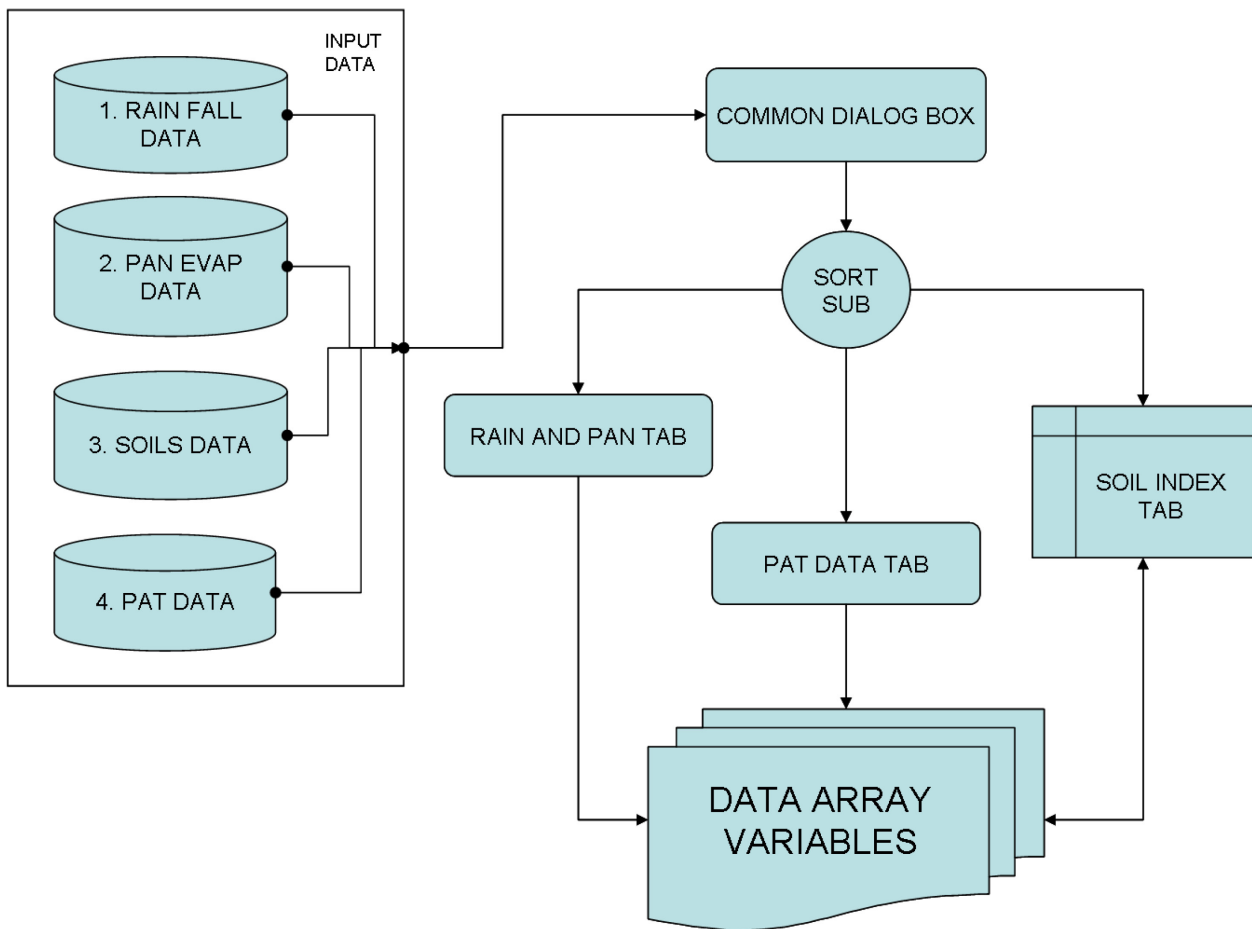


Figure 67. Input data programming flow diagram. The sorting sub-routines move the data to its appropriate tab and assigns them to their respective array.

The loaded data are displayed in tabs in the GUI of AQUA CHARGE. The rain and pan evaporation data are shown in the second tab (Figure 68), the soils data are shown in the third tab (Figure 69), and the PAT data are shown in the fourth tab (Figure 70).

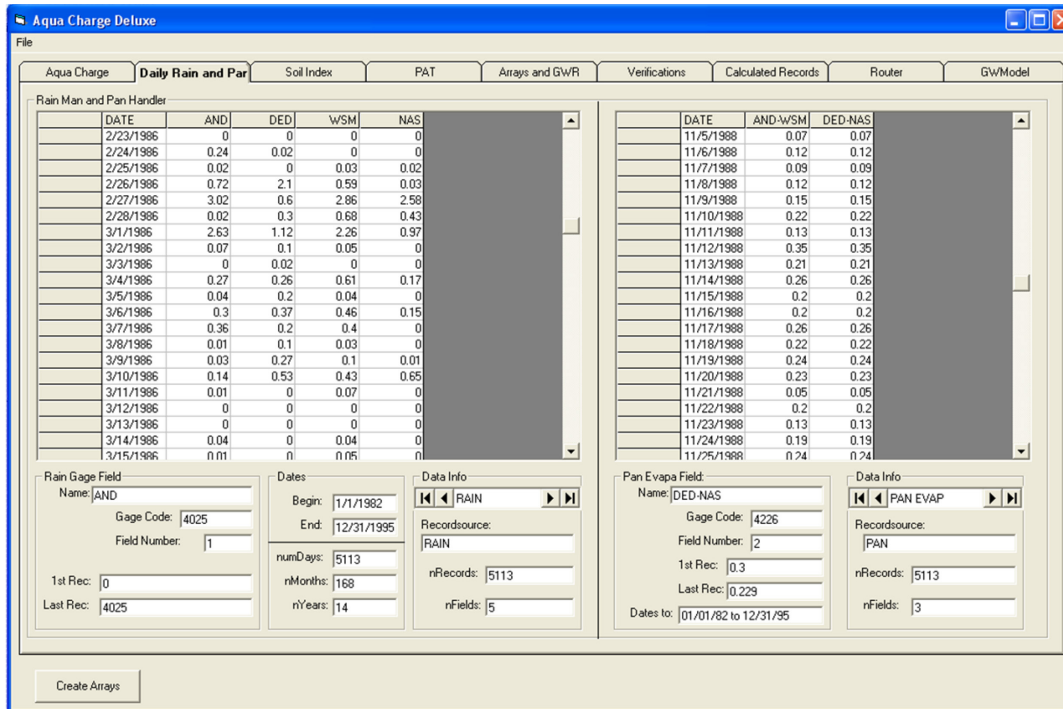


Figure 68. AQUA CHARGE Daily Rain and Pan Evaporation tab. This tab shows data information for the gaging stations.

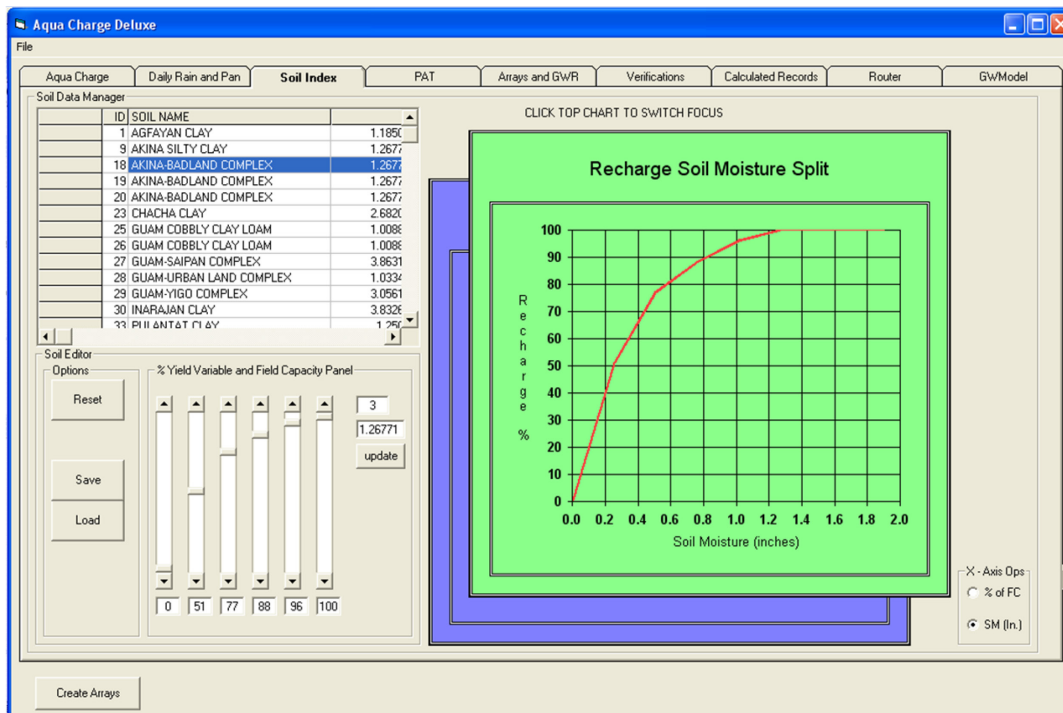


Figure 69. AQUA CHARGE Soil Index tab. Clicking on the front chart brings the back chart to the front and sets relationship curve on focus. The % Yield Variable and Field Capacity Panel lets the modeler adjust the curve shape and change the field capacity of a selected soil type. The SM curves can be saved or loaded.

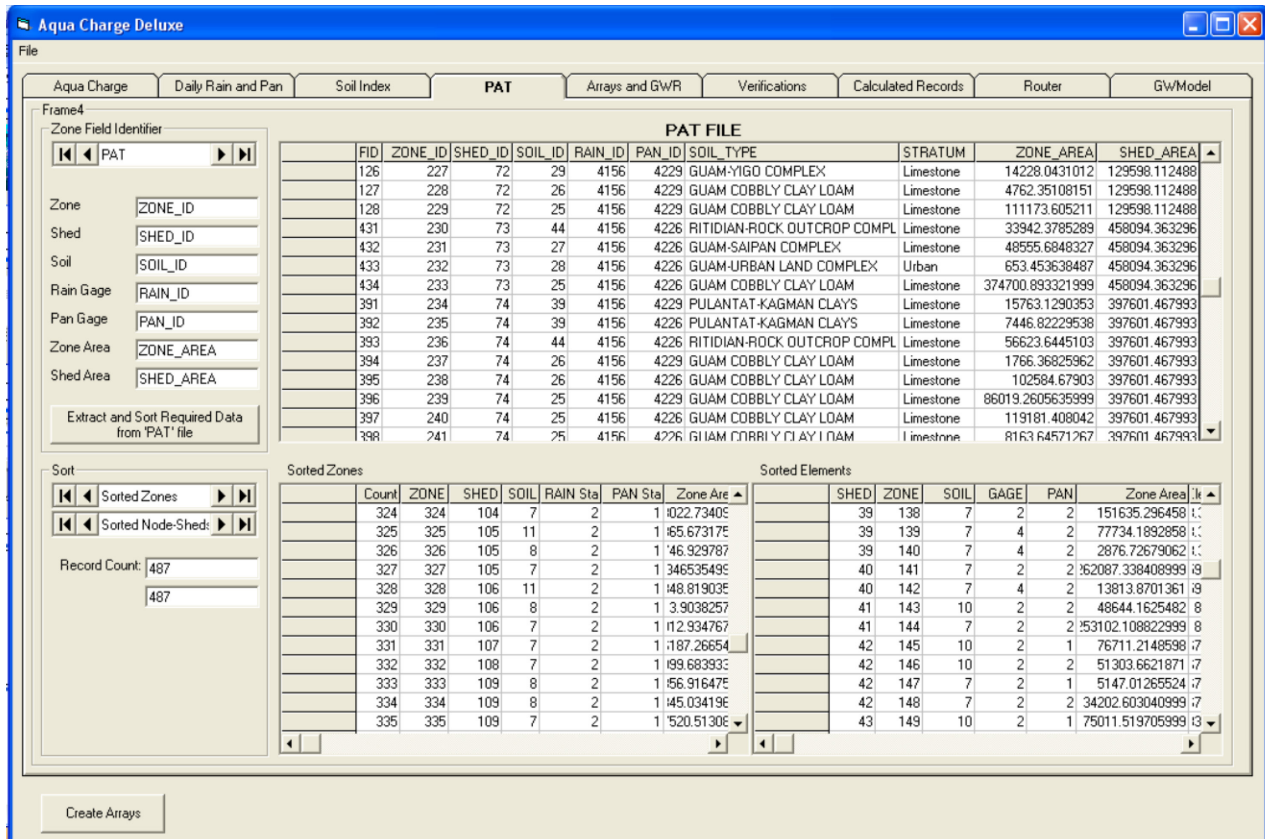


Figure 70. AQUA CHARGE PAT tab. This tab extracts the necessary fields and puts them in order.

The soil tab displays two soil curves (Recharge and ET), a list of soils in the domain, adjustment for the curves, view changes, and save and open buttons. Once the Excel file of soils properties is loaded, a default linear graph is displayed. Clicking on the chart will switch the display of either the recharge curve or the ET curve. Each soil in the table may be selected and the chart will show that soil's curve with the field capacity (FC). The view of the x-axis may be changed to display the percent of FC or FC in inches. The curves may be adjusted with the vertical control bars to the left of the chart. The adjusted curves may be saved to a special type text file and it may be opened for test and setting purposes. ET and recharge curve settings saves into file type extensions *.etp, and *.rep respectively.

The zone tab displays the PAT table. To the left of the table, the user may click the text box and select the proper field on the table. Once, the proper fields "Zone", "Shed", "Soil", "Rain Gage", "Pan Gage", "Zone Area", and "Shed Area" are selected, and the proper names of the field names in the PAT file are in their appropriate text box, the sorter button is clicked next to display an optimized ordering of the PAT file. This helps to speed up the calculation process. Only the selected fields are displayed during the sort.

Zone Recharge

The programming of recharge calculation for each zone is based on the simple mathematical model of the SM water budget/balance (E17) also described in Chapter 2.

$$SM_t = SM_{t-1} + P_t(1 - R\%_{(t-1)}) - PAN_t(ET\%_{(t)}) \quad (E17)$$

This equation manages only the SM budget. To determine recharge, we expand the equation:

$$P_t(1 - R\%_{(t-1)}) = P_t - P_t(R\%_{(t-1)}) \quad (E18)$$

The term $P_t(R\%_{(t-1)})$ is the percent ($R\%_{(t-1)}$) of rainfall (P_t) that goes into recharge amount for the period. This value is stored into a recharge array for each day and each zone. Also, excess SM (SM greater than FC) goes into recharge for that period (see Chapter 2).

Recharge is calculated within each unique zone area using its special attributes. For a specified zone, a water balance flow diagram (Figure 71) describes how the recharge calculation is programmed. The program sweeps through the entire spatial data for every zone on a daily basis. Zone recharges for every day and most calculation results are stored into an array variable.

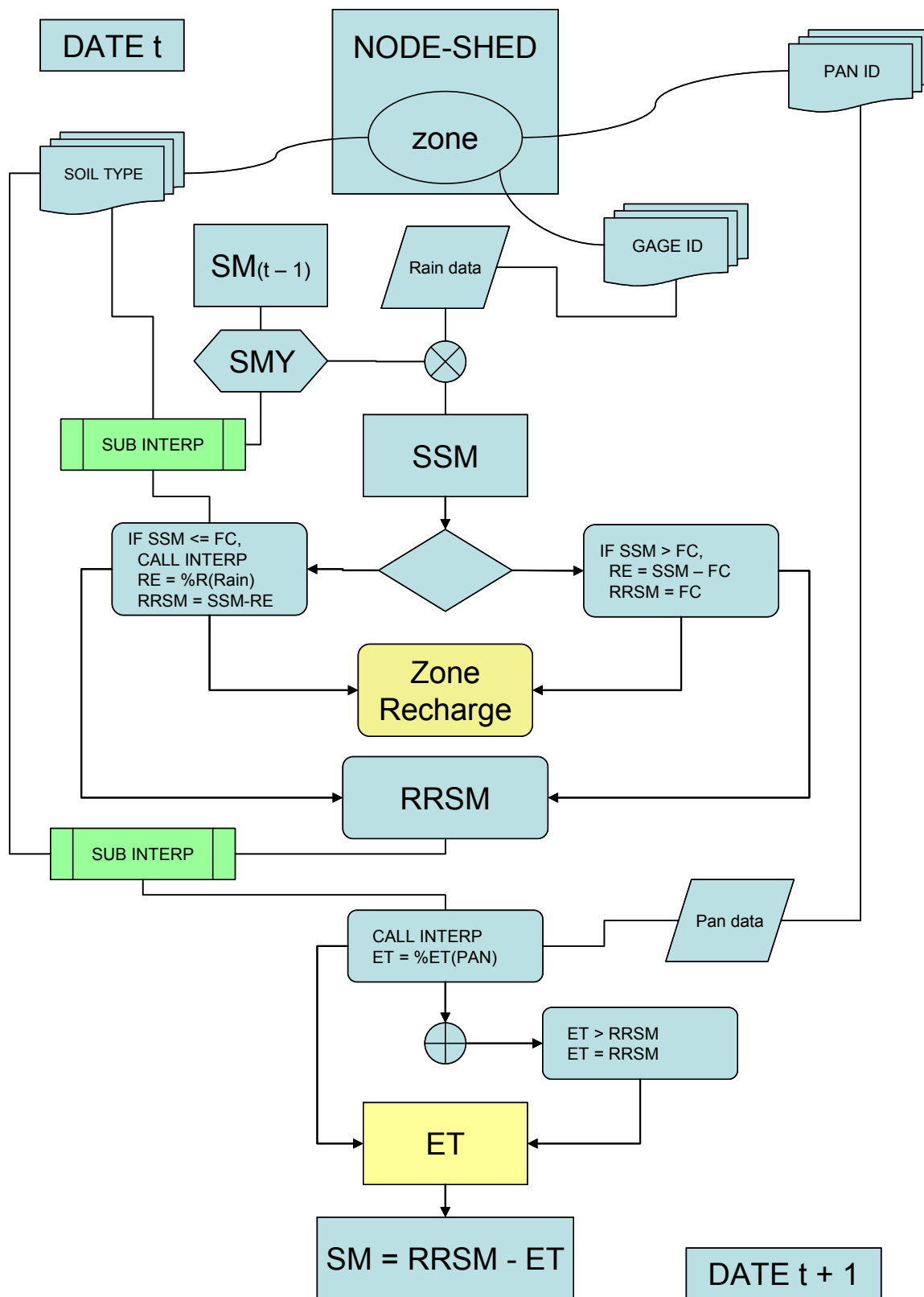


Figure 71. Programming flow diagram of zone recharge. A linear interpolation sub-routine solves the percent moisture splitters.

Area Weighted Average Recharge

In the same program loop, where the daily zone recharge is determined, the AWA daily recharge for the node-shed is being calculated (see Figure 72). A special algorithm and array setup does this instantly with the following code equation (E19):

$$AWR(d,s) = AWR(d,s) + \frac{zArea}{sArea} (zR(d,z)). \tag{E19}$$

$AWR(d,s)$ is an AWA recharge array variable for a given day number “d” and node-shed number “s”. $zArea$ and $sArea$ are zone area and node-shed area respectively. $zR(d,z)$ is the zone recharge for the day for a given zone. The AWAs were calculated for other values such as SM, change in SM, pan coefficients and so on. Once the AWAs for a node-shed are calculated, special algorithms were made to produce monthly sums and averages as well as yearly averages of selected values to produce monthly node-shed recharge (Figure 72) and a summary values tab (Figure 73).

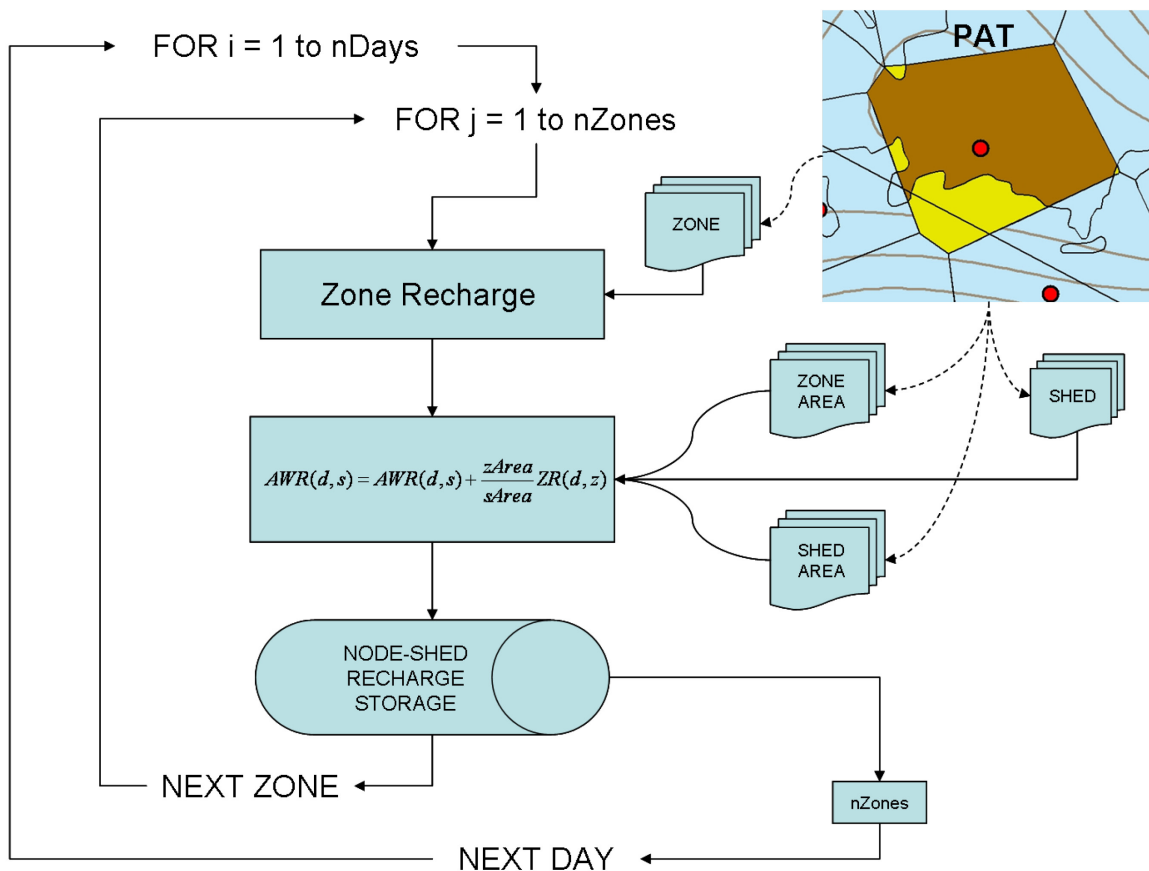


Figure 72. Programming flow diagram of area weighted average recharge. This is done in the same loop as zone recharge is calculated.

Vadose Flow Synthesis for the Northern Guam Lens Aquifer
 Methods, User Interface Design, and Code Development

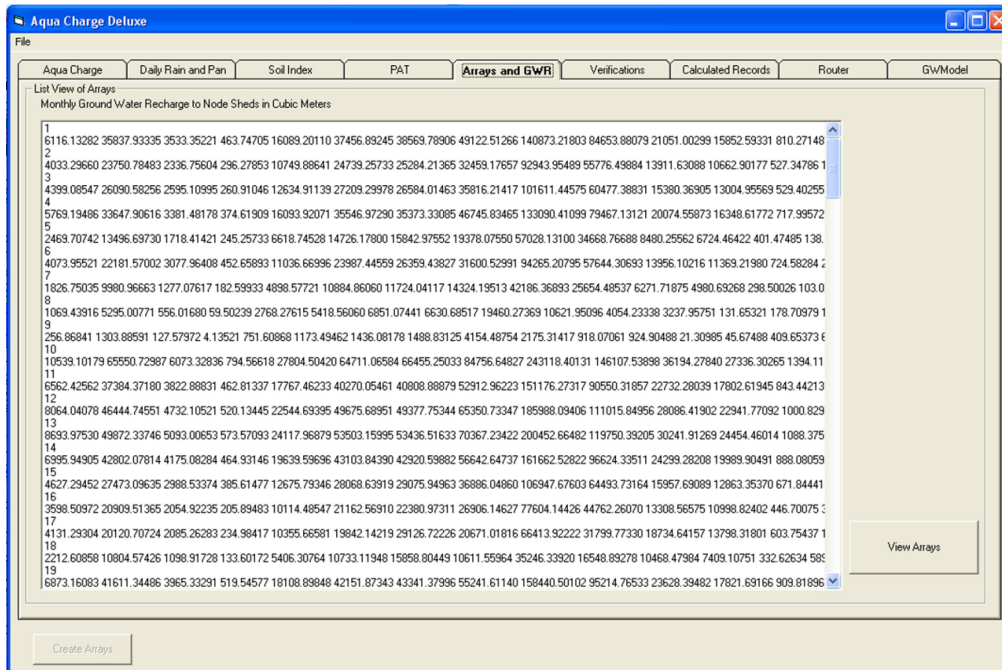


Figure 73. AQUA CHARGE Arrays and Groundwater Recharge tab. The values displayed here are monthly total AWA GW recharge in cubic meters for each node-shed or element, depends on GW modeler’s specification.

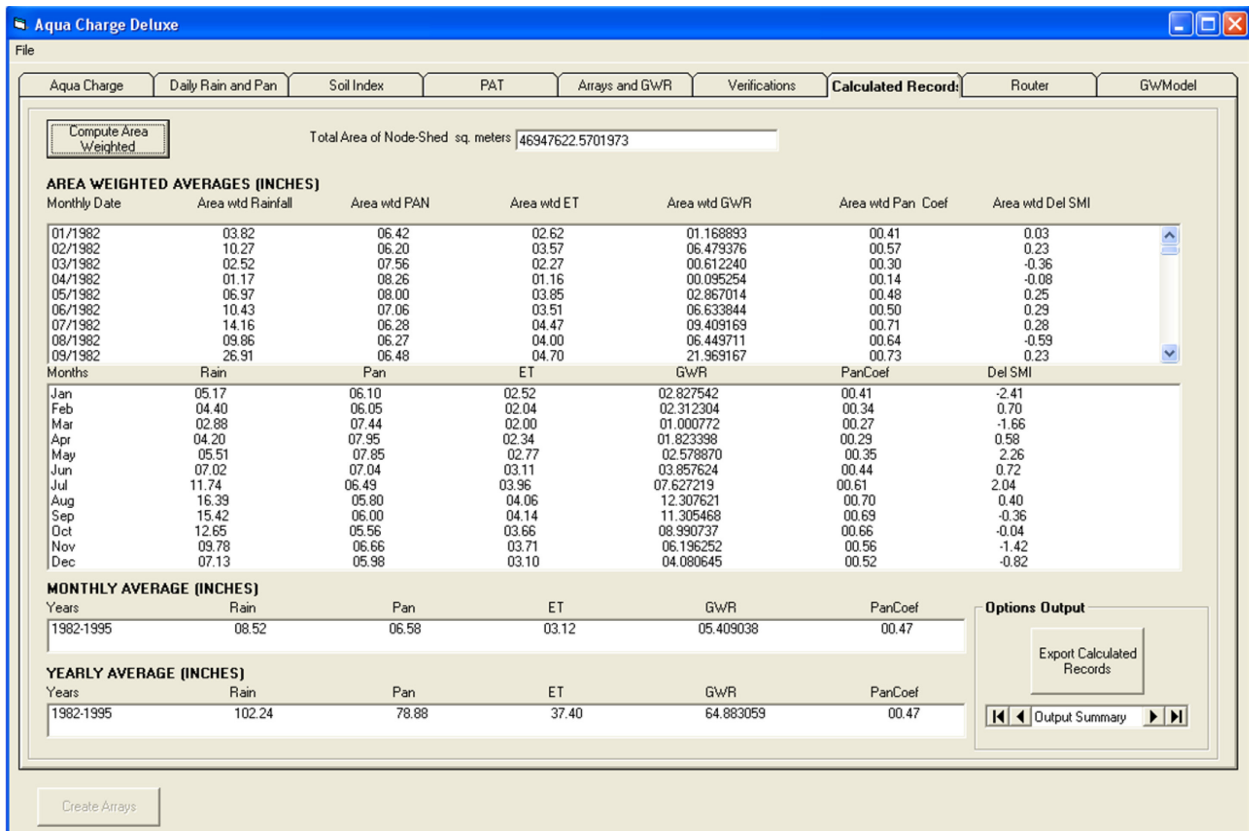


Figure 74. AQUA CHARGE Calculated Records tab.

Routing Recharge

A modified pulse routing technique is the way that water's time of travel and internal storage are accounted for in computing the recharge for each computational interval. Recharge's lag time and attenuation effect was simulated this way. First, the daily AWA recharge is split using an adjustable curve similar to splitting recharge and ET from the SM (see Figure 75). After the fast and slow recharges were split, they go to the routing algorithm. In the figure, the abbreviations FR and SR are the fast and slow routing algorithm respectively, T_s is the time in storage value (hours), t is the time of day in hours, and BR CAP is the bed rock capacity. The mathematical formula for routing is shown in Chapter 2.

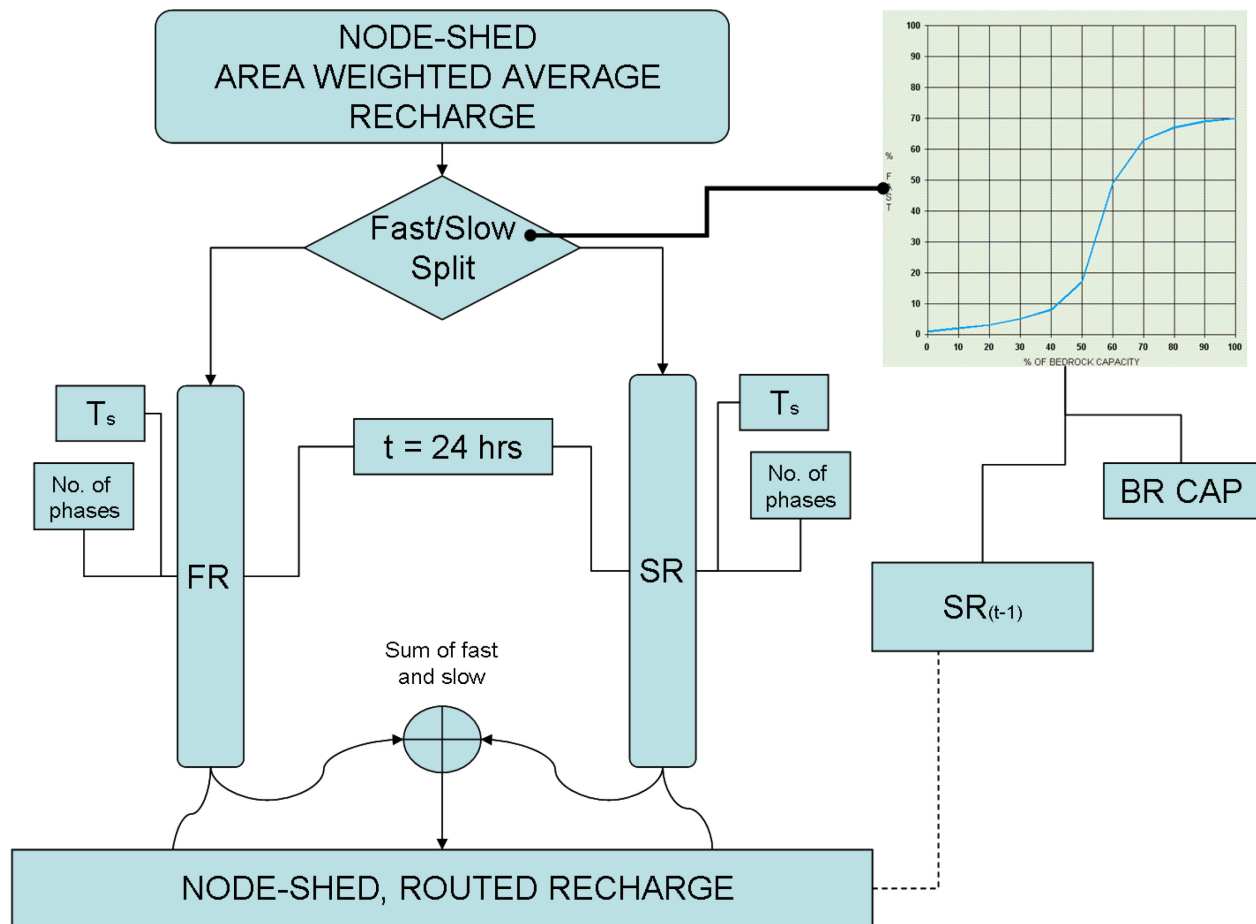


Figure 75. Programming flow diagram of the router.

The program is designed such that the user can change the number of phases and T_s for either the fast or slow recharge components of recharge, the bedrock capacity, and adjust the percent to fast flow curve. This allows the modeler to change the time lag and attenuation of the fast and slow recharge separately. The daily sum of both the fast and slow recharge produces the final vadose flow (recharge) synthesis. Again, the Visual Basic codes for the recharge synthesis model, Stages 1 and 2, are shown in the APPENDIX.

AQUA CHART Display of Recharge at M-11

After the routing process, the user may extract the synthesized recharge data to AQUA CHART for visual inspection. Figure 76 shows a special Excel chart, called AQUA CHART, displaying the synthesized recharge (top chart) response to rainfall (top axis). The green curve is slow recharge and the dark blue is the fast recharge. The sum of the slow and fast is the synthesized recharge (red). The second chart beneath shows observation well M-10a and M-11 measured data along with the daily tide fluctuations. Although the recharge and the well data are not directly comparable, the comparison gives the modeler a means to determine if any adjustments need to be made. The tide and observation well data can be found in Habana, 2008, APPENDICES E and F.

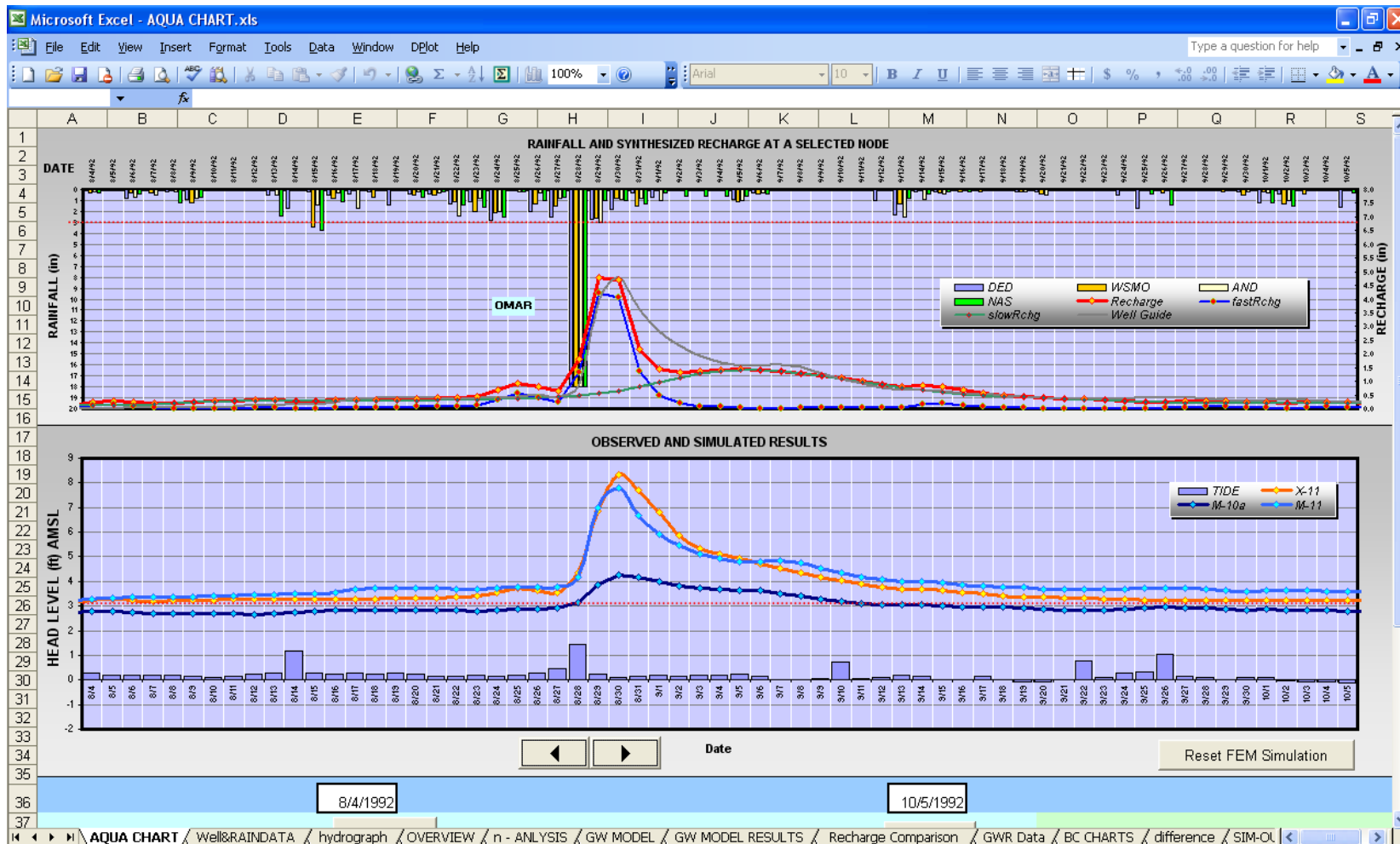


Figure 76. AQUA CHART. This is designed in Excel, top chart, displays rainfall data from the four gages, top axis, and a recharge synthesis (red) for observation well M-11, node-shed 59, bottom axis. The bottom chart displays observation well data M-10a (dark blue) and M-11 (light blue), daily average sea level data (near the bottom axis), and hydraulic model simulation for node-shed 59 (for observation well M-11, orange).

Recharge Synthesis Well Guide

Just as in streamflow synthesis or hydraulic modeling, many trial runs must be attempted to calibrate the many modeling parameters available in AQUA CHARGE. Since there are no recharge gages at the observation wells, there is no direct data to use and compare when determining the recharge synthesis results.

One way to determine the required routing parameters is to use a guide. The best guide we have is the observation well data showing response to recharge. The GW response measured in head can be converted to moisture in the porous media in terms of inch units. This can be used as a guide to assist in the calibration. A simple conversion of well head values using the porosity of the media is applied. If we considered a square meter top area column, as a unit area, of the GW rock media illustrated in Figure 77, a formula can be derived to determine the moisture input that would cause a particular response of the GW to recharge.

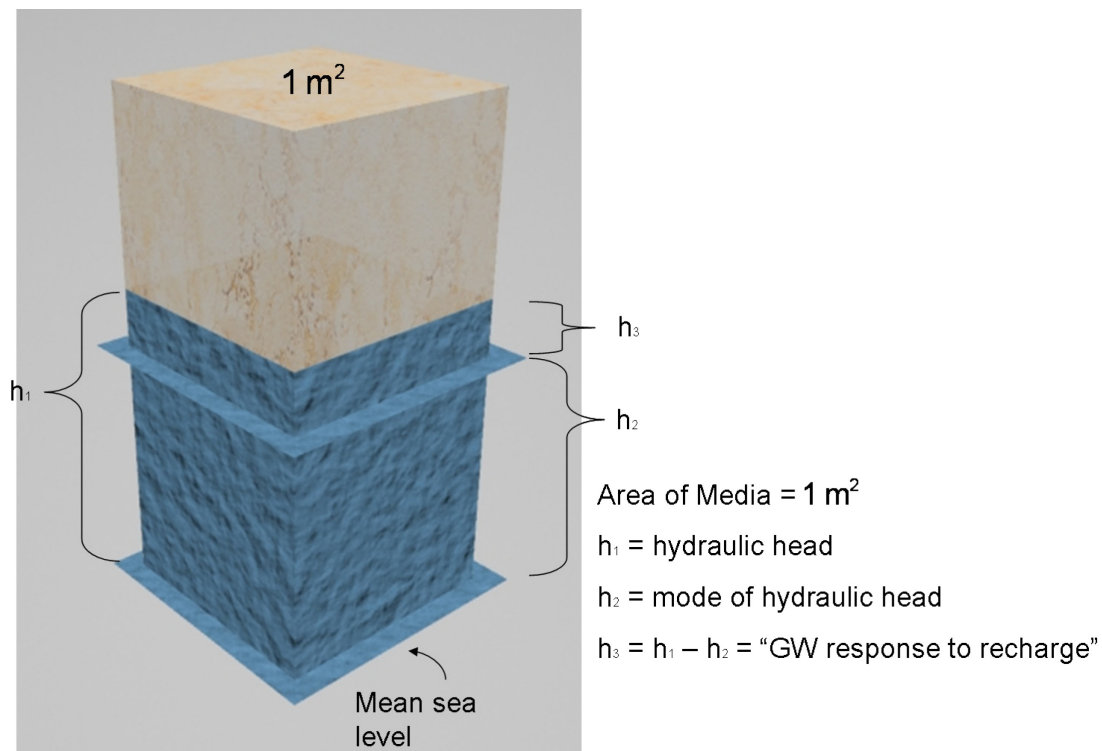


Figure 77. Properties of GW in a porous media.

We want to convert the hydraulic head in the media that is above the mode head of the observation well into its moisture equivalent in inches. The mode head above mean seal level is shown as h_2 in Figure 77. The head above the mode head is identified as h_3 in Figure 77. The value of h_3 is determined, depending on the conditions given, with the following condition equations (E20).

$$\begin{aligned} \text{If } h_1 > h_2, \text{ then } h_3 &= h_1 - h_2 \\ \text{If } h_1 < h_2, \text{ then } h_3 &= 0, \text{ (usually during rainless periods)} \end{aligned} \tag{E20}$$

The unit for h_3 is meters and converted to inches when displayed in AQUA CHART. Multiplying h_3 by the top area of the media, 1 m^2 , will give us the total volume of the saturated rock media. The aquifer's porosity, n (E21), assuming porosity is the same through out the rock media column, can give us the volume of the moisture in the void spaces:

$$n = \frac{\text{void volume (m}^3\text{)}}{\text{total volume (m}^3\text{)}} \quad (\text{E21})$$

A value of n equal to 0.09 was used for observation well M-11. This value was obtained from sampling values until it was near the synthesized recharge value through many test runs. For M-10a, n was set equal to 0.20. The volume of the moisture in the media can then be converted to a height in inches by dividing by the area and then converting it to inches (see Ex-1):

$$h_{\text{height of moisture}} = h_3 \left(\frac{1 \text{ m}^2 \text{ (area)}}{1 \text{ m}^2 \text{ (area)}} \right) \left(0.09 \frac{\text{m}^3}{\text{m}^3} \right) \left(39.37 \frac{\text{in}}{\text{m}} \right)$$

total volume divided by the area
 n
conversion factor

Ex-1

Ex-1 can be simplified to Equation 22. This equation can be applied to the known well head data and graphed as the well guide that will be an indicator of the recharge over time.

$$h = h_3 n \left(\frac{39.37 \text{ in}}{1 \text{ m}} \right) \quad (\text{E22})$$

The well guide curve is simply a scaled version of the observation well data. The porosity n acts as a scale multiplier and then converting the well guide to inches.

The modeler can use the well guide curve developed for a particular storm to determine the desired shape of the desired synthesized recharge curve. A good example of recharge responding to a high pulse amount of rainfall (15-18 inches, Lander, personal communication) occurred during Typhoon Omar's (1992). Figure 77 shows the output from the AQUA CHARGE models for this particular storm event. The well guide and the observation well level from which the Well guide was computed show a rapid rise in the water level in a just a few days. At the same time, water continues to drain from the aquifer, but the recharge is much faster than the rate which water is leaving the media vicinity. In this case the well heads reached heights of up to eight feet amsl. After the well heads reached a peak the aquifer begins to drain at a rate slower than it was filled and faster than the recharge can arrive to keep it up, since fast recharge is quickly diminished as it has ran out. This first phase of the drainage lasted approximately seven days. After seven days the well heads leveled nearly constant for about 4 days at five feet amsl. Then well heads fall at an even slower rate than in the first phase of the drainage. They return near the mode well level value after about ten days or more. From the day

of the typhoon to the time when the well level dropped to its mode, the event took approximately 25 days.

From observing the data from this storm, the modeler can infer that there was a rapid recharge that brought the water level up in only a couple of days. This fast recharge must have stopped at around the second day suggesting a narrow, and high amplitude curve similar to the fast recharge (dark blue) shown in Figure 78. The water in the observation well falls after its peak and then plateaus after a few days revealing the affect of the slow recharge's arrival which maintained the steady water levels around the ninth day. From these observations, the modeler uses the well guide to build the shape of the fast and slow recharge that might have caused the observed water levels for a particular storm. Thus the well guide is used to decide the models routing parameters, (the Number of Phases and Time of Storage), to be applied to the fast and slow flow components of recharge. A sample of the well guide for both M-11 and M-10a are in Habana, 2008, APPENDIX E

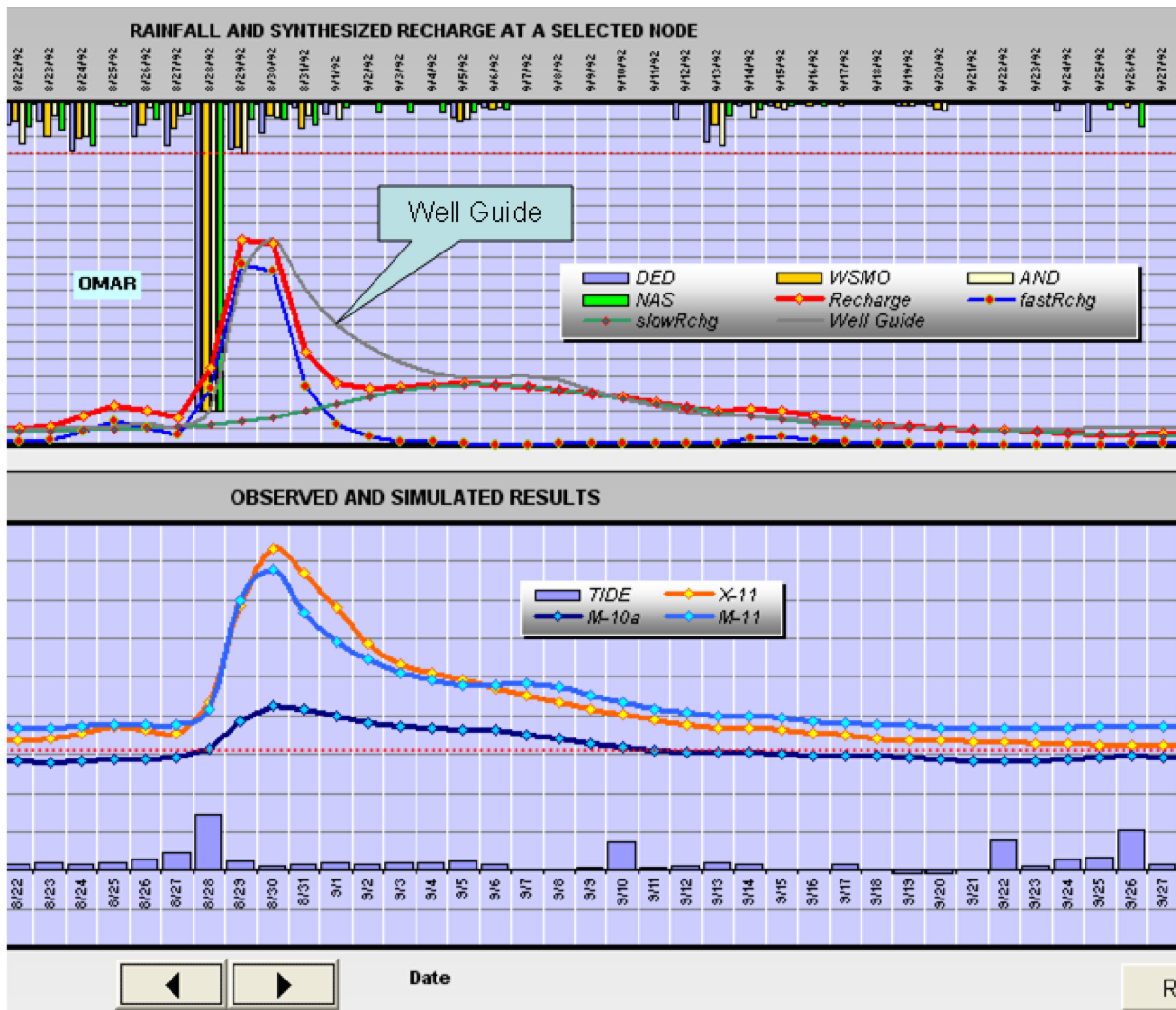


Figure 78. Sample of the Well Guide in AQUA CHART. The gray line in the recharge synthesis chart, to determine recharge parameter adjustment. The well guide is a scaled down image of the observatory well levels.

Hydraulic Model

The synthesized recharge output formatted for a hydraulic model is provided in cubic meters. The text-file output format begins with the node number followed by a space separated daily synthesized recharge as explained in Chapter 4. For this project, the finite element method GW program was designed as described in Chapter 3. Figure 79 shows AQUA CHARGE's interface for a simple finite element method GW model design based on Istok's code. The modeler uses the recharge output text file as recharge input data for the program. The program is hard connected to the FEMData, so pushing the Input Data button will open a common dialog box to select and load a saved recharge data file. The program continues to automatically load the FEMData (see Chapter 4). The Materials Properties option button allows the user to change the hydraulic conductivity ($K_{x/y}$, in the planar x and y directions) and the specific storage (S_s). The "GW3 TRANSIENT, SATURATED GROUNDWATER FLOW" button runs the simulation. When the computation is done, the modeler may select a node of interest in the OUTPUT DATA frame and send the simulation for that node to AQUA CHART. The modeler may examine the results; adjust the $K_{x/y}$ and the S_s to match the simulated computation to the observed data. One simple guideline to calibrating finite element parameters is reducing S_s increases the amplitude of the response while increasing $K_{x/y}$ diminishes the duration of the water level stand quickly back down. The regional $K_{x/y}$ is 5.8 km/day (Jocson, 1998) and the S_s is a small number in the order of 0.0001ft^{-1} (0.0003 m^{-1}) (Fetter, 2001). We used $K_{x/y}$ from 5.5 km/day to 9.5 km/day and S_s were between 0.0001 m^{-1} to 0.0006 m^{-1} . GW modelers may use different programs and conditions setup. This project's main goal was to provide a realistic recharge to GW models.

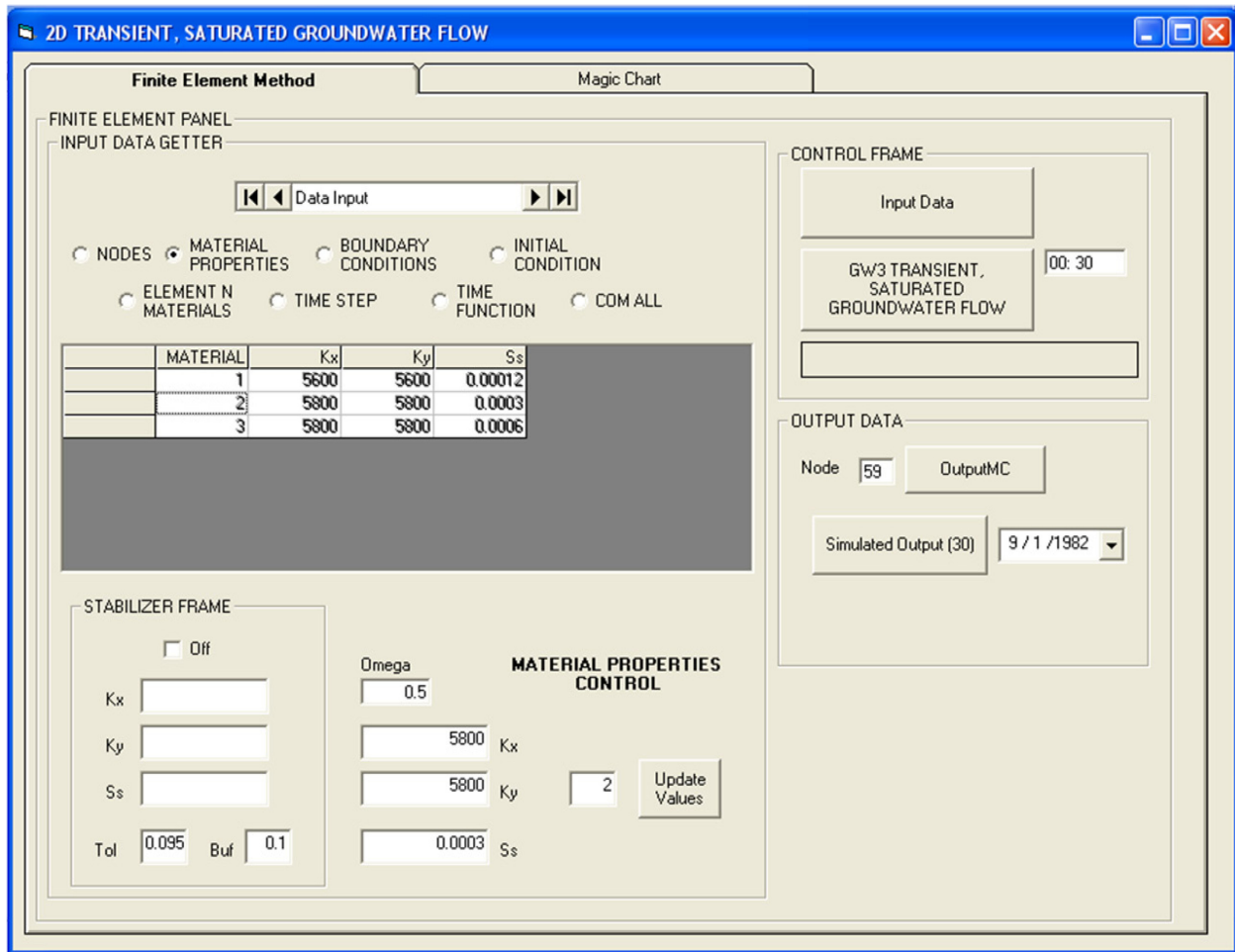


Figure 79. Finite Element Method program graphical user interface.

Interface Forms, Data, and Chart Connection Flow Diagram

All together, AQUA CHARGE's interface forms, data input/output, and charts are connected as shown in Figure 80. AQUA CHARGE needs the All-In-One input data to make the recharge and summary computations. AQUA CHARGE can also load and save ET/Recharge curve settings, display routed recharge for a selected node-shed in AQUA CHART, and produce output text files of routed recharge for hydraulic models or other studies. The finite element interface form, FEM, has a finite element input data called FEMData. The output recharge text

file can be used in the FEM and the results displayed into AQUA CHART. The next chapter is the user's manual.

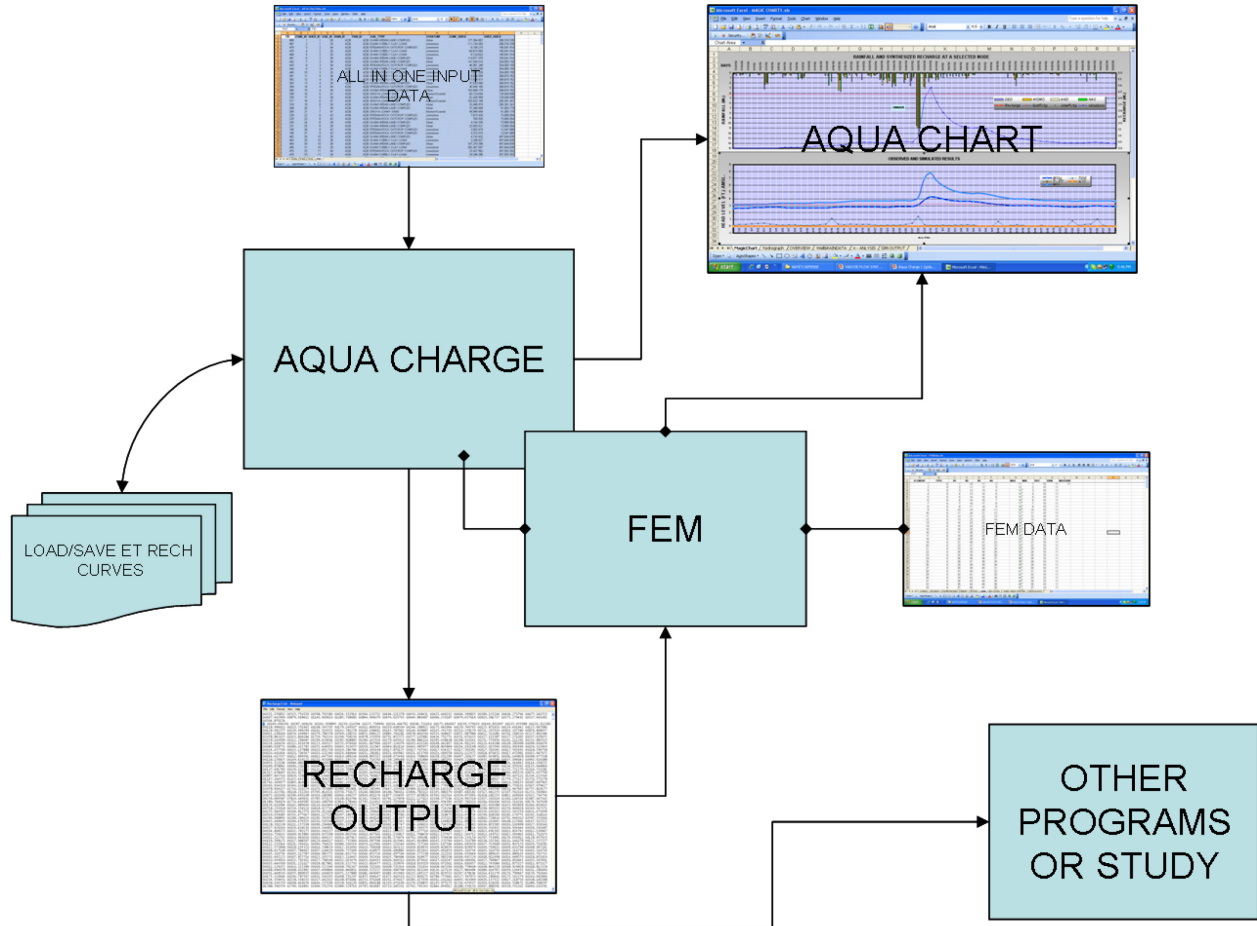


Figure 80. AQUA CHARGE program flow diagram connectivity.

AQUA CHARGE USER MANUAL

With the seemingly never ending need to upgrade to keep up with today's computer technology's rapid change and advancement, it is inevitable that AQUA CHARGE will one day become inoperable with the latest Personal Computer operating system. The computer programs mentioned in this project before AQUA CHARGE, such as SSARR, SWIG2D, and VADOSWIG for example, were ran and stored in floppy disks and designed before MICROSOFT® (MS) Windows XP. This shows that one day the AQUA CHARGE program too will need to be recoded to meet the changes. At the writing of this thesis, already, MS VB 2005 and MS Windows Vista had been introduced to the market. Just to mention another impediment, MS Office 2007 Excel's new file format with extension “*.xlsx” may not be compatible with VB 6.0 MSflexGrid data control that used the *.xls” extension. If we are lucky, the operating systems and programs are retro-compatible. Regardless, whenever that time comes, we provide you a user's manual for AQUA CHARGE, but not the obsolete computer.

Installation

The AQUA CHARGE software, the package contains the files and folders shown in Figure 81. The AquaCharge.msi installer file is run by clicking on the file icon. The Windows Setup Wizard (Figure 82) opens and instructions for loading the program are given for the user to follow; next to the installer is the program startup icon.

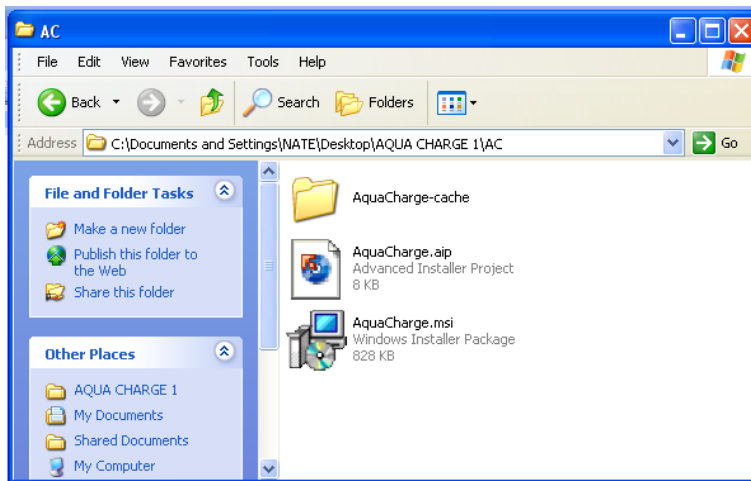


Figure 81. The program setup files.

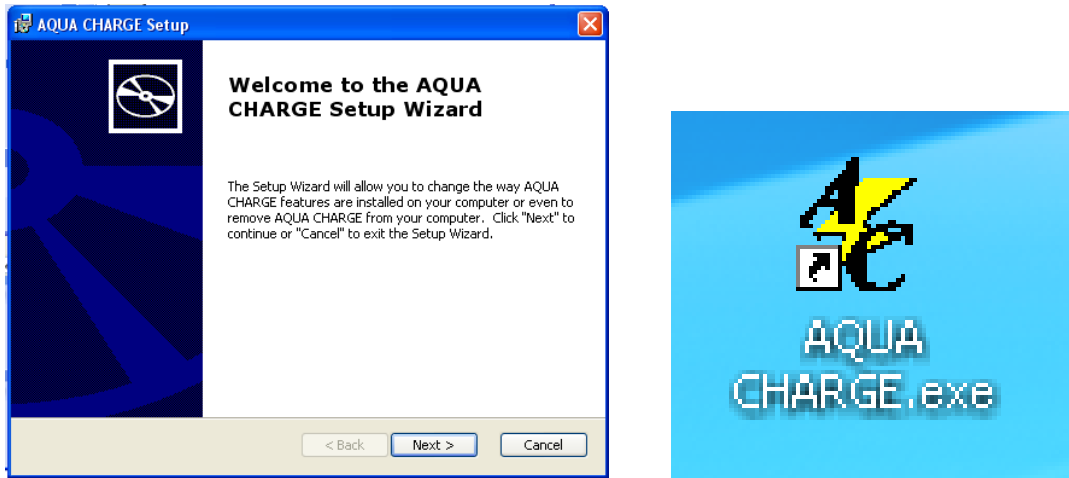


Figure 82. Windows installer Setup Wizard and the installed shortcut icon.

Stage 1 – Area Weighted Average Recharge

AQUA CHARGE was designed to run the conceptual model discussed in Chapter 2. The modeler begins by clicking the AQUA CHARGE.exe to run the application. The program launches (Figure 83) and it opens up a tab filled form (Figure 84). The input data are loaded next where the modeler may examine the input data tabs and make necessary adjustments to the soil curves in the soils tab. The PAT file needs to be checked to be sure that it is sorted; a command button accomplishes this. Next the, arrays and variables are prepared by activating another command button. The modeler can now run the Stage 1 recharge synthesis. The results are displays of monthly sums of recharge in cubic meters for every node-shed, a zone recharge calculation tab, and a calculated records tab.

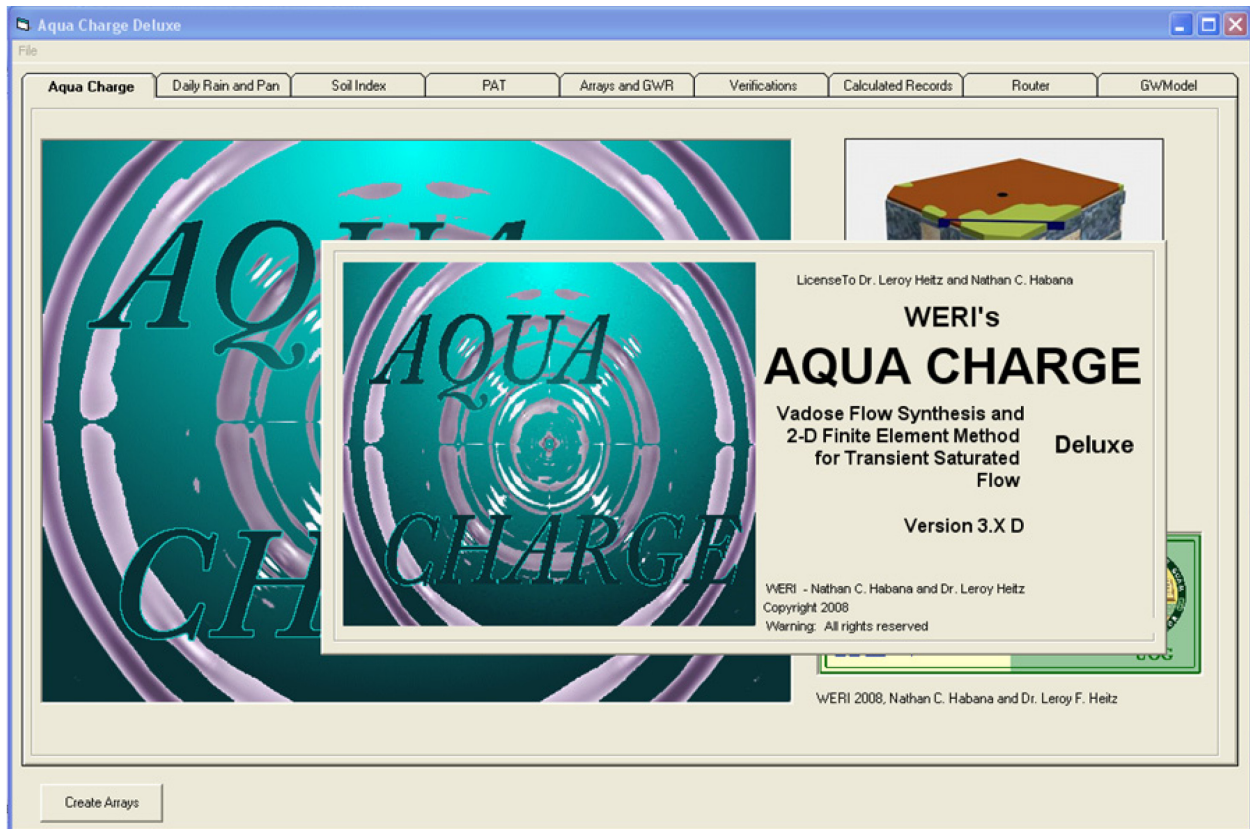


Figure 83. AQUA CHARGE Splash screen startup.

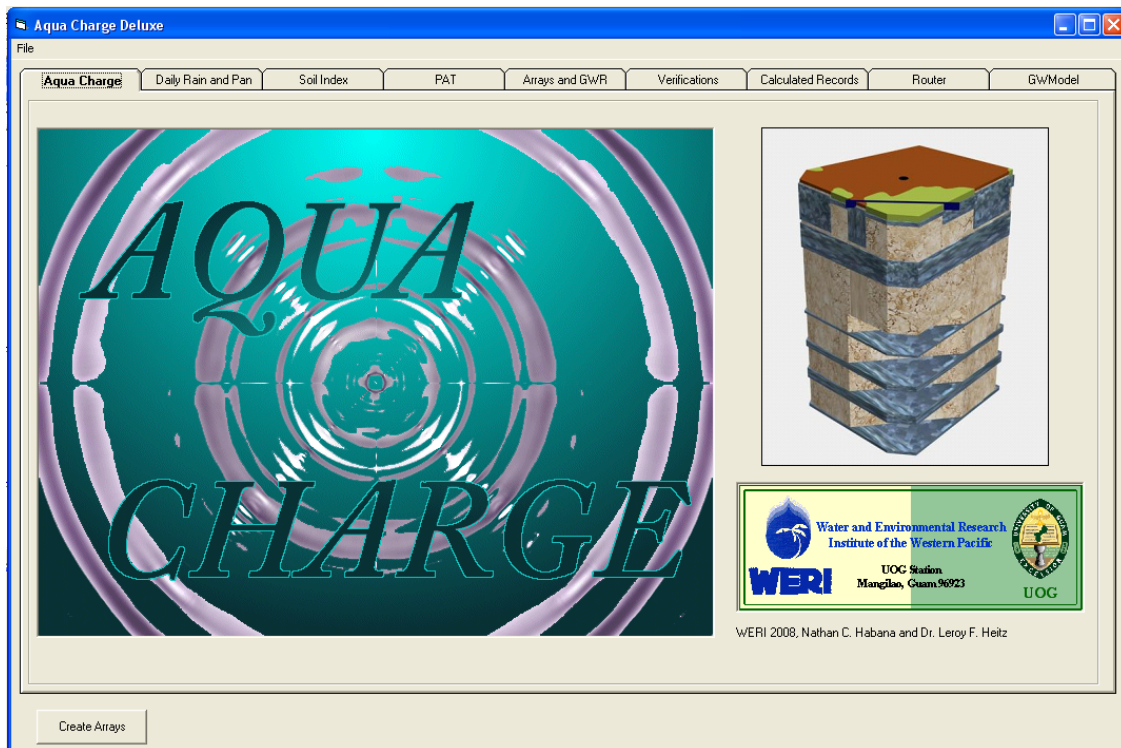


Figure 84. AQUA CHARGE program title cover tab.

Input Data

AQUA CHARGE requires four data files to run. The data files may be loaded individually, but the All-In-One data format in Excel file is the preferred method for fast loading. Before loading the data, the data should be formatted as explained in Chapter 4. For individual rain, pan, soil, and PAT loading, each Excel file's record sources must be defined and named as mentioned in Chapter 4. The data will not load if it is not in the format intended for the program. All of the mouse control for this program uses the "left click" mouse button control which will be referred to as "click." To load the data into the program, click on the file menu. A drop down menu, as shown in Figure 85, will appear and a common dialog box opens (Figure 86) for the modeler to select the All-In-One Data Excel file that holds the model's input data. These data include rainfall, pan evaporation, soils properties, and the Polygon Attribute Table (PAT) (Figure 84). Upon selecting the input data file, the data are loaded in their appropriated tabs. The PAT tab is on focus with a message box of instructions for extracting the PAT file data.

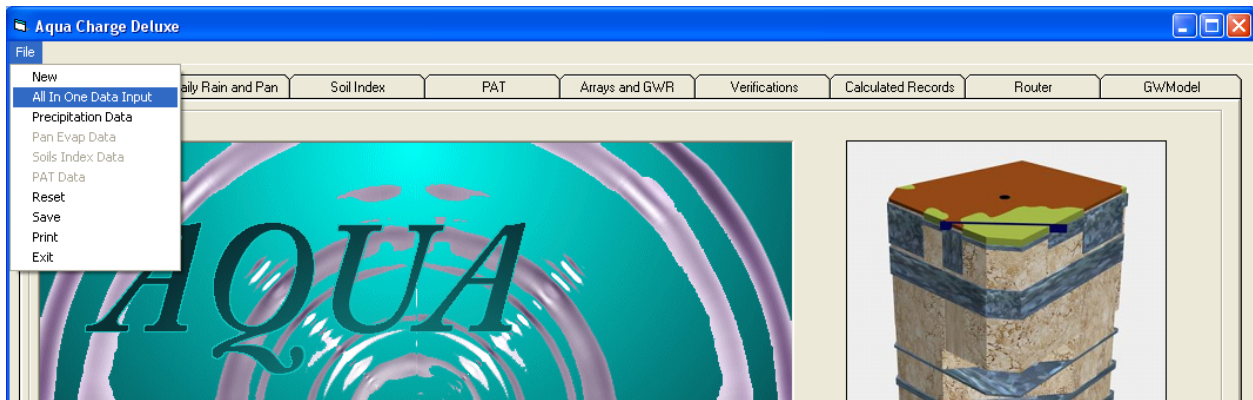


Figure 85. AQUA CHARGE file menu.

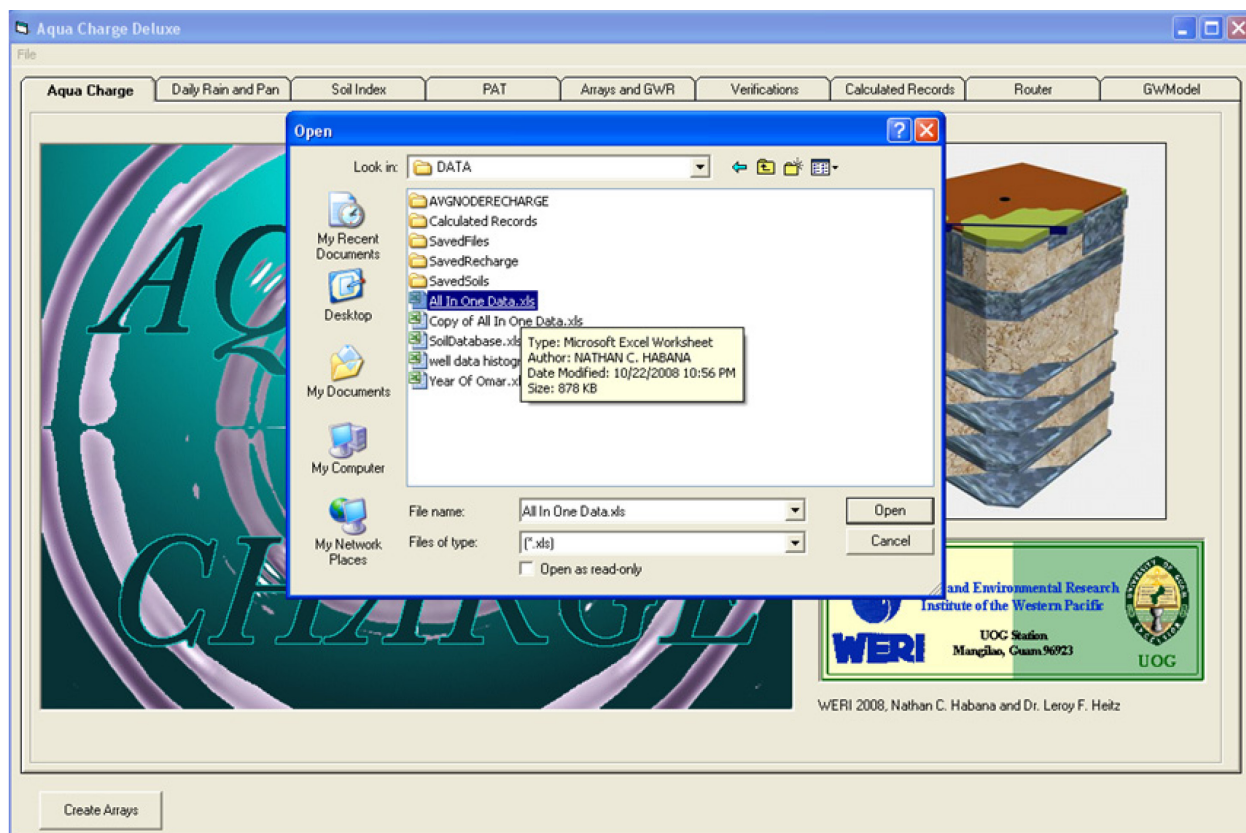


Figure 86. Data input common dialog box.

PAT Tab: The spatial data opens up the fourth tab and the data is loaded in the table. Figure 87 shows the message box that appears with instructions on how to select the appropriate fields to be extracted from the PAT data. In the Zone Field Identifier frame, to the left of the top PAT table, the modeler selects the appropriate field names for rain gage, pan gage, soil ID, zone number, element number, zone area, and element area as shown in Figure 88. These are the unique spatial attributes in the zone necessary to run AQUA CHARGE. The modeler may click on the text box and select the field on the table or simply type in the field name, which is case sensitive. Once the appropriate text boxes have the proper field names, the modeler needs to click on the sorter button titled “Extract and sort required field data from PAT file” to reorganize the data (Figure 89). This step is necessary so that the calculation process is done efficiently. The reorganization provides a smooth daily sweep throughout the zones which vastly improves calculation time.

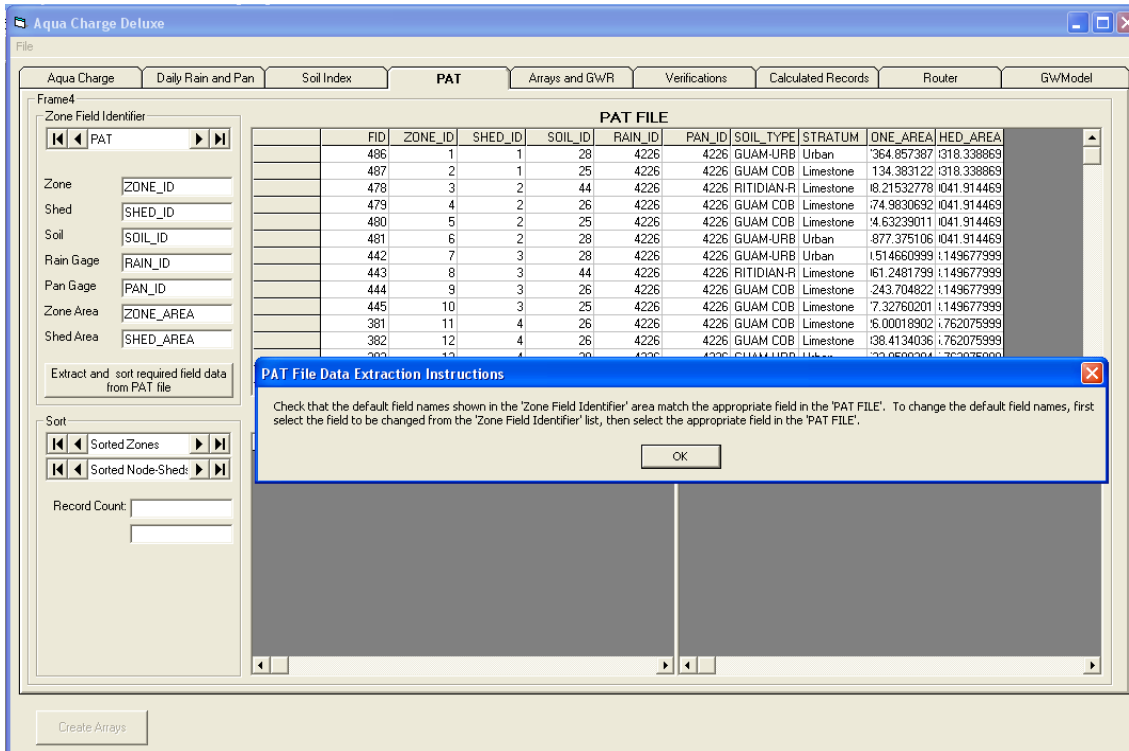


Figure 87. PAT tab data extraction instructions message box.

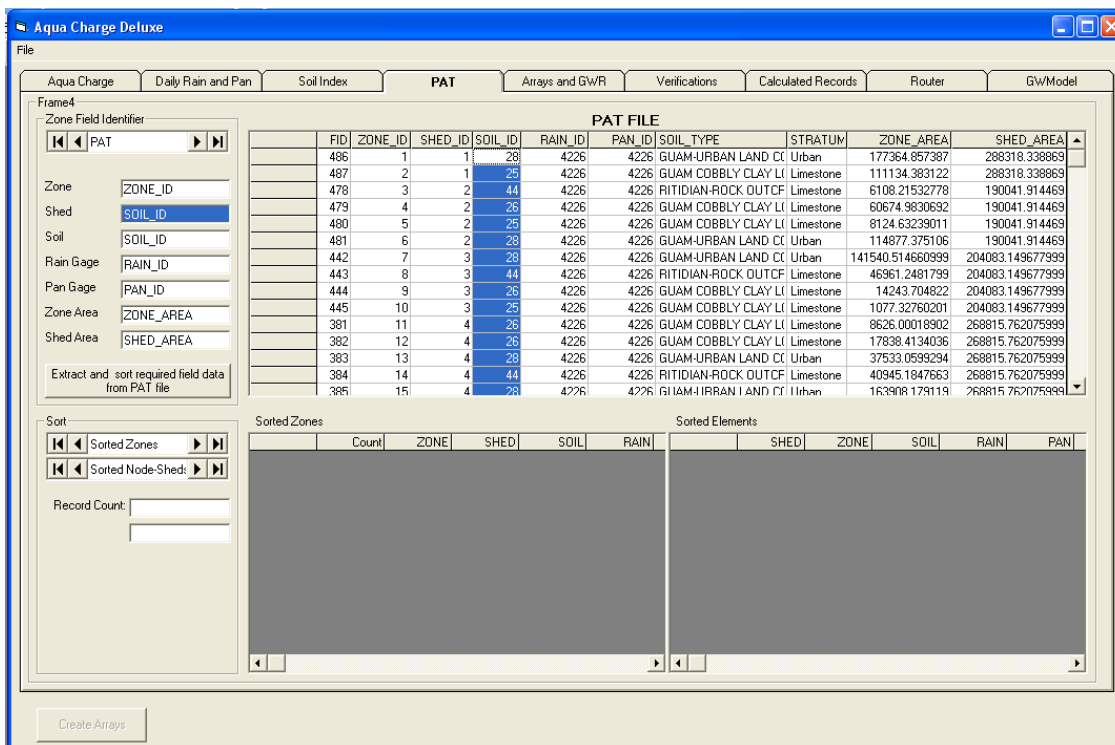


Figure 88. Zone field identifier text box and field name selection. The shed text box field name was changed to "SOIL_ID" simply selecting by clicking the text box and the field column name. It may also be changed by typing in the case sensitive field name in the text box.

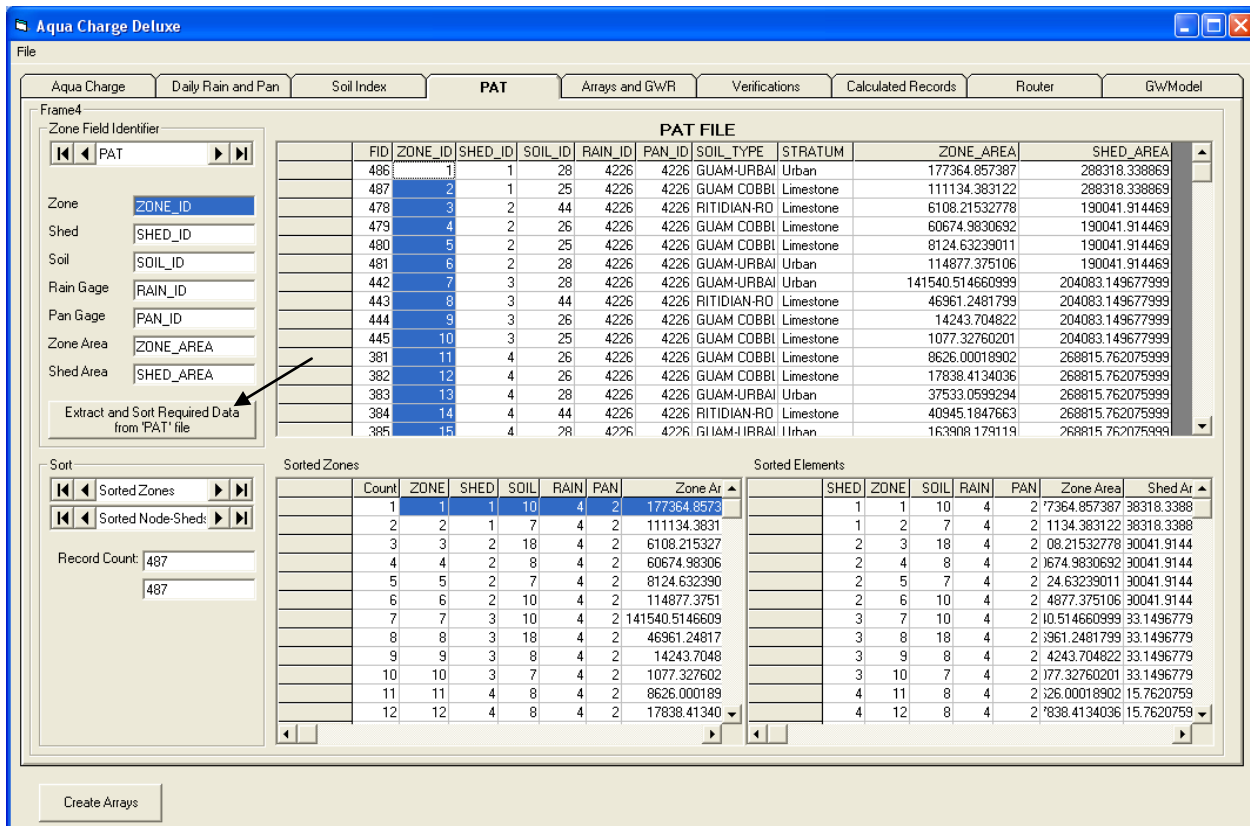


Figure 89. Extract and sort required field data from PAT file button. This prepares the spatial data for the program to use.

Daily Rain and Pan Tab: This tab displays the temporal rain and pan data in table form. The four rain gages and two pan gages are set up as two separate tables shown in Figure 90. The dates are on the first field followed by gage stations and their measured values are in inches for that day. Below each table is data information about the recordset for each gage. Clicking on a gage field will display the recordset information for the selected gage into the appropriate text boxes. This tab is useful for last visual scan of the temporal recordsets ensuring that there are no negative numbers, blank cells, or outrageous values. Chapter 4 explains the temporal data formats in detail.

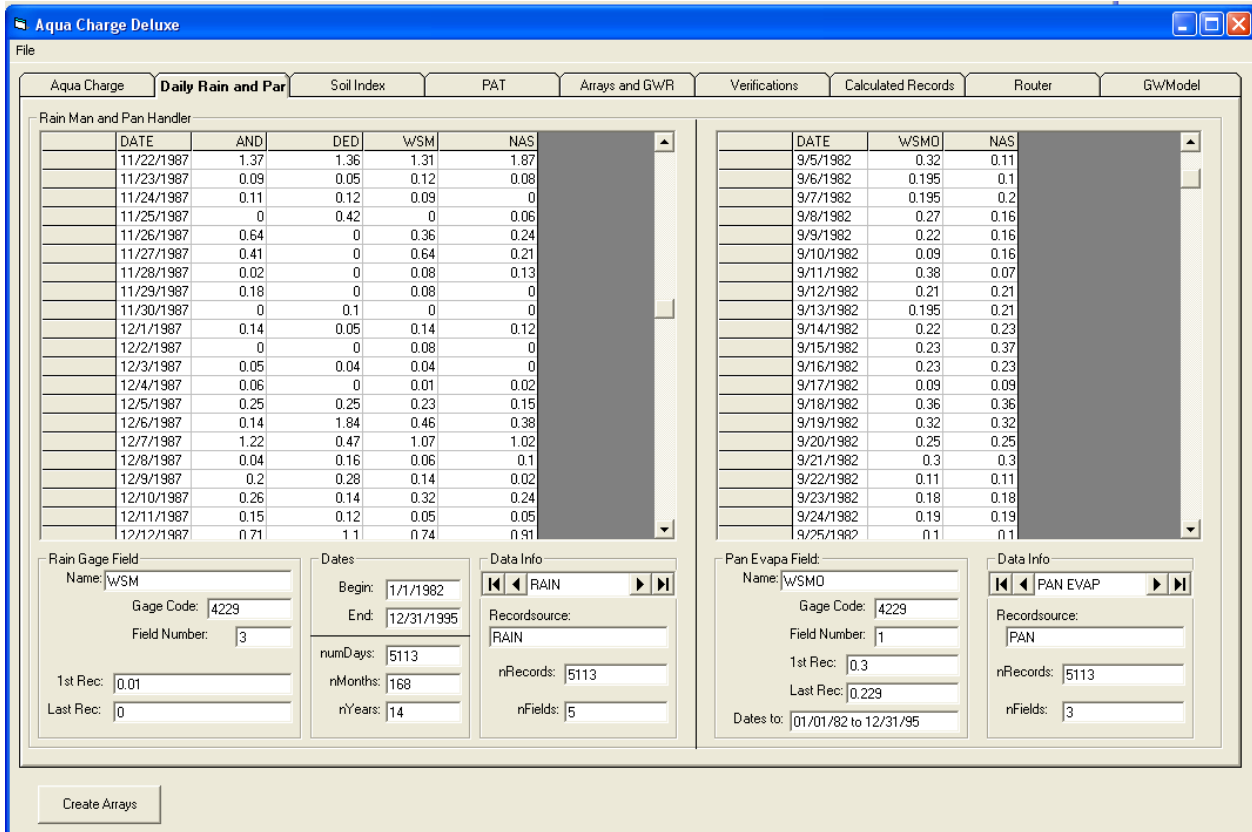


Figure 90. Daily rain and pan (evaporation) tab.

Soil Index Tab: This third tab allows the user to make changes to the soils curve and FC. A list of soils in the study area appears in the table (Figure 91). The table shows the soil id, soil name, and the FC. To the right of the table is the SM vs. recharge and ET curves for a selected soil. Clicking a row in the table puts the selected soil type data on the chart and in focus. Upon loading, the first soil listed in the table is displayed on the chart. Clicking on the top chart switches between views of ET or recharge curve (Figure 92). The x-axis option changes view from inches or percent of FC (Figure 93). The vertical bars allow the modeler to adjust the curve and explore different ET and recharge relationship curves (Figure 94). After selecting a soil type, the user may change the FC value (Figure 95). Once the curves are set, the modeler may save the curve configuration and load it later and use it (Figure 96). It is also helpful to save and keep the curve configurations for future reference or later use (Figures 96 to 98). In this project, three curve configurations were explored as mentioned in Chapter 2.

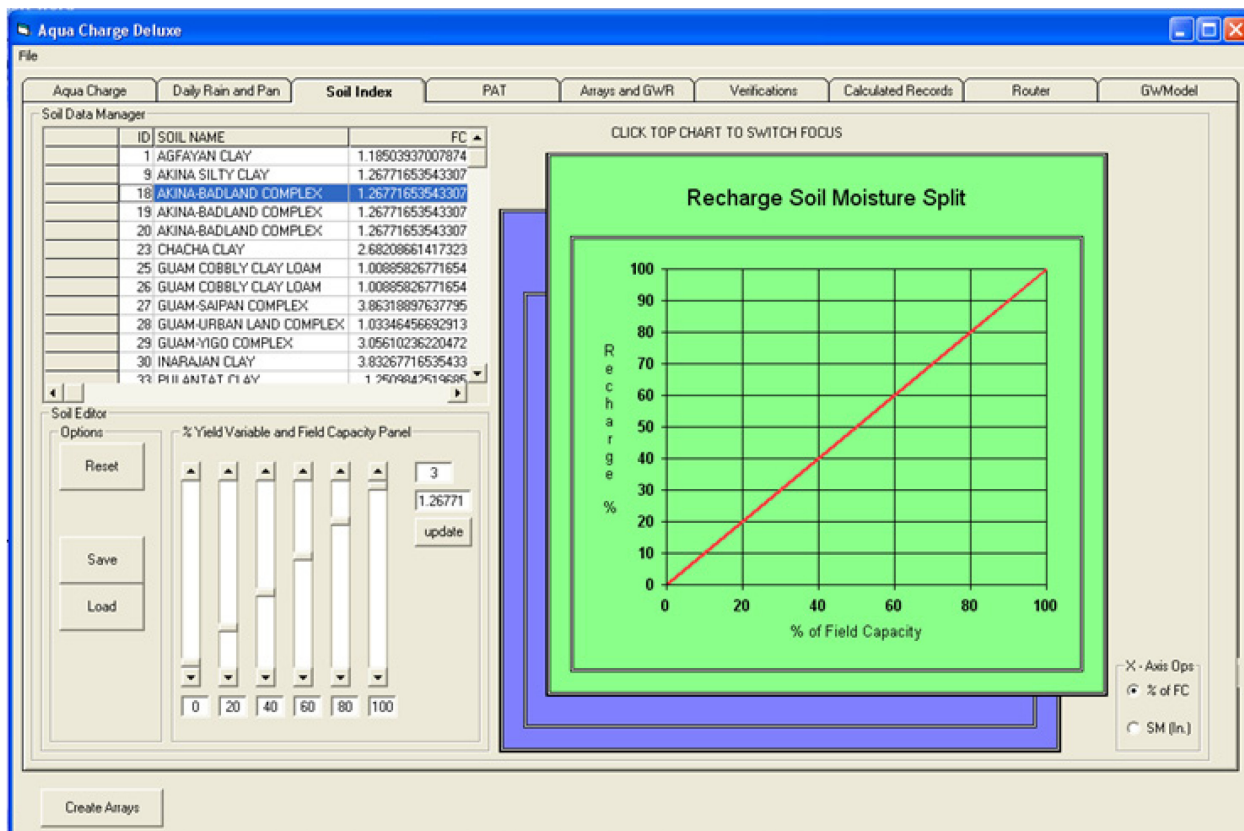


Figure 91. Soil Index tab.

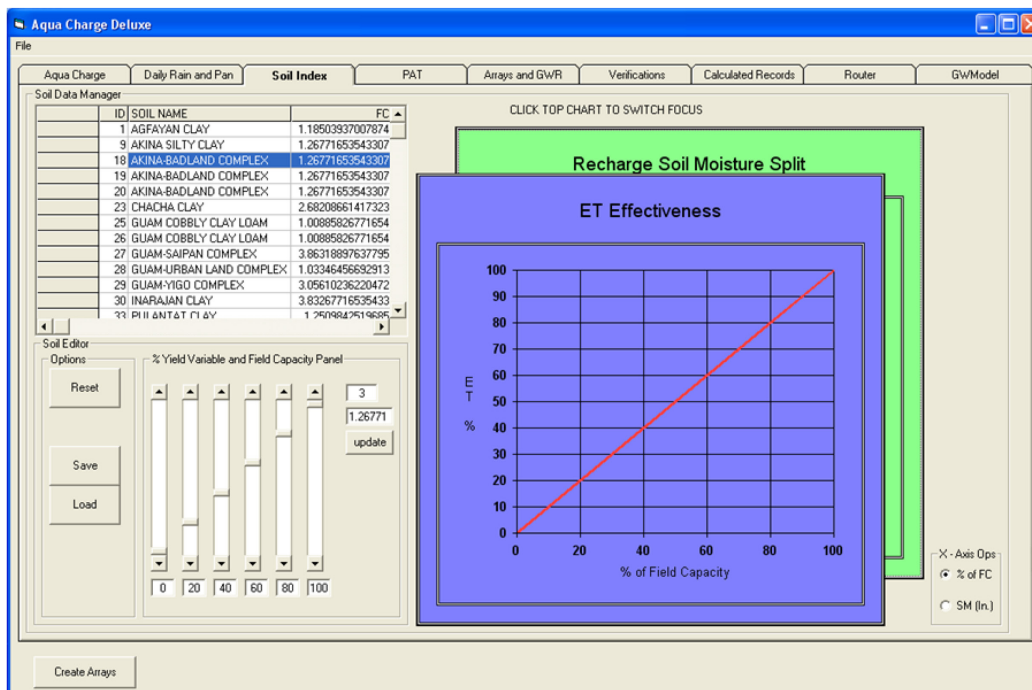


Figure 92. Switching focus on charts. The recharge chart on top (Figure 89) was clicked and the ET chart is now on focus.

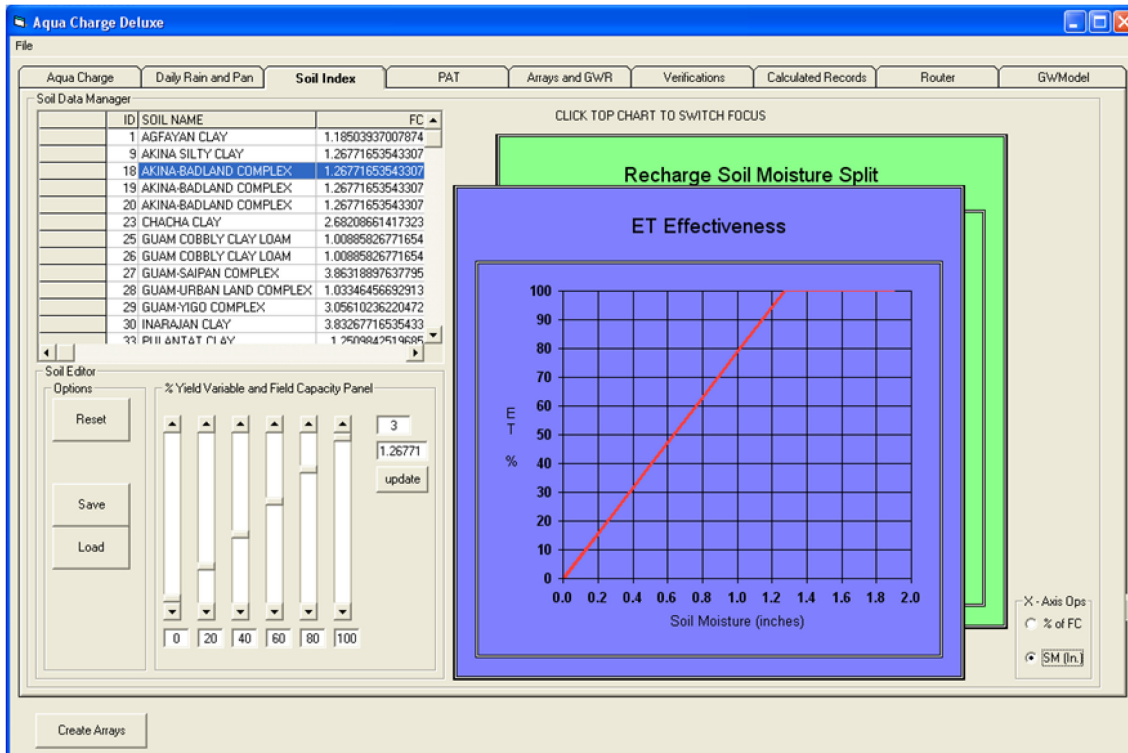


Figure 93. The x-axis options. The control allows the modeler to see the chart as Soil Moisture FC in inches or percent of FC.

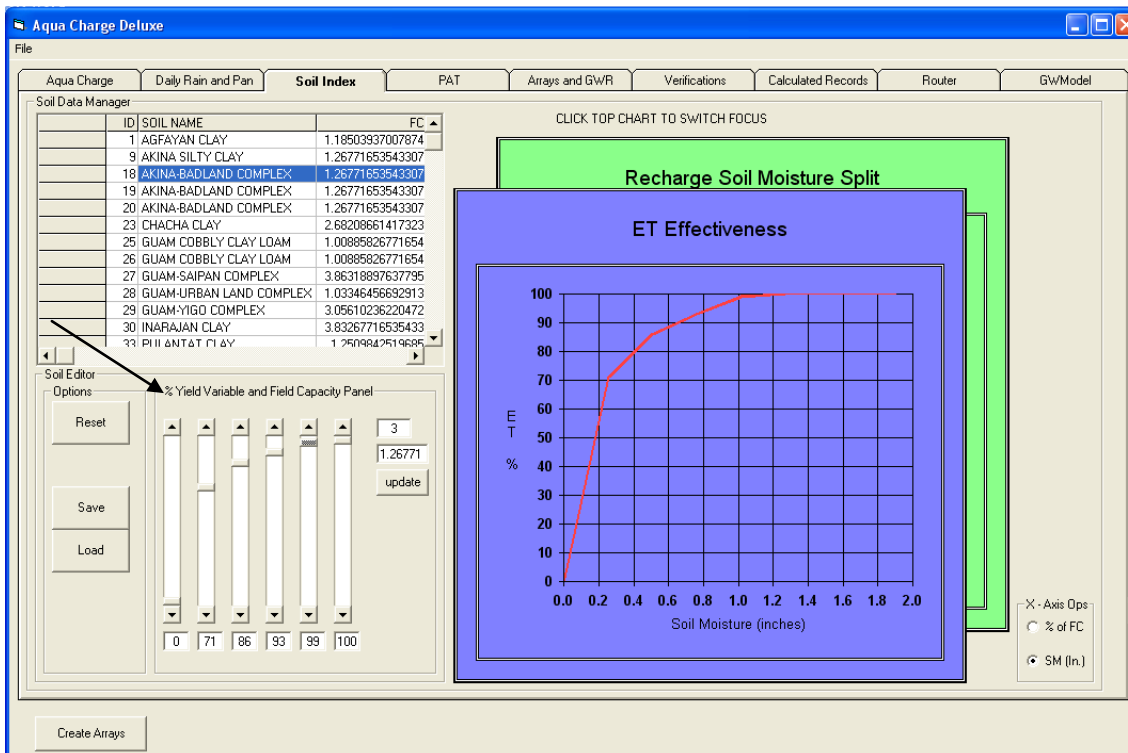


Figure 94. The Percent Yield Variable and Field Capacity frame.

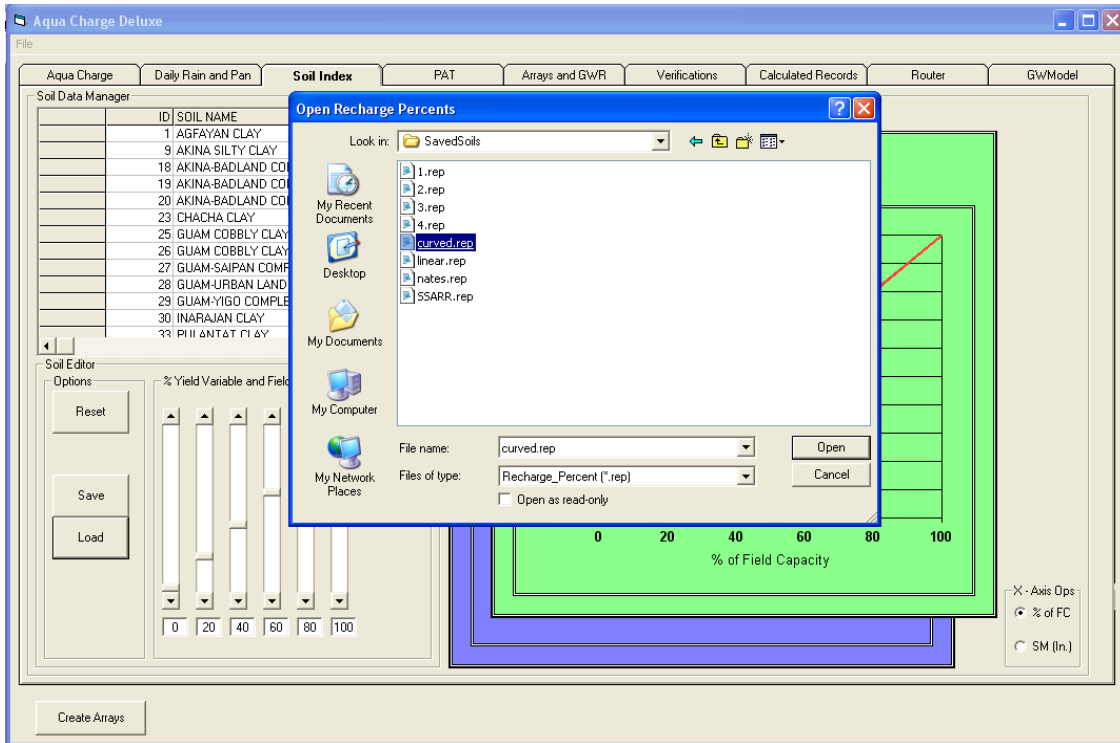


Figure 97. Loading saved curve settings.

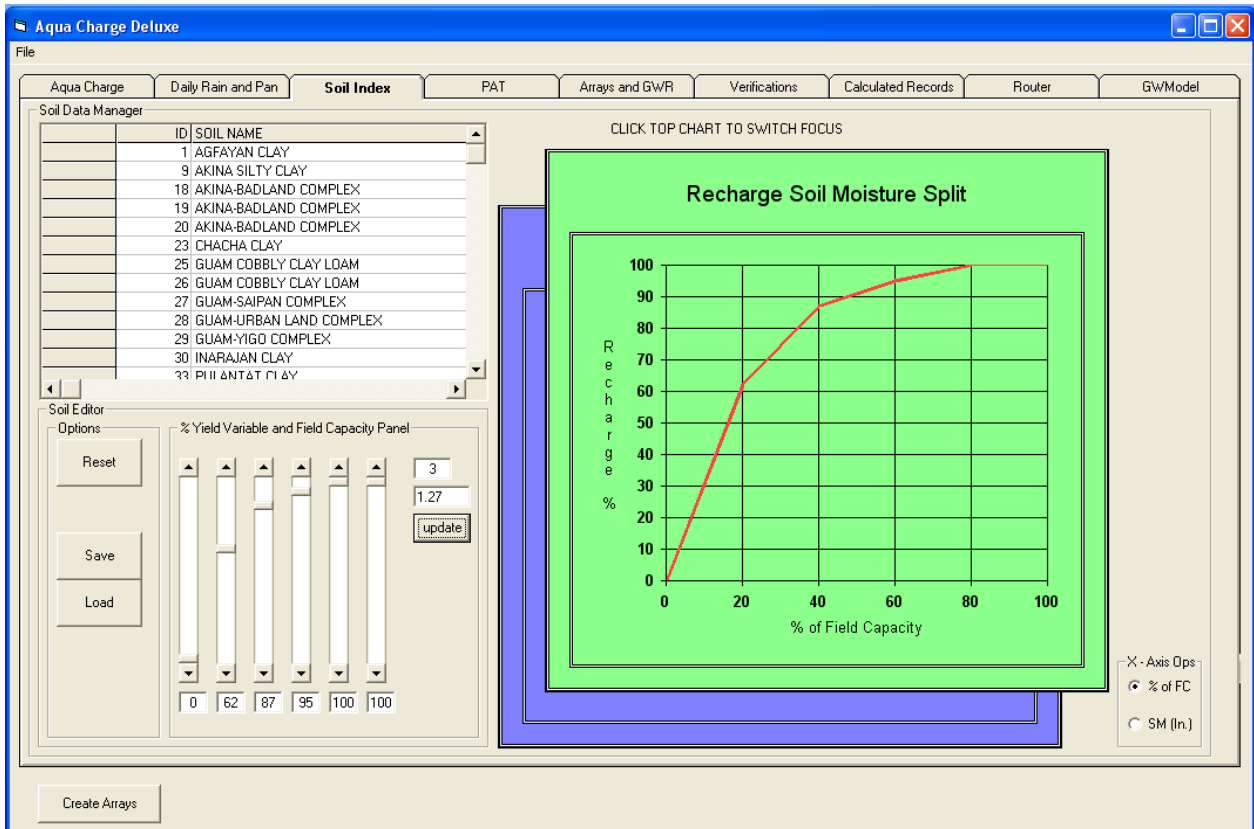


Figure 98. A loaded curve setting for recharge.

Array Variables

Now, all the data is loaded and is ready to be converted into array variables. The array button at the bottom left, as shown in Figure 99, is clicked and the fifth tab, Arrays and GWR, opens with a list box that displays the array values as shown in Figure 100. This step allows the modeler to see that all the loaded data was converted properly into their respective arrays. The modeler may also use this to double check the input data to confirm and accept the quality of the data before executing the recharge calculation.

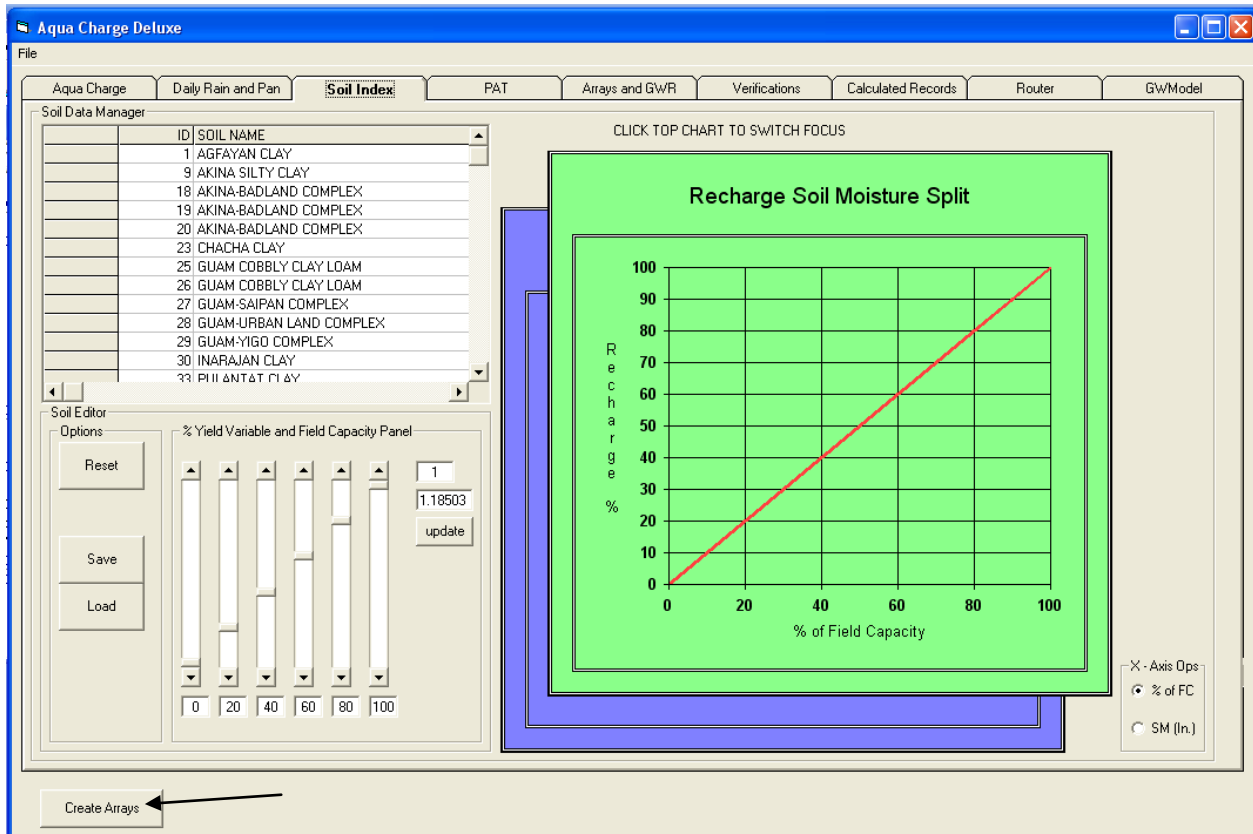


Figure 99. Create Arrays button. The button is located in the lower left corner of the AQUA CHARGE form.

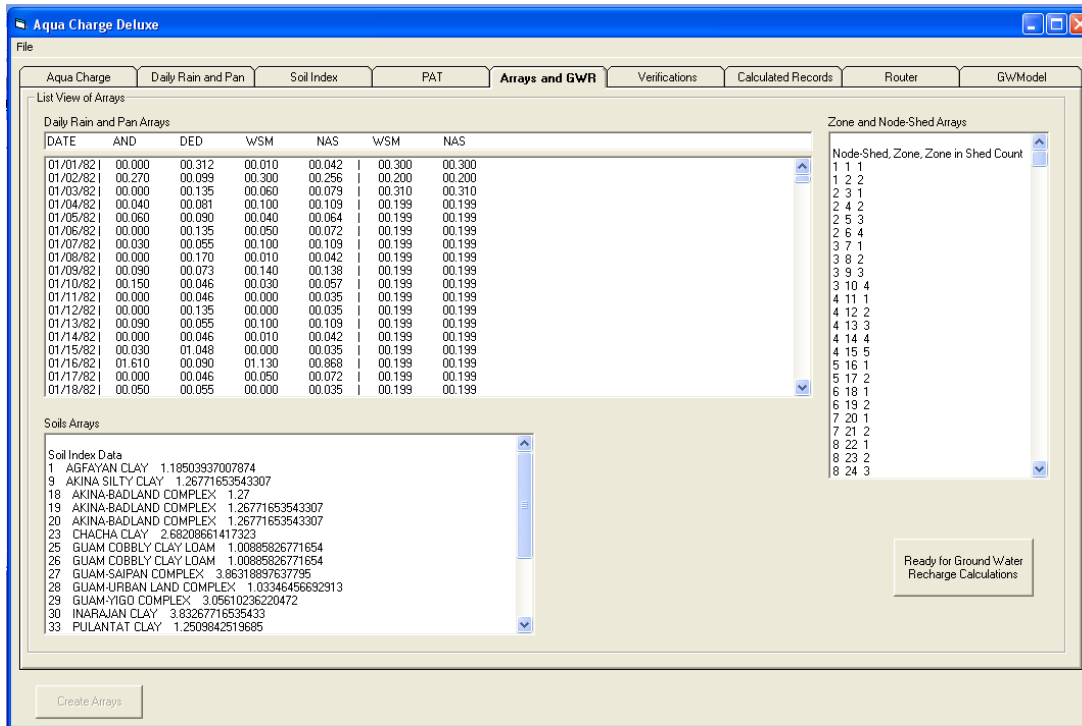


Figure 100. Arrays and GWR tab showing array values prepared.

Computational Interval and Recharge Calculation

With the array variables now set, the modeler can now make the recharge calculations. The “Ready for Ground Water Recharge Calculations” button located on the lower right part of the tab (Figure 101) is clicked to open a computational interval dialog box as shown in Figure 102. As mentioned earlier, the date range can only be set within the period where there are complete records of data in all of the temporal files. The modeler may enter an initial SM value (inches), for all the soils in the domain. A check box with label “Potential ET > Rainfall...” has a subroutine that has not been completed and is disabled and bypassed in this program. Clicking the “Cancel” command button will require the modeler to start all over and restart the program. Next, click on the “OK” button and the Stage 1 recharge for all the node-sheds in the domain is calculated. Some subroutines not mentioned are coded to calculate monthly and yearly averages. The daily AWA recharge (cubic meters) sum for the month for each node-shed is shown in a list box (Figure 103). Clicking the “OK” button also enables the power button for the Stage 2 routing tab.

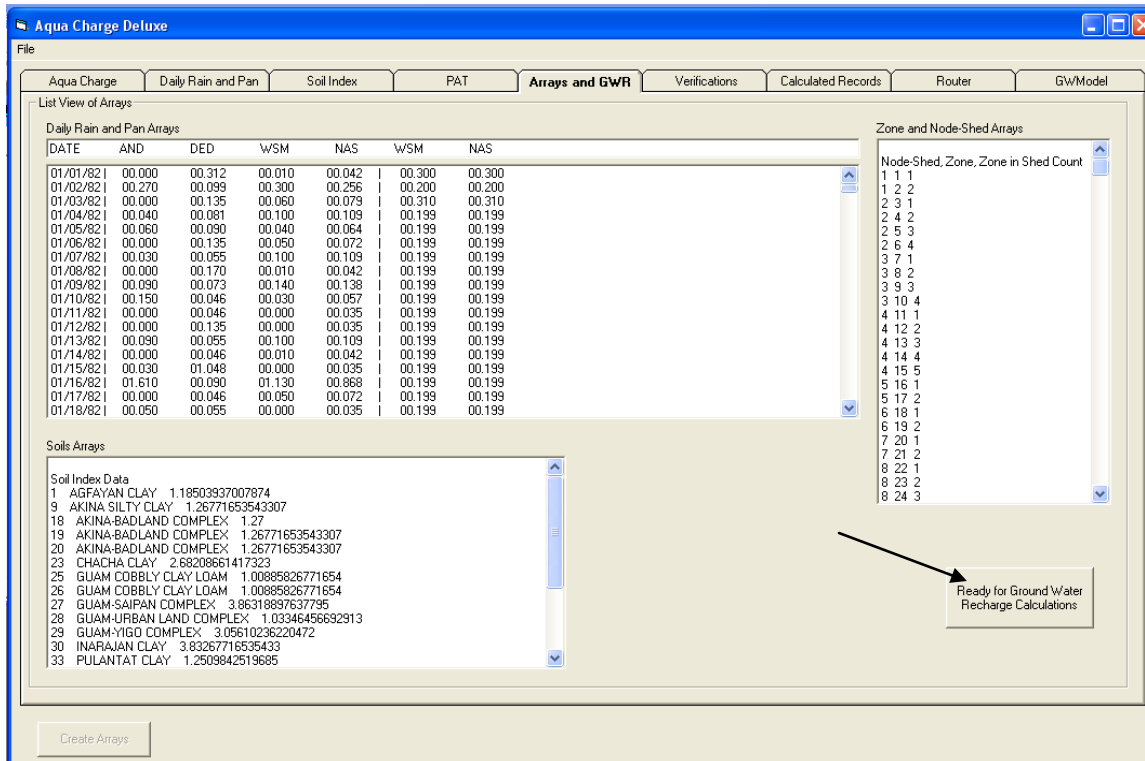


Figure 101. Ready for Groundwater Recharge Calculation button. The button opens the computational interval form.

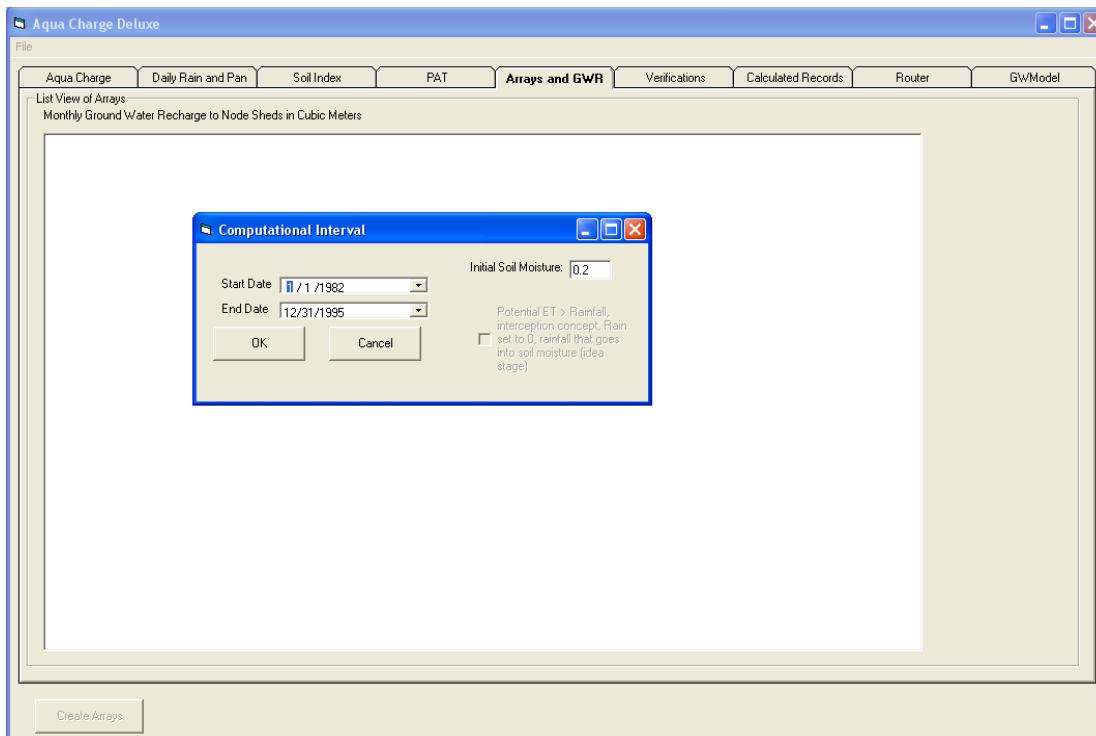


Figure 102. Computational Interval Form. This form allows the modeler to select within the recordset dates to compute the Stage 1 recharge calculation.

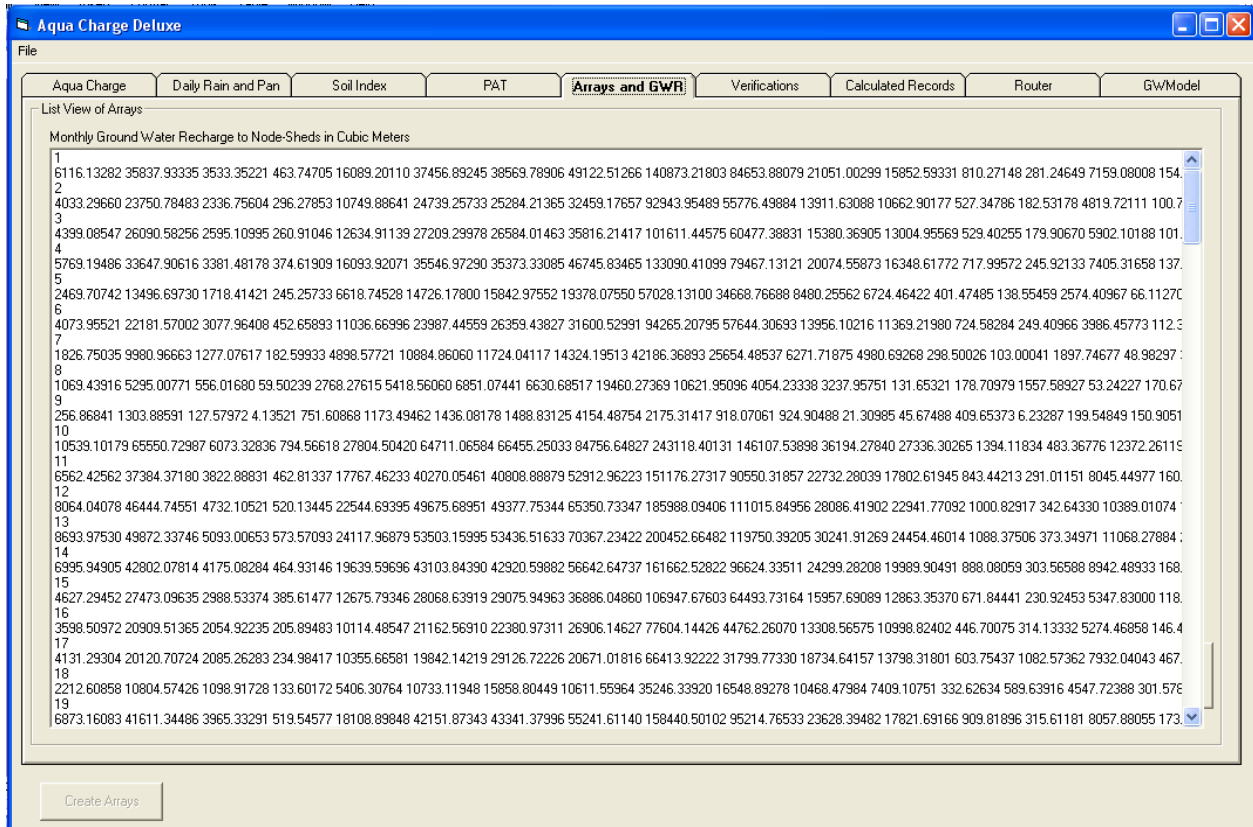


Figure 103. Monthly groundwater recharge to node-sheds list box. When calculation is done, the monthly GW recharge to node-sheds (cubic meters) is displayed in the list box.

Computation Verification Tab: A verification tab shows the calculation details so that the modeler can ensure that the computations were correct. This tab focuses on the zone recharge calculations (Figure 104). The list box on the top left hand corner allows the modeler to select a zone within an element to reveal the temporal, soil curves, and spatial values for that zone. This tab was an early form of the AQUA CHARGE program and was used to ensure that the algorithms were producing expected results.

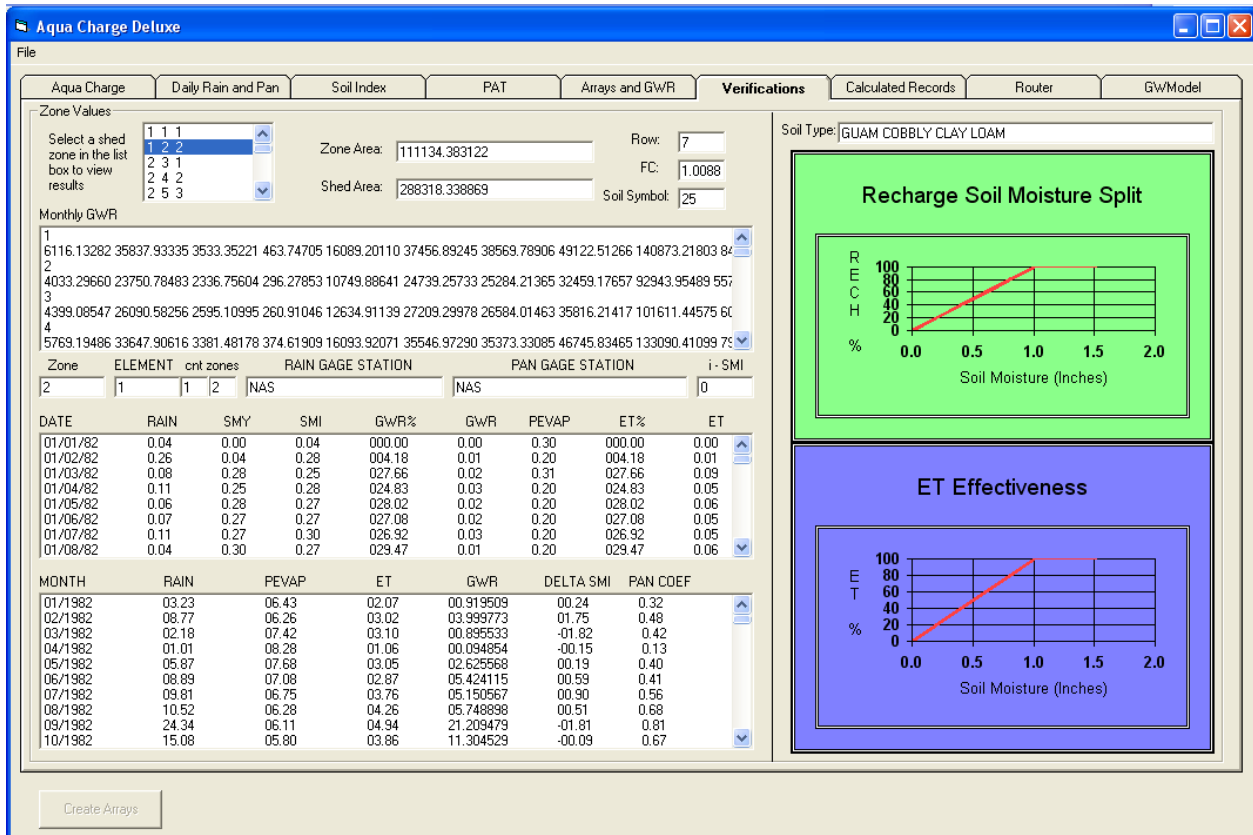


Figure 104. Verifications tab. This tab lets the modeler check and verify calculations for each zone.

Calculated Records Tab: A calculated records tab (Figure 105) shows the summary of the area weighted calculated values. These values are first calculated by clicking on the “Compute Area Weighted” command button on the top left corner. This tab reveals the AWAs of the entire domain. Monthly and annual weighted average recharges are provided. A button “Export Calculated Records” in the “MS Excel Output” frame at the lower right hand corner of the tab is enabled that allows the modeler to save the calculated records into an Excel File (Figure 106). The Excel file contains the records shown in Figures 107 to 110.

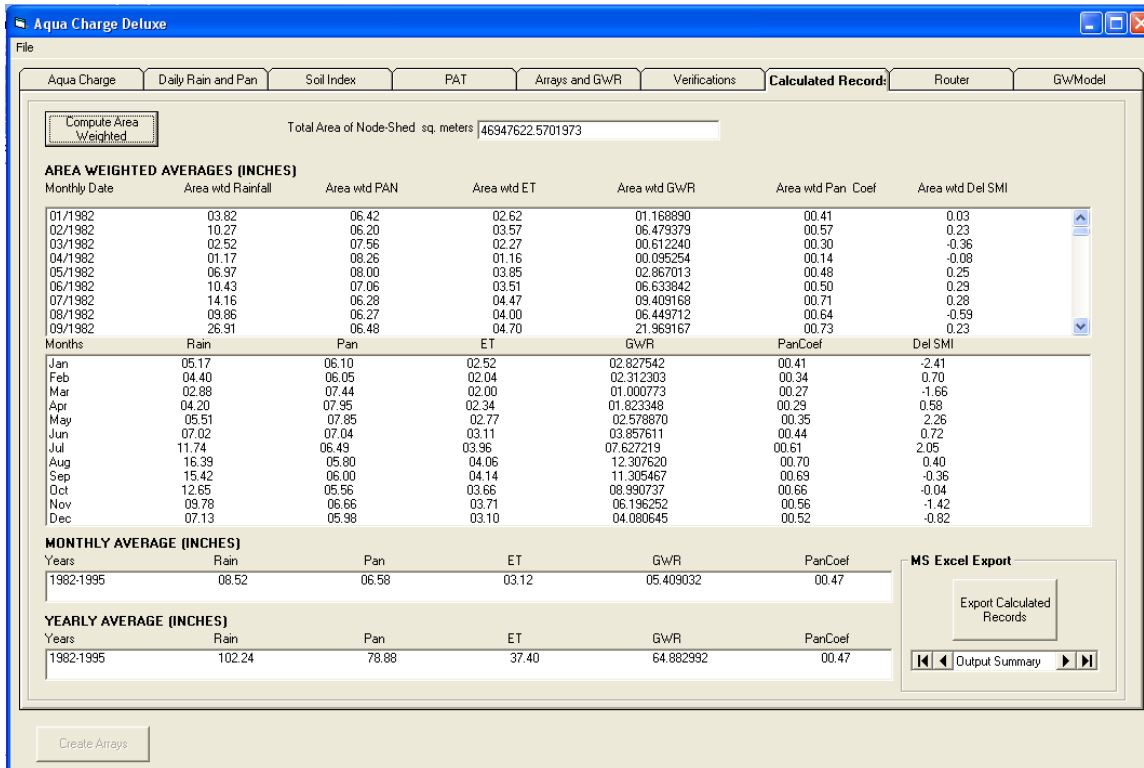


Figure 105. Calculated Records tab. This tab shows monthly and yearly summaries of calculations.

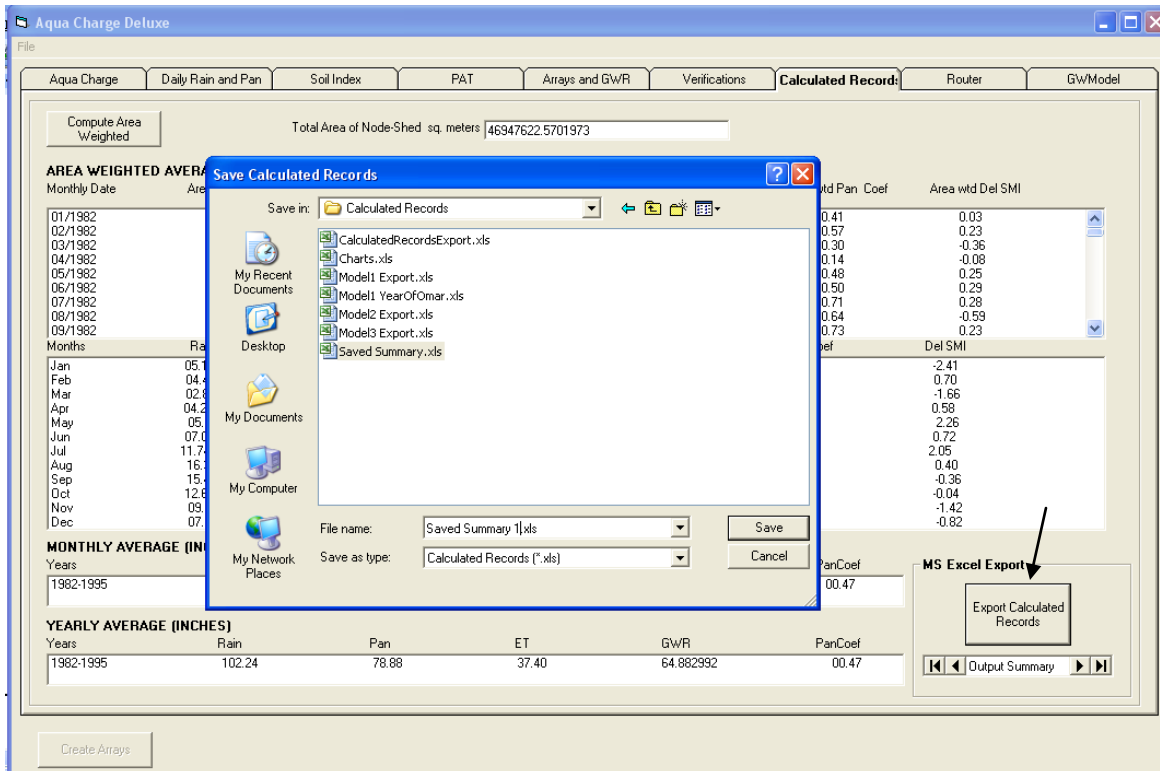


Figure 106. Export Calculated Records to an Excel file.

MONTHLY-YEARLY AVERAGES (Area Weighted, Inches)							
	YEARS	RAIN	PAN	ET	GWR	PAN COEF	
MONTHLY	1982-1995	8.52	6.58	3.93	4.705065	0.6	
YEARLY	1982-1995	102.24	78.88	47.18	56.438688	0.6	

Figure 107. Overall Monthly and Yearly average spreadsheet. Calculated Records exports monthly and yearly AWA (inches) of entire domain.

AVERAGES BY MONTH (Area Weighted, Inches)							
MONTH	RAIN	PAN	ET	GWR	PAN COEF	DEL SMI	
JAN	5.17	6.1	3.25	2.172308	0.53	-2.401396802	
FEB	4.4	6.05	2.55	1.845286	0.42	0.946765054	
MAR	2.88	7.44	2.47	0.659125	0.33	-1.24870197	
APR	4.2	7.95	2.8	1.577556	0.35	0.834656077	
MAY	5.51	7.85	3.35	2.18456	0.43	2.34562627	
JUN	7.02	7.04	3.56	3.571203	0.51	0.025972049	
JUL	11.74	6.49	5.04	6.62638	0.78	2.14924754	
AUG	16.39	5.8	5.12	11.288973	0.88	0.29107991	
SEP	15.42	6	5.14	10.322616	0.86	-0.3487128	
OCT	12.65	5.56	4.71	7.988634	0.85	0.054495272	
NOV	9.78	6.66	4.95	5.204764	0.74	-2.053909911	
DEC	7.13	5.98	4.27	3.019372	0.71	-0.776785342	

Figure 108. Averages by Month spreadsheet. AWA (inches) of entire domain.

MONTHLY AVERAGES (Area Weighted, Inches)						
MONTHLY DATE	RAINFALL	PAN	ET	GWR	PAN COEF	DEL SMI
1/1982	3.82	6.42	3.70	0.46	0.58	-0.18
2/1982	10.27	6.20	4.22	5.94	0.68	0.14
3/1982	2.52	7.56	2.69	0.18	0.36	-0.14
4/1982	1.17	8.26	1.29	0.04	0.16	0.00
5/1982	6.97	8.00	5.42	1.73	0.68	0.01
6/1982	10.43	7.06	4.94	5.38	0.70	0.33
7/1982	14.16	6.28	5.97	7.77	0.95	0.44
8/1982	9.86	6.27	5.26	5.33	0.84	-0.71
9/1982	26.91	6.48	5.32	21.44	0.82	0.16
10/1982	14.24	5.51	4.44	10.07	0.81	-0.21
11/1982	9.37	5.88	4.53	4.50	0.77	0.43
12/1982	7.17	6.24	4.89	2.76	0.78	-0.43
1/1983	1.49	6.97	1.70	0.05	0.24	-0.01
2/1983	1.65	6.18	1.67	0.09	0.27	0.00
3/1983	4.35	7.94	2.85	1.59	0.36	0.00
4/1983	1.45	8.61	1.69	0.05	0.20	0.00
5/1983	1.47	9.45	1.78	0.06	0.19	0.00
6/1983	0.77	9.28	0.99	0.03	0.11	0.00
7/1983	7.12	8.36	5.71	1.67	0.68	0.02
8/1983	10.74	6.43	5.42	5.10	0.84	0.33
9/1983	11.01	6.41	4.35	6.62	0.68	0.09
10/1983	11.22	6.00	5.41	5.52	0.90	0.32
11/1983	11.22	7.11	5.96	6.36	0.84	-0.71
12/1983	5.25	5.62	4.03	0.95	0.72	0.36
1/1984	3.10	5.46	3.09	0.51	0.57	-0.40
2/1984	4.27	6.15	3.19	1.19	0.52	0.00
3/1984	3.41	7.45	2.47	0.97	0.33	0.11
4/1984	2.08	8.05	1.53	0.27	0.19	0.39
5/1984	6.34	8.69	5.32	1.66	0.61	-0.33
Overall Monthly-Yearly Average						
Averages by Month						
Monthly Averages						
Node Shed Avg Recharge						

Figure 109. Monthly Averages spreadsheet. Monthly averages through the years, AWA (inches) of entire domain.

NODE SHED	RECHARGE
1	0.1178005295
2	0.1201455002
3	0.1359566079
4	0.1298665841
5	0.1007783110
6	0.1012219050
7	0.1054564406
8	0.0766550872
9	0.1290862956
10	0.1179076804
11	0.1236899106
12	0.1305768296
13	0.1287741563
14	0.1296163147
15	0.1195710642
16	0.1436706906
17	0.1826131373
18	0.1779542898
19	0.1170641109
20	0.1177925983
21	0.1324032310
22	0.1175294602
23	0.1175294602
24	0.1295819766
25	0.1582016835
26	0.1727809213
27	0.1805986407
28	0.1179256259
29	0.1177611063
30	0.1430109535
31	0.1236072655
32	0.1422727363

Figure 110. Node-shed Average Recharge spreadsheet.

Stage 2 – Routing

Now that recharge beneath the soil layer is done, the modeler may use a technique called routing to simulate the attenuated vadose flow to the lens. This is Stage 2 of the vadose-flow conceptual model which splits the fast and slow flows and uses the modified pulse routing technique described in Chapter 2. The interface is in the router tab (Figure 111). The modeler clicks open the router tab and clicks on the power button to enable the controls. If the modeler wants to use AQUA CHART to graph and view the recharge synthesis, the AQUA CHART button allows the modeler to select and open the AQUA CHART Excel file (Figure 112).

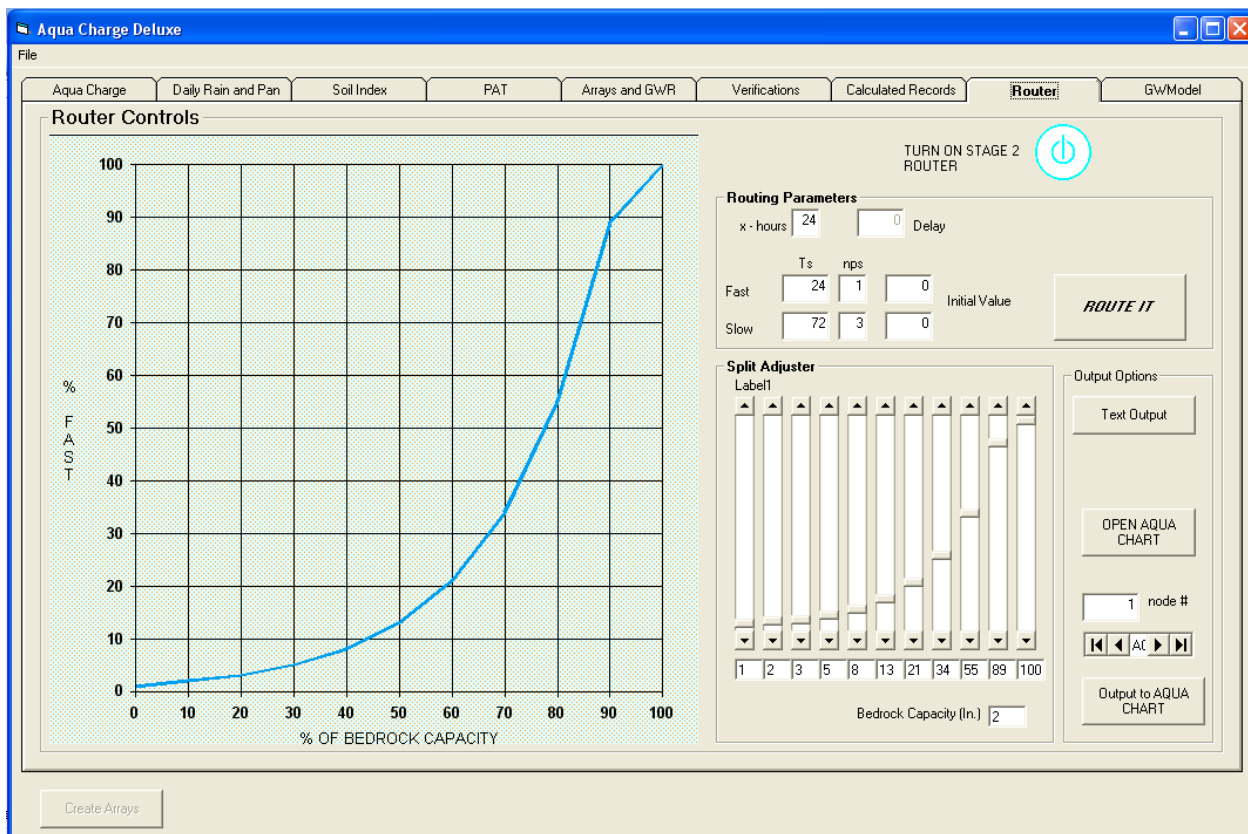


Figure 111. The routing tab.

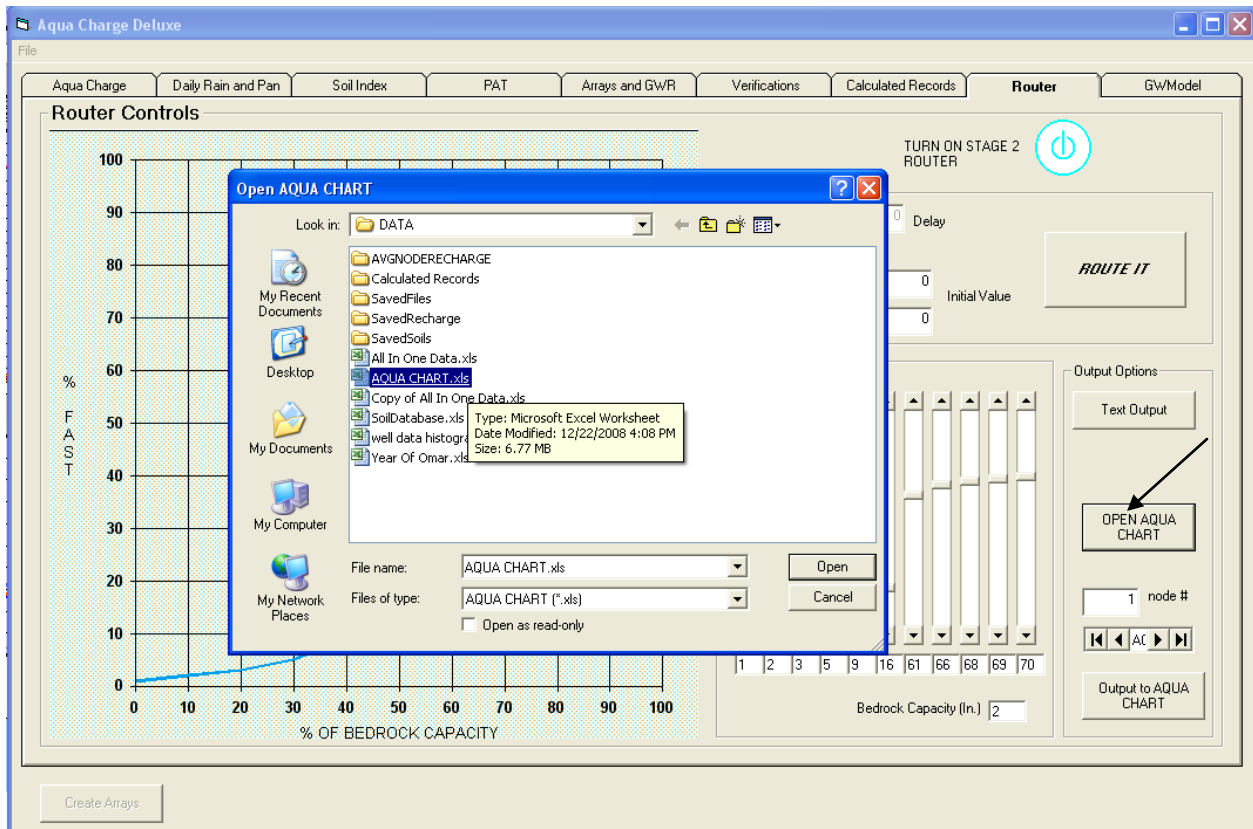


Figure 112. Open AQUA CHART command button.

Before any routing can be done, the modeler must adjust the percent curve splitter that determines the percentage of the AWA node shed recharge that will go to slow or fast routing. The percent to fast flow, in this model, depends on the previous day's slow flow bedrock moisture to determine the percent of bedrock capacity (BC) in the x-axis. The BC, in inches, can be entered in a text box below the vertical adjustment bars. The curve shape produces a small percent to fast recharge when the previous day's slow recharge and its percent of (BC) are small. As it approaches near BC, the percent to fast recharge rapidly increases. Then, it levels off around 45% to 75% since it can still continue to fill in the matrix pores with water that contribute to slow flow. This is considering the thick (greater than 100 feet) of granular matrix media of Barrigada Limestone. The vertical bars to the right of the chart allows the modeler to adjust the curve by moving them up or down or the modeler may input into the text box, beneath the bars, the percent value (Figure 113).

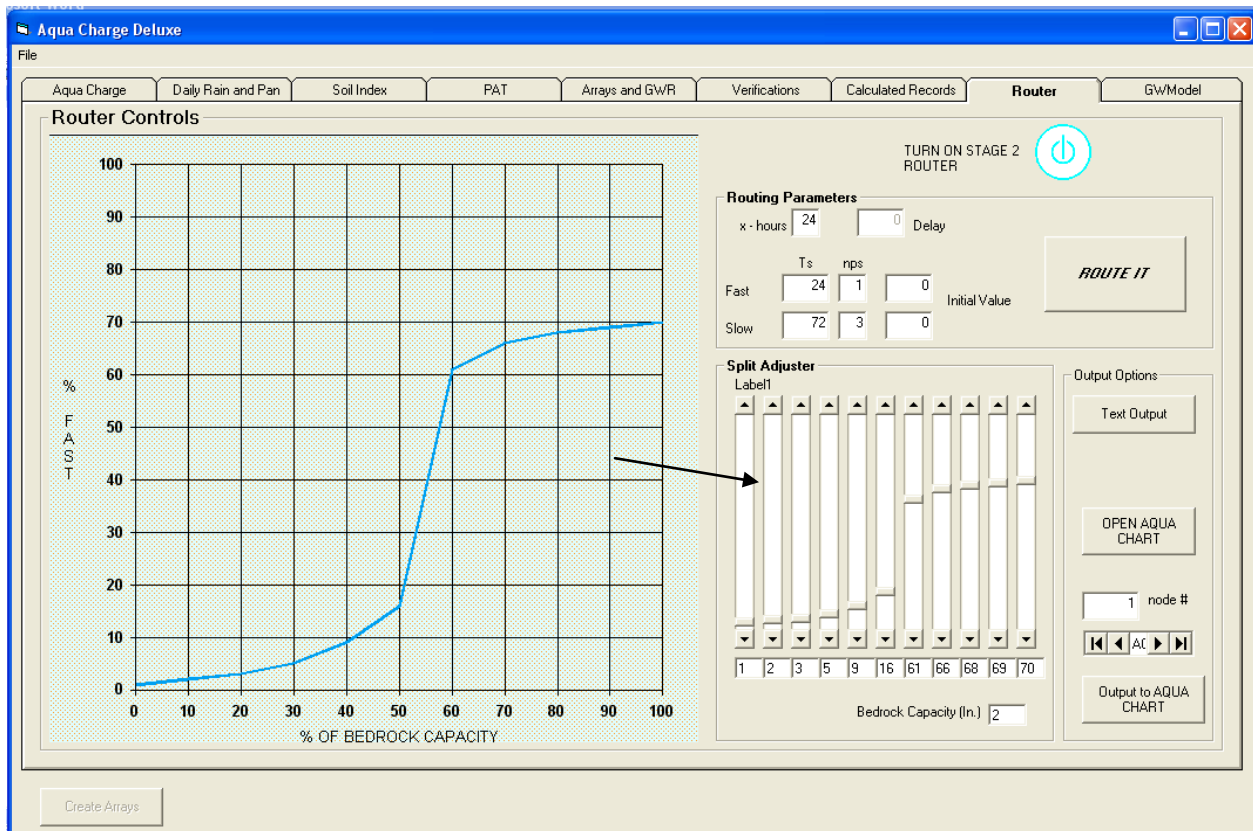


Figure 113. Percent Fast/Slow curve adjustment.

The routing parameters frame in the router tab is where the final adjustments are for synthesizing recharge. This is also where the command button “ROUTE IT” is placed that holds the routing execution code (Figure 114). Here is where the modeler enters values in the text boxes to control the attenuation and lag time of the fast and slow flow recharge. These variables are the same variables mentioned in the equation for routing in Chapter 2. The x-time is set to a 24 hour computational interval. In this case twenty four hours is set in the text box. Each fast and slow parameter have their own T_s (time of storage), nps (number of phases), and the initial value. In this project, the initial value is set to zero and the rest at their default settings. Simple guidelines to follow when using routing is when T_s is large, the curve response produced is wide and is good for simulating slow flow. And likewise, when T_s value is small, a narrower curve response is produced and is good for representing the fast flow recharge to the lens. Increasing the nps will increase the lag time. Routing begins by estimating the values, and then adjustments are made to the curve, the BC, T_s , and nps. The modeler continues to make changes using also the “well guide” (Chapter 5) to adjust the lag and attenuation of the fast and slow flows. The “output to AQUA CHART” button is continually used to send data to the AQUA CHART where the modeler can visually analyze the synthesized recharge results.

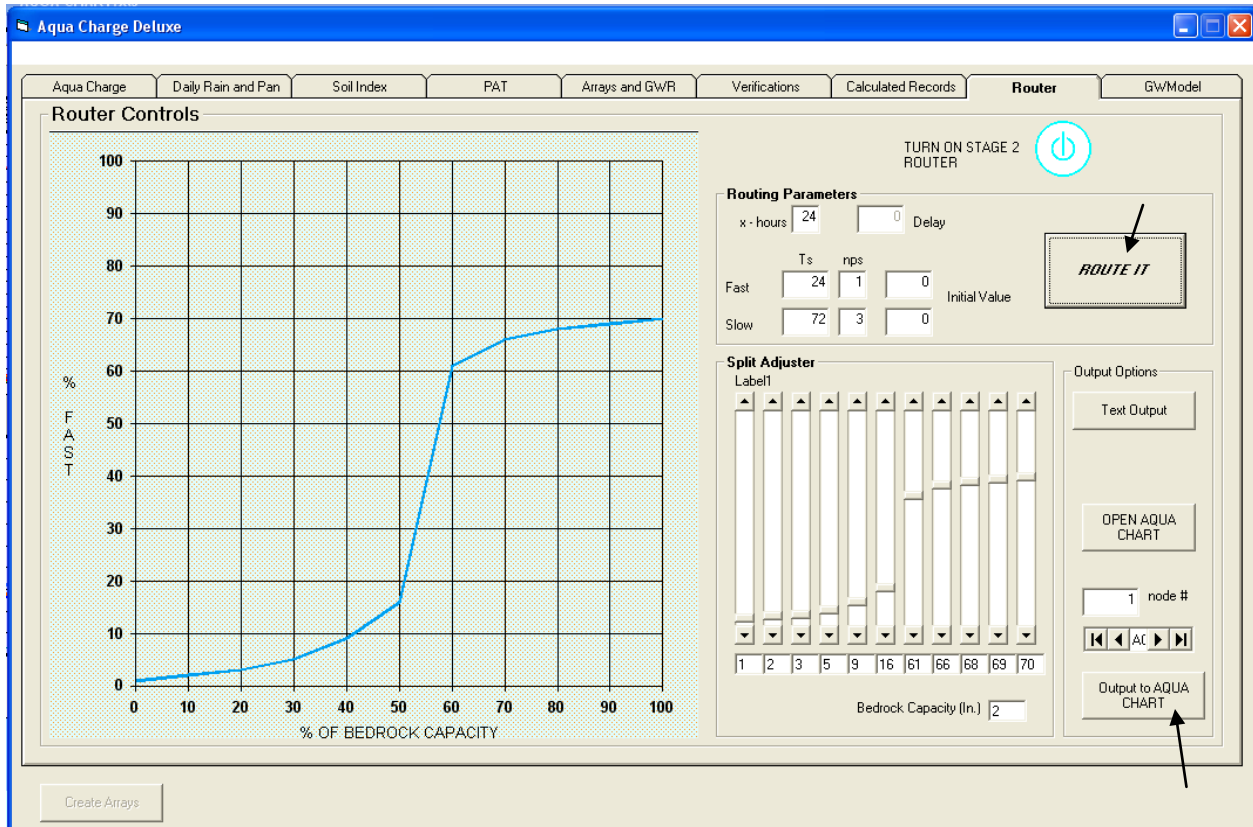


Figure 114. The ROUTE IT and Output to AQUA CHART command buttons.

AQUA CHART Output Monitor

First of all, any Excel worksheet file can be made to receive the routed output recharge and the simulated GW hydraulic head from a selected node and for all the nodes. That Excel file must have two named and defined recordsource, and the modeler can use the exported data in any way he or she sees as appropriate.

The first recordsource is the fast, slow, and the sum of fast and slow routed recharge, and a simulated GW head output for a selected node-shed number. The Excel file will have five field names; DATE, RECHARGE, FAST, SLOW, and XVAL (Figure 115). To name and define the recordsource, select insert on the menu bar and choose name on the dropdown menu and select define (Figure 116). Title the recordsource "RECHARGE" and select the range that covers the fields "RECHARGE" to "XVAL", and having the row value for the last number equal the number of days of computational period plus one (Figure 117). For example, for 1982 to 1995 years totals 5112 days, plus one equals 5113. So the 'Refers to:' data range selection box should read "=Sheet1!\$B\$1:\$E\$5113" where the end is numbered 5113 (Figure 117). Click the "Add" button and then the "OK" button to name and define the recordsource "RECHARGE." Again, this sheet is now ready to receive data for a selected node-shed number during the recharge synthesis and the finite element method simulation.

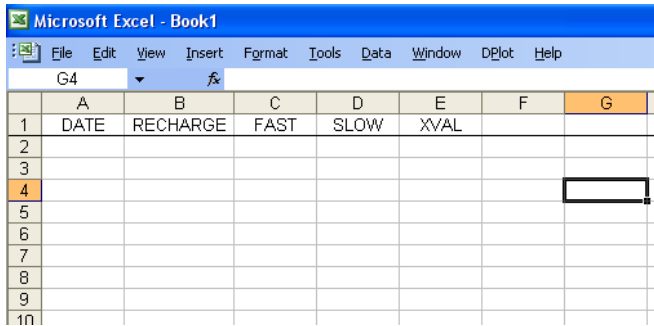


Figure 115. Field names setting.

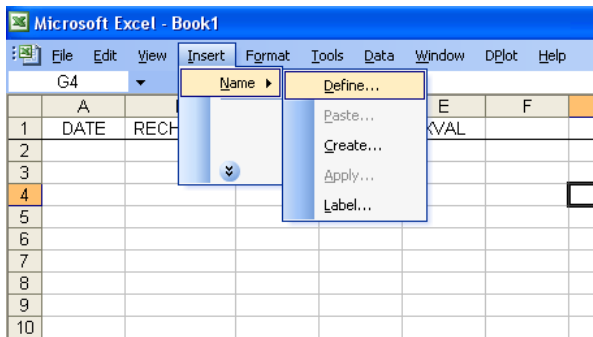


Figure 116. Insert, Name, and Define from the menu bar.

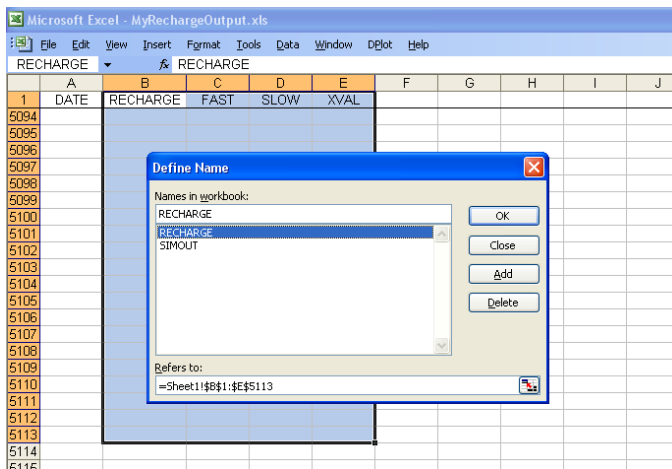


Figure 117. Defining names for recharge output to AQUA CHART.

The other recordsource was designed for data that may be transferred to GIS for interpolating and animating the entire domain after the GW simulation process. The field names for this second spreadsheet are “NODE”, and “X1 to X30.” The X1 to X30 represents the hydraulic head for day X1 to X30 (Figure 118). The NODE field is numbered from 1 to the total number of nodes, which in this project’s domain consist of 137 nodes. The entire range is selected from the “NODE” field to 137 to X30. The selection is named and defined as

“SIMOUT” and the Add and OK buttons are clicked (Figure 119). The file is saved as whatever name the modeler chooses (Figure 120). This file during the routing process may be opened using the OPEN AQUA CHART button in AQUA CHARGE’s Routing tab (see Figure 112). The Excel file is now ready to receive data from AQUA CHARGE during the routing and the finite element method process. More details for sending data to this recordsource are explained in the Finite Element Method Program section.

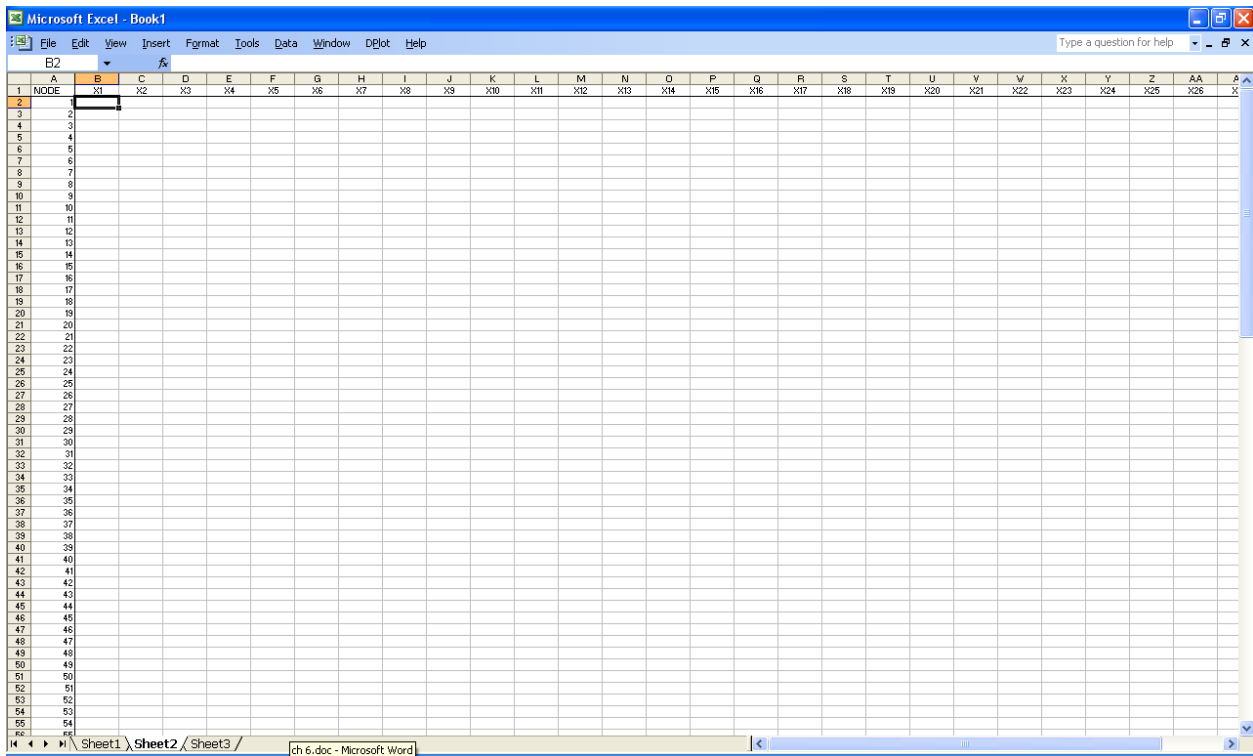


Figure 118. Field Names and Node numbers for SIMOUT.

Vadose Flow Synthesis for the Northern Guam Lens Aquifer
AQUA CHARGE User Manual

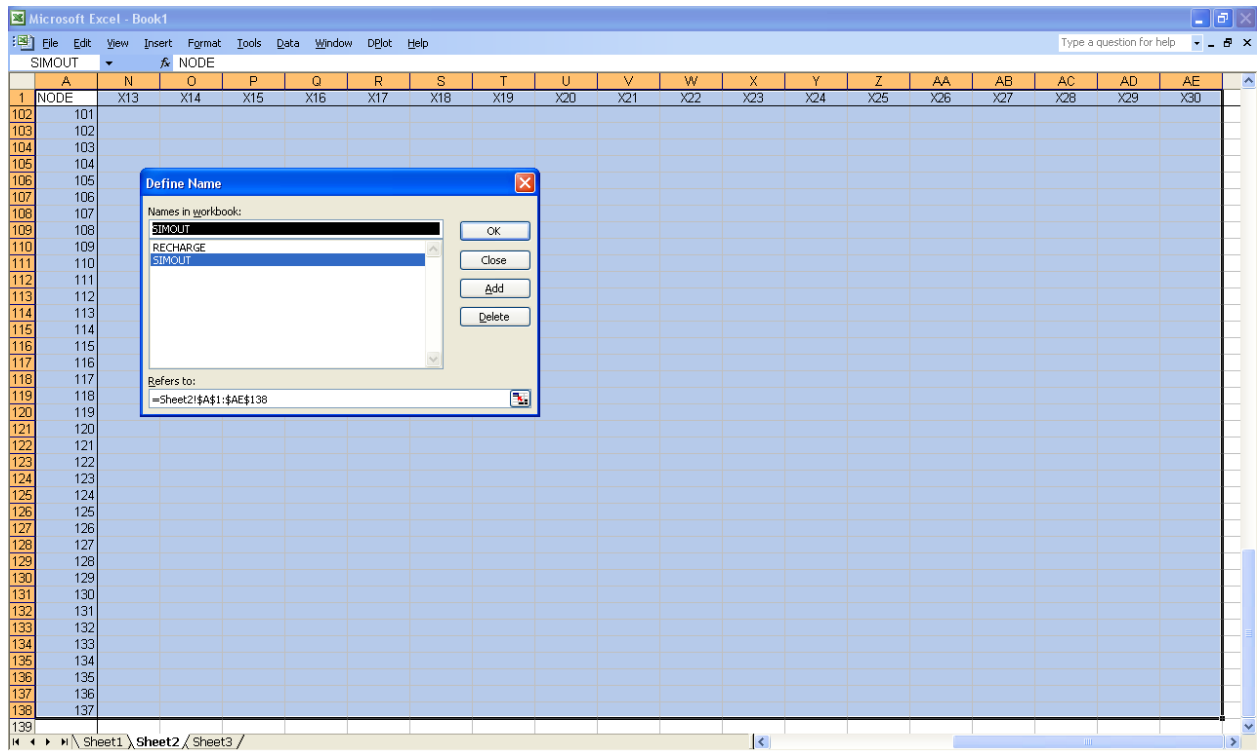


Figure 119. Define name for SIMOUT.

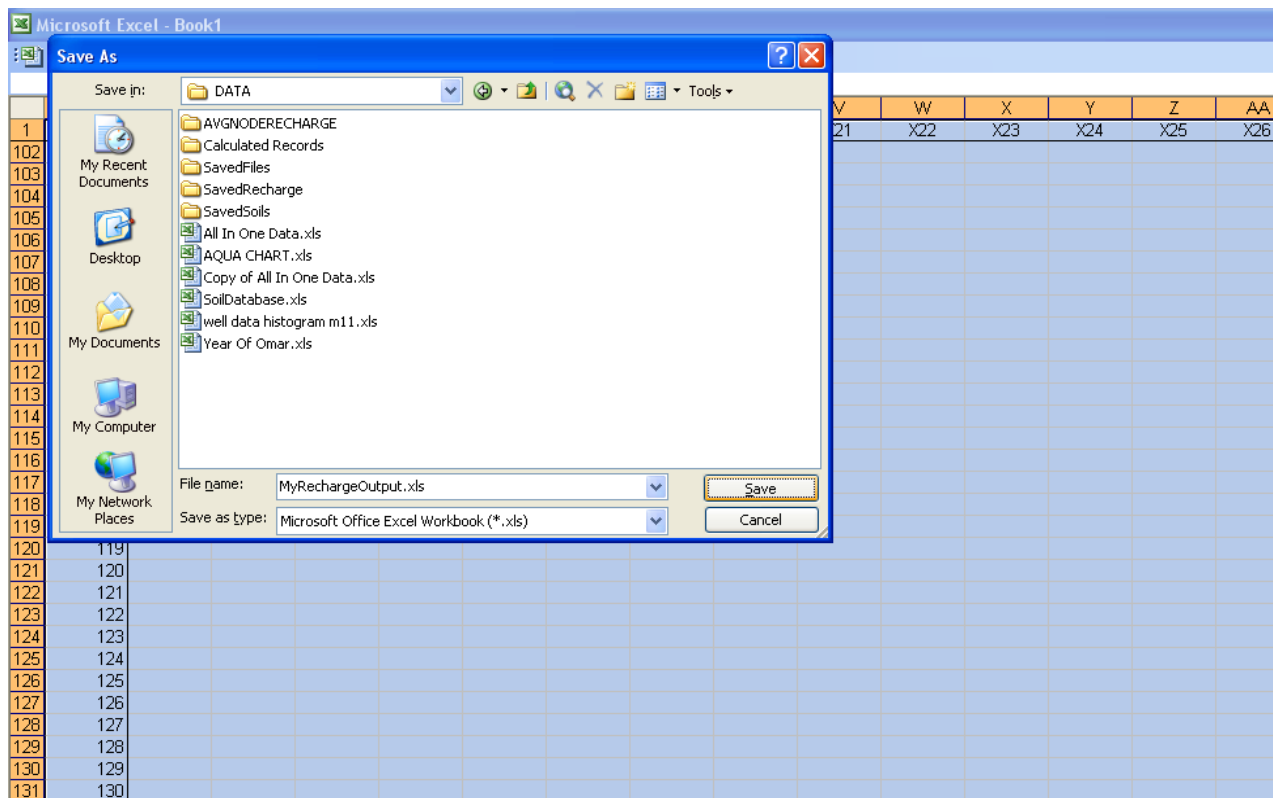


Figure 120. Save the file name.

With Excel's simple and popular charting flexibility and programmability, we were able to work with the data output and build AQUA CHART. The details to the design of AQUA CHART will not be provided. The modeler can use the flexibility of MS Excel to view the exported data however he/she may choose. Much other data was added to AQUA CHART and the extra spreadsheets were added to run data analysis.

However, using AQUA CHART, the modeler runs scenarios and makes adjustments while looking at the rainfall and output recharge synthesis data graph with the data graph from a selected observation well. AQUA CHART was designed and programmed in Microsoft Excel's Visual Basic environment that allows the modeler to easily scroll horizontally through years of meteorological data, synthesized recharge, and observation well response with all aligned in time (Figure 121).

After the routing is completed, the modeler may select a node and send the data to the AQUA CHART. The modeler analyzes the synthesized recharge graph with the observation well graph and to determine if it should be tried in the hydraulic model. The two results (recharge and well level) are not directly comparable, but the comparison can be useful for determining any necessary adjustments to the soils curves, the fast flow curve, or the routing parameters to visually determine whether more or less attenuation is required. A good method to use is the well guide described in Chapter 5. AQUA CHART has two control buttons that allows the modeler to scroll to the left or to the right of the date axis and a number entry cell for entering the number of days to scroll back and forth. The buttons for scrolling in the date axis have black arrow heads that point in the direction of scroll.

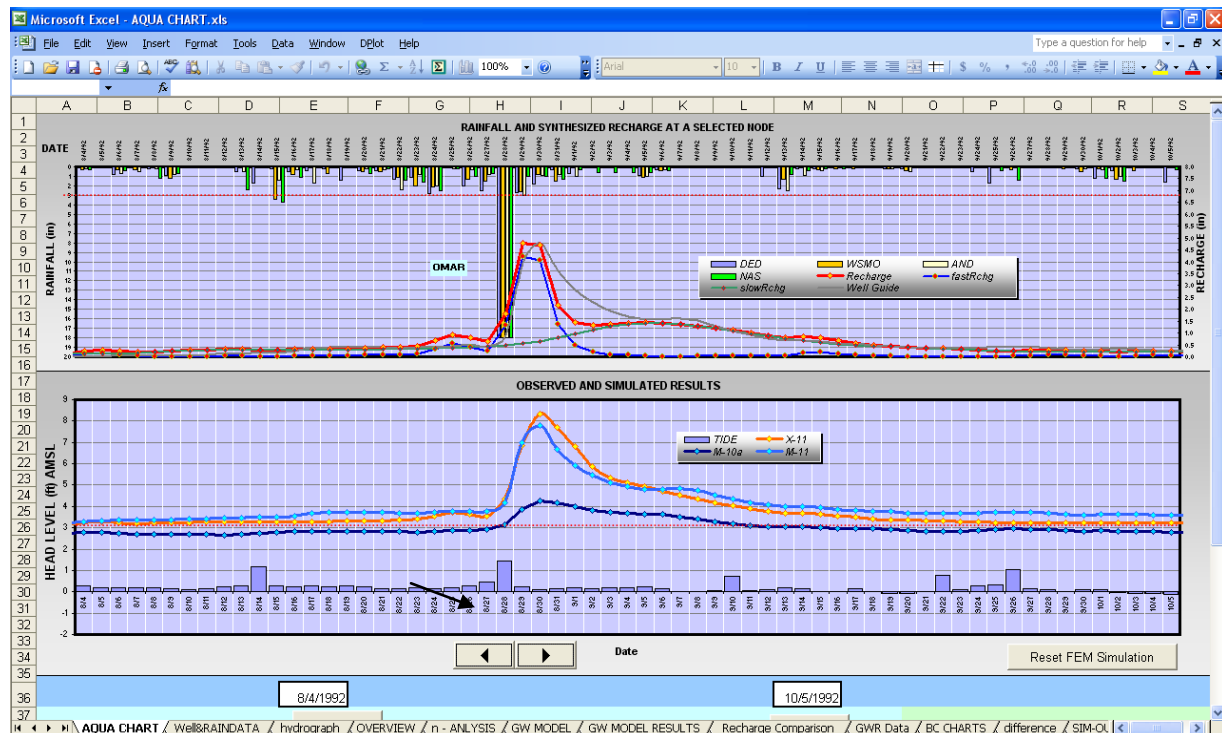


Figure 121. AQUA CHART interface. The top chart shows rainfall from four gages on the secondary axis as bars. The primary axis holds the recharge, fast, slow, and guide curves. The chart below it is the observation well levels (blue), the tide (blue bars), and the simulation (orange). An arrow points to the date axis scroll buttons.

Text File Recharge Output For Hydraulic Models

After the routing is executed, the modeler may want to apply the synthesized recharge to a GW hydraulic model. AQUA CHARGE can save a data text file of the synthesized recharge in units of cubic meters per day (Figure 122). This text file may be imported into a hydraulic model such as the finite element method. To extract the data, in the router tab and in the output options frame, click on the text output button. A common dialog box opens to facilitate in saving the file. The format for this data is as described in Chapter 4.

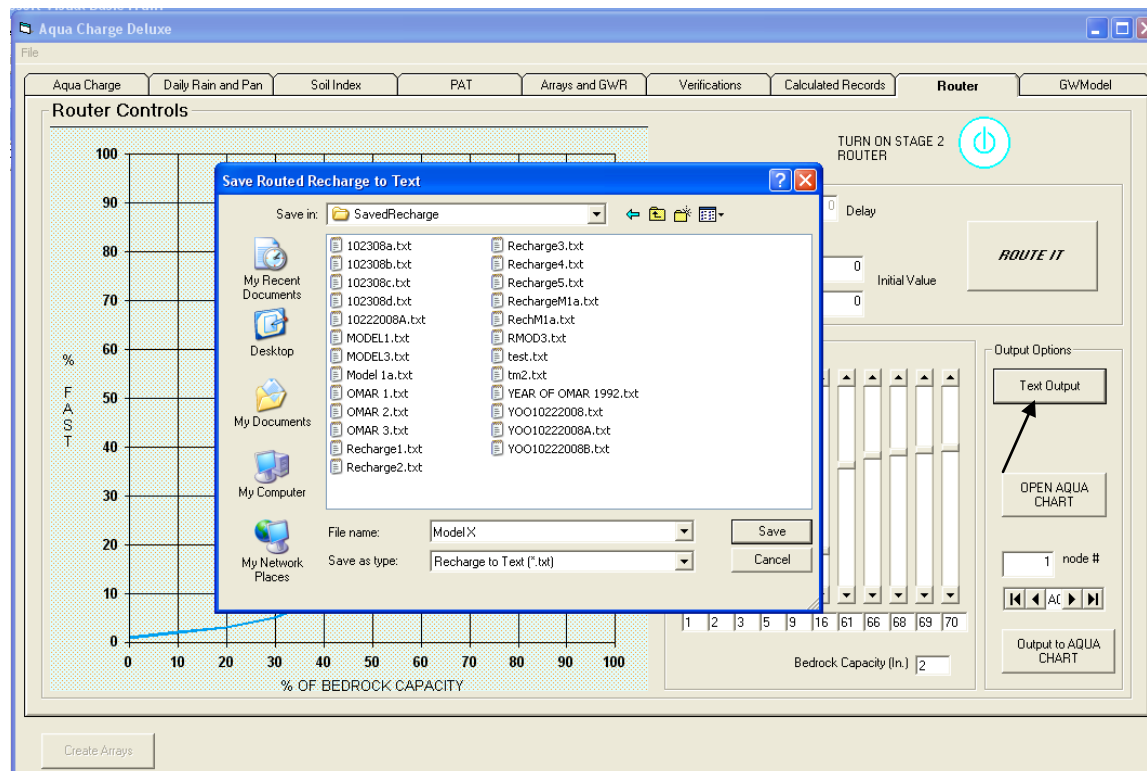


Figure 122. Saving the routed recharge to a text file.

AQUA CHARGE Finite Element Method Program

A Finite Element Method, 2-D, transient, saturated GW flow model was added to AQUA CHARGE and is located in the last tab called GWModel. The VB 6.0 form had reached its capacity for adding controls from the tool box that it had to be constructed on another form. The last tab has a button (Figure 123) that opens up the 2-D Transient, Saturated Groundwater Flow form (Figure 124). The finite element method was added to receive the recharge output text file. The purpose for this was to match GW modeling simulation to observed well response from the synthesized recharge. Details for this topic are described in Chapter 3.

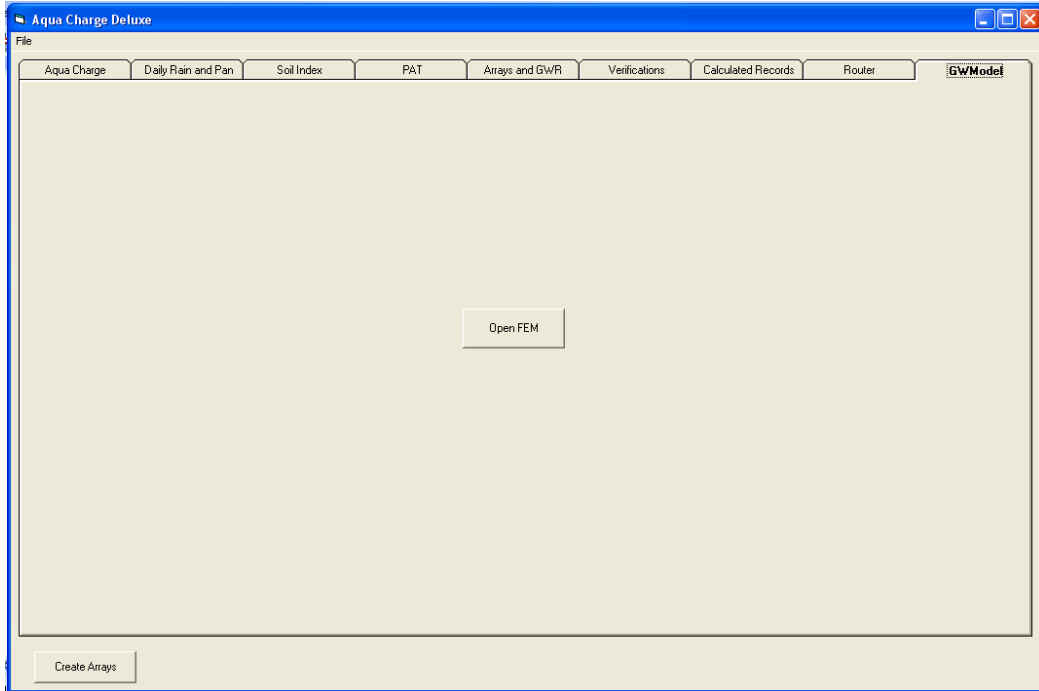


Figure 123. AQUA CHARGE GWModel tab. The GW model tab has a button that opens up the 2-D transient saturated-flow program form interface.

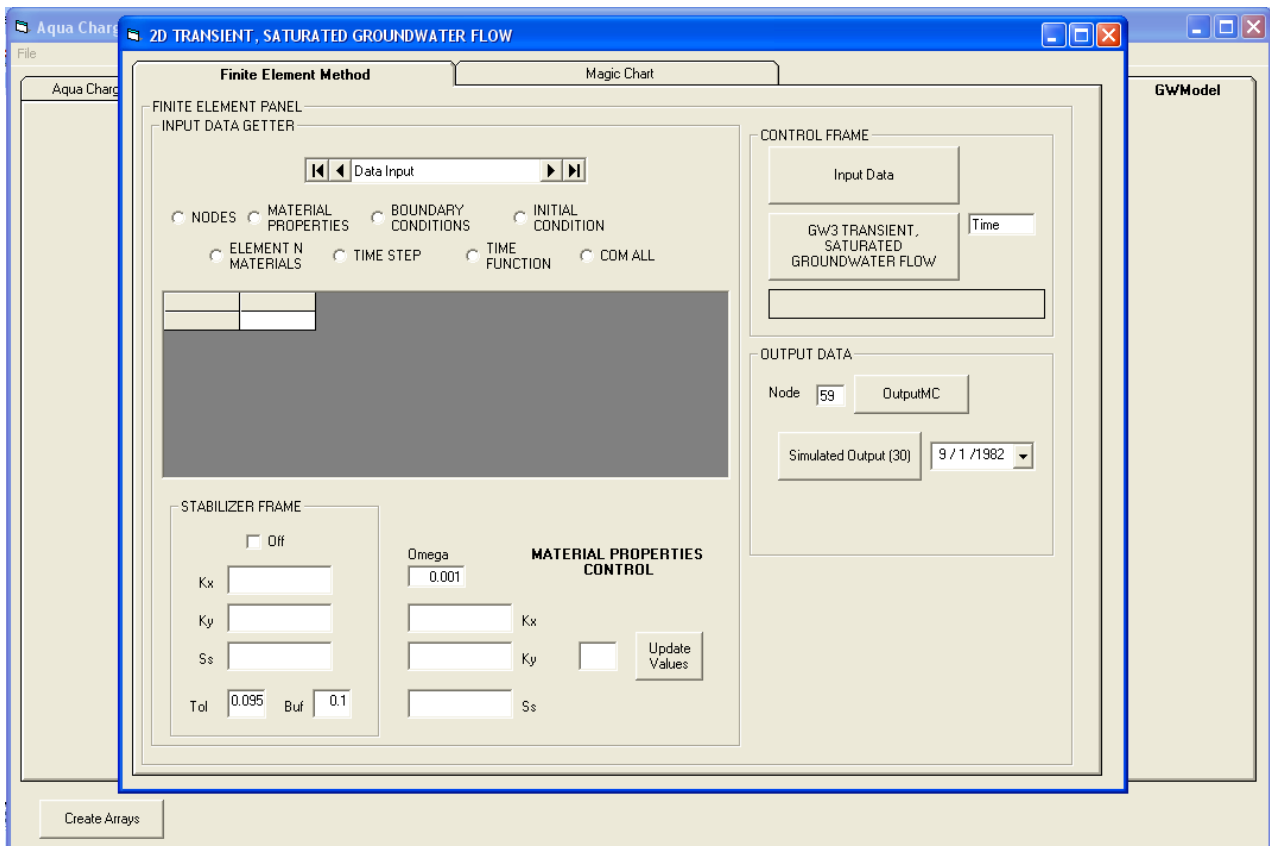


Figure 124. Finite element program interface.

The input data button opens the common dialog box to select the FEMData.xls and the recharge text file (Figure 125). Again, the FEMData holds data recordsource and recordsets as information of the mesh domain design. After the FEMData has been selected, a second common dialog box appears to select the recharge file text file (Figure 126). The recharge text file is the final recharge synthesis known as Stage 2 of the conceptual model for the entire domain.

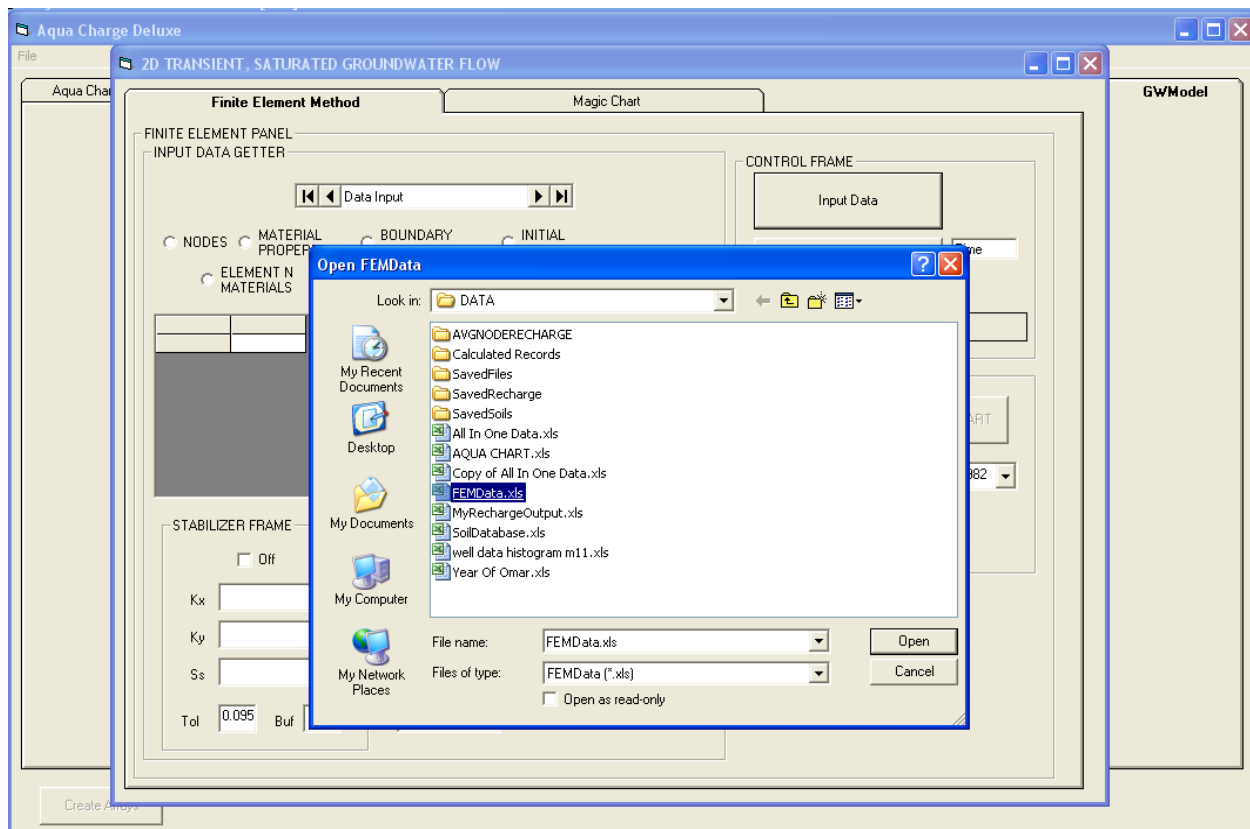


Figure 125. Opening FEMData.

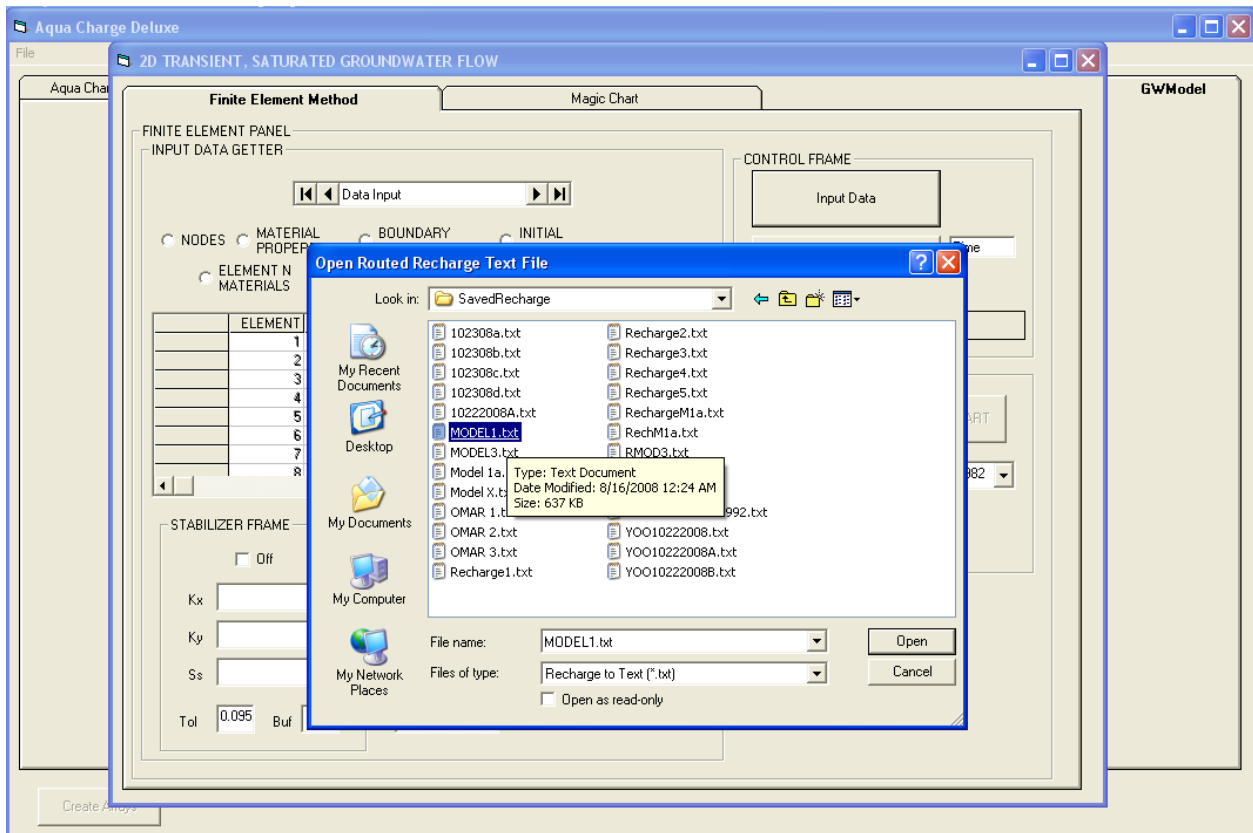


Figure 126. Opening the recharge text file.

Once the input data is loaded, the modeler may look at the data through the table and by selecting an options button. The **NODES** option displays the node number, its x and y coordinates, the material type, and the area of the node-shed for that particular node (Figure 127). The **ELEMENT N MATERIALS** option shows the element number and its surrounding nodes in counterclockwise order and also its material property number (Figure 128). The **MATERIAL PROPERTY** option shows three material properties identified as numbers with its $K_{x/y}$ value and S_s value (Figure 129). When this option is selected, the modeler may change the $K_{x/y}$ by clicking the material number row, changing the values in the text box in the **MATERIAL PROPERTIES CONTROL**, and clicking the “Update Values” command button (Figure 130). The **TIME STEP** option shows the daily time step value as one (Figure 131). The **TIME FUNCTION** was controlled in the finite element sub routine code, so it is not used as input data. The **COM ALL** option displays important variables such as number of nodes, number of elements, the mesh type shape, and so on (Figure 132).

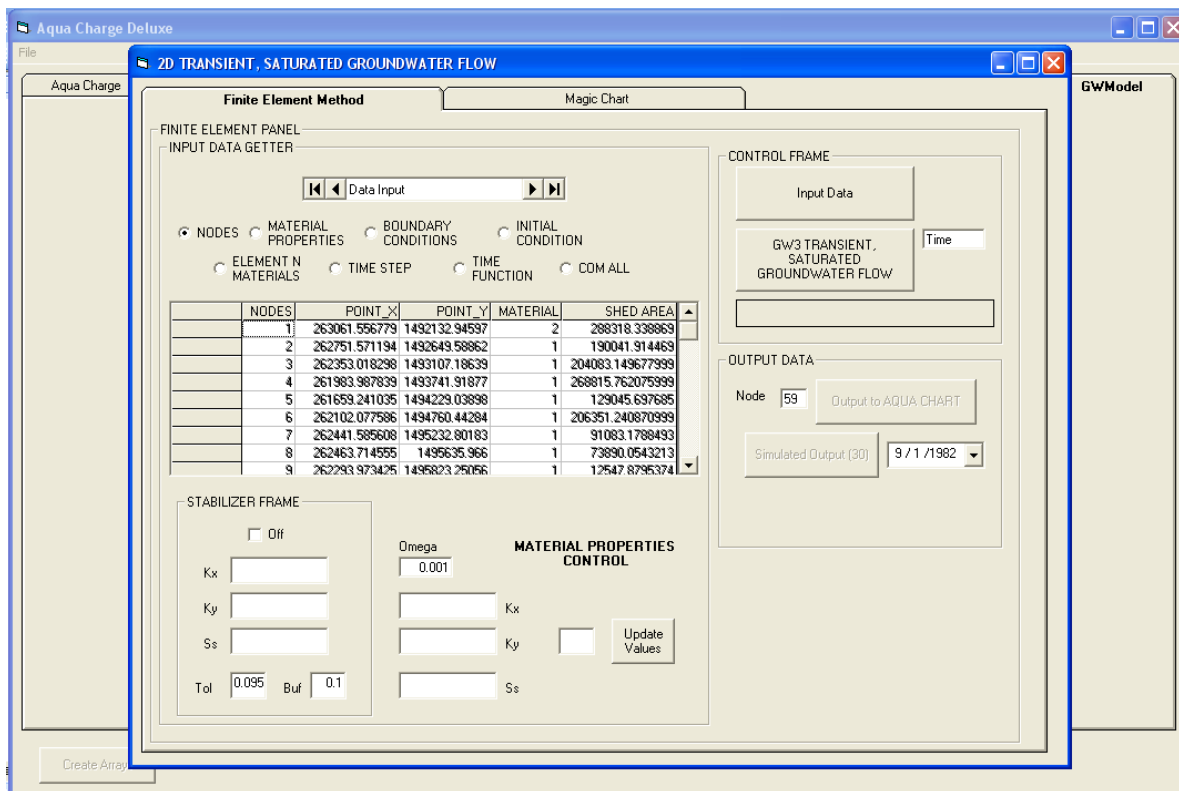


Figure 127. NODES option button.

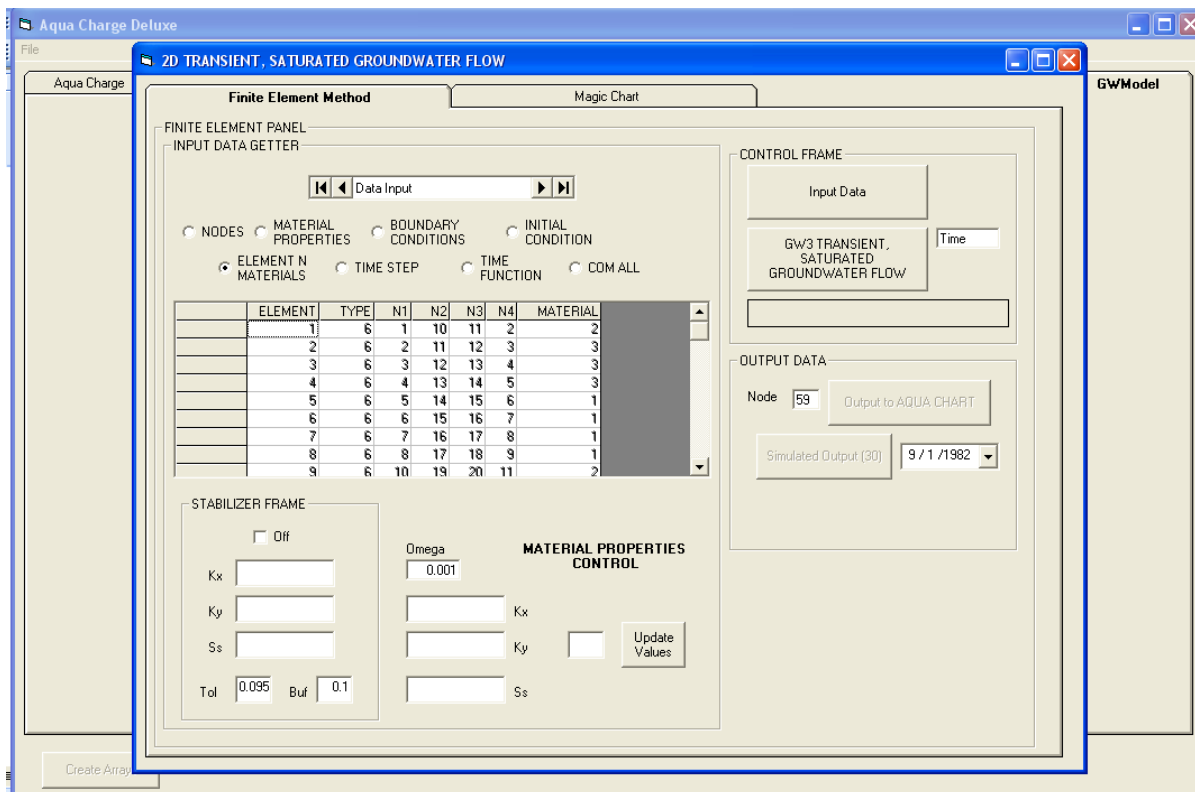


Figure 128. ELEMENT N MATERIALS option button.

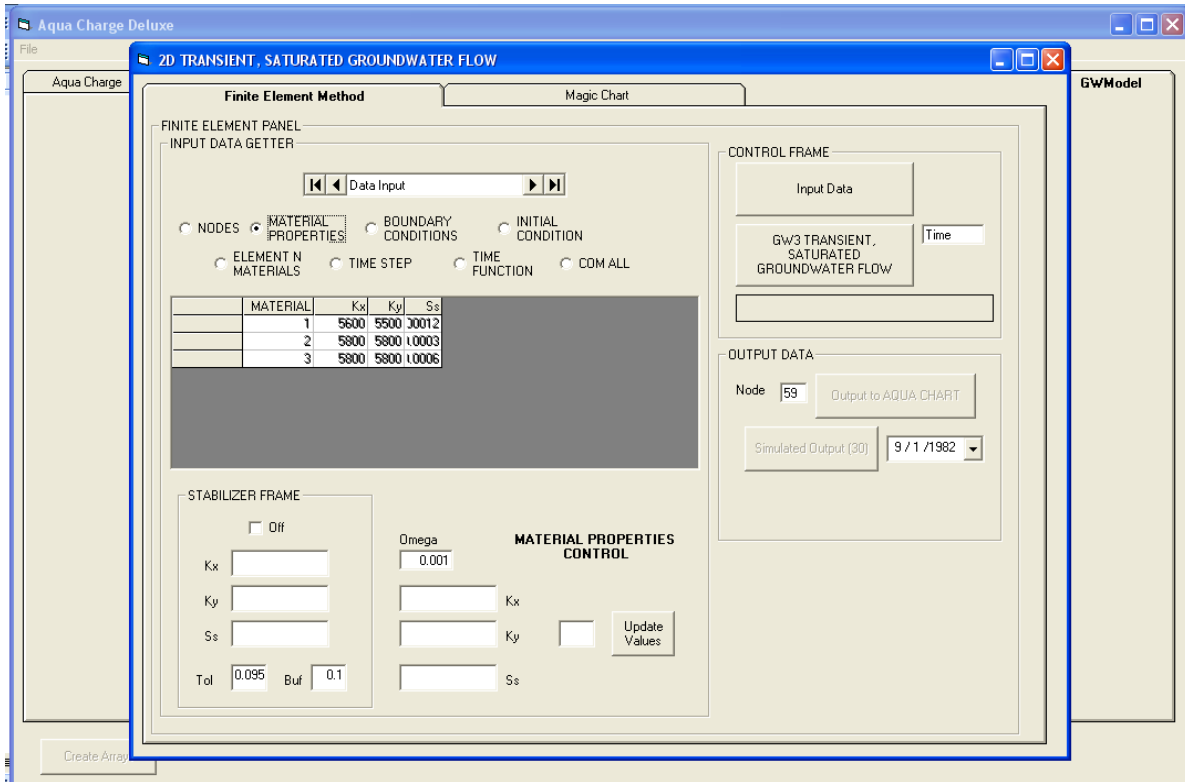


Figure 129. MATERIALS PROPERTIES options button.

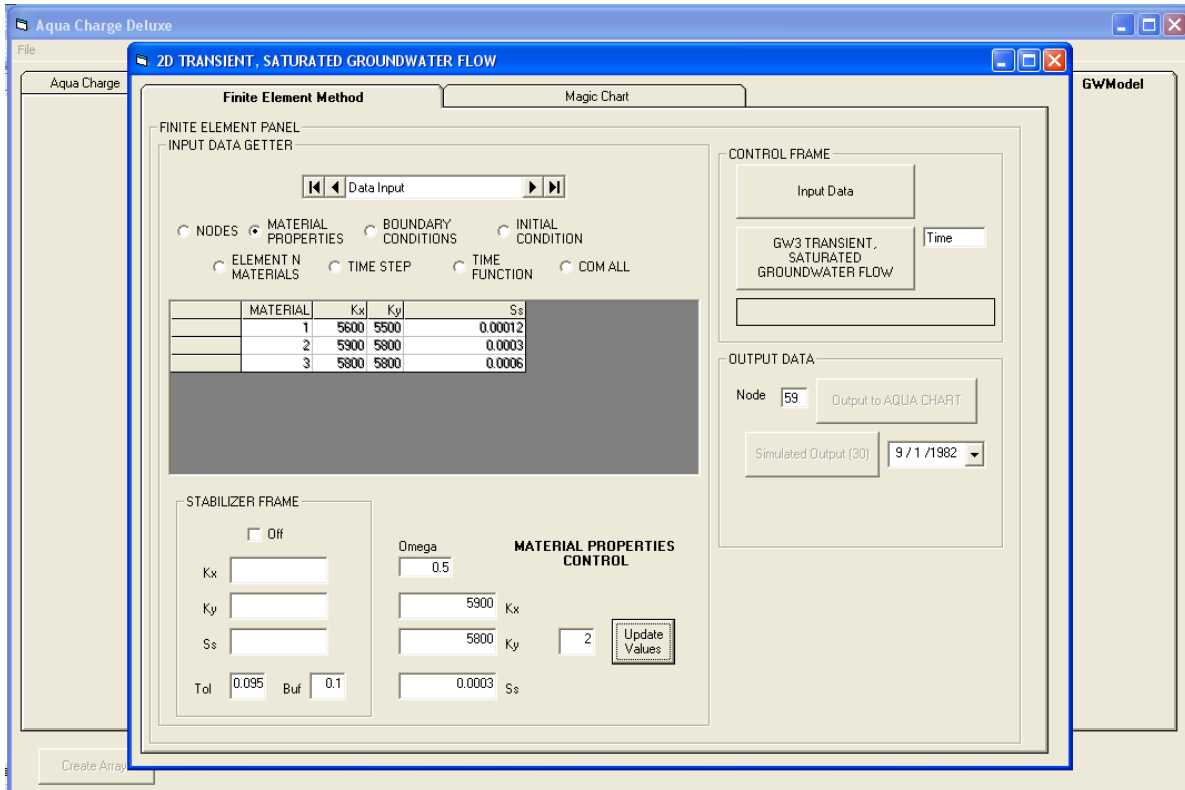


Figure 130. Changing the materials properties data.

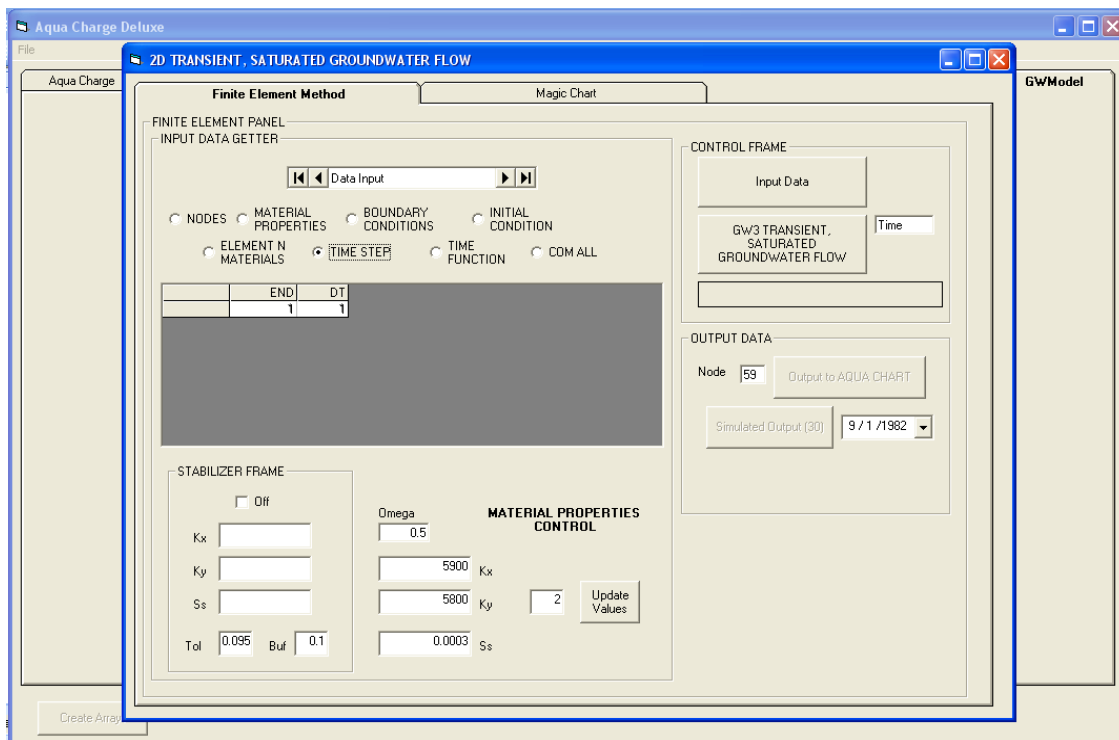


Figure 131. TIME STEP Options.

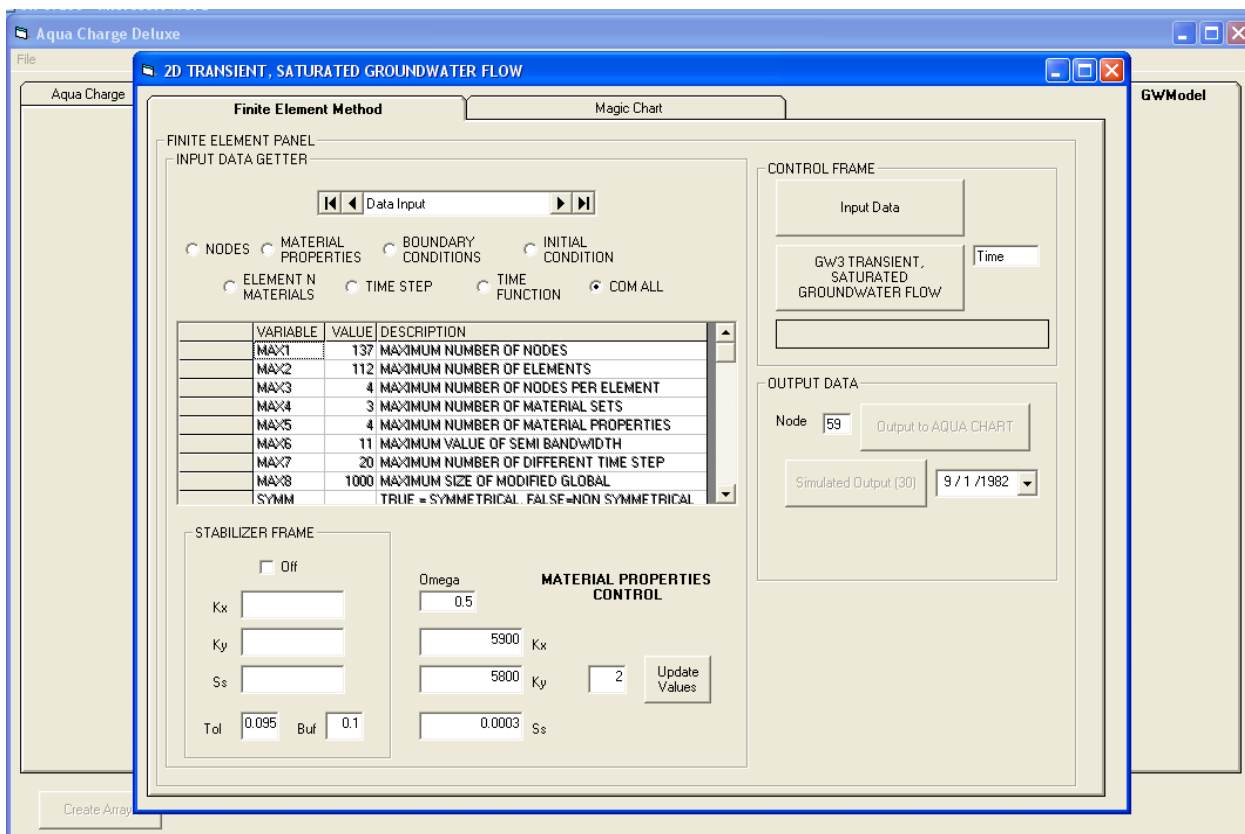


Figure 132. COMALL Options.

If all the input data is loaded properly, the modeler can click the “GW3 TRANSIENT, SATURATED GROUNDWATER FLOW” button (Figure 133) to run the finite element code. The GW3 is a subroutine from Istok’s code for a transient saturated flow model. A simplified explanation of the equations involved is in Chapter 3. When the program is done running, the modeler may select a node to chart the results in daily time steps using the “Output to AQUA CHART” command button (Figure 134). The modeler will be prompted to open AQUA CHART if it is not opened already (Figure 135). AQUA CHART displays the results on the bottom chart (Figure 136).

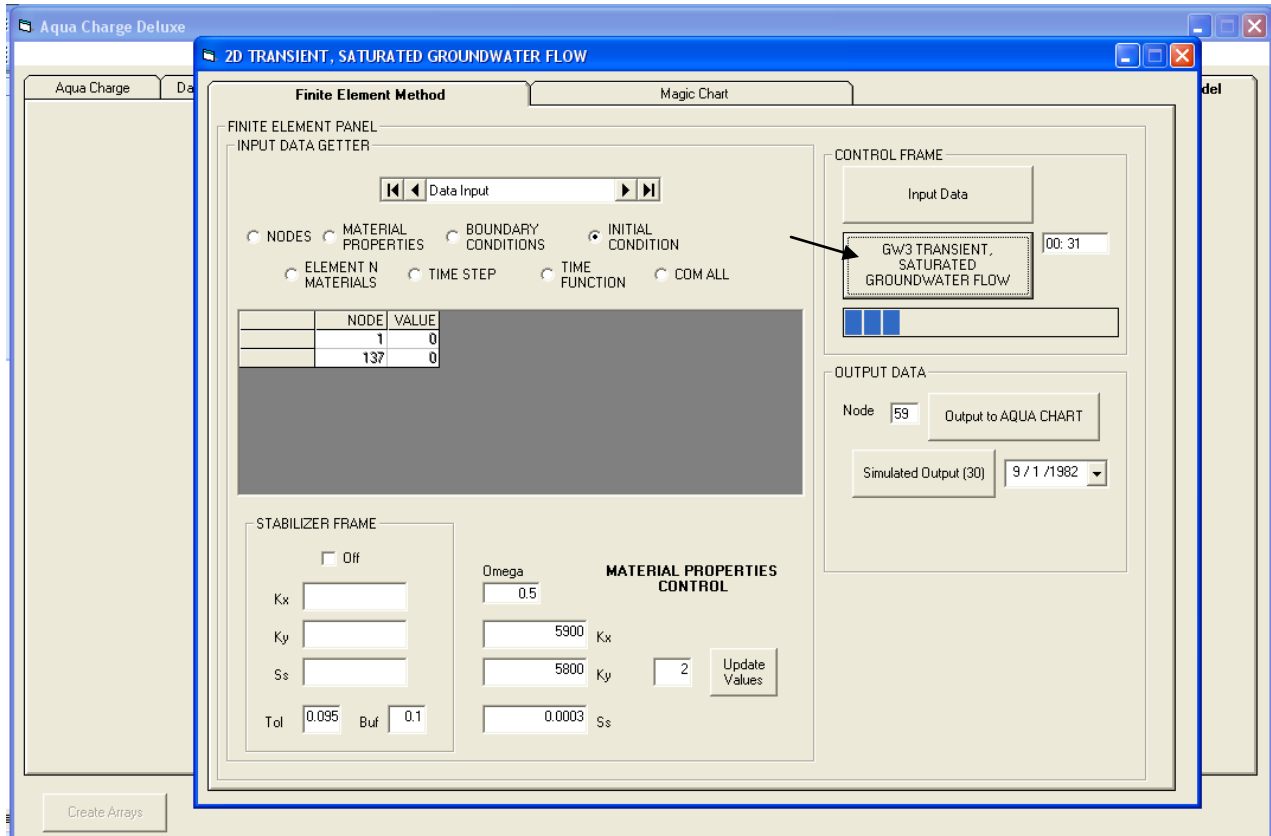


Figure 133. GW3 (Istok) Transient, Saturated groundwater flow button.

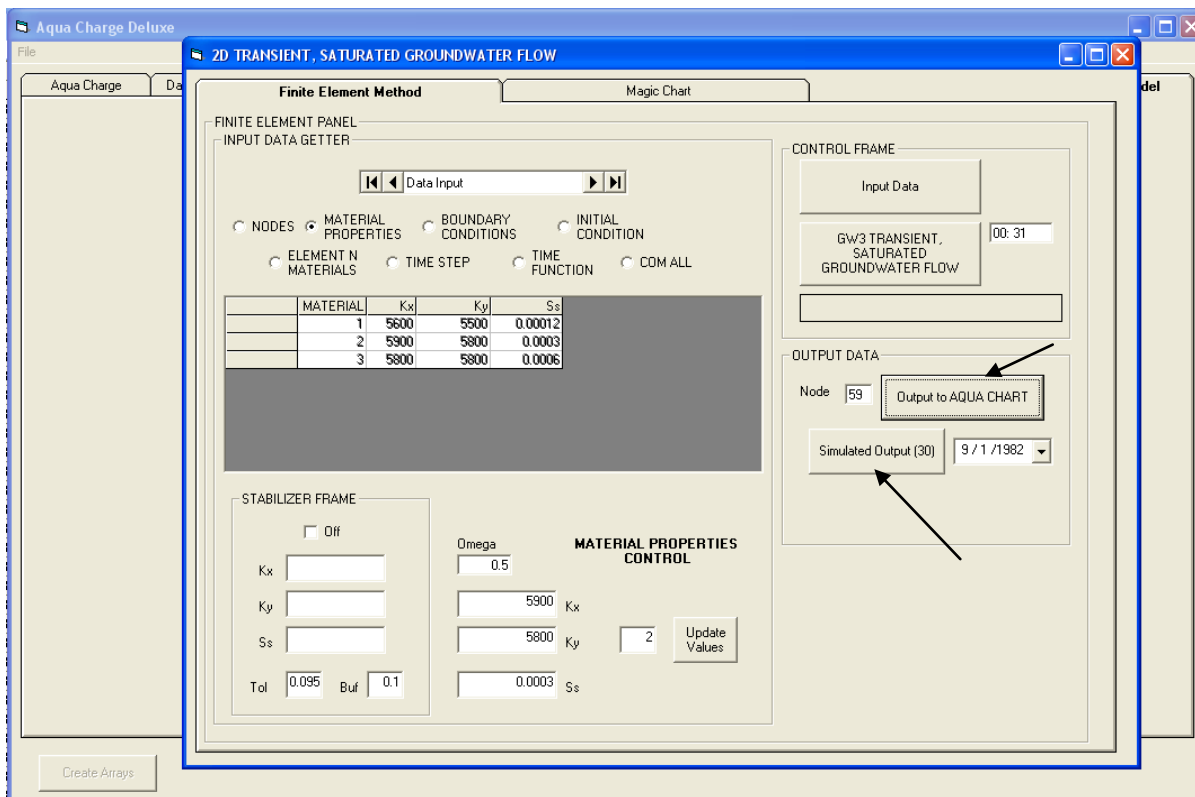


Figure 134. Output to AQUA CHART and Simulated Output (30) button.

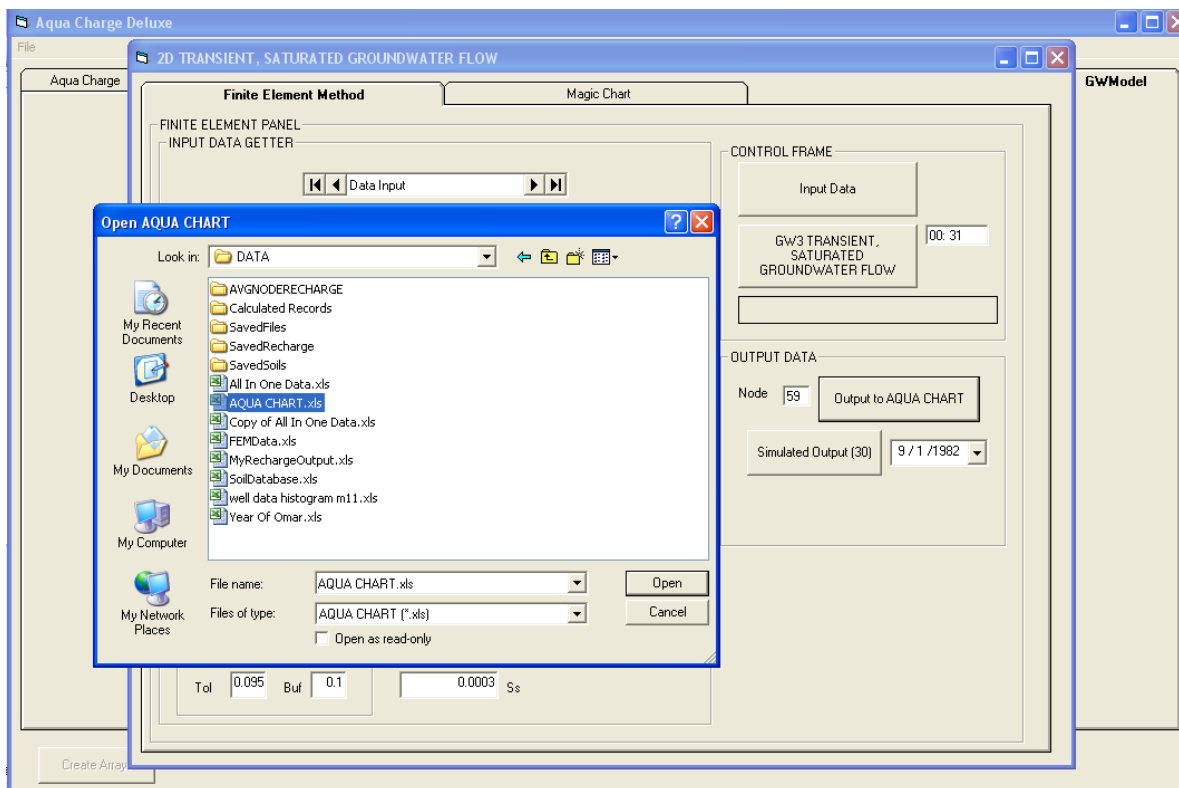


Figure 135. Select AQUA CHART if not opened, common dialog box pop up.

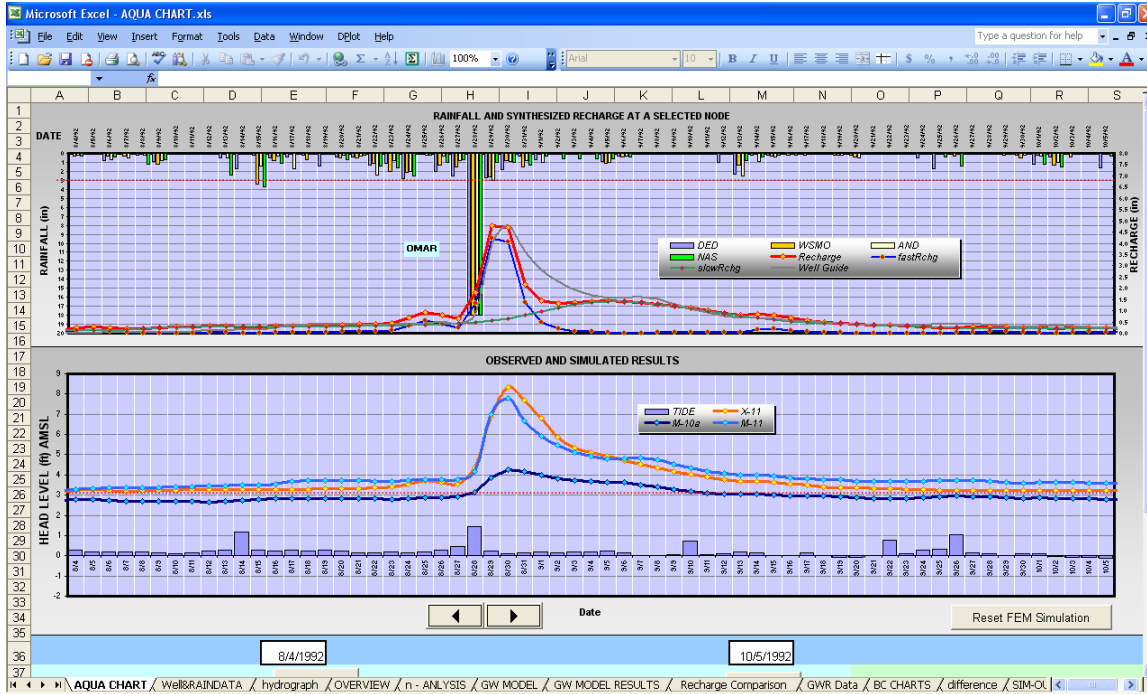


Figure 136. Simulation charted (orange).

The “Simulated Output (30)” command button was designed for creating the animation data. The modeler may select a start date, in this case 9/1/1982, results from the start date to 9/30/1982, 30 days, for each node is exported to the SIMOUT recordsource in AQUA CHART (Figure 137). The node number has x-y coordinates that can be joined in GIS. The values for each X(day) number can be interpolated in the GIS using the *Spline* function tool. The images may be saved and animated using a movie program such as ADOBE® Premier Pro (Figures 138 and 139).

The “Simulated Output (30)” was the last button created and concludes the user’s manual. The next chapter shows the results of sample runs and a discussion on identifying its limitations and making improvements to the program. An output simulation data for September 1 to 30, 1982, are shown in Habana, 2008, APPENDIX J.

Vadose Flow Synthesis for the Northern Guam Lens Aquifer
AQUA CHARGE User Manual

The image shows a screenshot of a Microsoft Excel spreadsheet titled "MAGIC CHART1.xls". The spreadsheet is a "SIMOUT" output file, with columns labeled A through AA and rows numbered 1 through 55. The data is organized into columns representing different nodes (X1 to X26) and rows representing time steps. The values are numerical, representing simulation results. The spreadsheet interface includes the standard Excel menu bar (File, Edit, View, Insert, Format, Tools, Data, Window, DPlot, Help) and a search bar at the top right. The bottom of the spreadsheet shows a navigation bar with tabs for "MagicChart", "WellRAINDATA", "hydrograph", "OVERVIEW", "n - ANALYSIS", "GW MODEL", "GW MODEL RESULTS", "Recharge Comparison", "GWR Data", "BC CHARTS", and "SIM-OUTPUT".

Figure 137. SIM OUTPUT spreadsheet in AQUA CHART.

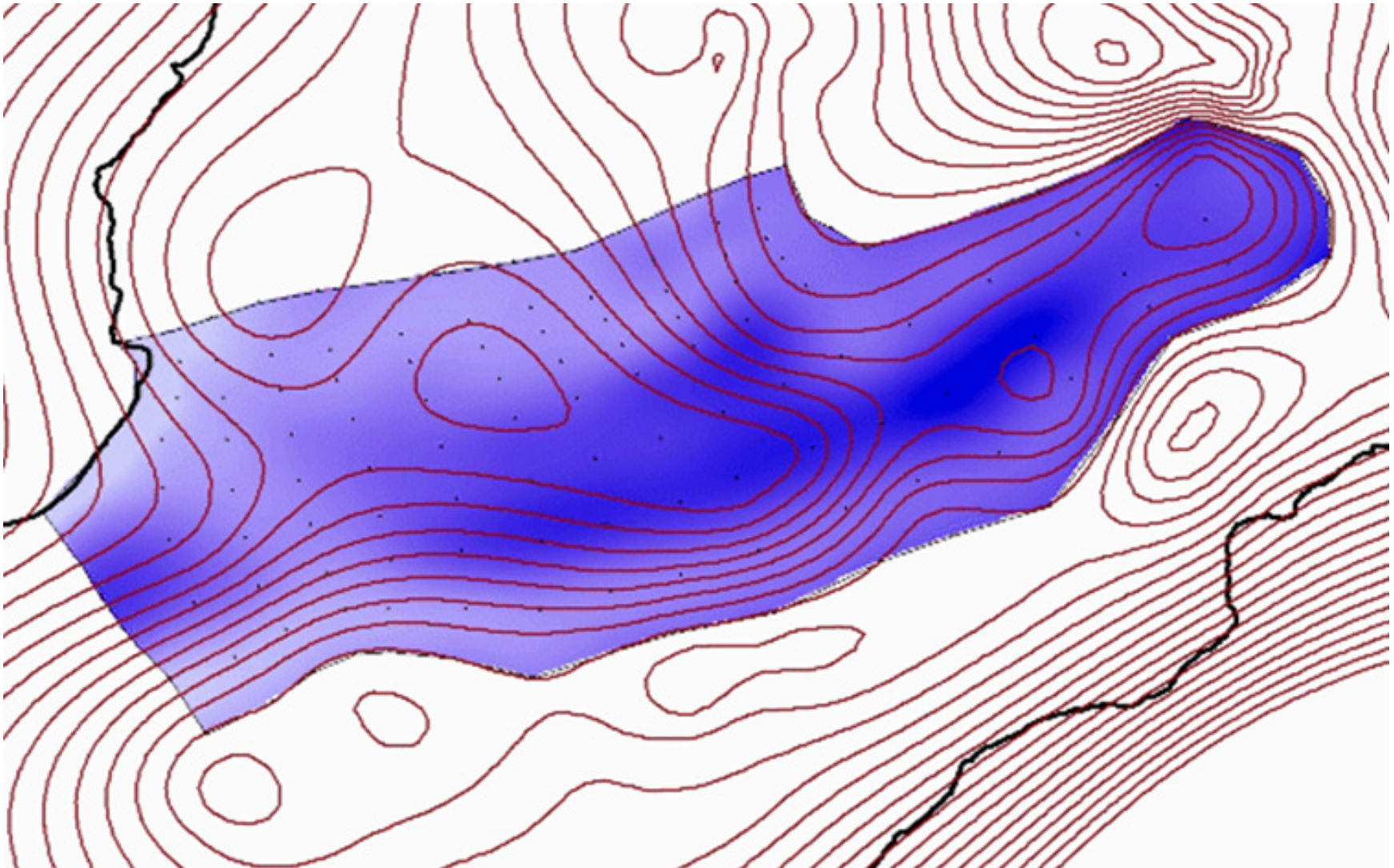


Figure 138. X12 animation frame. Day 12, 9/12/1982, finite element simulation response to recharge results.

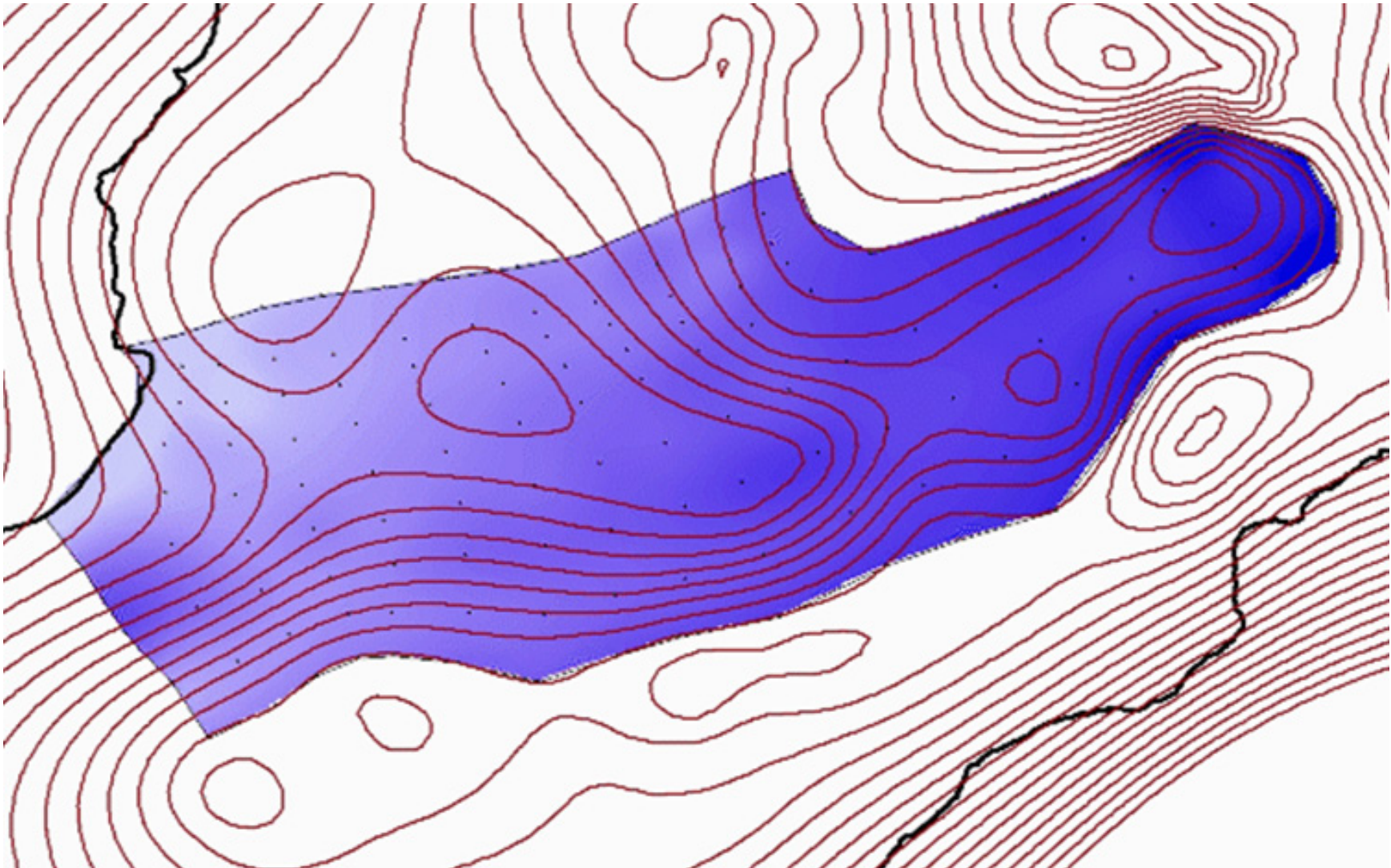


Figure 139. X29 animation frame. Day 29, 9/29/1982, finite element simulation response to recharge results.

RESULTS AND DISCUSSIONS

This chapter reveals the results for synthesizing recharge and the outcome of adding the synthesized recharge as inflow flux into a simple two-dimensional (2-D) finite element groundwater (GW) model. Three trial soil model conditions were applied since it was one of our objectives to explore how soil moisture (SM) affects recharge. The summaries of Stage 1, area weighted average (AWA) recharge, were computed first for each model. The summary results were compared to past estimates of annual recharge and the AWA recharges were sent to the router. The well guide (see Chapter 5) was used to shaping the synthesized recharge. Next, the selected soil model condition that had been routed is applied to the finite element model to simulate the GW dynamics and response to recharge. Adjustments were made to the hydraulic model until the simulation closely resembled the observatory well data.

Soil Model Conditions

The three SM conditions, mentioned in Chapter 2, were applied and the results for Stage 1, AWA recharge and other AWA calculated values are displayed in the following pages. The results for all the models allowed us to explore simple weighted average statistical summaries. The AWA recharge and evapotranspiration (ET) by month was charted as a bar graph showing the difference between the three models. The computational interval ran was set to the available temporal data from 1982 to 1995 and the initial SM was set to 0.2 in.

Soil Model Condition 1

This model set both SM curves as linear relationships. The ET soil model is known as the Thornthwaite Model. The chart curve settings used are shown in Figure 140. This was a good starting run for the modeling process since the first few attempted trials are usually uncertain. Since the soils field capacity (FC) values are fairly low, significant amounts of rainfall would yield most of the infiltration as recharge. It is the moisture amounts within the soil's FC that affects the percentage that becomes recharge and ET. Since the FC is so small, even small daily rainfall amounts can produce recharge for the day. These small amounts in a day add up though when summed by months or year and converted to volume in a large area node-shed

Vadose Flow Synthesis for the Northern Guam Lens Aquifer
Results and Discussions

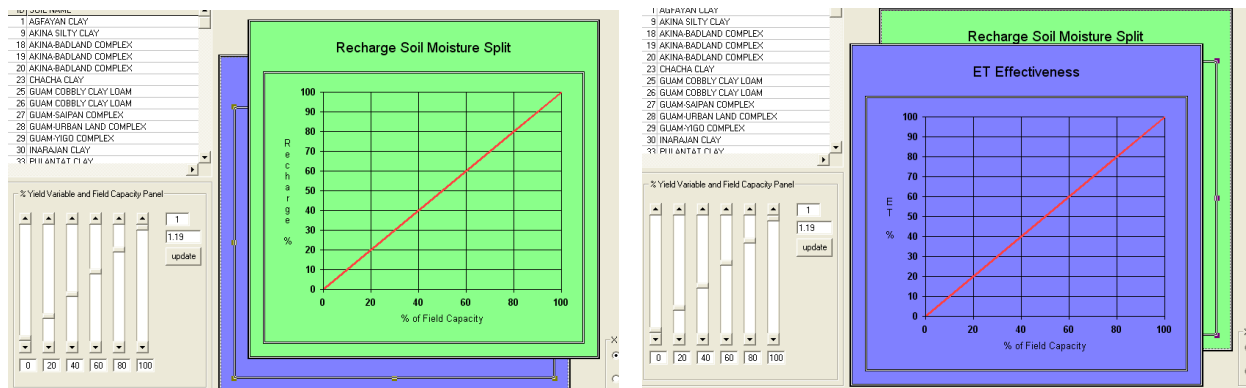


Figure 140. Model 1 soil conditions. Recharge is linear (green) and ET is Thornthwaite model (blue).

Table 1 shows the results of using linear and Thornthwaite for recharge and ET respectively. Approximately 65% of the annual rainfall becomes recharge. This result is similar to the estimates Dr. Mink made in the early 1990s where 60 to 70 percent of annual rainfall goes into recharge (Mink, 1991).

AVERAGES BY MONTH (Area Weighted, Inches)

MONTH	RAIN	PAN	ET	GWR	PAN COEF	DEL SMI
JAN	5.17	6.1	2.44	2.92	0.40	-2.66
FEB	4.4	6.05	1.93	2.43	0.32	0.61
MAR	2.88	7.44	1.97	1.03	0.27	-1.62
APR	4.2	7.95	2.23	1.92	0.28	0.77
MAY	5.51	7.85	2.66	2.68	0.34	2.49
JUN	7.02	7.04	2.92	4.04	0.42	0.80
JUL	11.74	6.49	3.67	7.88	0.57	2.56
AUG	16.39	5.8	3.55	12.86	0.61	-0.19
SEP	15.42	6	3.74	11.70	0.62	-0.42
OCT	12.65	5.56	3.41	9.21	0.61	0.38
NOV	9.78	6.66	3.51	6.42	0.53	-2.08
DEC	7.13	5.98	2.99	4.18	0.50	-0.63

MONTHLY-YEARLY AVERAGES (Area Weighted, Inches)

	YEARS	RAIN	PAN	ET	GWR	PAN COEF
MONTHLY	1982-1995	8.52	6.58	2.92	5.61	0.44
YEARLY	1982-1995	102.24	78.88	35.00	67.24	0.44

Table 1. Soil Model Condition 1 calculated records.

Soil Model Condition 2

This model has a highly pronounced ET, since it uses the Viemeyer Model. At just 20% of FC, 96% of potential ET (total pan evaporation amount) was reduced from the soil if it was available. By 50% of FC, 100 % of potential ET is reduced in the SM. If the available SM is less than effective ET from the chart model, then that ET was set equal to the SM. All of the SM would be evapotranspired and the final SM is zero. The SM curve settings in the Soil Index tab were shaped as shown in Figure 141. The recharge was held linear as in Model 1.

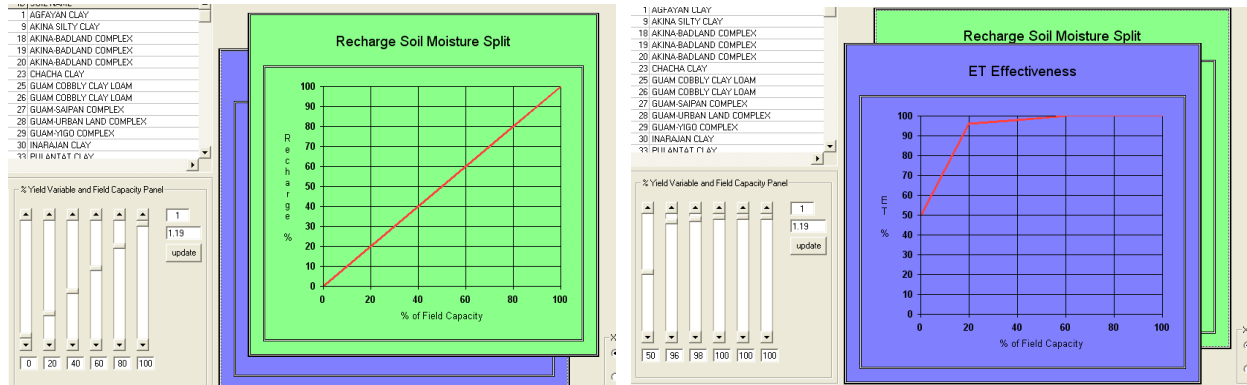


Figure 141. Model 2 soil conditions. Recharge is linear (green) and ET is Viemeyer model (blue).

Table 2 shows the significant increase in ET in the monthly and yearly averages differing from Table 1. The high ET curve setting reduced the SM more than it did with Model 1. For the next day, small initial SM means less going to recharge. Since the recharge percent depends on the previous day's SM and the high ET leaves little to no SM for the next day, the recharge value was decreased in this model condition. The Monthly-Yearly Averages show ET as nearly as much as recharge.

AVERAGES BY MONTH (Area Weighted, Inches)

MONTH	RAIN	PAN	ET	GWR	PAN COEF	DEL SMI
JAN	5.17	6.10	3.30	2.04	0.54	-2.31
FEB	4.40	6.05	2.66	1.70	0.44	0.45
MAR	2.88	7.44	2.51	0.48	0.34	-1.56
APR	4.20	7.95	2.85	1.26	0.36	1.27
MAY	5.51	7.85	3.66	1.72	0.47	1.80
JUN	7.02	7.04	4.16	2.88	0.59	-0.25
JUL	11.74	6.49	5.38	6.09	0.83	3.67
AUG	16.39	5.80	5.12	11.26	0.88	0.11
SEP	15.42	6.00	5.35	10.10	0.89	-0.56
OCT	12.65	5.56	4.85	7.77	0.87	0.36
NOV	9.78	6.66	4.93	5.04	0.74	-2.75
DEC	7.13	5.98	4.27	2.89	0.71	-0.44

MONTHLY-YEARLY AVERAGES (Area Weighted, Inches)

	YEARS	RAIN	PAN	ET	GWR	PAN COEF
MONTHLY	1982-1995	8.52	6.58	4.09	4.44	0.62
YEARLY	1982-1995	102.24	78.88	49.04	53.22	0.62

Table 2. Soil Model Condition 2 calculated records. The summaries show an increase in ET due to the rapidly ascending curve setting with the Viemeyer Model. This in turn favored the high percent of SM reduction that affected the yield to recharge for the next day.

Soil Model Condition 3

The curve settings for this model increases the percentage split for both recharge and ET. The SM curve settings in the Soil Index tab are shown in Figure 142. Both produced high yields for recharge and ET, with a recharge average higher than Model 2. This model though only moves 55% of the rainfall into recharge which is much lower than Mink’s estimate.

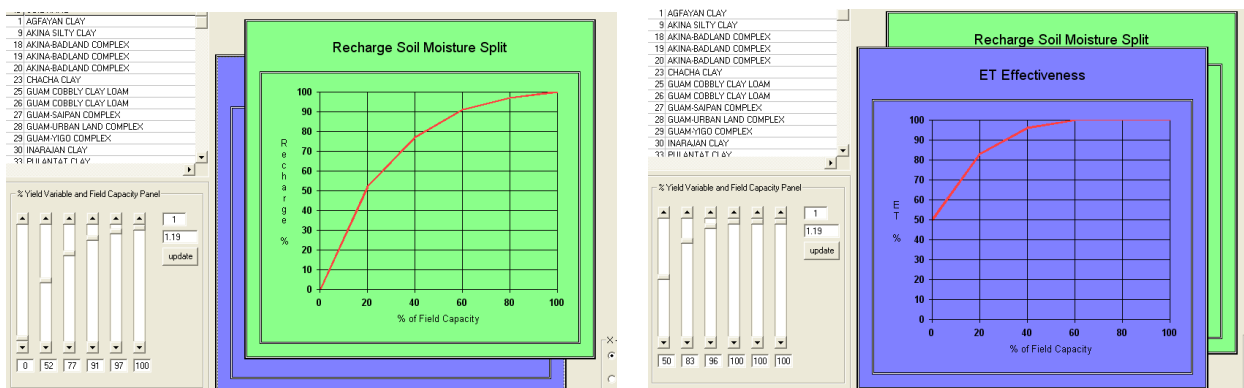


Figure 142. Model 3 soil conditions. Recharge was curved (green) and ET was Pierce (blue).

AVERAGES BY MONTH (Area Weighted, Inches)

MONTH	RAIN	PAN	ET	GWR	PAN COEF	DEL SMI
JAN	5.17	6.1	3.05	2.26	0.50	-1.85
FEB	4.4	6.05	2.52	1.86	0.42	0.28
MAR	2.88	7.44	2.38	0.60	0.32	-1.34
APR	4.2	7.95	2.73	1.40	0.34	1.09
MAY	5.51	7.85	3.51	1.90	0.45	1.50
JUN	7.02	7.04	3.91	3.14	0.56	-0.46
JUL	11.74	6.49	5.05	6.48	0.78	2.85
AUG	16.39	5.8	4.8	11.51	0.83	1.13
SEP	15.42	6	5.13	10.33	0.85	-0.66
OCT	12.65	5.56	4.58	8.07	0.82	-0.04
NOV	9.78	6.66	4.6	5.32	0.69	-1.95
DEC	7.13	5.98	3.91	3.27	0.65	-0.73

MONTHLY-YEARLY AVERAGES (Area Weighted, Inches)

	YEARS	RAIN	PAN	ET	GWR	PAN COEF
MONTHLY	1982-1995	8.52	6.58	3.85	4.68	0.59
YEARLY	1982-1995	102.24	78.88	46.15	56.11	0.59

Table 3. Soil Model Condition 3 calculated records. Again, the summaries show sensitivity in soil condition matters. The curved relationship of SM vs. recharge against a Pierce model ET curve resulted increased the yield in favor of recharge. This shows that curving the recharge slightly can draw more moisture to split towards recharge than to ET.

The results of the three soil model conditions are summarized in the following figures. The overall average by month and year in are shown in a bar chart, Figures 143 and 144.

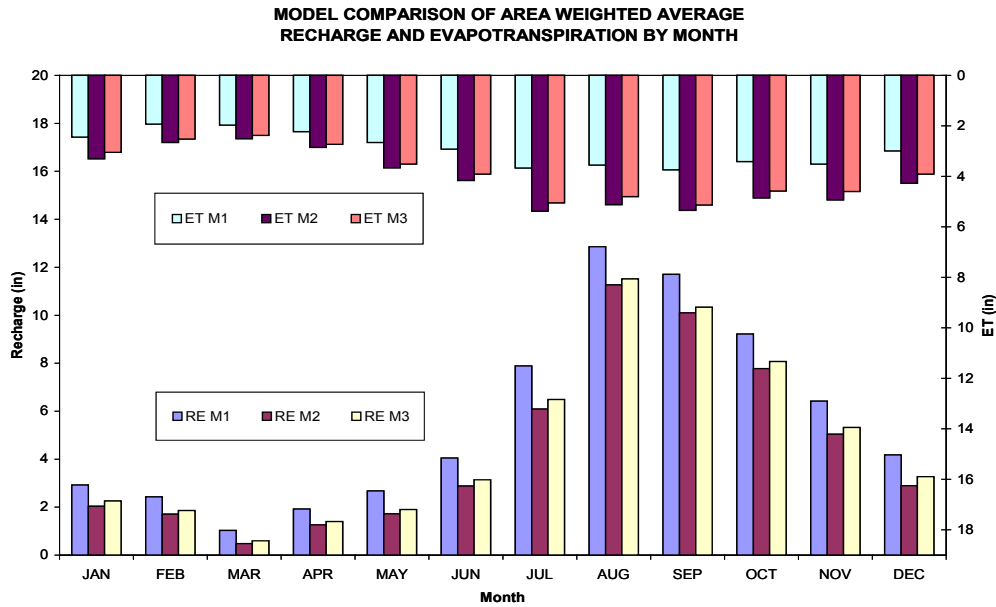


Figure 143. Monthly model comparison bar chart. Soil Model comparison chart shows ET values (top secondary axis) and Recharge (primary axis) for the three models.

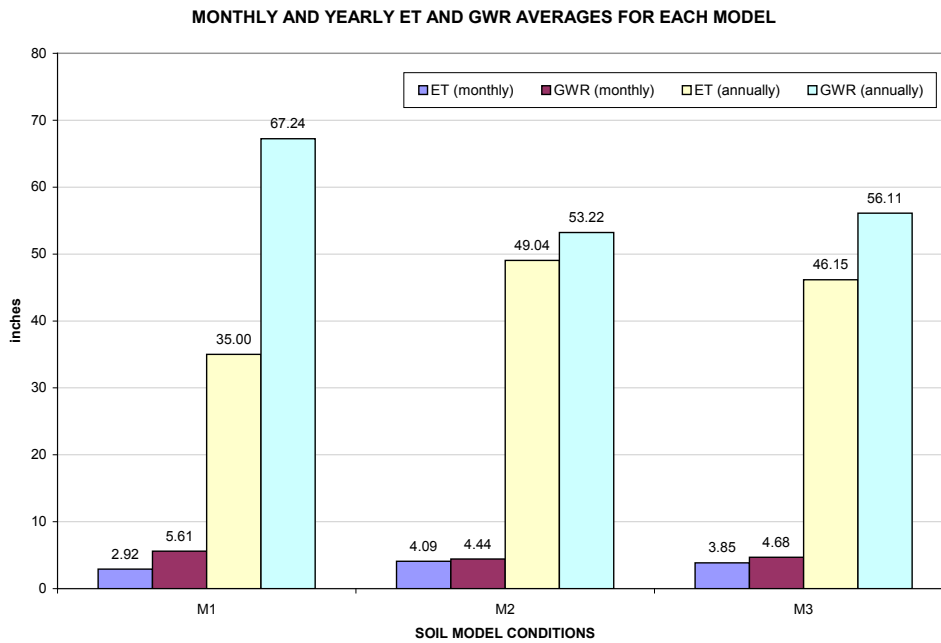


Figure 144. Monthly and yearly ET and GW recharge model comparison bar chart. Three soil model conditions as Models M1, M2, and M3, charting overall monthly and yearly AWA for ET and recharge.

AQUA CHARGE is able to compute all the month's overall AWA summaries from 1982 to 1995. Table 4, in the next page, displays each month's average through the years 1982 to 1995 for a Model 1 soil condition. It also calculates the average recharge for each node-shed (Table 5)

*Vadose Flow Synthesis for the Northern Guam Lens Aquifer
Results and Discussions*

MONTHLY AVERAGES (Area Weighted, Inches)

MNTH DATE	RAIN	PAN	ET	GWR	PAN COEF	DEL SMI	MNTH DATE	RAIN	PAN	ET	GWR	PAN COEF	DEL SMI
1/1982	3.82	6.42	2.55	1.21	0.40	0.05	1/1989	3.15	6.16	1.91	1.17	0.31	0.06
2/1982	10.27	6.20	3.28	6.73	0.53	0.26	2/1989	11.50	6.04	2.89	8.28	0.48	0.33
3/1982	2.52	7.56	2.34	0.59	0.31	-0.40	3/1989	1.25	7.55	1.20	0.28	0.16	-0.24
4/1982	1.17	8.26	1.16	0.10	0.14	-0.08	4/1989	11.59	8.20	3.72	7.48	0.45	0.39
5/1982	6.97	8.00	3.49	3.24	0.44	0.24	5/1989	4.16	7.17	2.57	1.48	0.36	0.11
6/1982	10.43	7.06	3.26	6.78	0.46	0.39	6/1989	9.57	6.80	4.21	5.47	0.62	-0.11
7/1982	14.16	6.28	4.27	9.57	0.68	0.32	7/1989	12.53	6.62	4.02	8.42	0.61	0.10
8/1982	9.86	6.27	3.91	6.64	0.62	-0.70	8/1989	13.03	5.12	3.62	9.62	0.71	-0.20
9/1982	26.91	6.48	4.68	21.90	0.72	0.32	9/1989	17.29	5.84	3.54	14.05	0.61	-0.30
10/1982	14.24	5.51	3.42	11.17	0.62	-0.35	10/1989	11.57	5.20	2.97	8.39	0.57	0.21
11/1982	9.37	5.88	3.21	5.76	0.55	0.40	11/1989	9.22	5.90	2.59	6.12	0.44	0.51
12/1982	7.17	6.24	3.73	3.85	0.60	-0.41	12/1989	4.81	4.98	2.98	2.30	0.60	-0.47
1/1983	1.49	6.97	1.38	0.21	0.20	-0.09	1/1990	14.89	5.24	2.76	12.36	0.53	-0.23
2/1983	1.65	6.18	1.37	0.29	0.22	-0.01	2/1990	2.71	6.32	1.92	0.84	0.30	-0.06
3/1983	4.35	7.94	1.85	2.54	0.23	-0.04	3/1990	3.17	7.13	2.27	0.93	0.32	-0.03
4/1983	1.45	8.61	1.30	0.22	0.15	-0.07	4/1990	2.88	7.80	2.09	0.68	0.27	0.10
5/1983	1.47	9.45	1.30	0.11	0.14	0.06	5/1990	5.87	7.47	2.97	2.47	0.40	0.43
6/1983	0.77	9.28	0.62	0.06	0.07	0.08	6/1990	6.32	7.57	3.75	2.73	0.50	-0.16
7/1983	7.12	8.36	3.64	3.00	0.44	0.18	7/1990	13.38	5.74	4.17	9.18	0.73	0.03
8/1983	10.74	6.43	3.43	6.73	0.53	0.58	8/1990	18.52	4.38	2.44	15.73	0.56	0.35
9/1983	11.01	6.41	3.53	7.76	0.55	-0.28	9/1990	24.75	7.88	5.47	19.77	0.69	-0.48
10/1983	11.22	6.00	3.87	7.12	0.64	0.23	10/1990	8.95	6.42	3.67	4.96	0.57	0.31
11/1983	11.22	7.11	4.00	7.70	0.56	-0.48	11/1990	18.37	6.86	3.96	14.48	0.58	-0.06
12/1983	5.25	5.62	3.00	2.02	0.53	0.23	12/1990	17.74	6.44	3.42	14.16	0.53	0.16
1/1984	3.10	5.46	2.39	1.09	0.44	-0.38	1/1991	5.91	6.75	3.26	3.08	0.48	-0.43
2/1984	4.27	6.15	2.28	2.06	0.37	-0.06	2/1991	3.66	6.04	1.77	1.89	0.29	0.00
3/1984	3.41	7.45	1.53	1.54	0.21	0.34	3/1991	2.59	6.94	2.18	0.74	0.31	-0.32
4/1984	2.08	8.05	1.47	0.50	0.18	0.11	4/1991	6.39	6.75	2.27	4.03	0.34	0.09
5/1984	6.34	8.69	3.86	2.63	0.44	-0.15	5/1991	5.02	7.39	2.57	1.74	0.35	0.71
6/1984	8.45	5.88	2.81	5.53	0.48	0.11	6/1991	7.20	5.69	3.36	4.21	0.59	-0.37
7/1984	10.98	6.23	3.00	7.66	0.48	0.42	7/1991	14.07	6.12	3.79	10.09	0.62	0.19
8/1984	24.12	5.13	3.63	20.47	0.71	0.01	8/1991	14.30	5.52	2.63	12.09	0.48	-0.42
9/1984	15.42	5.79	4.09	11.49	0.71	-0.16	9/1991	13.90	5.84	3.93	9.53	0.67	0.44
10/1984	8.27	5.56	3.34	5.05	0.60	-0.13	10/1991	14.14	5.33	2.66	11.35	0.50	0.13
11/1984	12.77	5.98	4.05	8.74	0.68	-0.01	11/1991	14.99	5.52	3.76	11.47	0.68	-0.24
12/1984	7.15	5.76	2.57	4.39	0.45	0.18	12/1991	4.40	5.35	2.52	2.18	0.47	-0.29
1/1985	7.04	6.33	3.31	4.41	0.52	-0.68	1/1992	8.09	6.53	3.31	4.99	0.51	-0.21
2/1985	4.37	6.64	2.02	1.72	0.30	0.63	2/1992	1.34	6.80	1.11	0.24	0.16	-0.01
3/1985	4.75	8.40	3.26	2.24	0.39	-0.75	3/1992	3.14	7.87	1.94	0.68	0.25	0.52
4/1985	5.50	7.92	2.34	2.98	0.30	0.18	4/1992	3.90	8.52	2.89	1.64	0.34	-0.63
5/1985	11.31	6.12	3.13	7.99	0.51	0.19	5/1992	4.06	7.87	1.80	1.52	0.23	0.74
6/1985	15.32	6.61	4.11	10.92	0.62	0.28	6/1992	4.39	7.03	2.30	2.24	0.33	-0.15
7/1985	9.97	6.88	3.92	5.87	0.57	0.18	7/1992	8.53	6.32	3.46	5.13	0.55	-0.06
8/1985	18.79	5.79	3.71	15.01	0.64	0.07	8/1992	43.58	5.51	3.88	39.37	0.70	0.34
9/1985	19.21	6.60	4.54	14.79	0.69	-0.12	9/1992	8.66	5.84	3.39	5.70	0.58	-0.44
10/1985	7.92	6.43	3.76	4.63	0.59	-0.48	10/1992	14.39	5.47	3.55	10.90	0.65	-0.06
11/1985	5.86	5.94	2.66	3.19	0.45	0.01	11/1992	12.90	5.63	3.25	9.74	0.58	-0.09
12/1985	8.57	5.89	3.17	5.10	0.54	0.29	12/1992	1.94	6.61	1.62	0.44	0.25	-0.12
1/1986	1.03	6.48	1.36	0.30	0.21	-0.62	1/1993	2.14	6.31	1.68	0.53	0.27	-0.07
2/1986	6.99	5.37	2.08	3.93	0.39	0.98	2/1993	4.83	5.85	2.05	2.77	0.35	0.01
3/1986	3.91	7.02	2.54	2.21	0.36	-0.84	3/1993	1.38	7.35	1.25	0.24	0.17	-0.12
4/1986	8.13	6.86	3.05	4.36	0.44	0.72	4/1993	1.65	8.54	1.28	0.33	0.15	0.03
5/1986	9.94	6.53	3.92	6.42	0.60	-0.41	5/1993	1.69	9.17	1.48	0.23	0.16	-0.02
6/1986	9.02	5.75	3.59	5.37	0.62	0.06	6/1993	2.67	8.63	1.62	0.79	0.19	0.26
7/1986	13.90	6.20	3.88	10.05	0.63	-0.03	7/1993	8.53	6.94	2.45	5.50	0.35	0.58
8/1986	23.08	6.95	4.36	18.84	0.63	-0.12	8/1993	16.28	5.48	3.12	13.06	0.57	0.10
9/1986	9.10	6.14	3.06	6.23	0.50	-0.19	9/1993	12.52	4.74	3.09	9.36	0.65	0.08
10/1986	16.71	5.86	3.13	12.84	0.53	0.74	10/1993	13.13	5.73	3.75	9.60	0.65	-0.22
11/1986	4.58	6.38	3.14	2.04	0.49	-0.60	11/1993	7.48	5.88	3.12	4.63	0.53	-0.27
12/1986	11.95	5.46	3.14	8.50	0.57	0.32	12/1993	6.54	5.65	3.38	3.20	0.60	-0.04
1/1987	3.88	6.28	2.49	1.38	0.40	0.01	1/1994	5.31	5.43	2.38	2.58	0.44	0.34
2/1987	5.41	6.00	2.20	3.71	0.37	-0.50	2/1994	2.48	5.01	1.89	1.14	0.38	-0.55
3/1987	2.33	7.55	1.79	0.48	0.24	0.06	3/1994	3.93	6.52	2.59	1.26	0.40	0.08
4/1987	1.98	8.46	1.71	0.40	0.20	-0.14	4/1994	3.76	7.15	2.73	1.23	0.38	-0.20
5/1987	0.89	9.18	0.82	0.07	0.09	0.00	5/1994	8.40	7.71	3.22	5.14	0.42	0.03
6/1987	2.54	7.84	1.37	0.77	0.17	0.40	6/1994	5.21	7.01	3.12	1.91	0.45	0.18
7/1987	15.51	6.62	4.09	11.59	0.62	-0.17	7/1994	13.28	5.64	3.12	9.56	0.55	0.59
8/1987	7.77	6.13	3.59	3.82	0.59	0.36	8/1994	7.50	5.83	3.65	4.46	0.63	-0.60
9/1987	11.47	5.84	3.30	8.05	0.57	0.12	9/1994	20.45	5.15	2.79	17.07	0.54	0.58
10/1987	17.45	5.20	3.33	14.40	0.64	-0.28	10/1994	12.17	4.97	3.10	9.27	0.62	-0.20
11/1987	9.48	10.54	4.94	4.94	0.47	-0.40	11/1994	4.43	5.72	2.70	2.14	0.47	-0.41
12/1987	8.18	7.09	3.28	4.63	0.46	0.27	12/1994	6.98	5.98	2.94	3.86	0.49	0.19
1/1988	8.89	6.16	3.08	5.90	0.50	-0.10	1/1995	3.68	4.95	2.28	1.71	0.46	-0.31
2/1988	1.23	6.25	1.17	0.27	0.19	-0.21	2/1995	0.88	5.81	0.94	0.13	0.16	-0.19
3/1988	1.54	7.55	1.34	0.29	0.18	-0.09	3/1995	2.05	7.30	1.51	0.33	0.21	0.21
4/1988	2.90	8.20	2.00	0.77	0.24	0.13	4/1995	5.49	7.94	3.18	2.17	0.40	0.14
5/1988	3.02	7.67	2.39	0.62	0.31	0.01	5/1995	8.01	7.43	3.67	3.82	0.49	0.53
6/1988	9.61	6.80	3.56	5.88	0.52	0.16	6/1995	6.78	6.57	3.20	3.91	0.49	-0.34
7/1988	14.15	6.52	4.39	9.43	0.67	0.32	7/1995	8.22	6.42	3.20	5.10	0.50	-0.07
8/1988	9.00	6.76	3.88	5.54	0.57	-0.42	8/1995	12.92	5.91	3.82	8.64	0.65	0.47
9/1988	8.94	5.84	3.27	5.05	0.56	0.62	9/1995	16.19	5.64	3.75	13.05	0.66	-0.61
10/1988	14.83	5.20	3.85	10.87	0.74	0.11	10/1995	12.10	5.03	3.30	8.43	0.66	0.37
11/1988	7.57	5.67	3.69	4.49	0.65	-0.60	11/1995	8.64	10.19	4.04	4.44	0.40	0.16
12/1988	3.68	5.82	2.47	1.41	0.42	-0.20	12/1995	5.40	6.86	3.69	2.45	0.54	-0.74

Table 4. Soil Model 1 overall monthly summary.

AWA RECHARGE FOR EACH NODE-SHED (Inches)

NODE-SHED	AVERAGE RECHARGE	NODE-SHED	AVERAGE RECHARGE	NODE-SHED	AVERAGE RECHARGE	NODE-SHED	AVERAGE RECHARGE
1	0.146	36	0.191	71	0.190	106	0.189
2	0.149	37	0.145	72	0.190	107	0.191
3	0.165	38	0.147	73	0.196	108	0.191
4	0.159	39	0.177	74	0.203	109	0.205
5	0.129	40	0.189	75	0.191	110	0.191
6	0.132	41	0.191	76	0.191	111	0.191
7	0.136	42	0.191	77	0.191	112	0.194
8	0.092	43	0.191	78	0.191	113	0.207
9	0.149	44	0.191	79	0.191	114	0.191
10	0.146	45	0.190	80	0.191	115	0.191
11	0.152	46	0.158	81	0.190	116	0.191
12	0.160	47	0.180	82	0.194	117	0.189
13	0.158	48	0.190	83	0.192	118	0.196
14	0.159	49	0.191	84	0.191	119	0.191
15	0.150	50	0.191	85	0.191	120	0.190
16	0.173	51	0.191	86	0.191	121	0.188
17	0.213	52	0.191	87	0.192	122	0.190
18	0.207	53	0.191	88	0.190	123	0.195
19	0.145	54	0.191	89	0.191	124	0.191
20	0.146	55	0.178	90	0.192	125	0.191
21	0.162	56	0.190	91	0.191	126	0.191
22	0.146	57	0.191	92	0.189	127	0.189
23	0.146	58	0.191	93	0.191	128	0.232
24	0.158	59	0.191	94	0.191	129	0.191
25	0.188	60	0.191	95	0.191	130	0.188
26	0.203	61	0.191	96	0.191	131	0.191
27	0.210	62	0.191	97	0.192	132	0.187
28	0.146	63	0.191	98	0.190	133	0.187
29	0.146	64	0.190	99	0.184	134	0.164
30	0.173	65	0.202	100	0.191	135	0.168
31	0.152	66	0.190	101	0.191	136	0.191
32	0.171	67	0.191	102	0.191	137	0.188
33	0.190	68	0.191	103	0.191		
34	0.191	69	0.191	104	0.190		
35	0.191	70	0.191	105	0.188		

Table 5. Soil Model 1 AWA recharge for each node-shed. Highlighted node-sheds 41 and 59 where observation wells M-10a and M-11 are situated respectively.

Routing

The recharge output from each soil model was passed through the router to see which soil model produces results that best simulate those described by the guide. Each soil model produced different results that were superimposed in order to visually evaluate their significant difference.

A few trials were made by changing the parameters in soil model 1. Changes were made until the results reflected the guide values as described in Chapter 5. When the routing produced results that were viable, the routing parameters and settings were maintained for the other two remaining models. The results for routing all three models were overlaid in a chart (See Figure 145) so that their differences could be revealed.

Visual analysis of the results led us to determine that there were no significant differences between the models. The simple reason behind that was the soil layers were rather thin. Significant rainfall that was much greater than the FC of the soils would cause most of the SM to yield to recharge. In daily time steps, difference of results between the soil models was not significant. When the results are summed in monthly and yearly steps, significant differences occur as the daily values add up. When rainfall was about the same as the FC, the SM that was driven to recharge were rather small since the curves determining recharge, especially for Models 1 and 2, were the same.

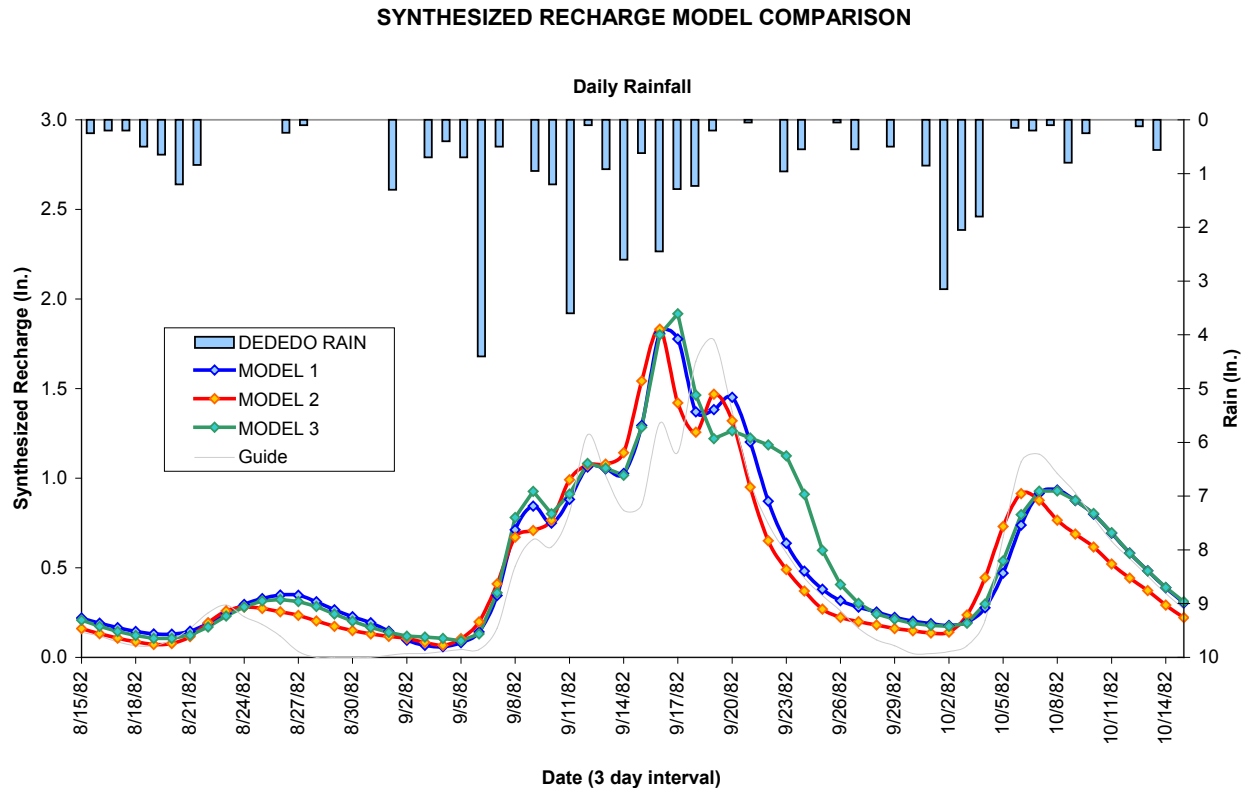


Figure 145. Synthesized recharge model comparison graph. The difference between the three models when routed during a multiple complex pulses of rain. Soil Models 1 and 2 are nearly comparable and follow the guide closely. Soil Model 3 extends out more since the recharge is greater for the SM curve setting. The result causes Model 3 to extend out further than the other two models. Model 2 is slightly decreased since the ET effectiveness is increased with the Viemeyer model.

With the results of routing the three models and finding visually that the differences between the three were small for each day; we used the simpler Model 1 soil condition for the rest of the modeling. The small differences between each model are probably due to the thin soil layers of each soil type resulting in small FCs. Also, the similarity of Model 1's annual average results to Mink's estimate, yielding 65% of rainfall into recharge, makes Model 1 a good candidate for the choice of soil model configuration. The results for routing Model 1 with

temporal data from 1982 to 1995 are shown in the following figures, chronologically, and their figure captions explain each graph analysis (Figures 147 to 169). The interesting routing findings are the *Single, Double, and Multi-Pulse Recharge* and *Plateau Recharge* graph forms. These have fast recharge pulse(s) from significant pulses of rain followed by a slow recharge tail. The *Plateau Recharge* has a small rise of fast recharge that flattens and stays nearly constant for a few days, then drops back down to zero, producing a recharge image of a plateau. The routing parameters and settings are shown in Figure 146.

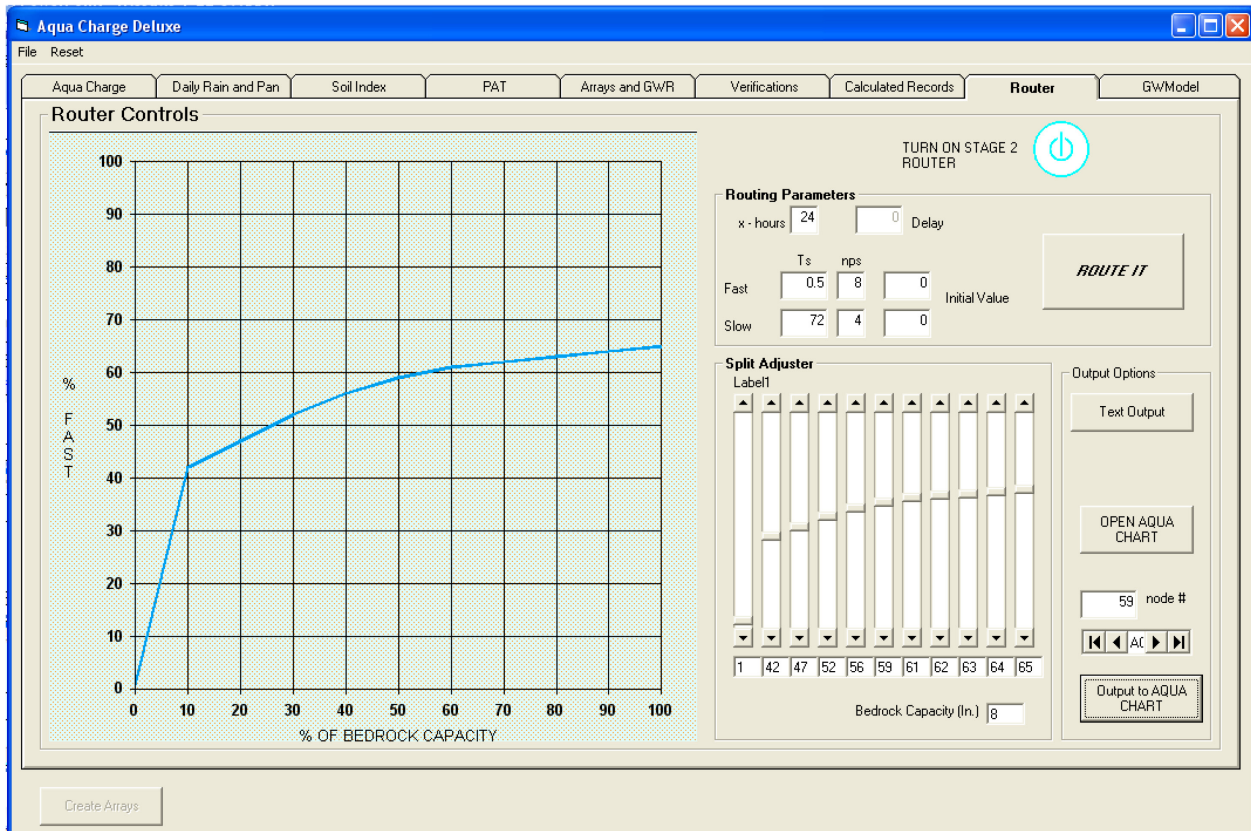


Figure 146. Router parameters and curve settings. Parameters and settings for the router used to generate the following recharge syntheses. For fast recharge, the routing parameters are $T_s = 0.5$ hours and $nps = 8$. Slow recharge $T_s = 72$ hours and $nps = 4$.

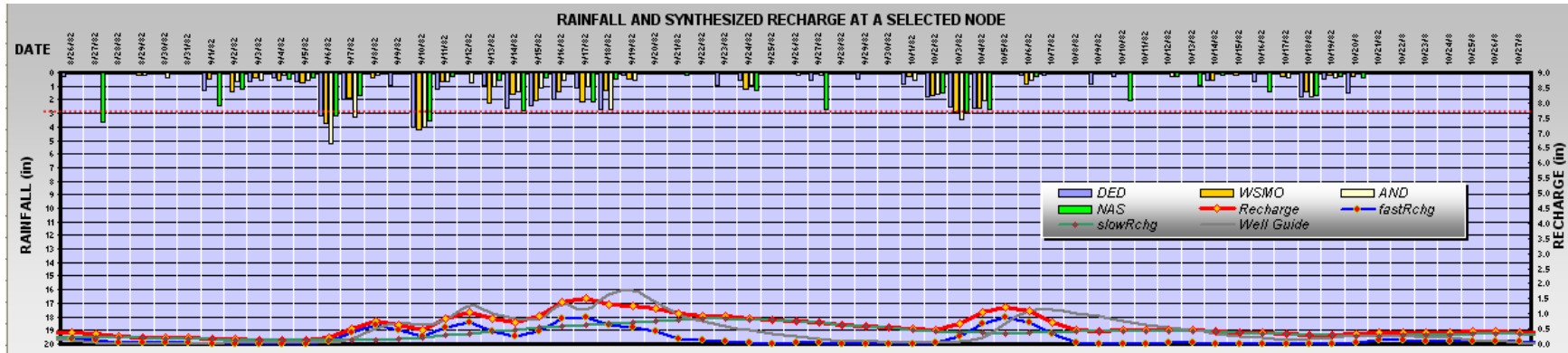


Figure 147. Multi-pulse recharge synthesis for a stormy month of September 1982. These are results from node-shed 59, point of Observation Well M-11, experiencing Dededo rainfall. The total recharge (red line) for each day is the sum of the fast (blue line) and slow (green line) recharges. The grey line is the well guide as illustrated in Chapter 5.

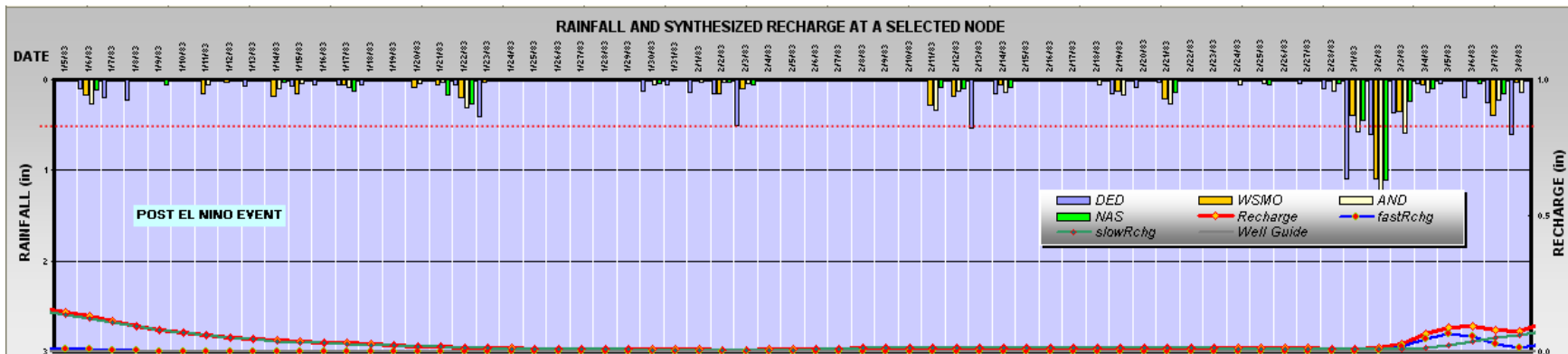


Figure 148. Post El Niño, in the dry season of 1983, shows extremely small slow recharge in a dry vadose. Y-axis was rescaled and red dotted line is at 0.4 inches for the rainfall axis. Even rain pulses at 0.5 inches show no noticeable recharge. This event of dryness continues to mid August of 1983.

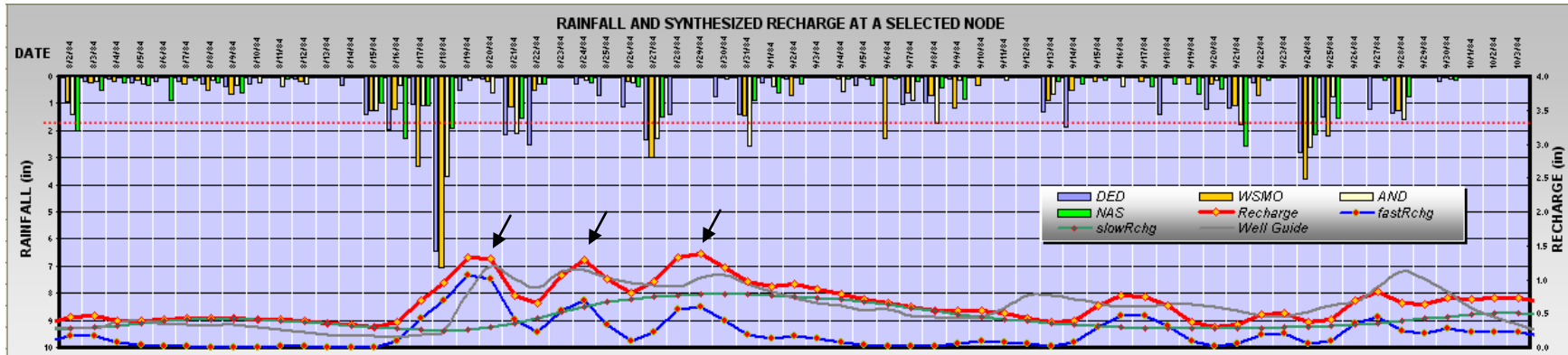


Figure 149. Recharge synthesis for September 1984 shows a *Multi-pulse Recharge*. August and September months experience most of the rainfall in the wet season in Guam. Three fast recharge pulses coincide with the three well hump responses in the guide (arrows). Some misaligned pulses raise questions as to the adequacy of the Thiessen polygon method for handling the rainfall spatial data (see Obvious Errors section in this Chapter).

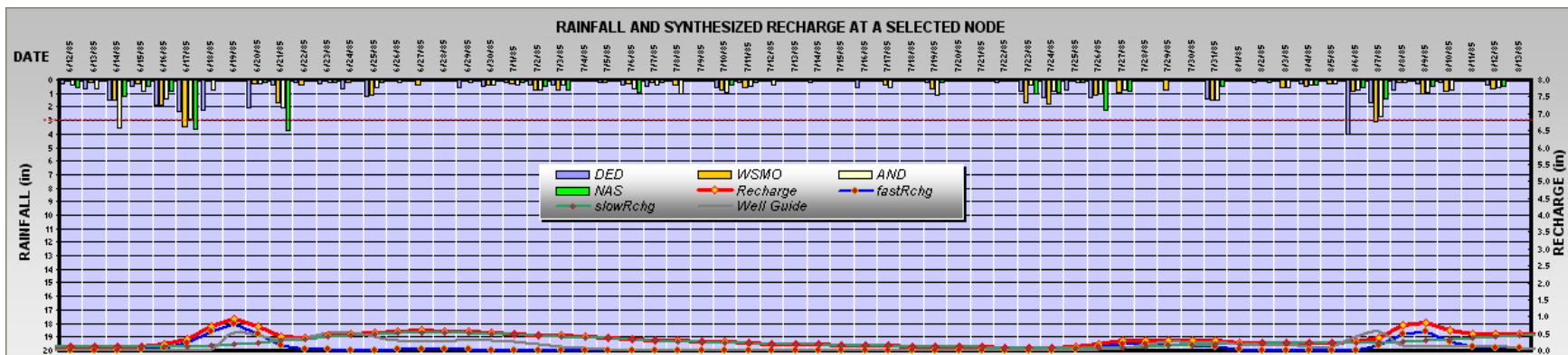


Figure 150. Small pulses of rainfall producing small recharge, summer rainfall of 1985. Many small pulses of rain produce long slow recharge.

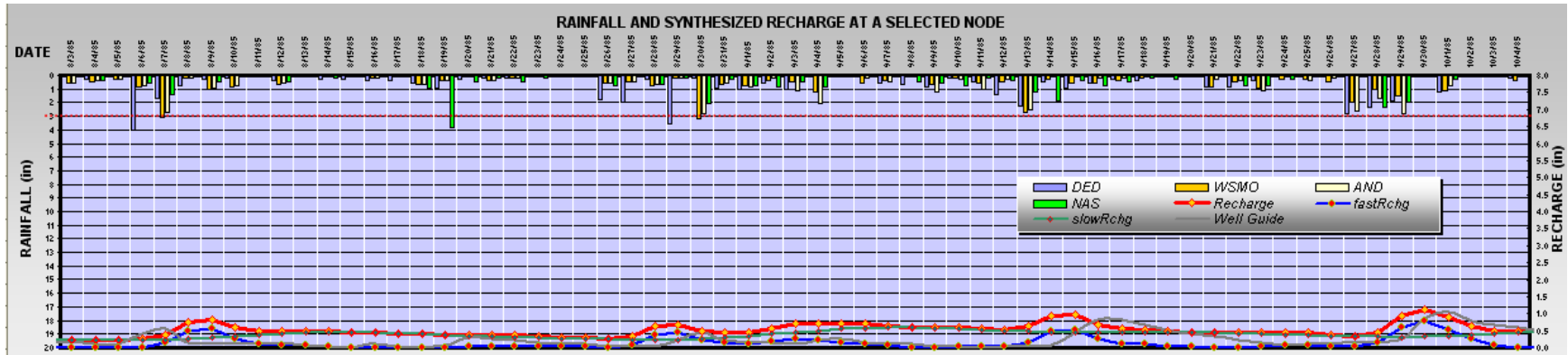


Figure 151. More small pulses of rain showing fast recharge pulses from 3 to 4 inches of rain, August and September months of 1985. Small rain pulses result in misaligned recharge pulses; this is due to scattered showers that may not simulated properly by the Thiessen Polygon Method for varied spatial rainfall distribution.

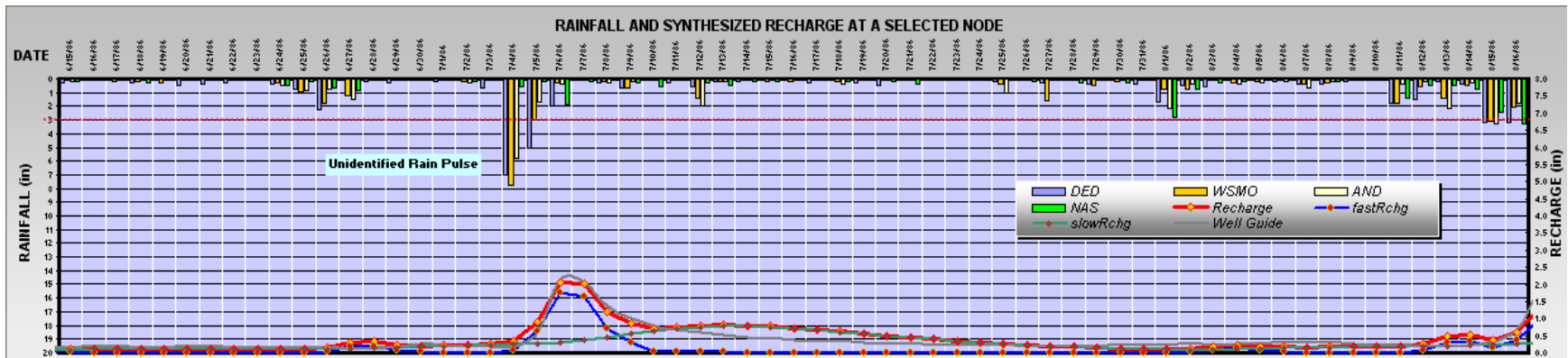


Figure 152. Two rain pulses, a day apart, greater than 3 inches producing a wide but small fast recharge, Summer of 1986. Significant pulses of rainfall from storms and typhoons increases the chance of a wider distribution of nearly equal rain quantities which are more likely to produce an acceptable recharge synthesis.

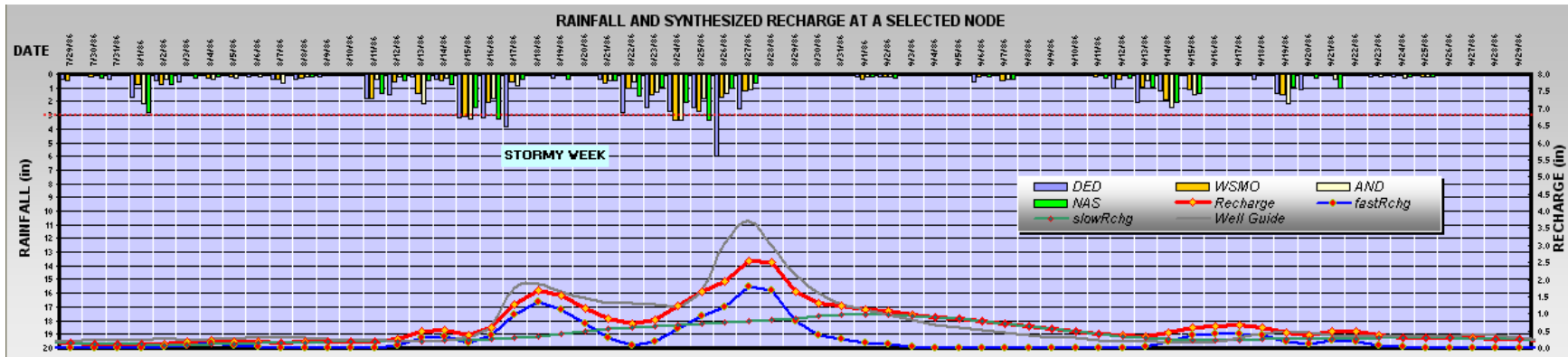


Figure 153. Recharge for a stormy week in August, 1986 (El Niño Year). The rainfall pulse for Dededo on August 24, 1986 does not meet the guide values during this fast recharge possibly due to rain data error. These data errors are explained in Obvious Errors section in this Chapter.

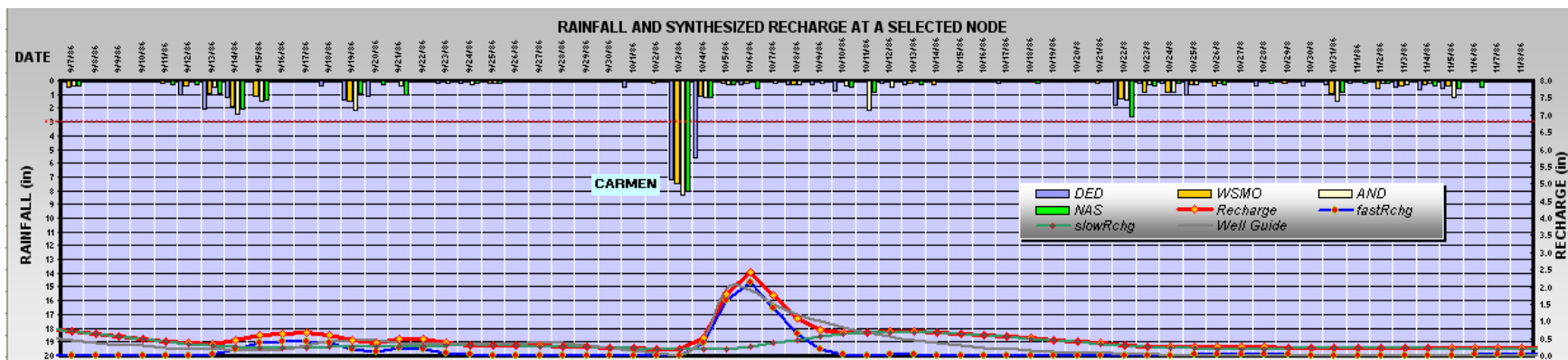


Figure 154. Synthesized recharge for Typhoon Carmen's rain pulse.

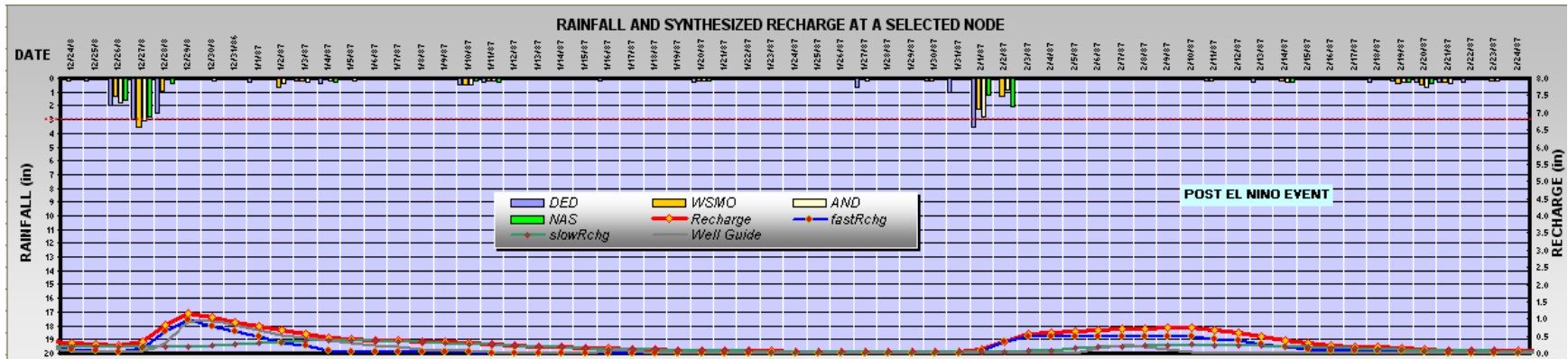


Figure 155. Synthesized recharge for December 1986 to February of 1987, the beginning of the dry season. A Plateau Recharge during February shows the gradual rise to flat lining of fast recharge.

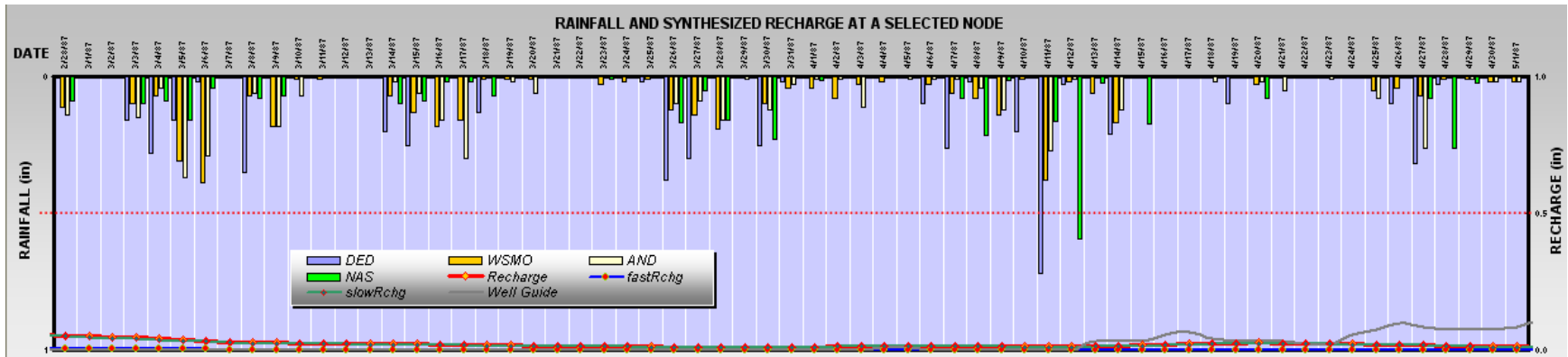


Figure 156. Post El Niño event, during the seriously dry months of February to May of 1987, shows less than 0.1 inches of recharge synthesis; rescaled on both y-axes to 1 inch (red dotted line is at 0.5 inches on both value axes).

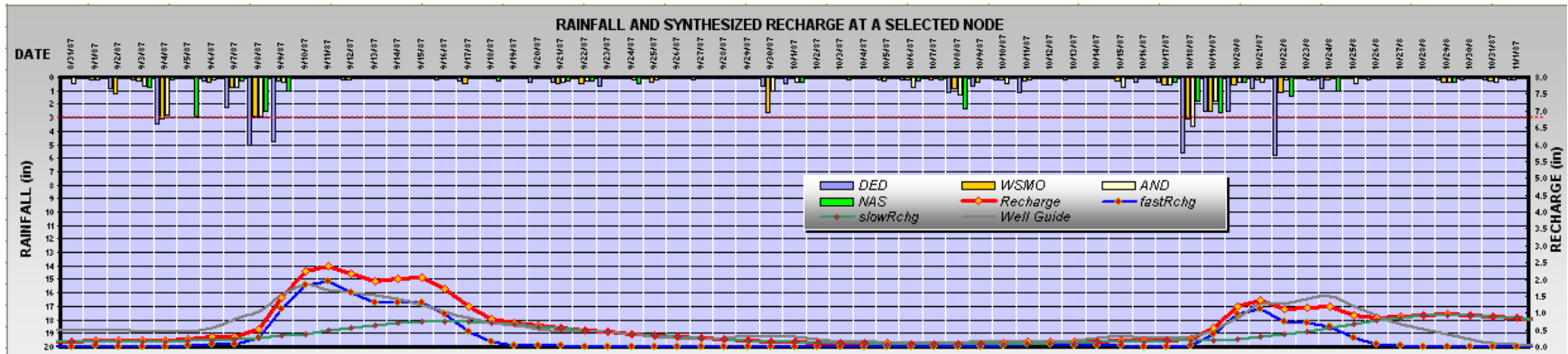


Figure 157. September and October, 1987, rainy months producing widely spread fast recharge.

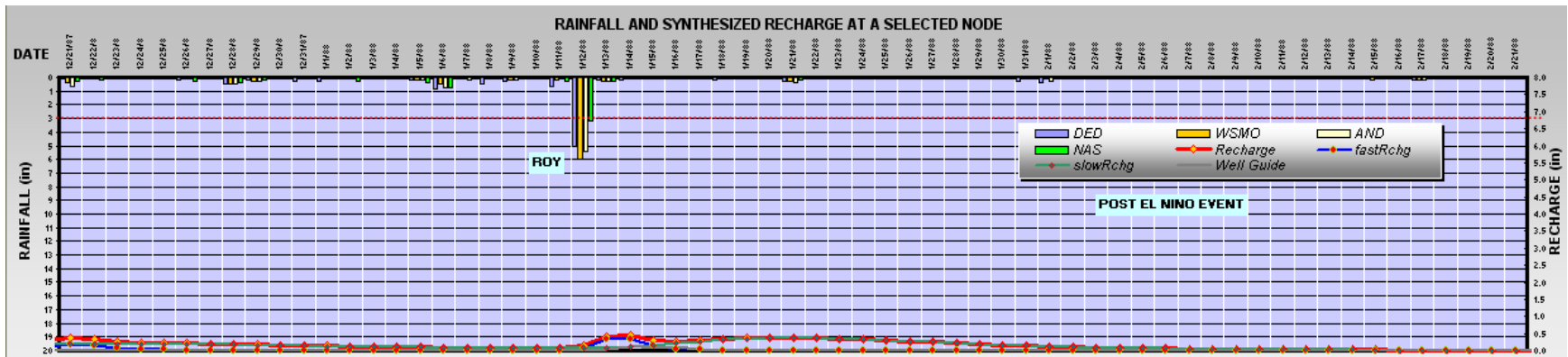


Figure 158. An unprimed vadose zone sends Typhoon Roy's 5 inches of rain mostly to slow recharge.

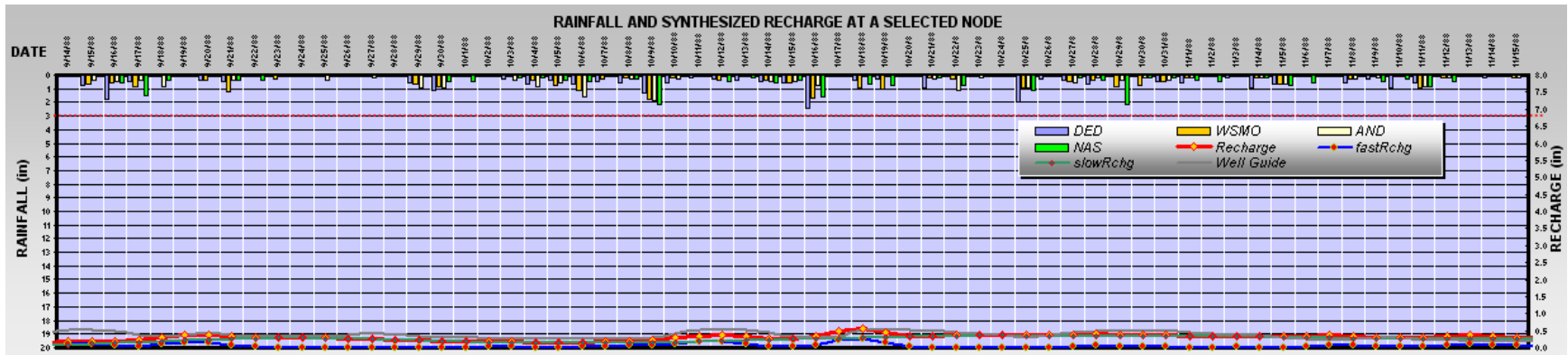


Figure 159. Small rainfall pulses (less than 3 inches) during a supposedly wet season in September to November of 1988, producing long, wide, and small slow recharge.

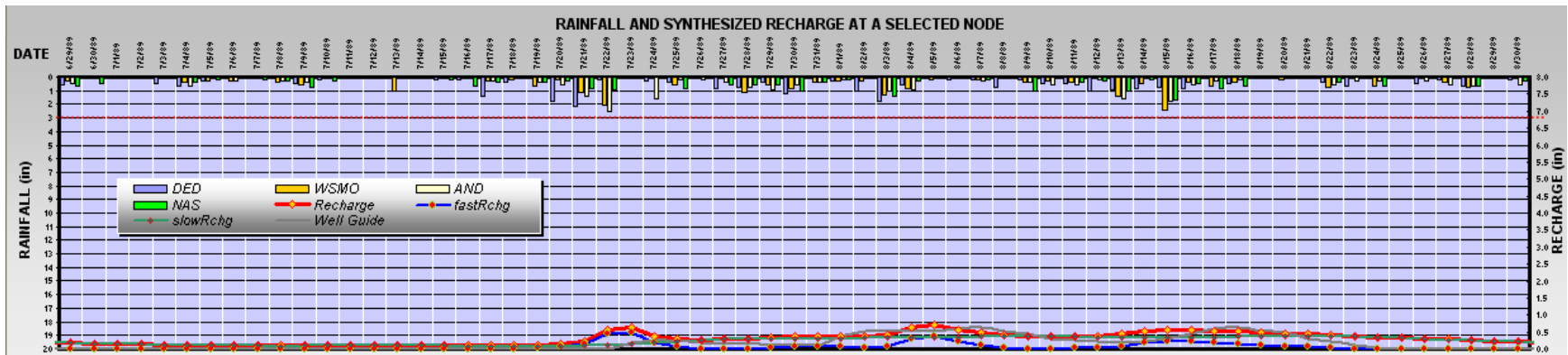


Figure 160. Another group of small rainfall pulses (less than 3 inches) during the early wet season, mid summer, 1989.

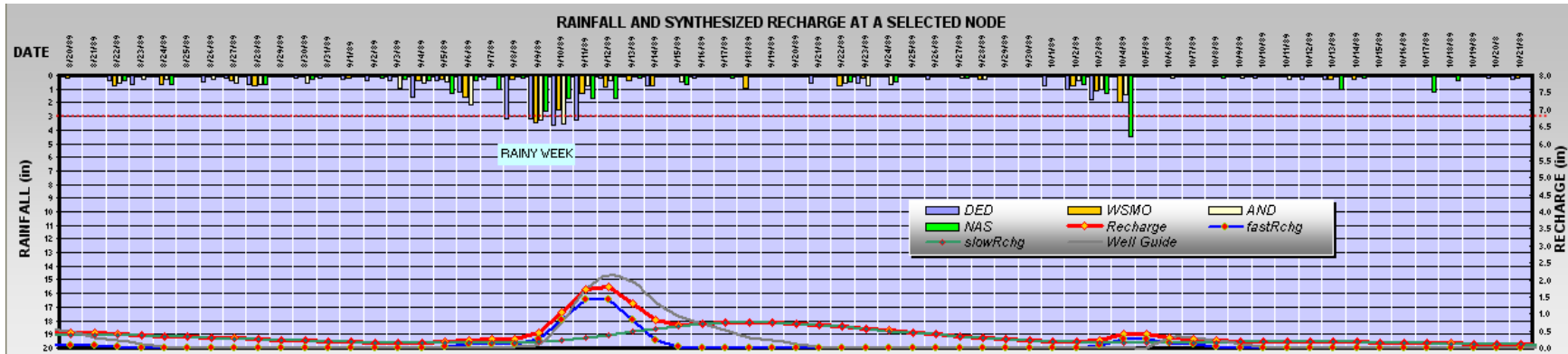


Figure 161. A near normal distribution of pulses of rain in September of 1989 produces a wide fast recharge synthesis.

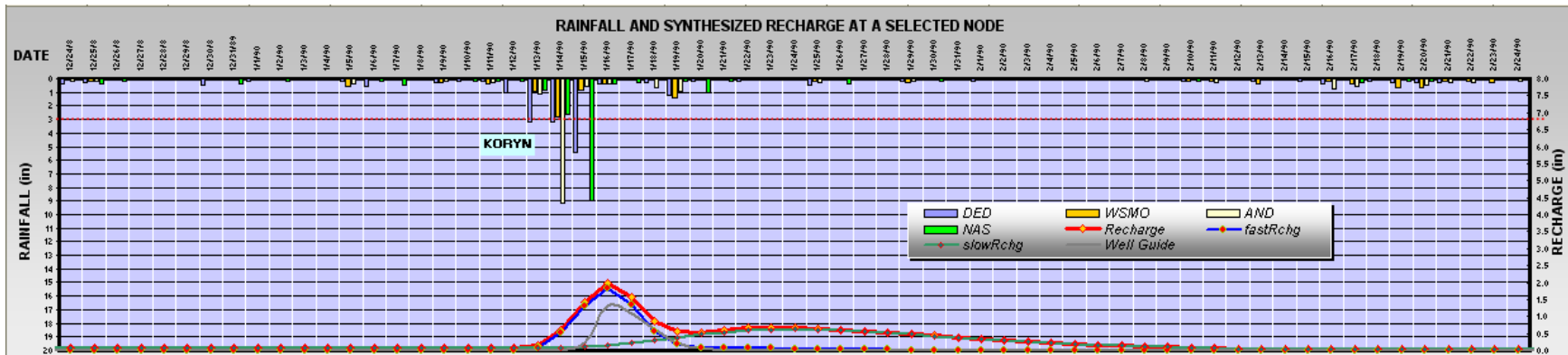


Figure 162. Typhoon Koryn, mid January of 1990, recharge synthesis was greater than the well guide (gray line).

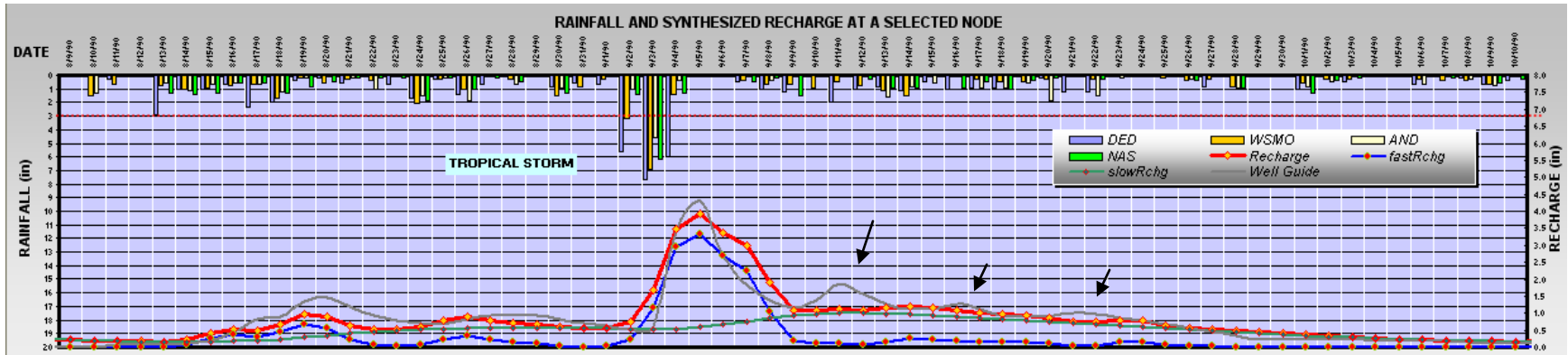


Figure 163. Tropical storm in September of 1989. The guide shows three GW responses (black arrows) where the rain pulses from the data were not enough to cause fast recharge to follow the guide curve during those times. This should have been another example of a *Multi-pulse Recharge*, because the well guide has noticeable well responses and a fast recharge pulse will normally cause this to occur.

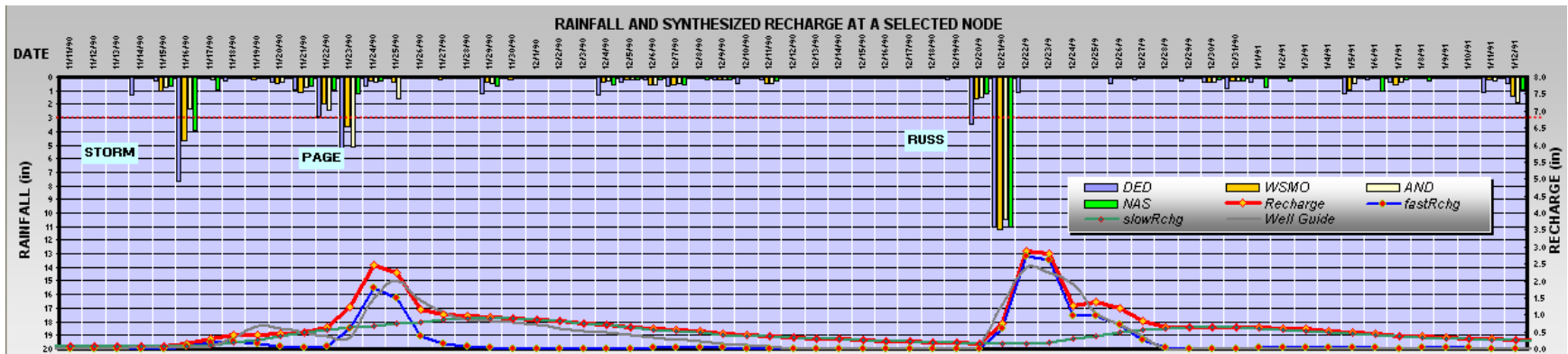


Figure 164. Three significant storm pulses in November and December of 1990.

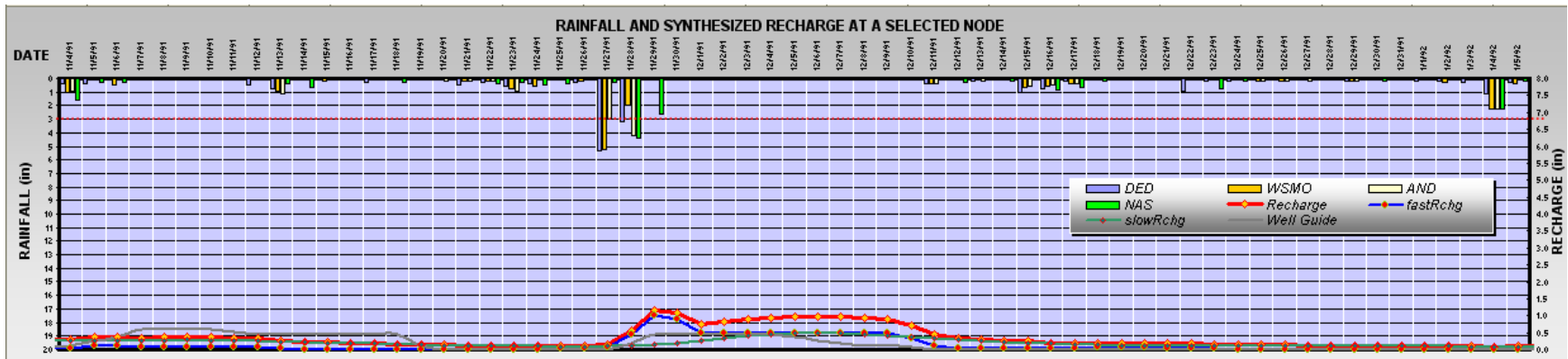


Figure 165. A Plateau recharge from two rain pulses in late November 1991.

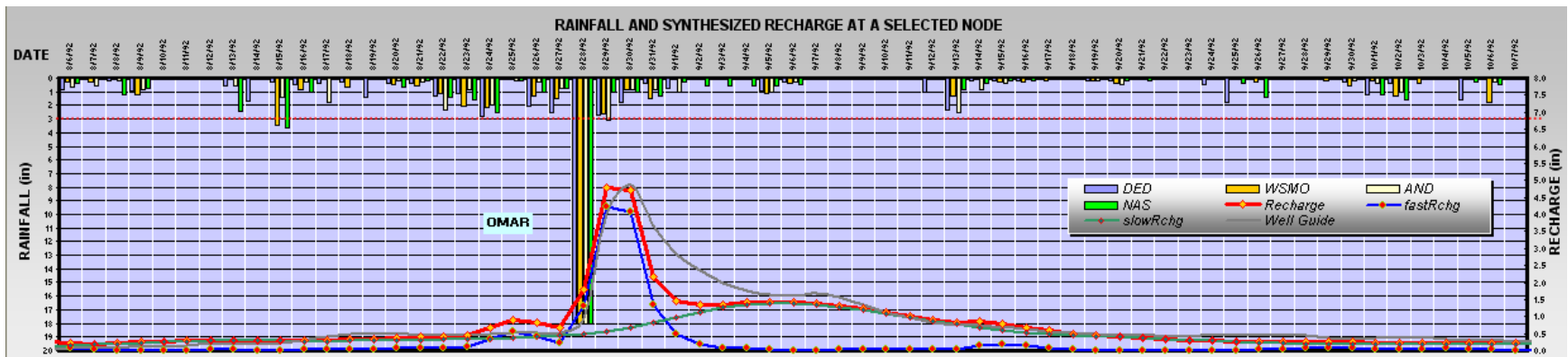


Figure 166. Single Pulse Recharge of Typhoon Omar, late August 1992, poured more than 15 inches of rain (Lander, Personal Communication). The classic shape of GW response measured at the well, shown by the guide, helped in the understanding of fast and slow recharge and setting the parameters for the router (see The Guide, Chapter 5).

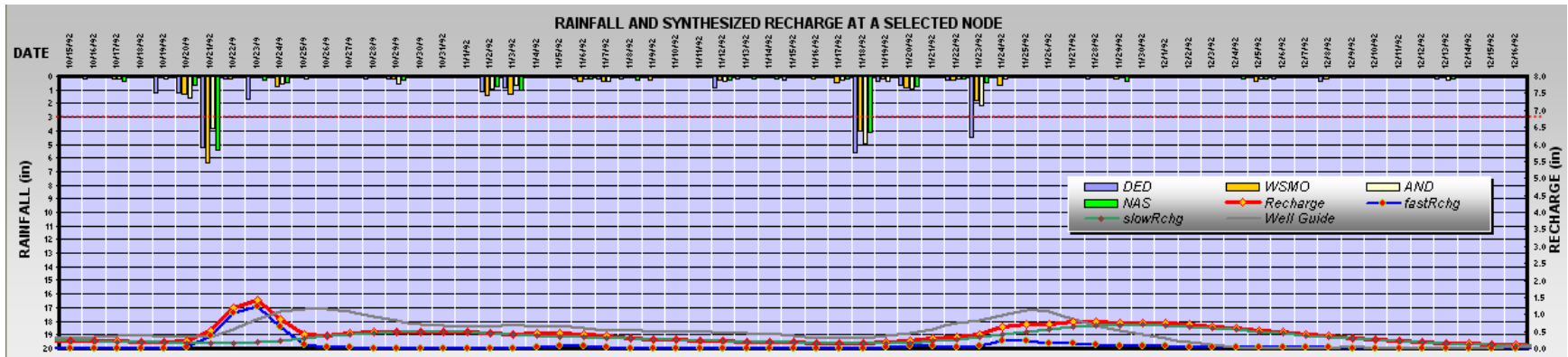


Figure 167. Small *Single Pulse Recharge* from October of 1992. The second recharge synthesis did not produce a good fast recharge pulse from the two rain pulses about a week apart.

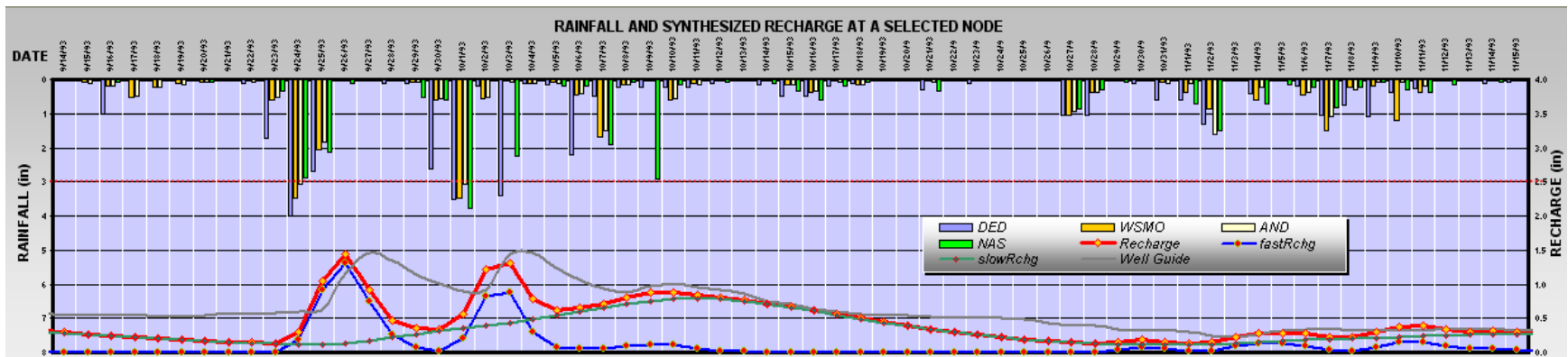


Figure 168. A *Double Pulse Recharge* will cause the GW to respond, slowly drain some, respond on the next pulse and slowly drain again, and then a long slow recharge comes behind and slows down the draining forming a long tail end. September of 1993, y-axes rescaled.

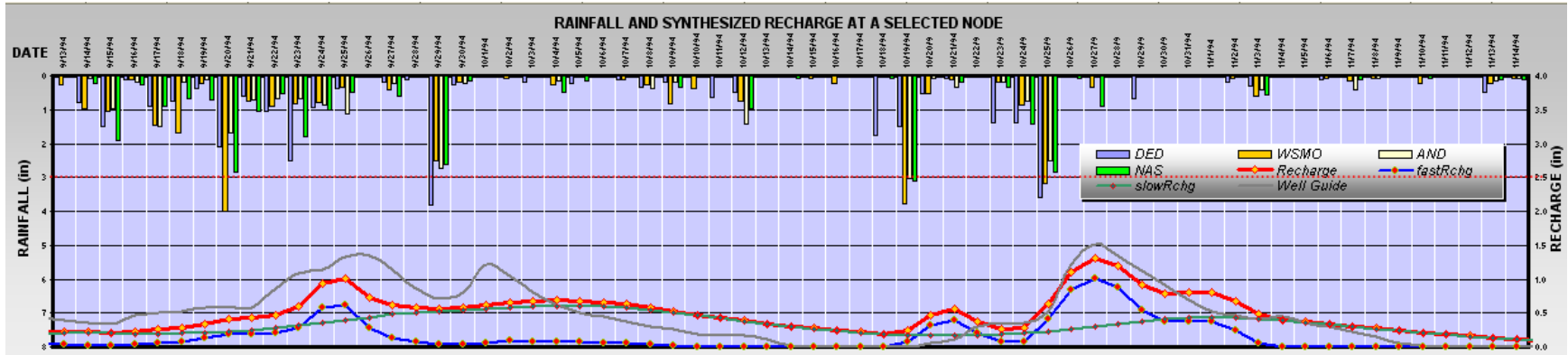


Figure 169. Recharge synthesis for mid October 1994, *Double Pulse Recharge*, y-axes rescaled. The left group of recharge fell short of the well guide.

Spatial Variations

The design of the AQUA CHARGE program was made to account for as much spatial variation as possible in order to assure near reality results. The next set of figures and Table 6 illustrates the differences between node-sheds. To simplify this investigation, we examined the results during the time frame of Typhoon Omar. The spatial variations are not significant in some node-shed areas. It could be possible that the difference between one node-shed and another, under the same Thiessen Polygon, is small. Some cases the difference is noticeable, even under the same Thiessen Polygons, which is probably due to the node-shed surface and soil layer variation that affects the AWA recharge. These are demonstrated in the following Figures 170 to 173. The router parameters and settings remain the same.

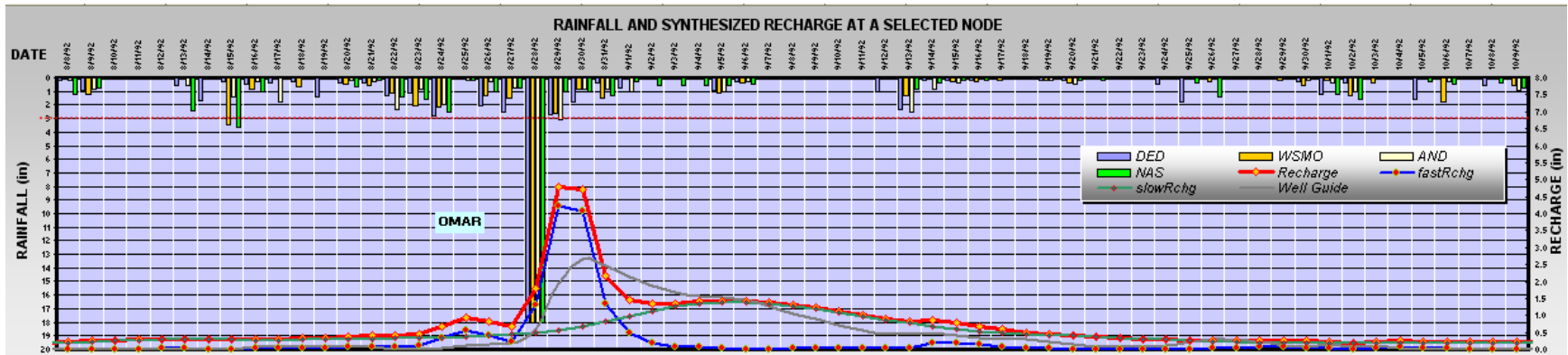


Figure 170. Recharge synthesis during Typhoon Omar at node-shed 41, M-10a. It is similar to the recharge synthesis at node-shed 59. The well guide is less pronounced than at M-11 for reasons that affect well response other than recharge. Well response here is also due to the different rock media porosity, storativity, hydraulic conductivity, and location of the point which is located in a lower hydraulic head gradient zone than M-11. The well guide mode was 2.8 feet and the porosity was set at 0.15.

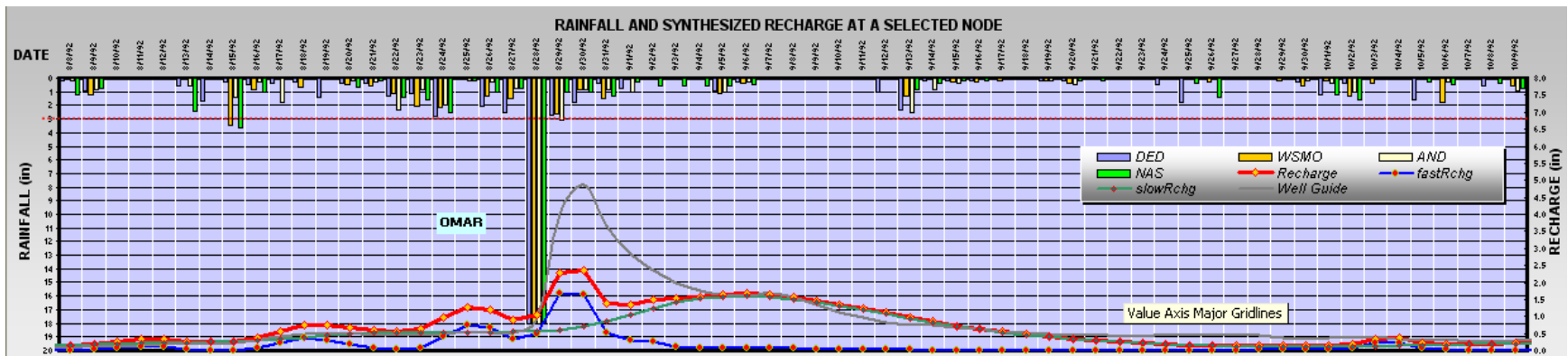


Figure 171. Synthesis for node-shed 1, Typhoon Omar, shows spatial variation of recharge. The rain and pan evaporation gages Thiessen Polygon for this node-shed correspond to the NAS gaging station (Guam International Airport, Tiyan).

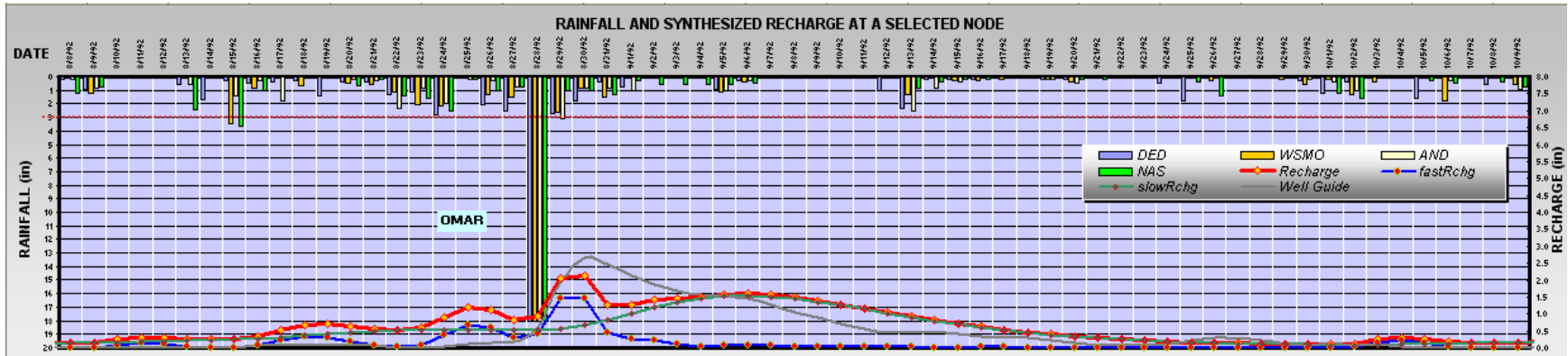


Figure 172. Synthesis for node-shed 6 (Tumon bay coastal area), during Typhoon Omar, is similar recharge to node-shed 1. This shows the spatial variation is greatly dependent on the Thiessen Polygon for discriminating gage area of influence.

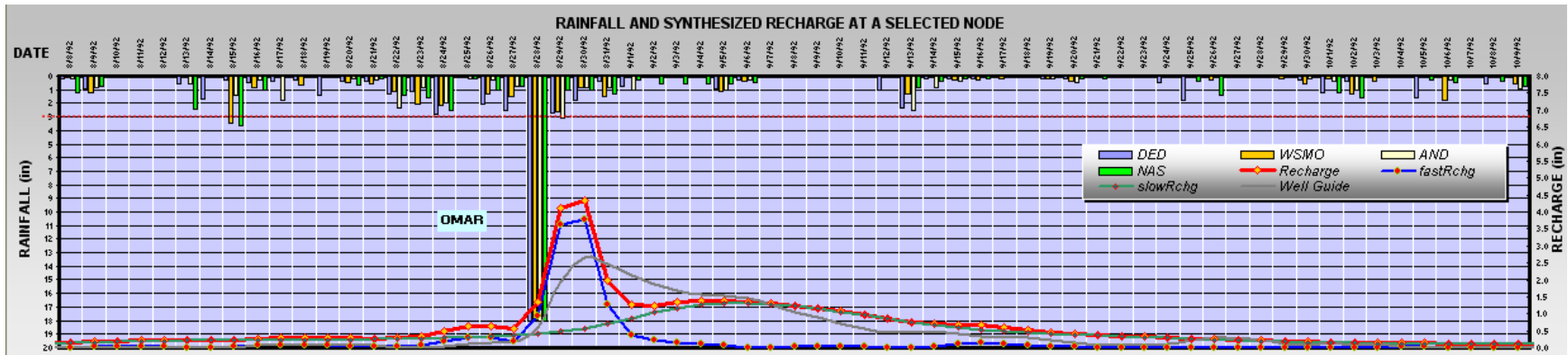


Figure 173. Node-shed 134, an allogenic recharge node-shed, is smaller than the observation well node-sheds recharge during Omar

DATE	ns 6 Tumon Bay Coast	ns 41 Observation Well M-10a	ns 59 Observation Well M-11	ns 130 far inland node- shed	ns 134 allogenic recharge
8/26/1992	1.11864	0.80832	0.80803	0.7920	0.65378
8/27/1992	0.82155	0.65873	0.65852	0.6457	0.55805
8/28/1992	0.94671	1.79465	1.79507	1.7846	1.33884
8/29/1992	2.04953	4.78158	4.78360	4.7777	4.10601
8/30/1992	2.12090	4.71773	4.71969	4.7147	4.34901
8/31/1992	1.27758	2.16728	2.16784	2.1603	1.98576
9/1/1992	1.27861	1.45118	1.45142	1.4443	1.25984
9/2/1992	1.42305	1.32753	1.32773	1.3216	1.25185
9/3/1992	1.44788	1.35026	1.35050	1.3453	1.32898
9/4/1992	1.50539	1.41898	1.41928	1.4149	1.38270
9/5/1992	1.57523	1.43567	1.43600	1.4324	1.36888
9/6/1992	1.59892	1.40427	1.40461	1.4015	1.33178
9/7/1992	1.56779	1.36525	1.36551	1.3617	1.30250
9/8/1992	1.49339	1.30288	1.30303	1.2981	1.24893
9/9/1992	1.39370	1.21496	1.21505	1.2098	1.16975
9/10/1992	1.28384	1.11374	1.11377	1.1084	1.07677
9/11/1992	1.17157	1.00628	1.00625	1.0007	0.97616
9/12/1992	1.05464	0.89551	0.89545	0.8900	0.87060
9/13/1992	0.93083	0.81599	0.81546	0.8195	0.76403
9/14/1992	0.80633	0.84434	0.84204	0.8741	0.69171
9/15/1992	0.70444	0.79833	0.79566	0.8264	0.68806
9/16/1992	0.62140	0.67502	0.67330	0.6458	0.67427
9/17/1992	0.53943	0.58156	0.58046	0.5323	0.59762
9/18/1992	0.46251	0.48727	0.48690	0.4606	0.51160
9/19/1992	0.39683	0.44634	0.44011	0.4233	0.45895
9/20/1992	0.34173	0.40909	0.40286	0.3901	0.41392

Table 6. Spatial variation of recharge for selected nodes. This table shows the spatial variation of recharge synthesis clearly for the node-shed (**ns**) selected. The highlighted date is when Typhoon Omar arrived and passed over Guam. Each value for each node-shed for the given date can differ from another in the thousandths and ten thousandths. These variations will further differentiate if there were more rain gages in the domain.

The router is sensitive to changes in curve settings and parameters. Figure 174 shows changing the T_s value and the number of phases affects the fast flow curve. It was best to change one parameter at a time sampling as it was confusing to keep track on the changes that caused a difference in results.

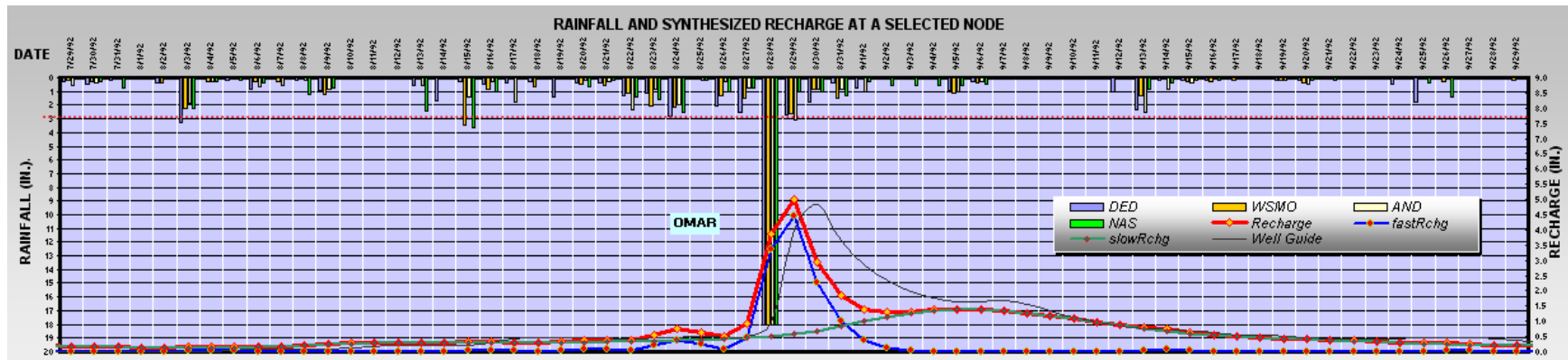


Figure 174. Results of changing fast flow parameters. Recharge synthesis at node-shed 59 during Typhoon Omar, changed router parameter and settings. This time, $T_s = 24$ hours and $nps = 1$ for fast flow. The other parameters and curve setting was kept the same as in Figure 142.

Next, the recharge syntheses were used as flux for the GW model. Each node-shed recharge synthesis is entered as flux to each node in daily time steps to the hydraulic model. We used Figure 142 parameters and settings for the recharge synthesis and made adjustments to the GW model for the calibration process.

Hydraulic Model Results

The hydraulic model or GW model allowed us to load the FEM Data and then the synthesized recharge data text file to prepare and store the input data for GW modeling computations. The hydraulic model was crucial to validating any recharge synthesis. The hydraulic model converted the computed recharge into GW hydraulic head values that were compared to actual measured values of head. The comparisons that follow deem the program design in its entirety to be adequate.

History Matching

The adjustments went tediously back and forth from the recharge synthesis to the GW Model until a reasonable match was accomplished. This history matching allowed us to determine the entire modeling integrity of the AQUA CHARGE and finite element programs as it simulates GW response to the recharge synthesis, making a close estimate of the real world observation. In this project, history matching is our means of calibration of all modeling parameters that affect output from time the rain pulse hits the ground surface until it is changed to GW recharge and finally as , the GW moves through the aquifer system to the sea coast. The goal was to achieve model simulations that responded similarly to the observation well level records. A match helps us verify, as hydrologic and hydraulic modelers understands, that AQUA CHARGE, in its attempt to model vadose flow synthesis, could be a great alternative method to producing good recharge estimates at a daily time step. It will also allow us to have control of the spatially complex vadose zone. This is could be quite useful for further studies such as contaminant transport through the GW system. With control of the vadose zone, the model can help us make near accurate predictions of the behavior water in the rock media. It also helped identify errors that may one day be corrected in order to make improvements for any following research projects.

Many sample runs were carried out during the calibration process for M-11, node-shed and node number 59. The understanding of the NGLA geology and the well guide played a large role in determining the parameter settings to produce a particular shape to the recharge synthesis. The GW model was calibrated using the recharge in the same manner. A few sample runs are shown next in the following Figures 175 to 190.

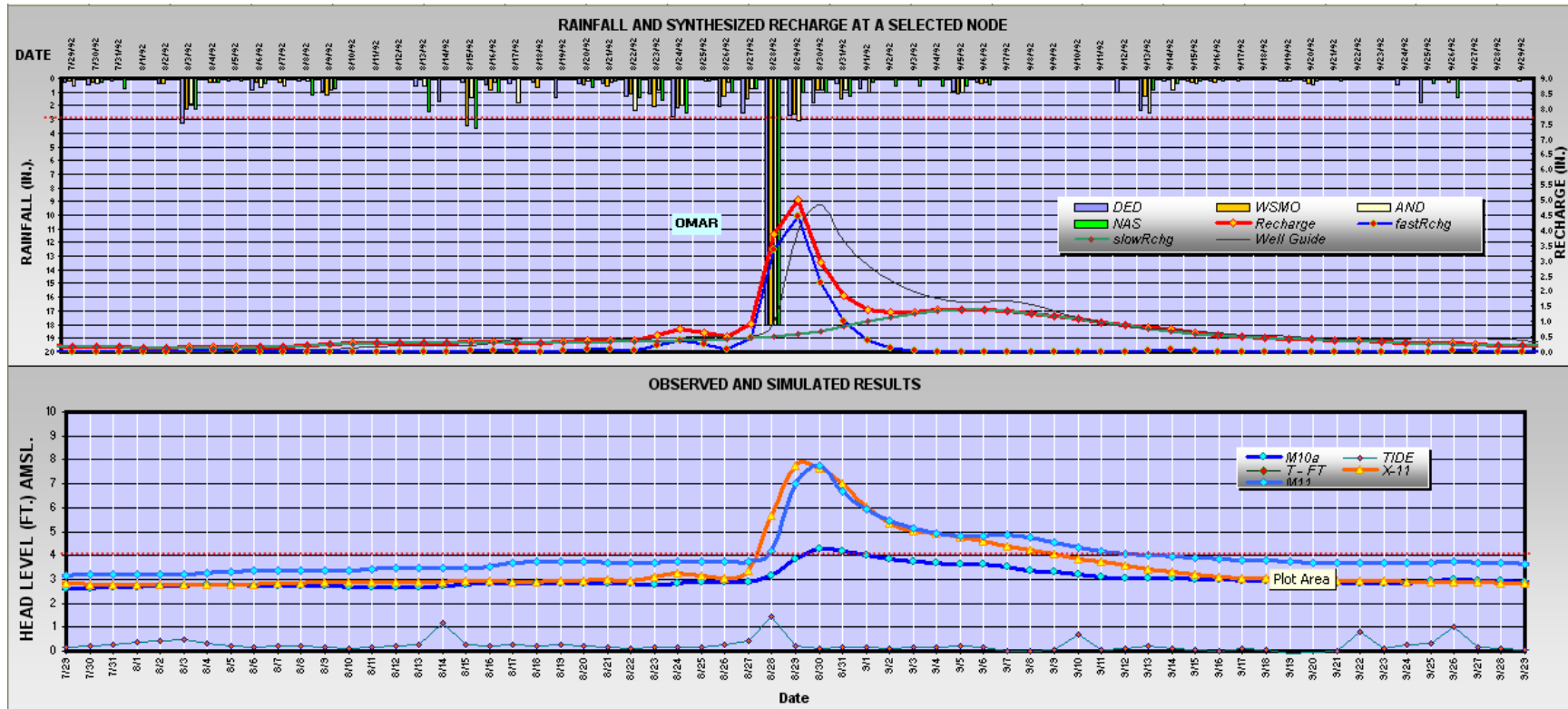


Figure 175. Typhoon Omar recharge synthesis (red line, top chart) at node-shed 59 (Well M-11) and GW model simulation (orange line, lower chart) near matches observation well hydrograph's (light blue, lower chart) response to recharge.

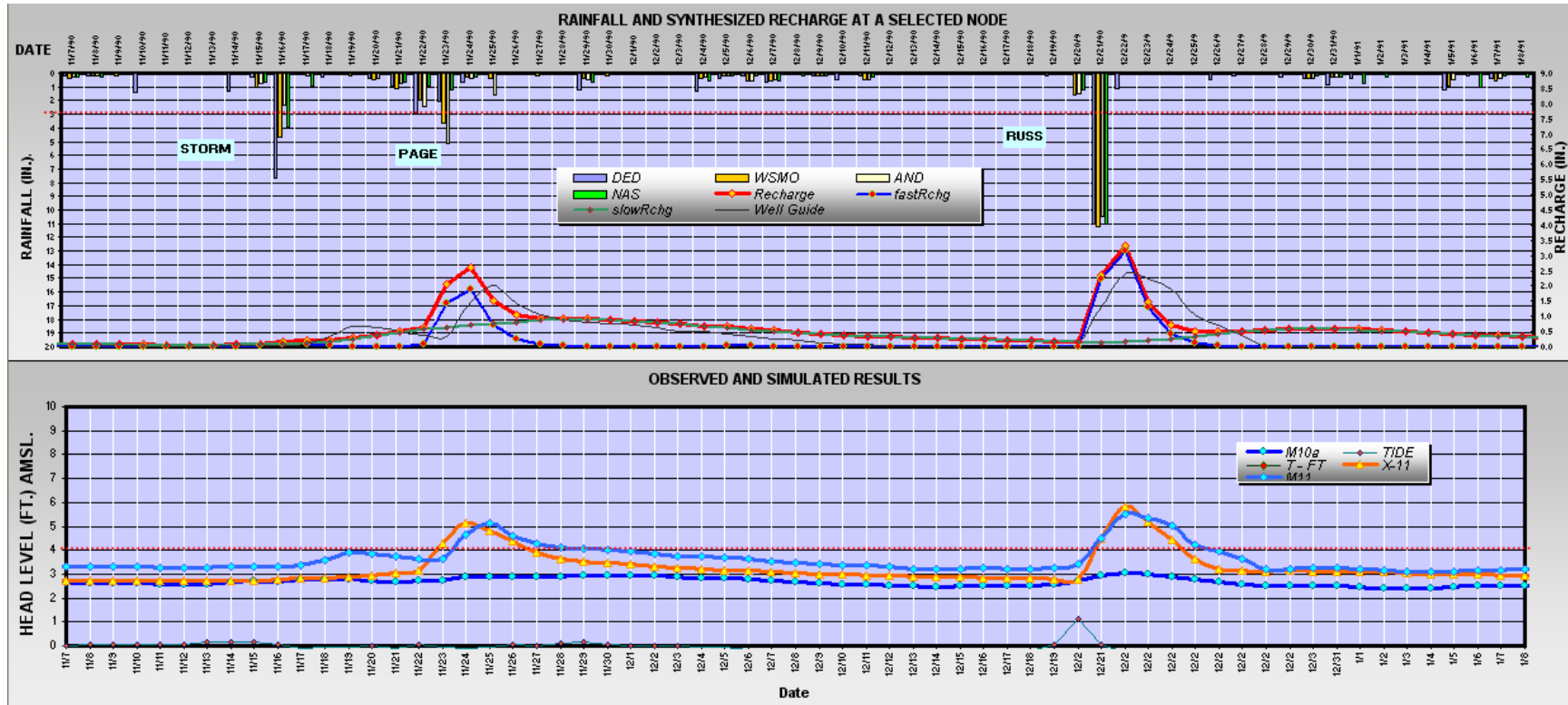


Figure 176. Three storms in November to December of 1990, where the first storm rain pulse had no fast recharge pulse. The drain portion of the simulation, after the peaks of the two responses, could have been made to drain slower by decreasing the hydraulic conductivity and adjusting the specific storage to maintain the peaks.

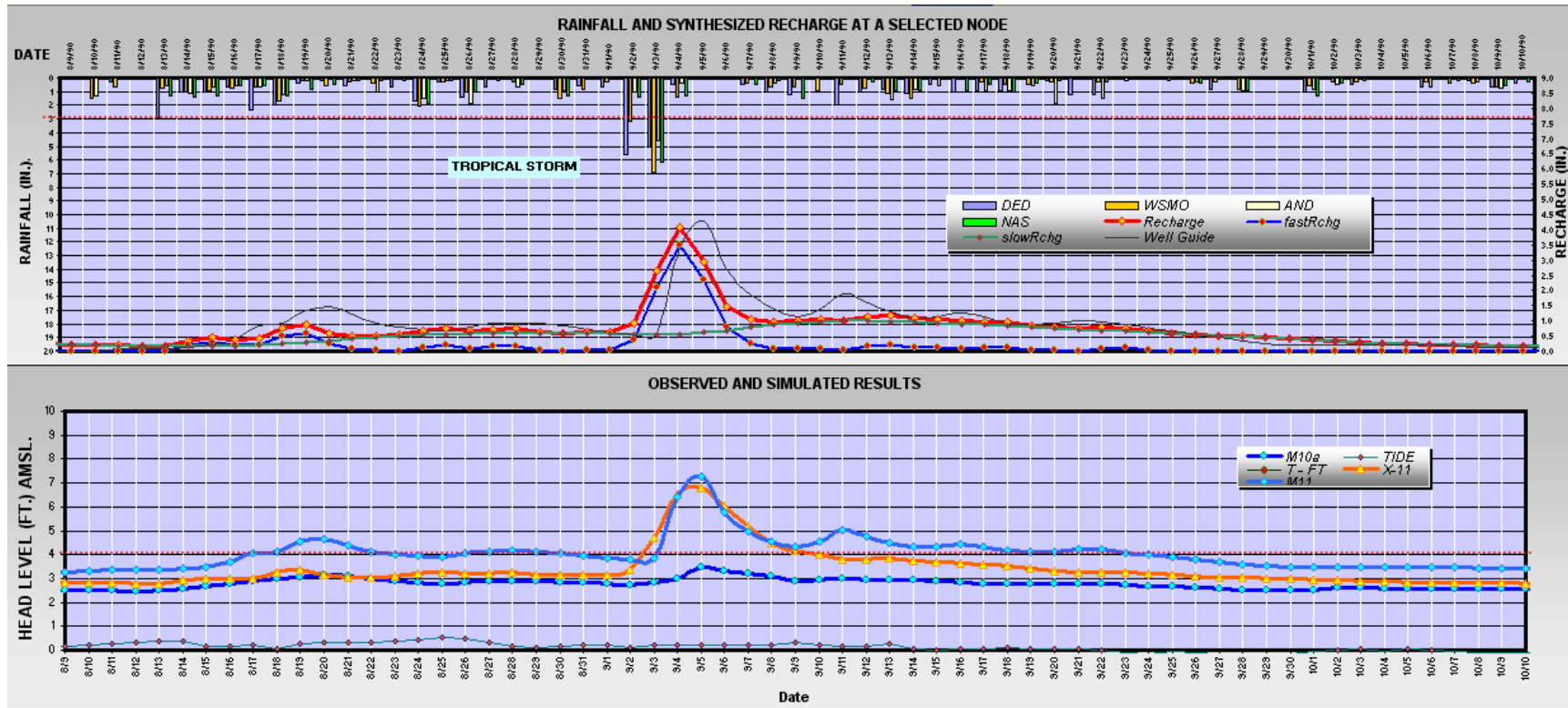


Figure 177. A tropical storm in August and September of 1990. The recharge synthesis did not have high enough rain pulses to produce the successive recharge pulse during the synthesis. The observation well reveals a *multi-pulse recharge* but the GW model can only produce responses from the recharge pulses.

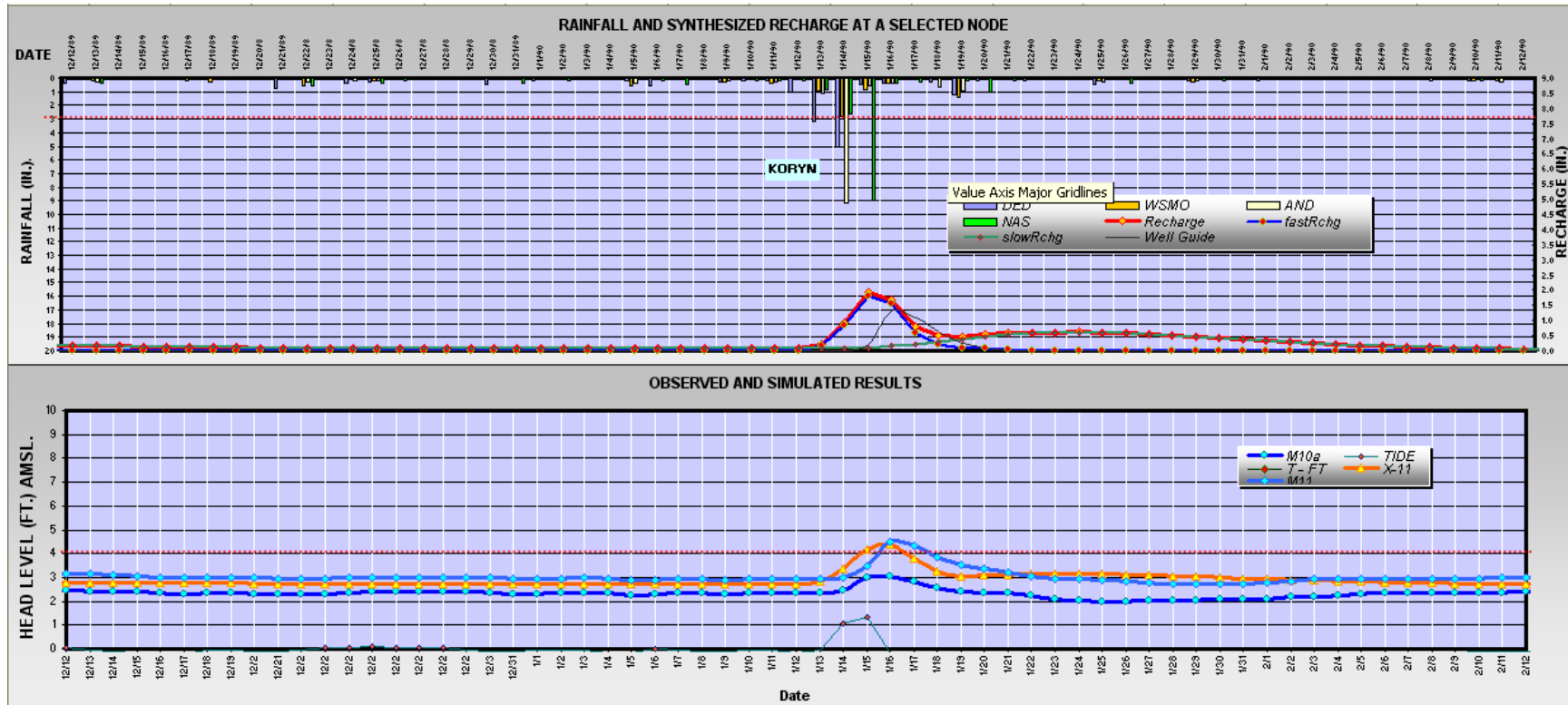


Figure 178. Typhoon Koryn, January of 1990. The GW simulation is slightly misaligned signifying the recharge synthesis might require an increase in lag time by increasing the number of phases or it could again be possible rain data error.

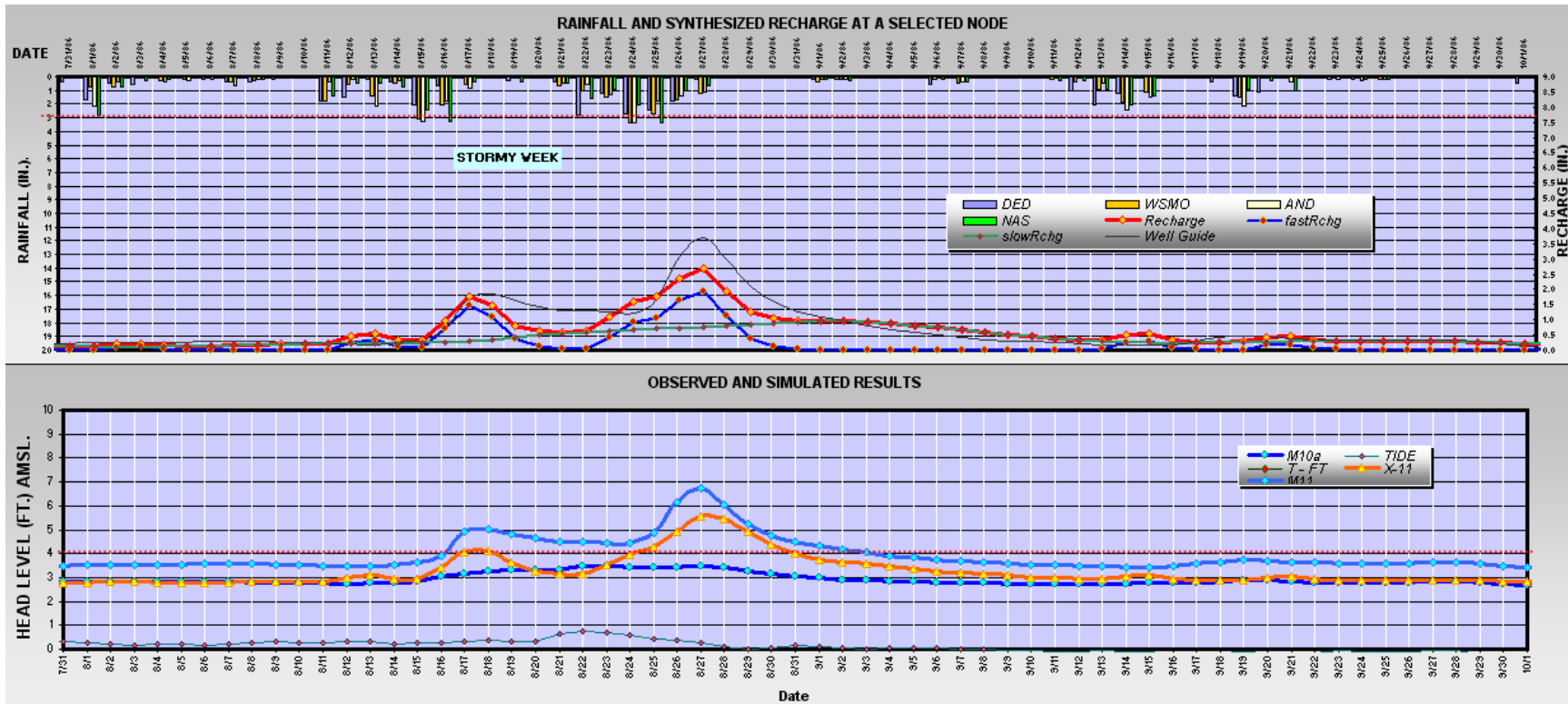


Figure 179. A stormy week, late August of 1986, shows a *Double Pulse Recharge* produced from a wide distribution of rain pulses. It is not clear if it is an error of the rain data, the ET or recharge SM curve settings. The max rain fall measured for the Dededo gage was not more than 4 inches. The GW simulation could not respond high enough with the recharge synthesis flux input to match the observation well chart.

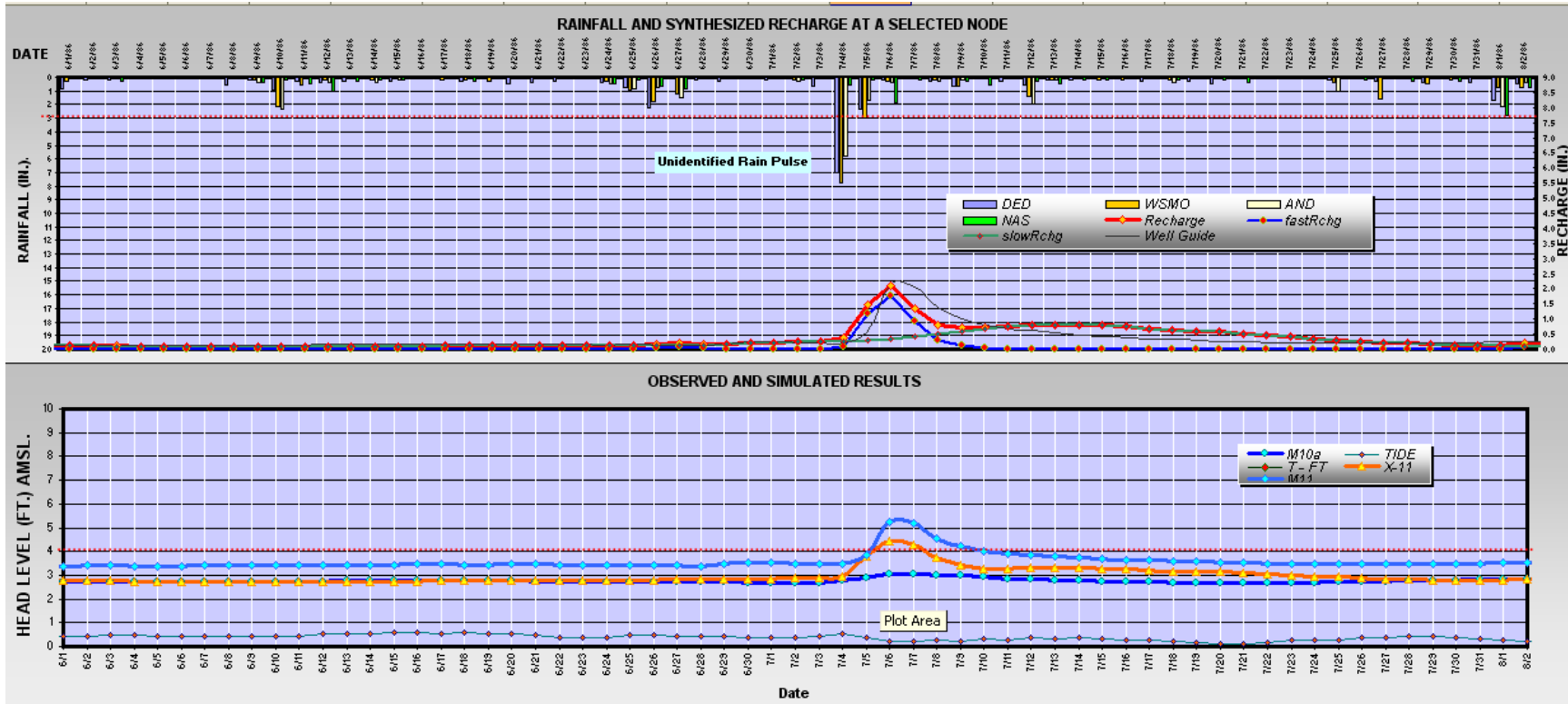


Figure 180. This GW simulation is lower than the observed data by a foot or less which is a result of underestimating the frequent hydraulic gradient which the GW model is specified when there is no recharge. This is more of a GW modeling issue than a recharge synthesis problem.

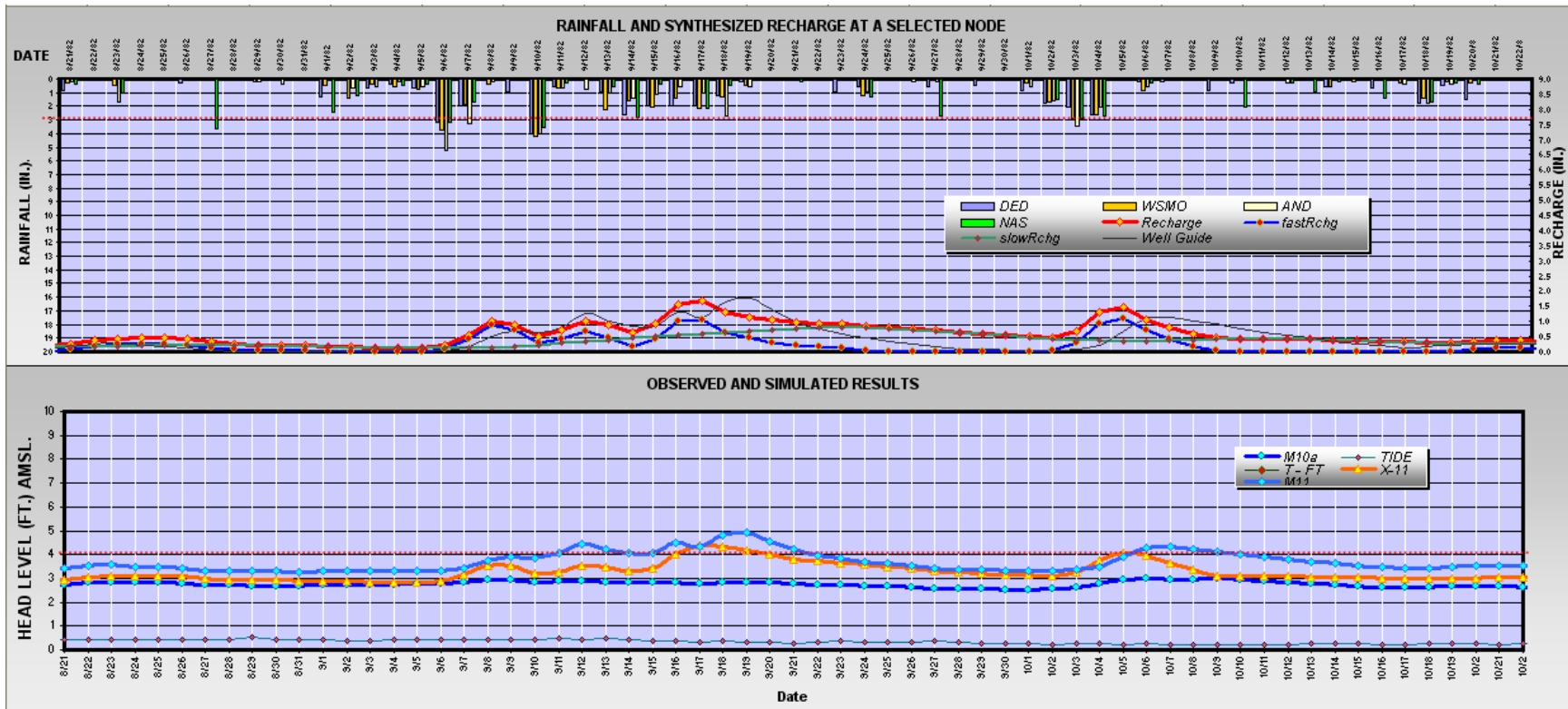


Figure 181. GW simulation of a multi-pulse recharge, September-October 1982.

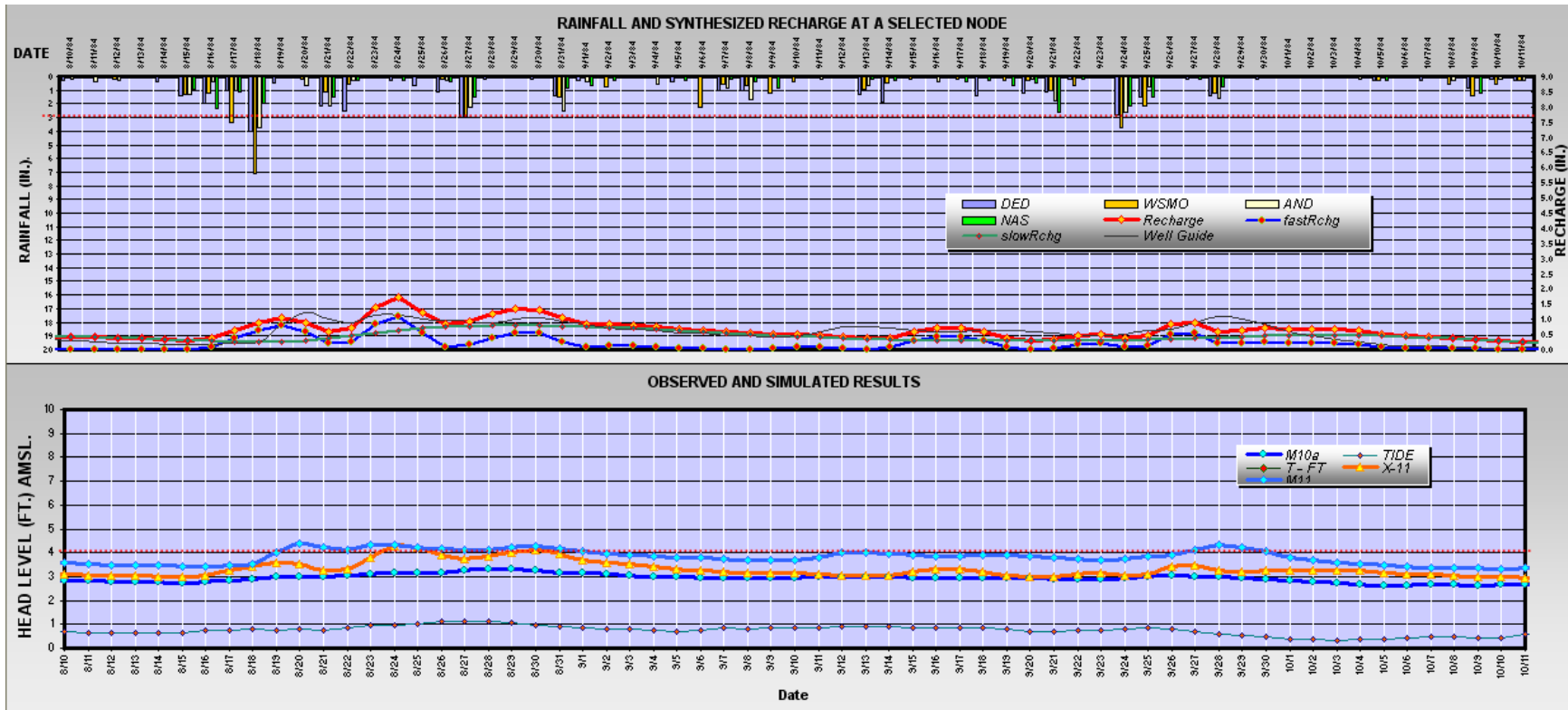


Figure 182. Small amplitude *multi-pulse recharge* simulation, August-September 1984.

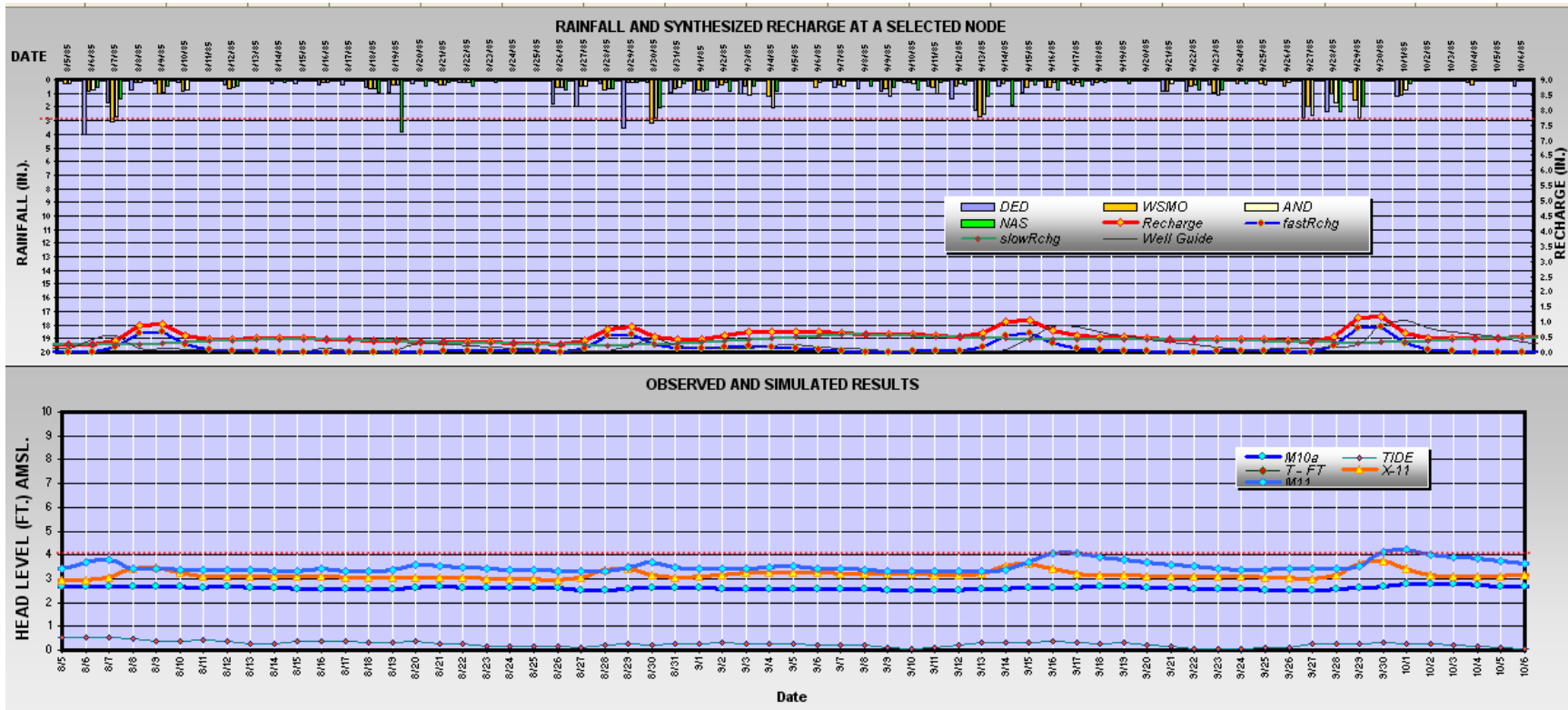


Figure 183. Small pulses of recharge during August-September of 1985 show misalignment for both synthesis and simulations.

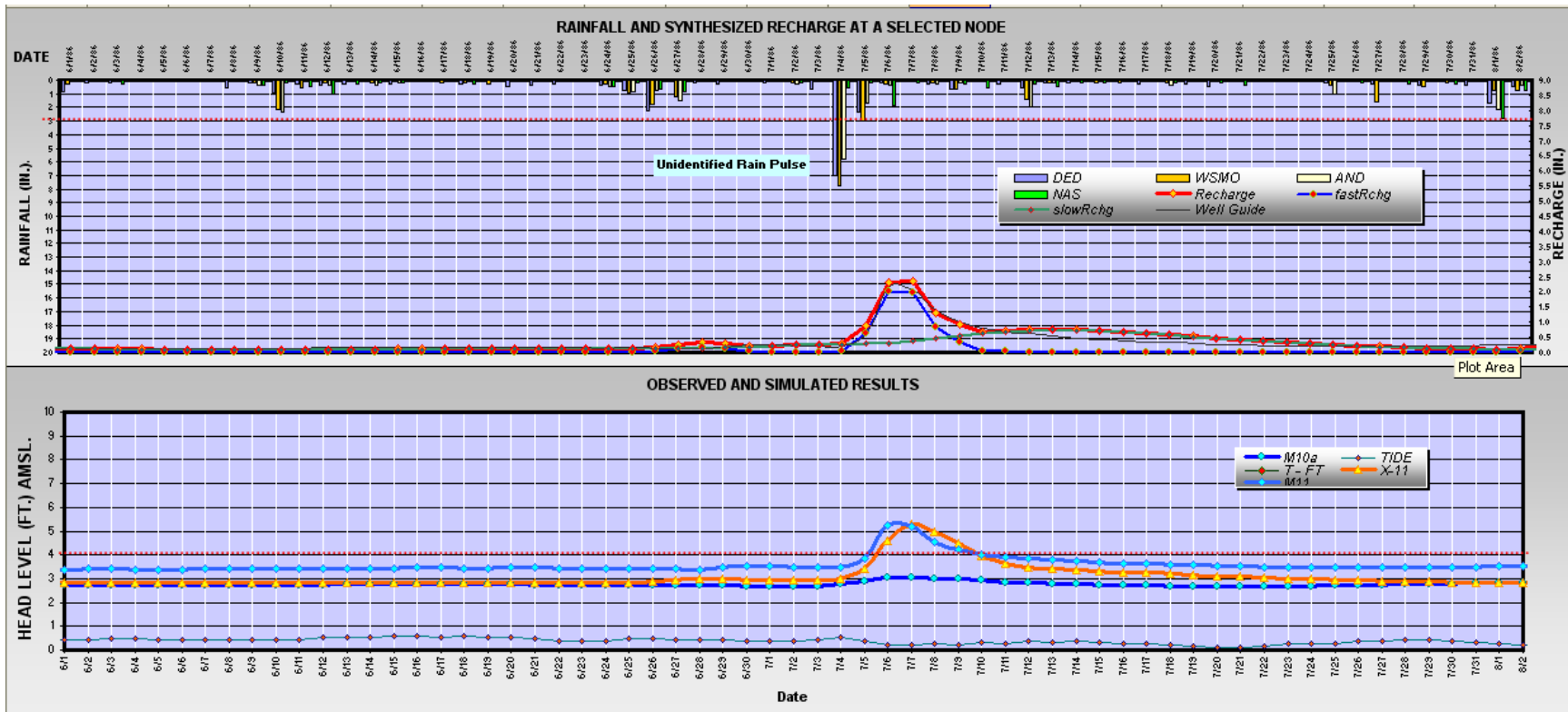


Figure 184. Simulation during an unidentified rain pulse in the summer of 1986.

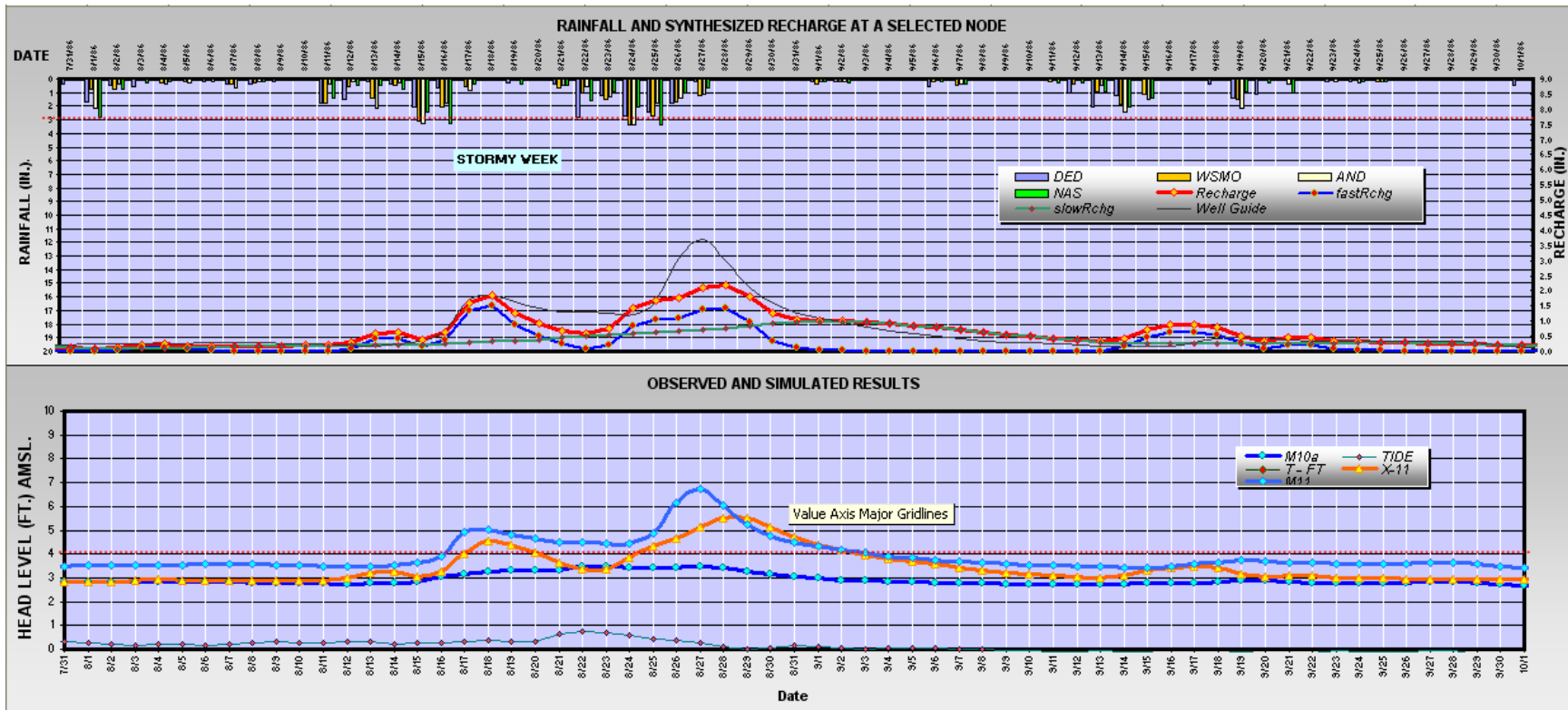


Figure 185. Simulation for August-September of 1986.

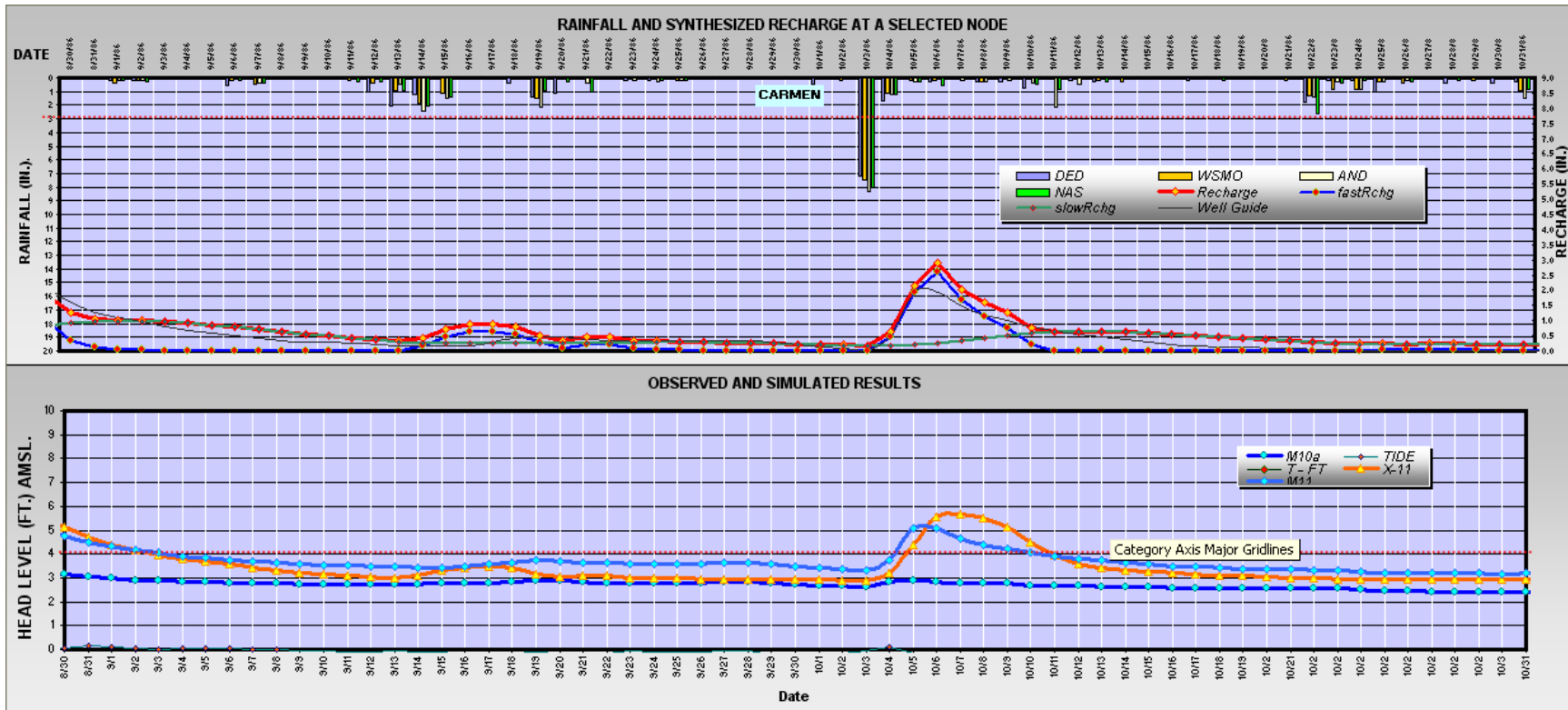


Figure 186. Typhoon Carmen, early October of 1986, rain pulse, recharge synthesis, and simulated response.

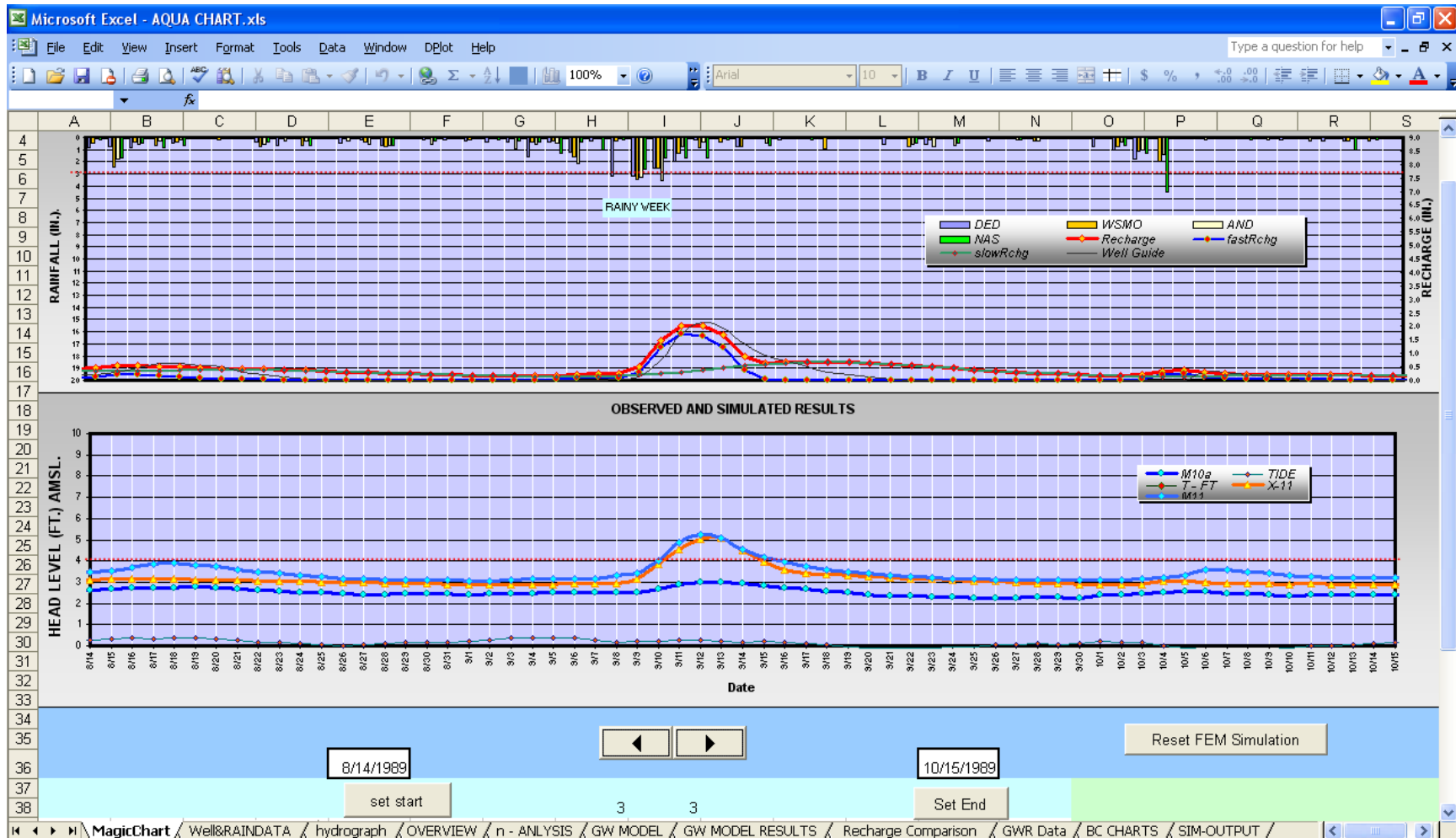


Figure 187. One of the best simulations matches thus far during a rainy week. This figure also shows the scroll buttons control and its design in Excel.

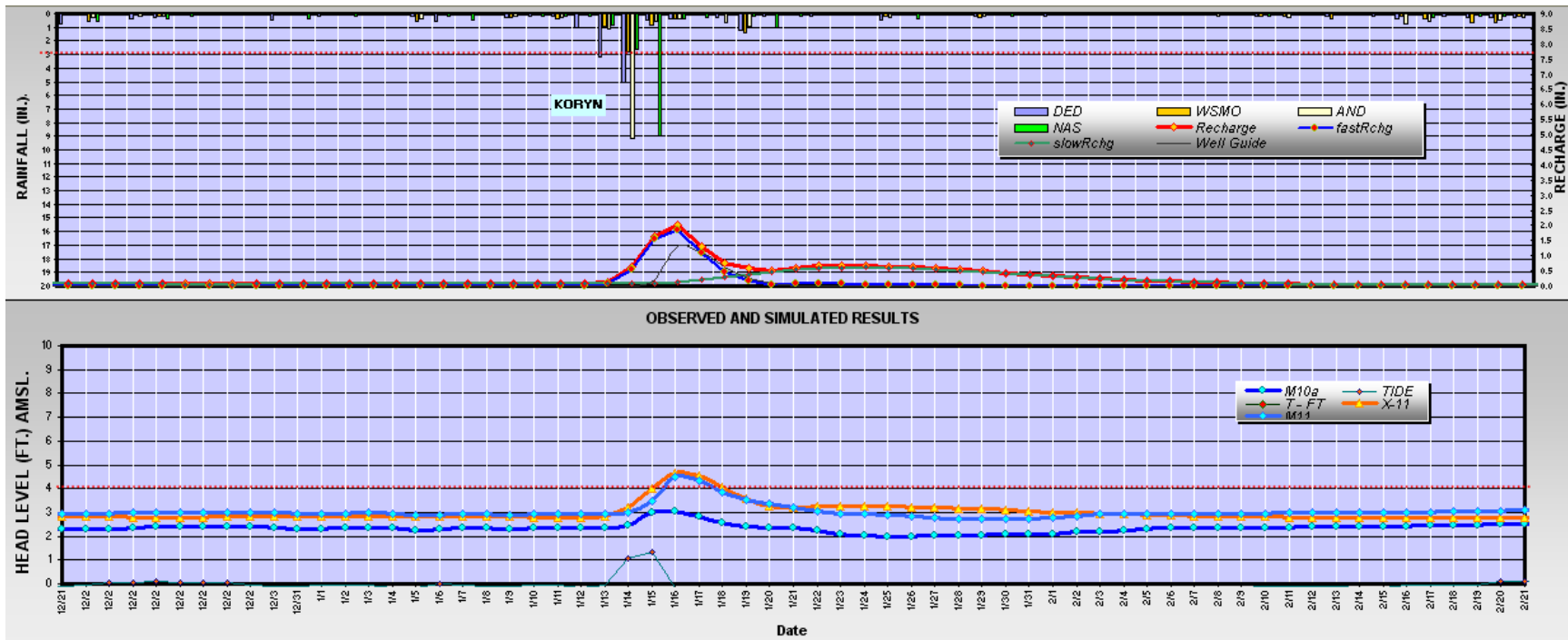


Figure 188. Typhoon Koryn simulation closely approximates the observed data.

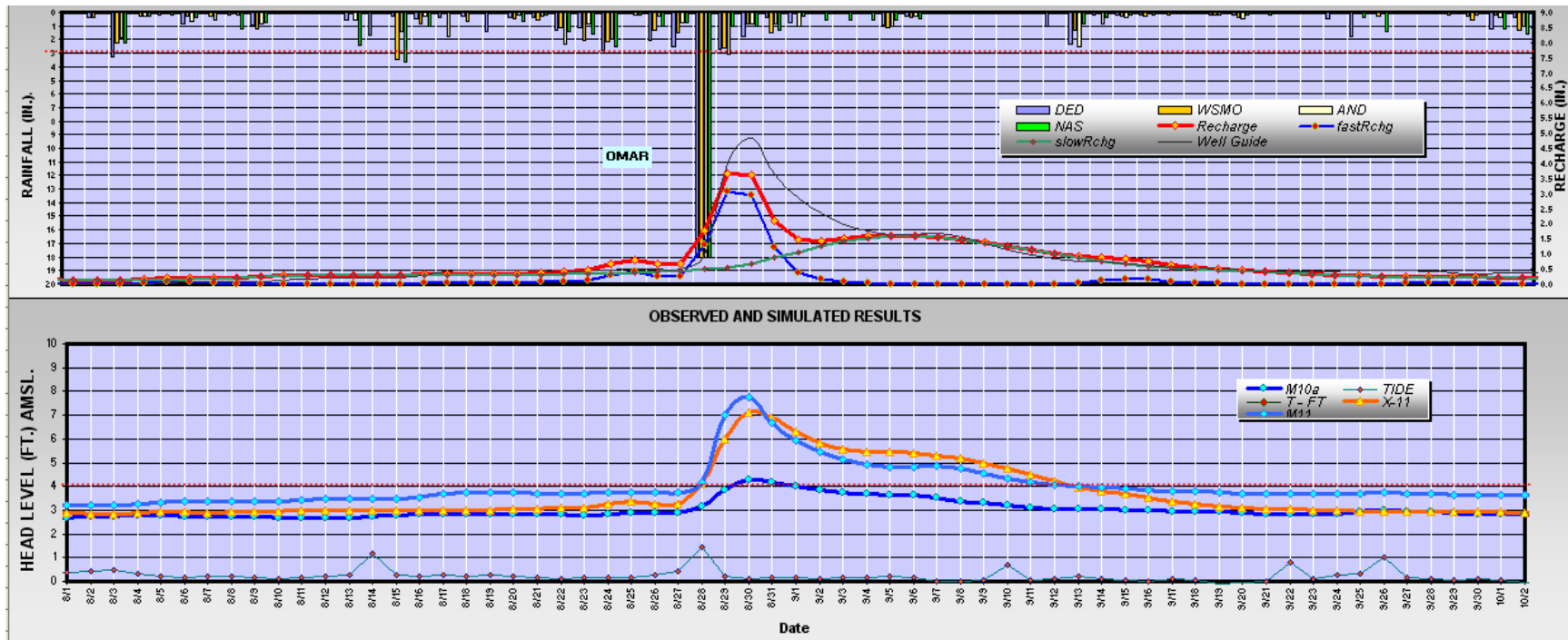


Figure 189. A simulation of Typhoon Omar needs more amplitude in the recharge synthesis fast flow to produce the extra foot at the peak in the simulation.

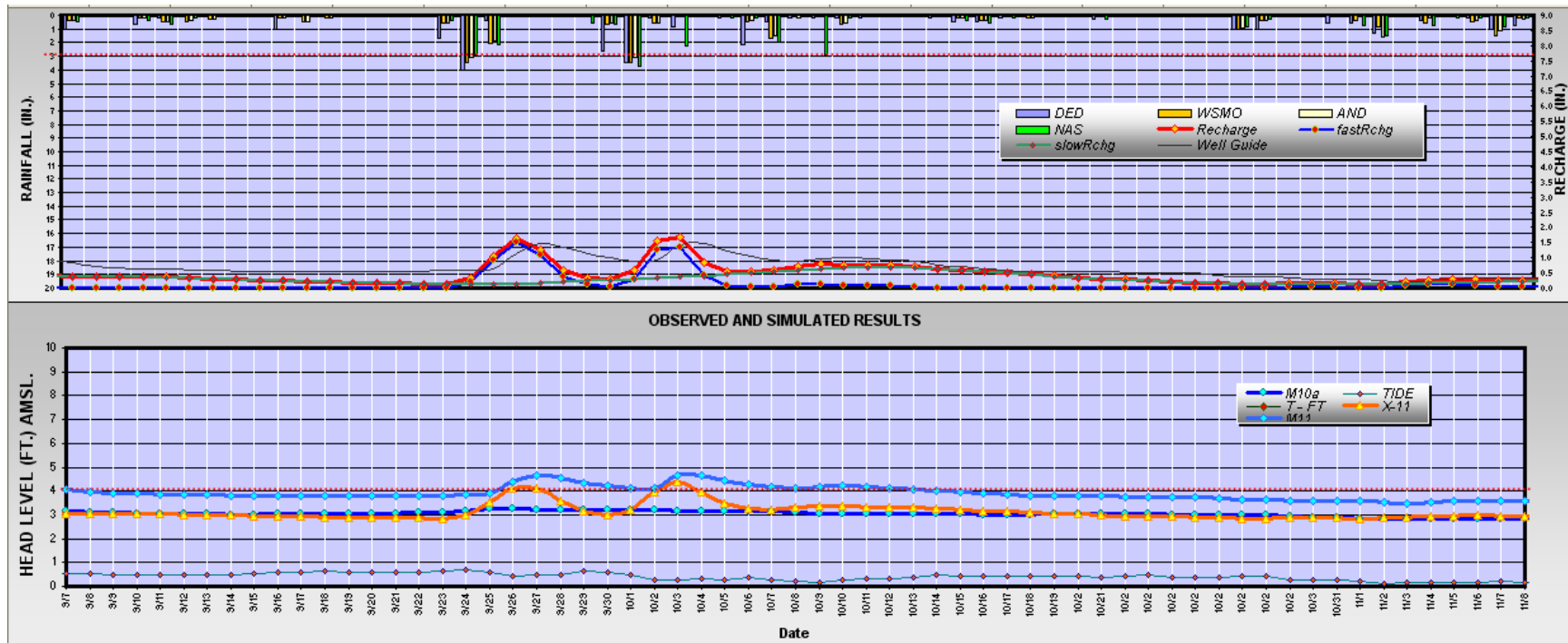


Figure 190. This figure shows that sometimes, results are not as expected and the GW modeling might need adjusting or reconfiguring.

GW Model Simulations for M-11 and M-10a

The final settings and AQUA CHART results for this project for recharge synthesis and GW model are shown next. The parameter settings for the GW model are shown in figure 191. M-10a, node 41, and allogenic recharge receiving nodes used material 3. Observation well M-11, node-shed and node number 59, hydraulic conductivity was set to 5500 m/day and the specific storage was set to 0.00012. The rest of the nodes used Jocson’s 5800 m/day regional hydraulic conductivity (Jocson, 1998) and the specific storage was set to 0.0002 m⁻¹. The results for M-10 are shown in Figures 192 to 206.

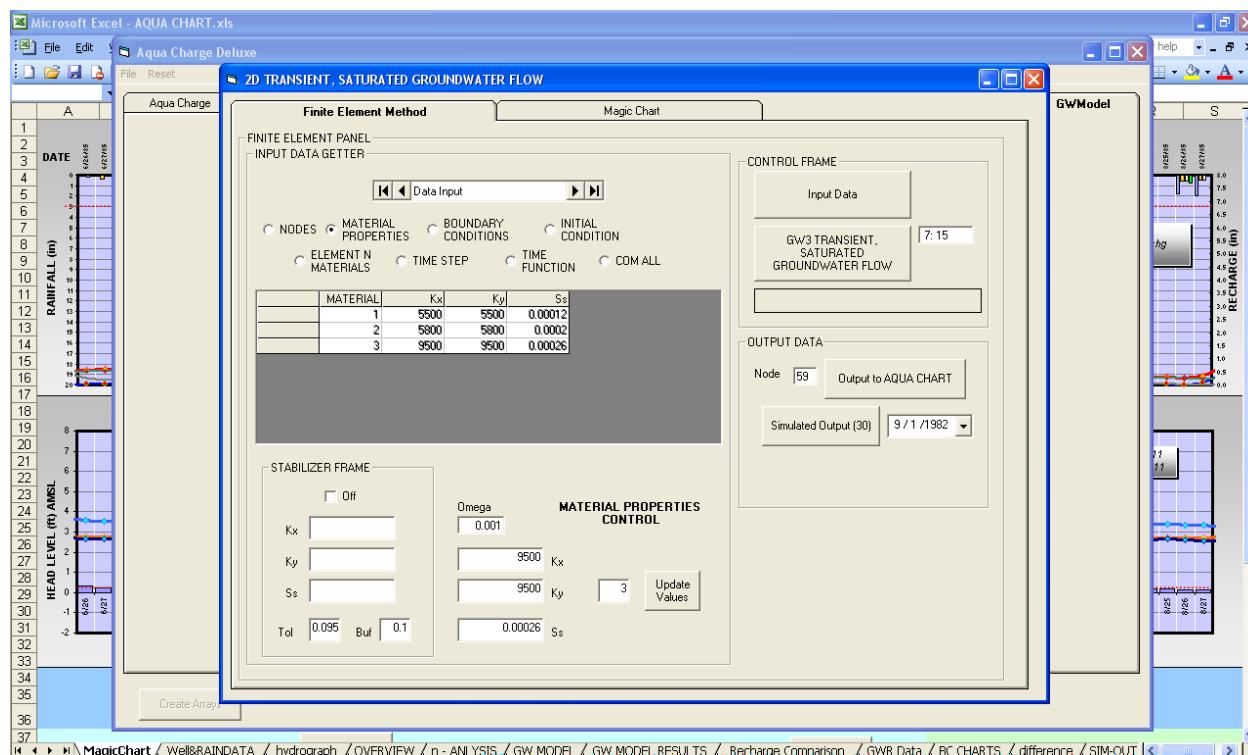


Figure 191. Final materials properties setting for GW model.

Final synthesis and simulation results for M-11:

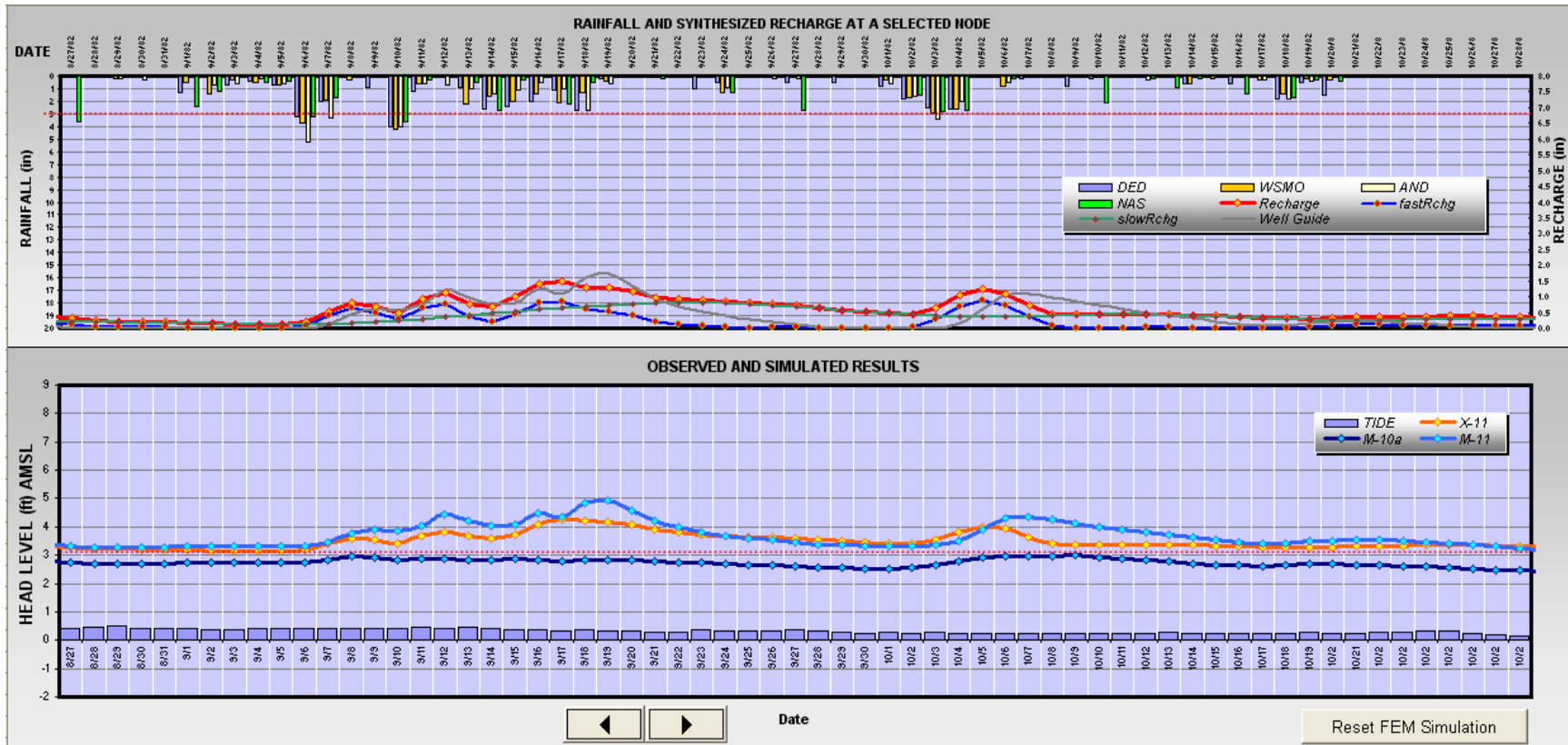


Figure 192. September 1982

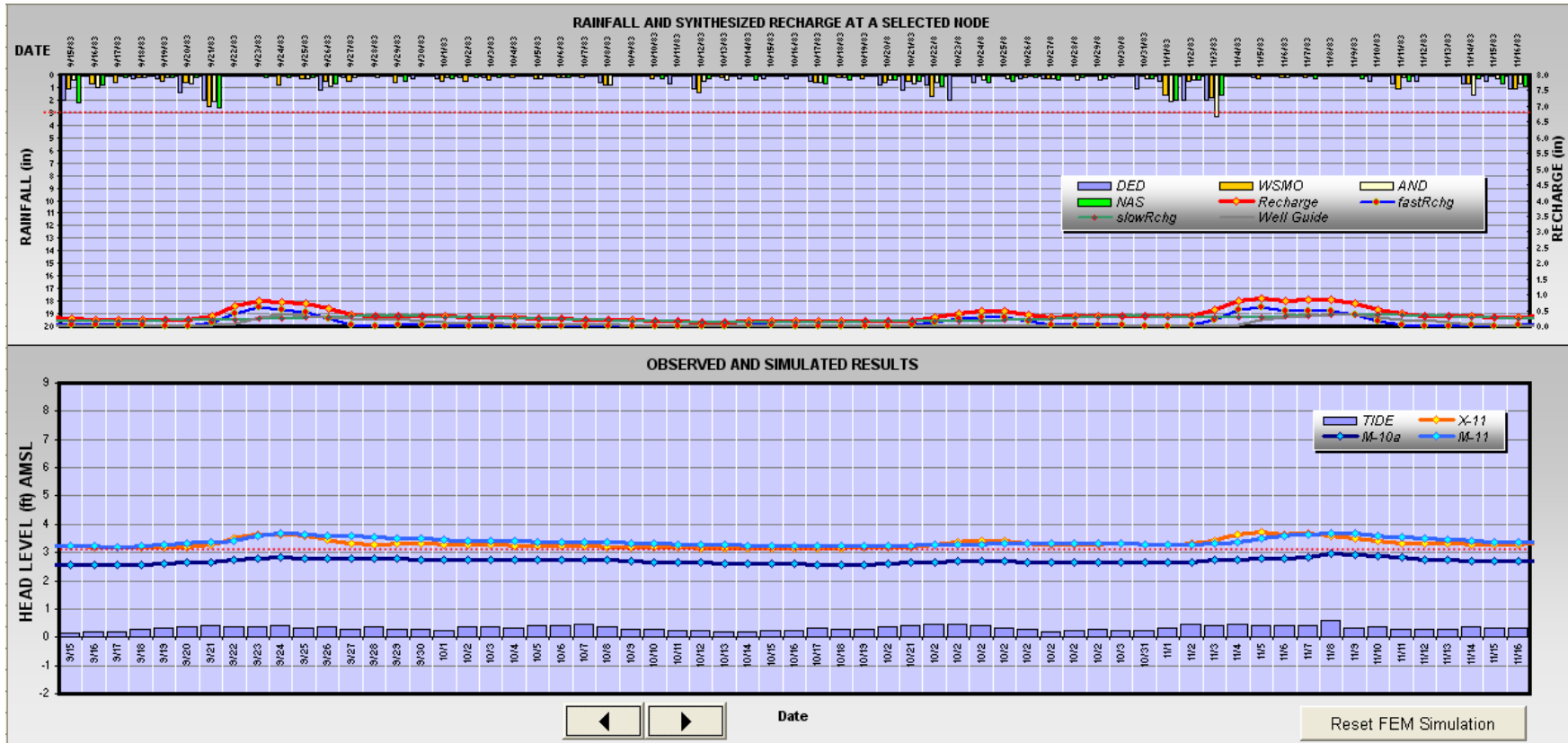


Figure 193. Small rainy season, September and October of 1983.

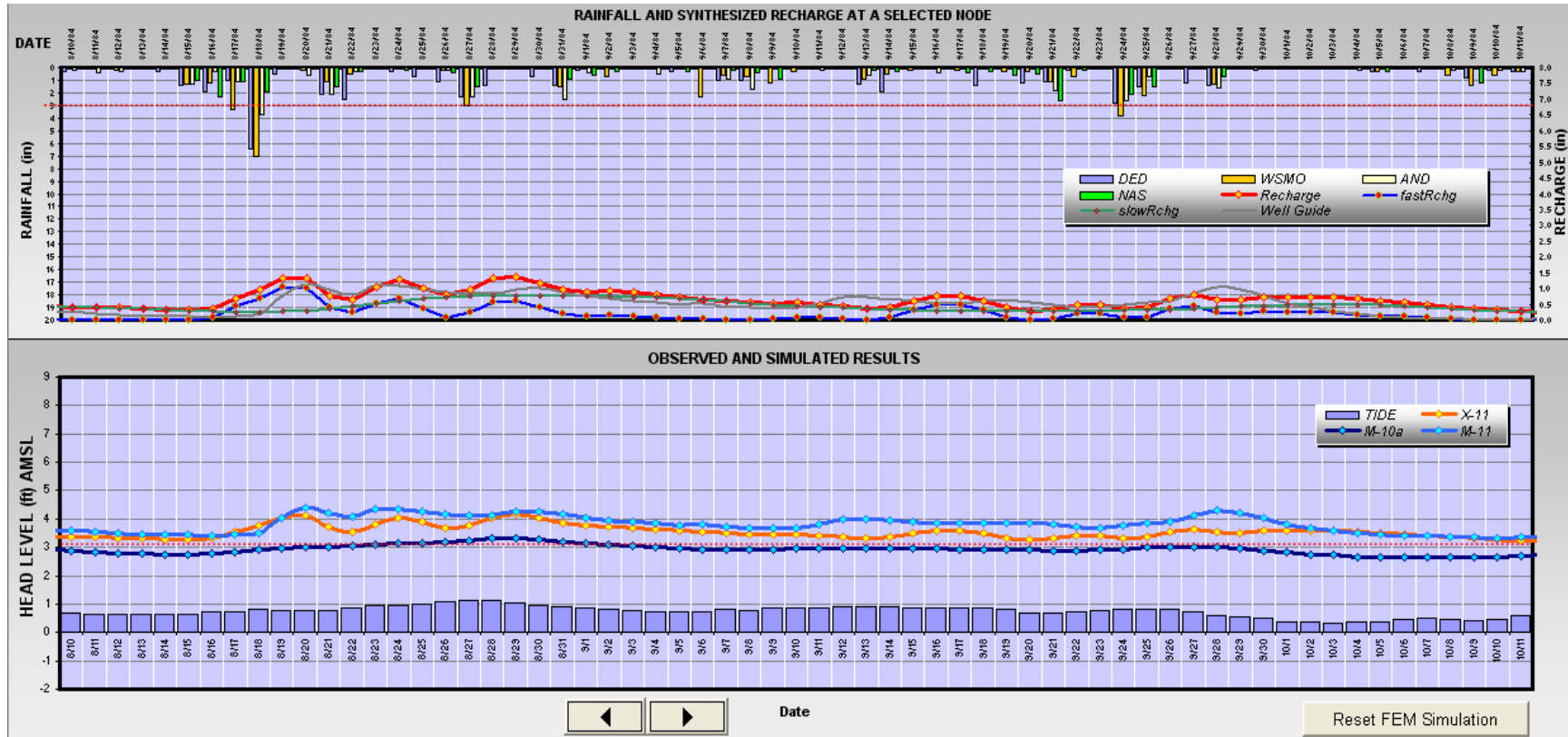


Figure 194. August to October of 1984.

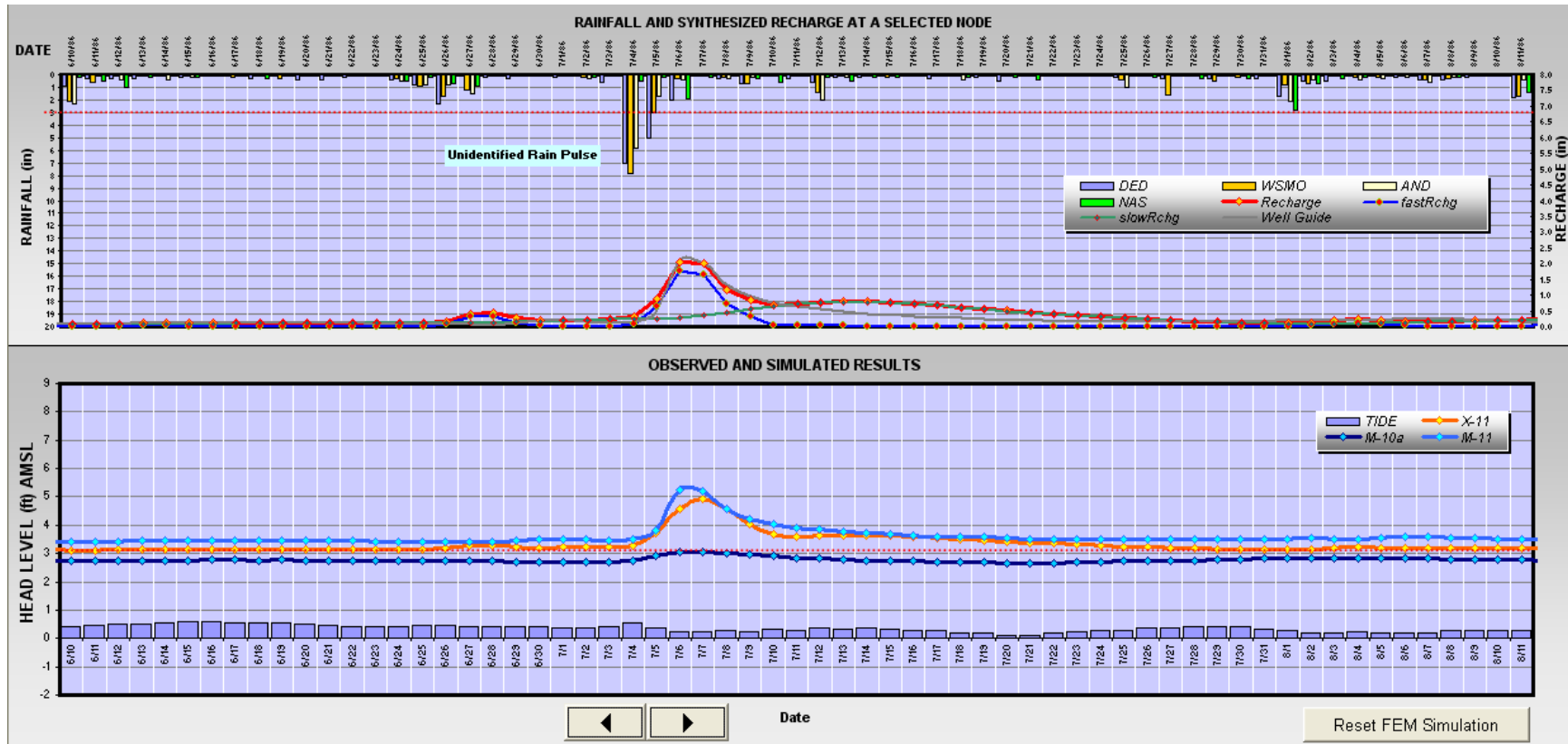


Figure 195. An unidentified rain pulse mid summer of 1986.

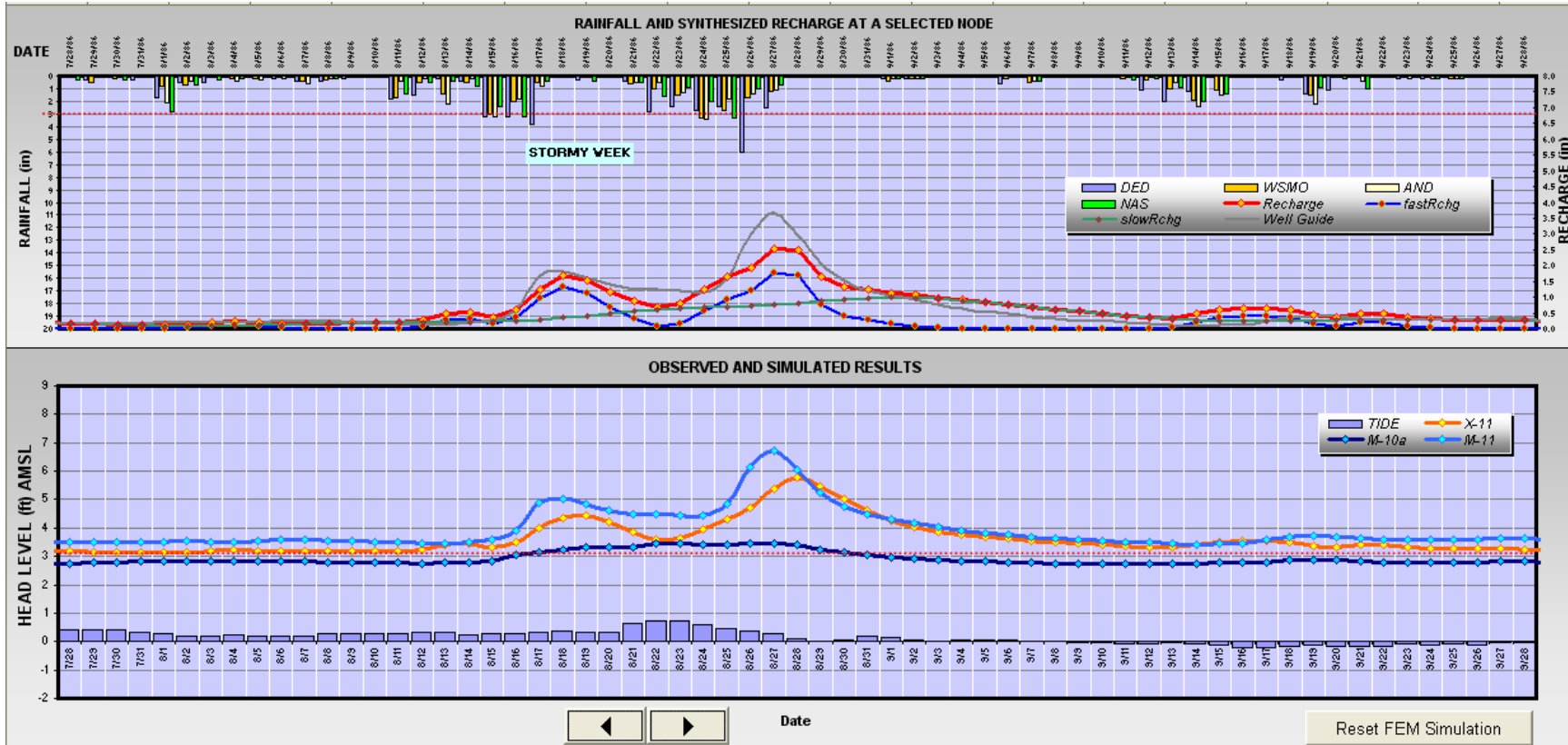


Figure 196. A stormy week in August of 1986. The tail end in the GW model captured the draining smoothly.

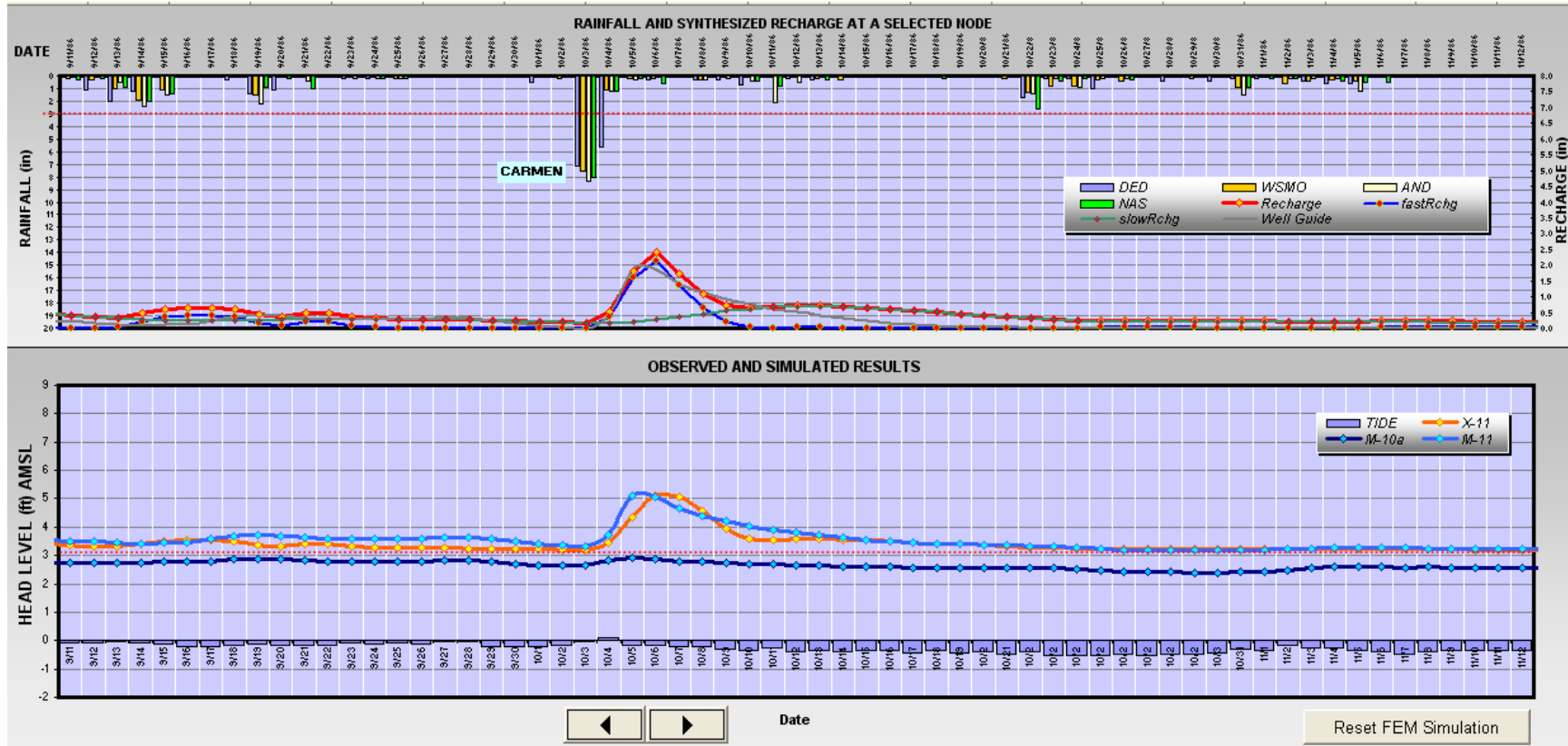


Figure 197. Typhoon Carmen, October 1986.

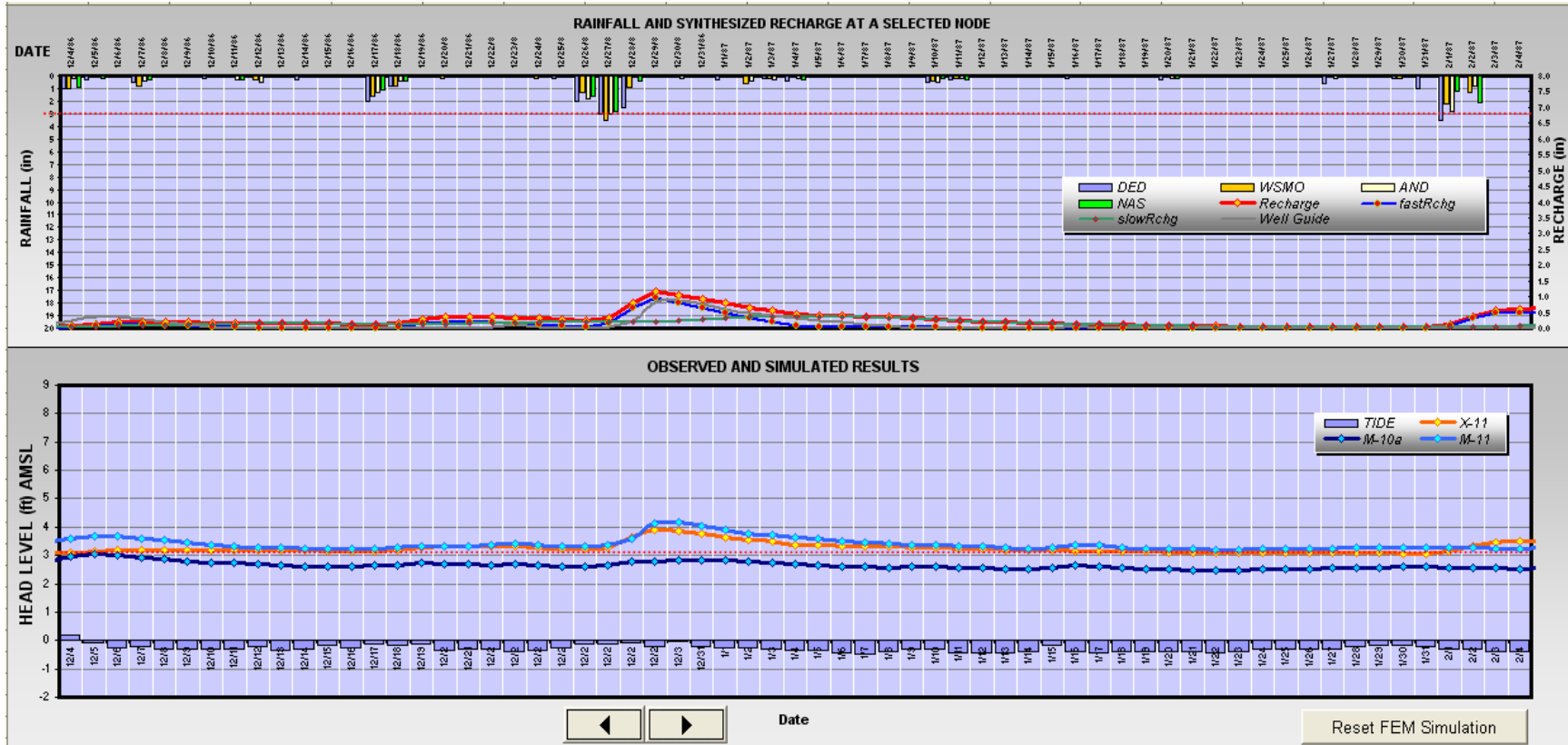


Figure 198. December of 1986.

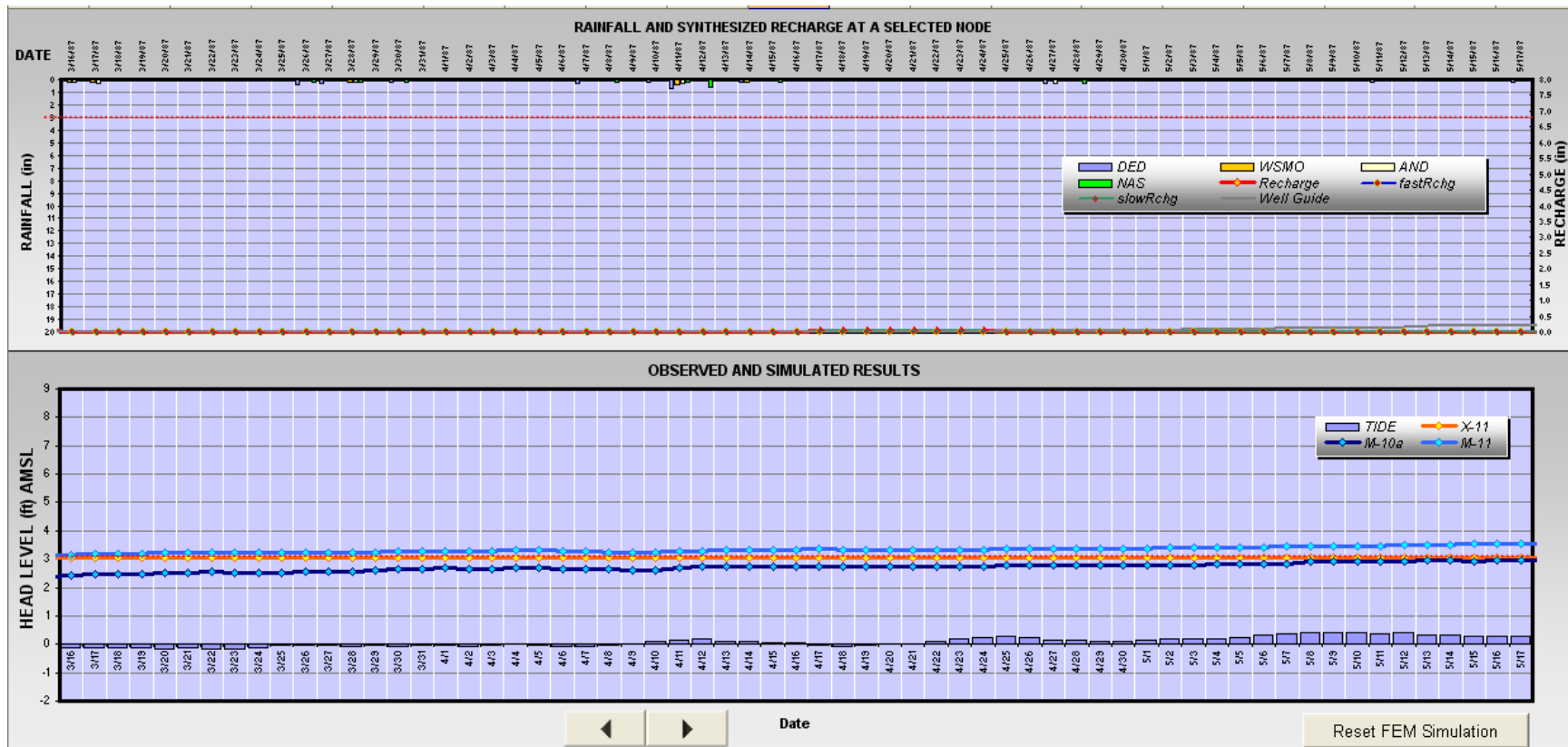


Figure 199. Post El Nino, 1987, with no recharge, shows the rising daily mean tide lifting the lens. The simulation holds its mode position steady when there is no recharge.

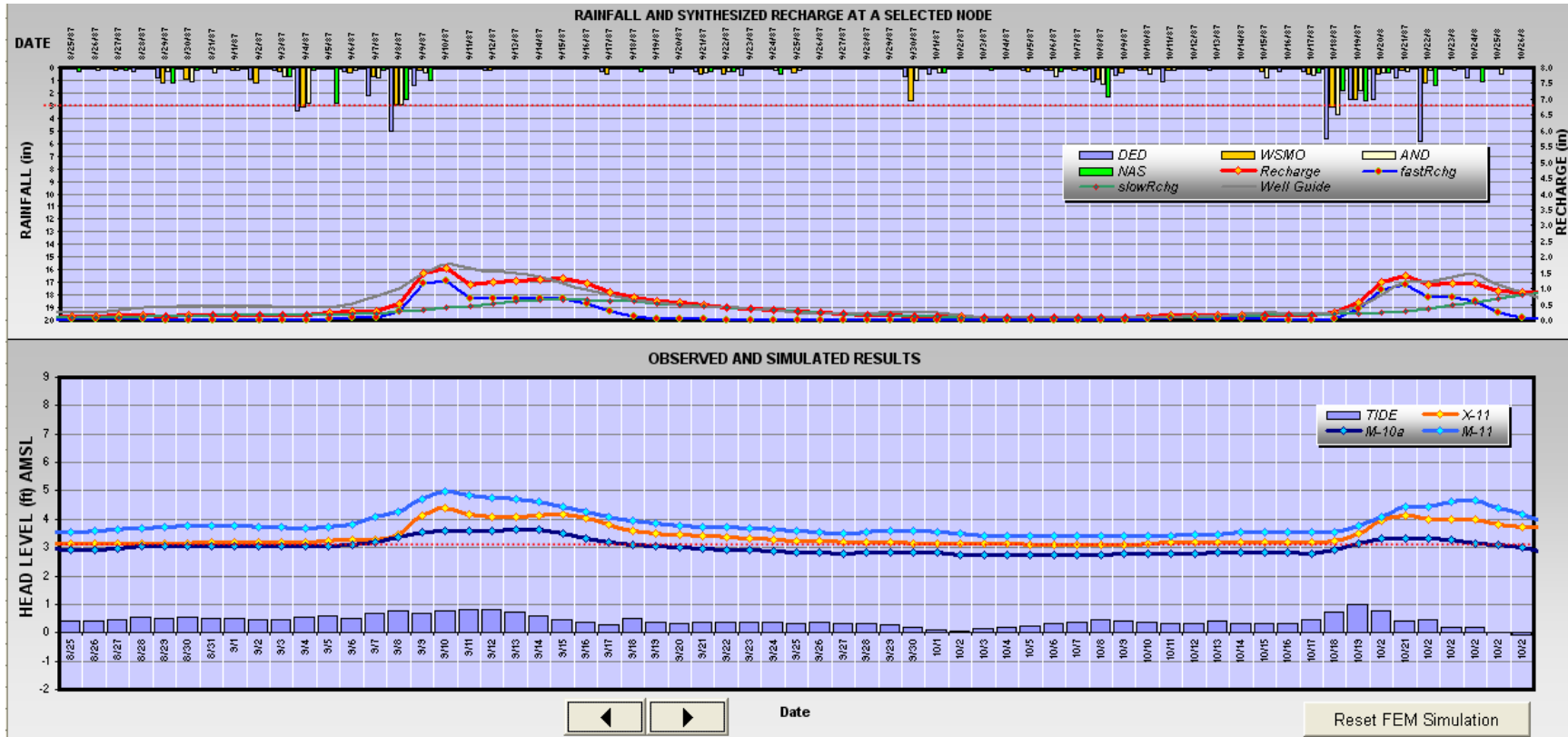


Figure 200. The rising tide affects history matching since the GW model does not handle tide effects well.

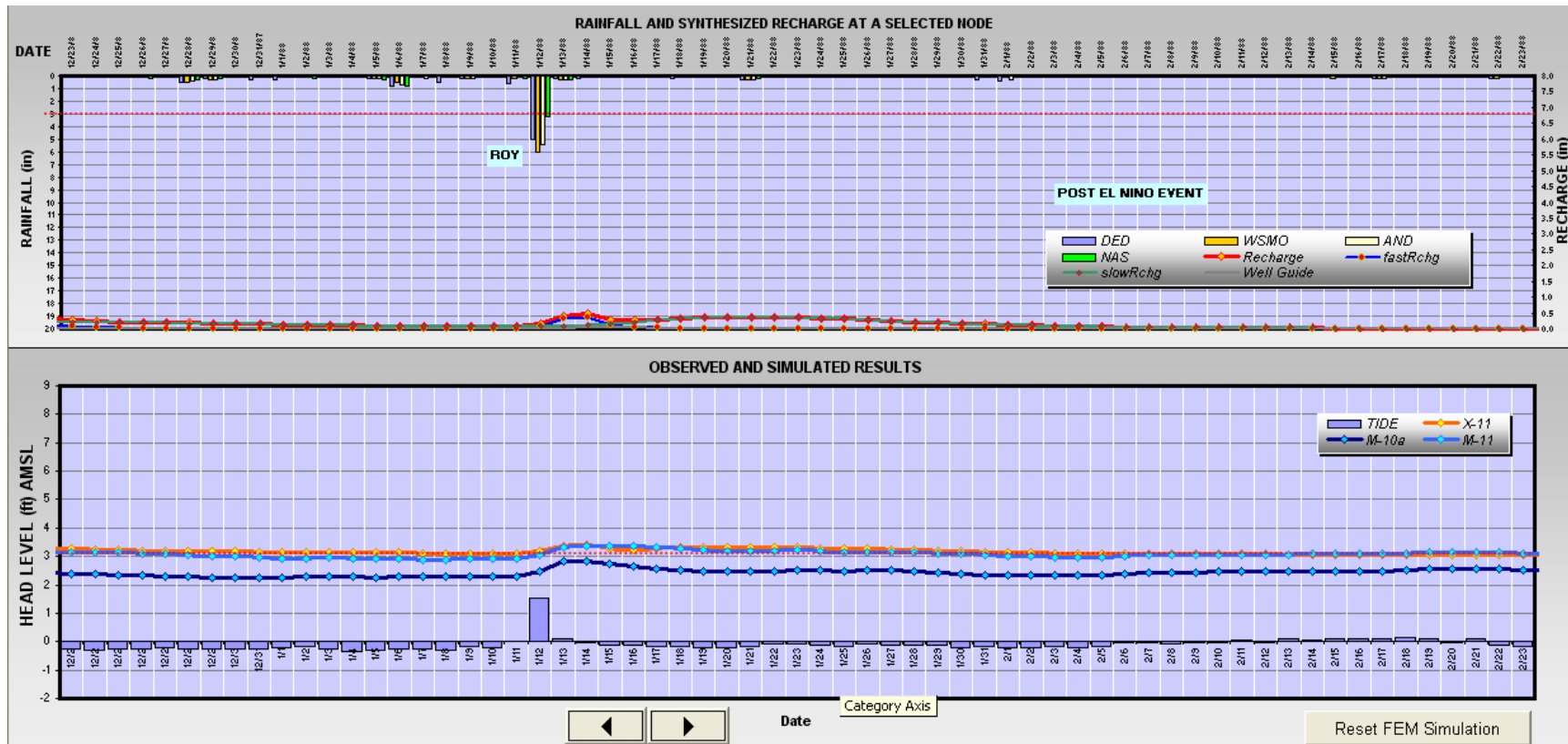


Figure 201. Typhoon Roy’s rain pulse drew a small recharge response due to a dry, unprimed, vadose. The GW simulation is a near match to M-11’s data.

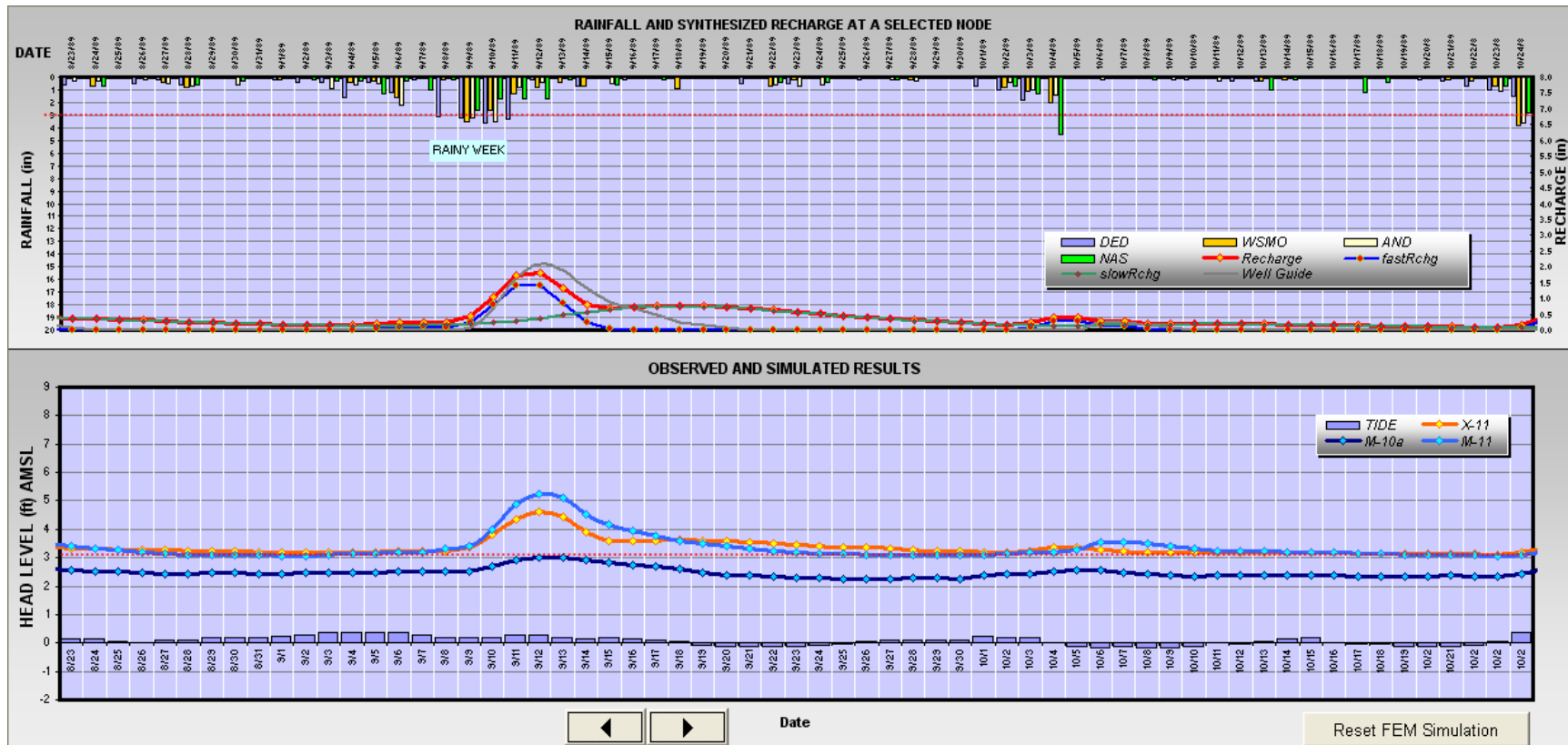


Figure 202. Rainy week in September of 1989 produced a smooth curved recharge. The GW simulation nearly captures the curved GW response.

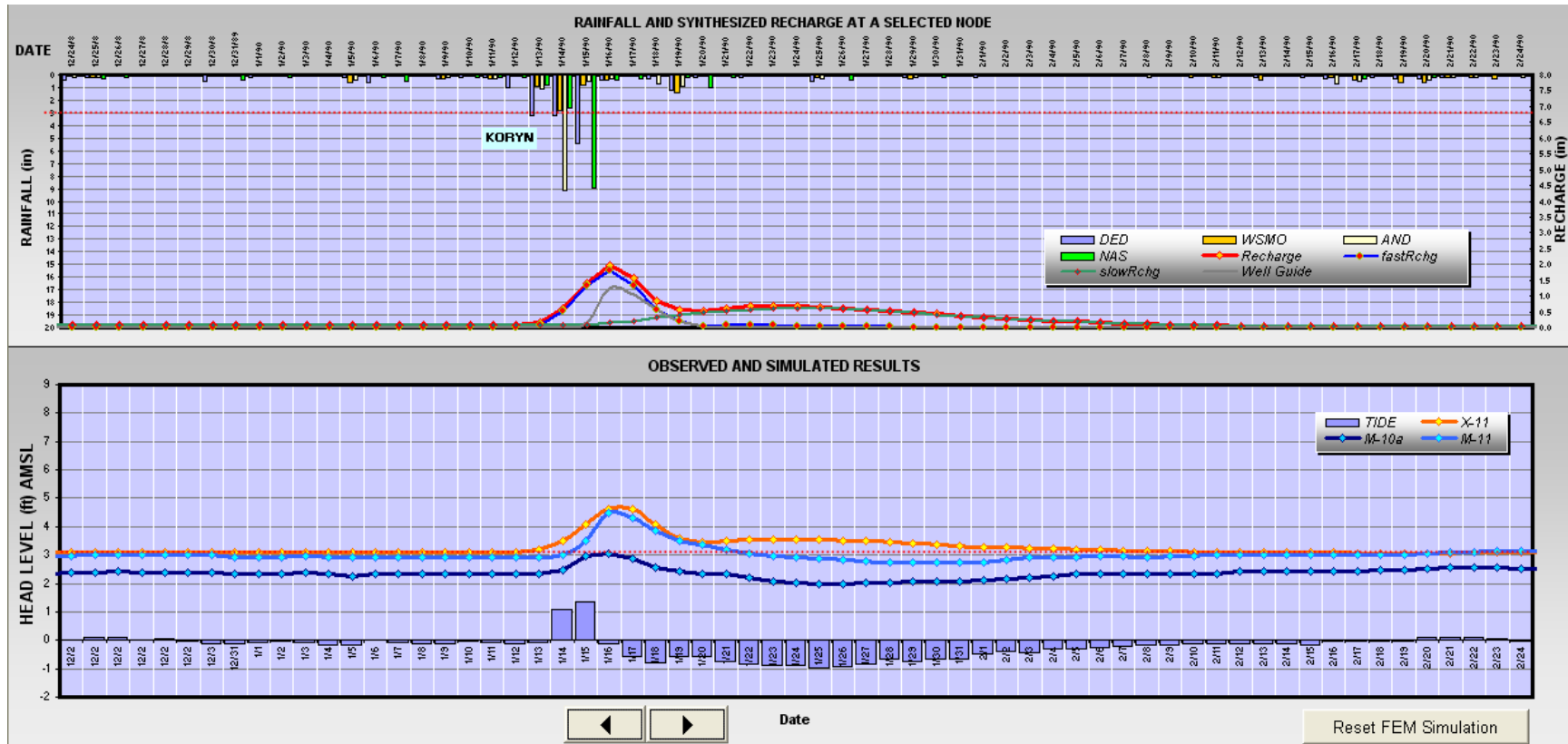


Figure 203. Typhoon Koryn, January of 1990, the tide influence draws down the on the M-11 well level.

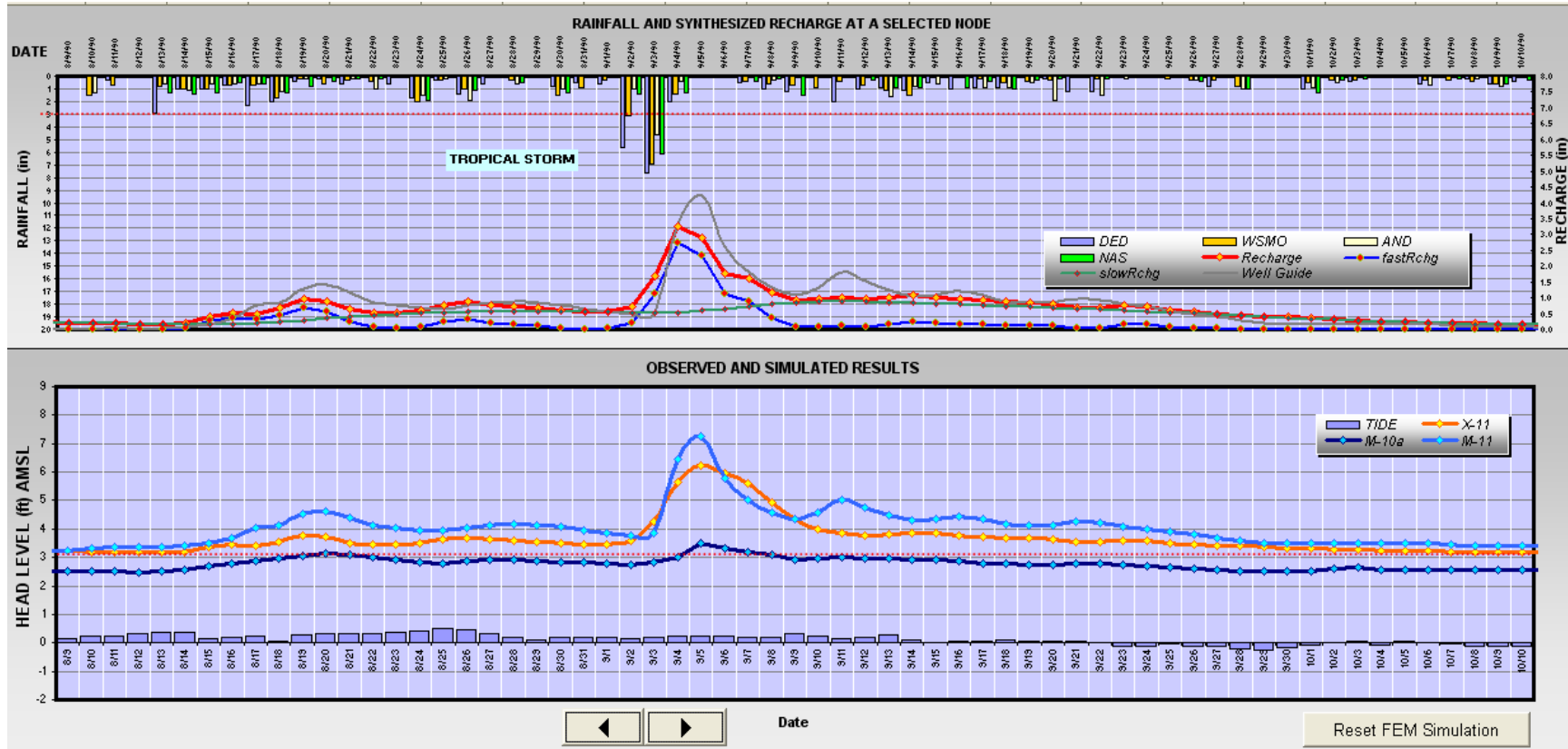


Figure 204. A complex multi-pulse recharge during a tropical storm and rainy months of August and September of 1990.

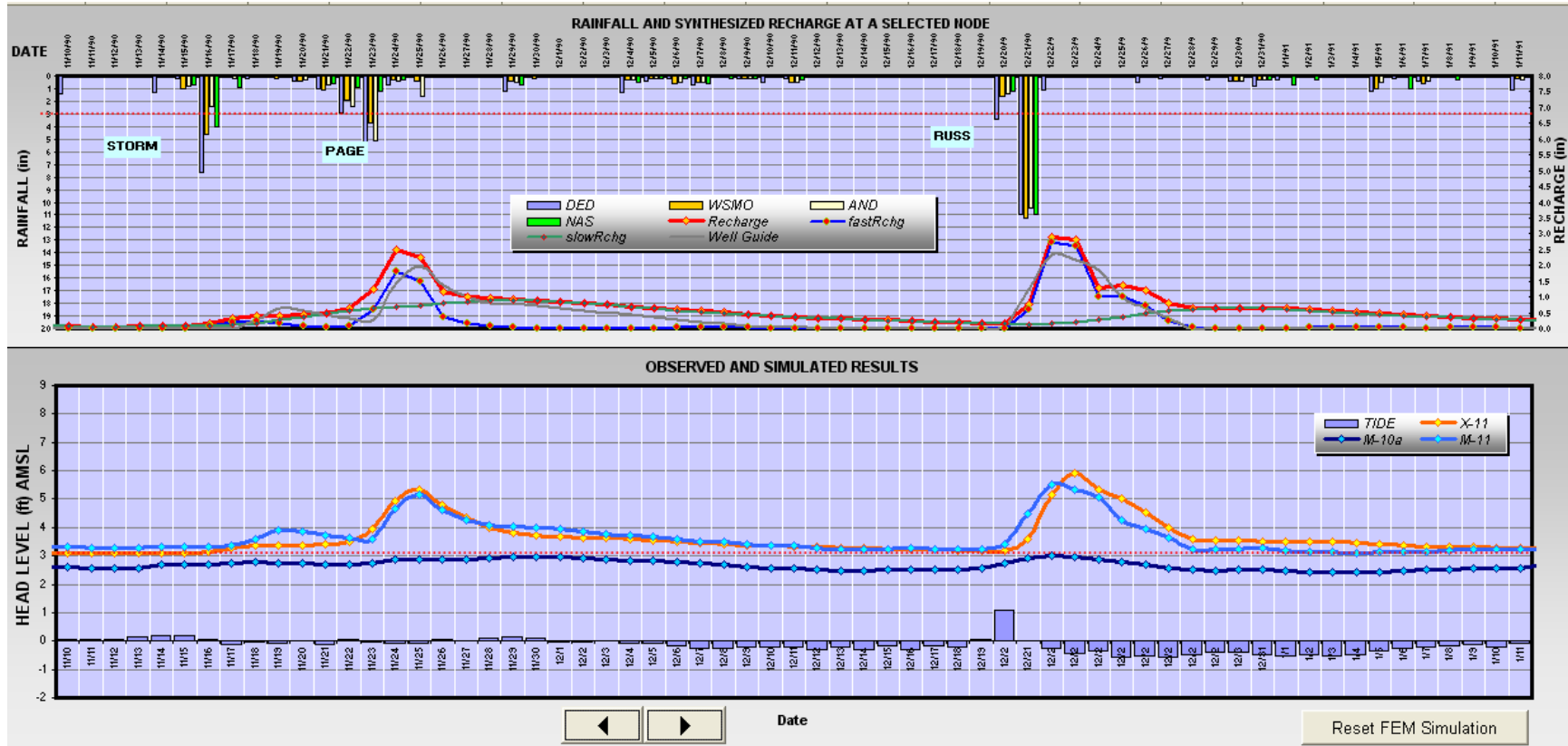


Figure 205. Three storms near the end of 1990.

Figure 206. The Category 3 Typhoon Omar, August 28, 1992.

Final synthesis and simulation results for M-10a: Observation well M-10a data shows GW response to rain pulses that are significantly less than observation well M-11. Calibrating to M-10a required the hydraulic conductivities in the GW model to be increased to at least 9500 m/day and the specific storage to 0.00026 m⁻¹. These parameters allowed the recharge to reach the water table and drain out rapidly, having no time to form significant hydraulic head fluctuations to recharge input as was seen in M-11. Although it takes a storm type rain pulse to get M-10a to respond, being closer to the shore than M-11, the well hydraulic head experiences response tidal influence much readily. Its higher hydraulic conductivity, greater porosity and specific storage, the media allows the water to flow easily that the tides rise and fall greatly affect the hydraulic head position even during no recharge. A figure 207 to 215 displays the results for M-10a

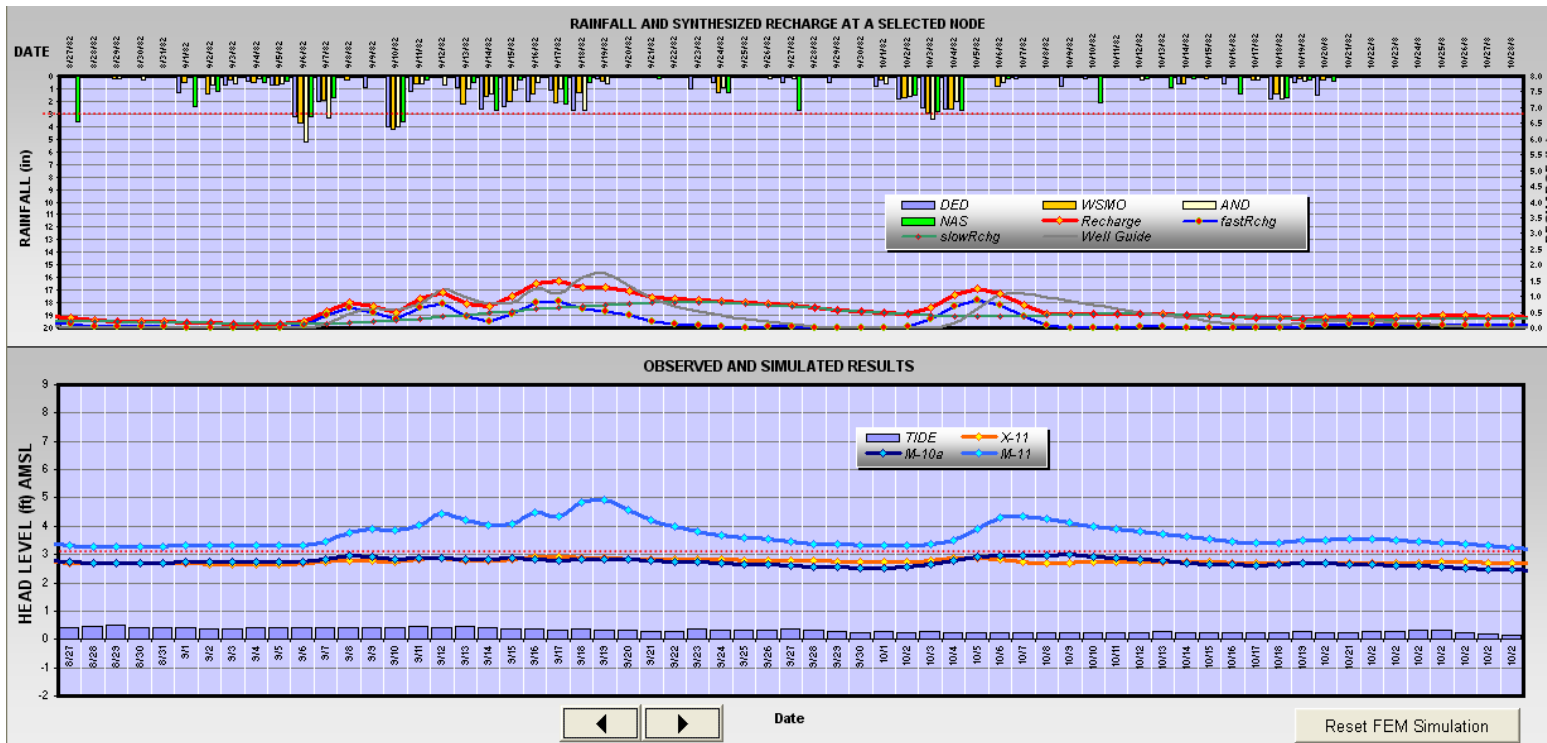


Figure 207. A multi-pulse recharge, September 1982, at M-10a causes the GW at that point respond so small compared to M-11.

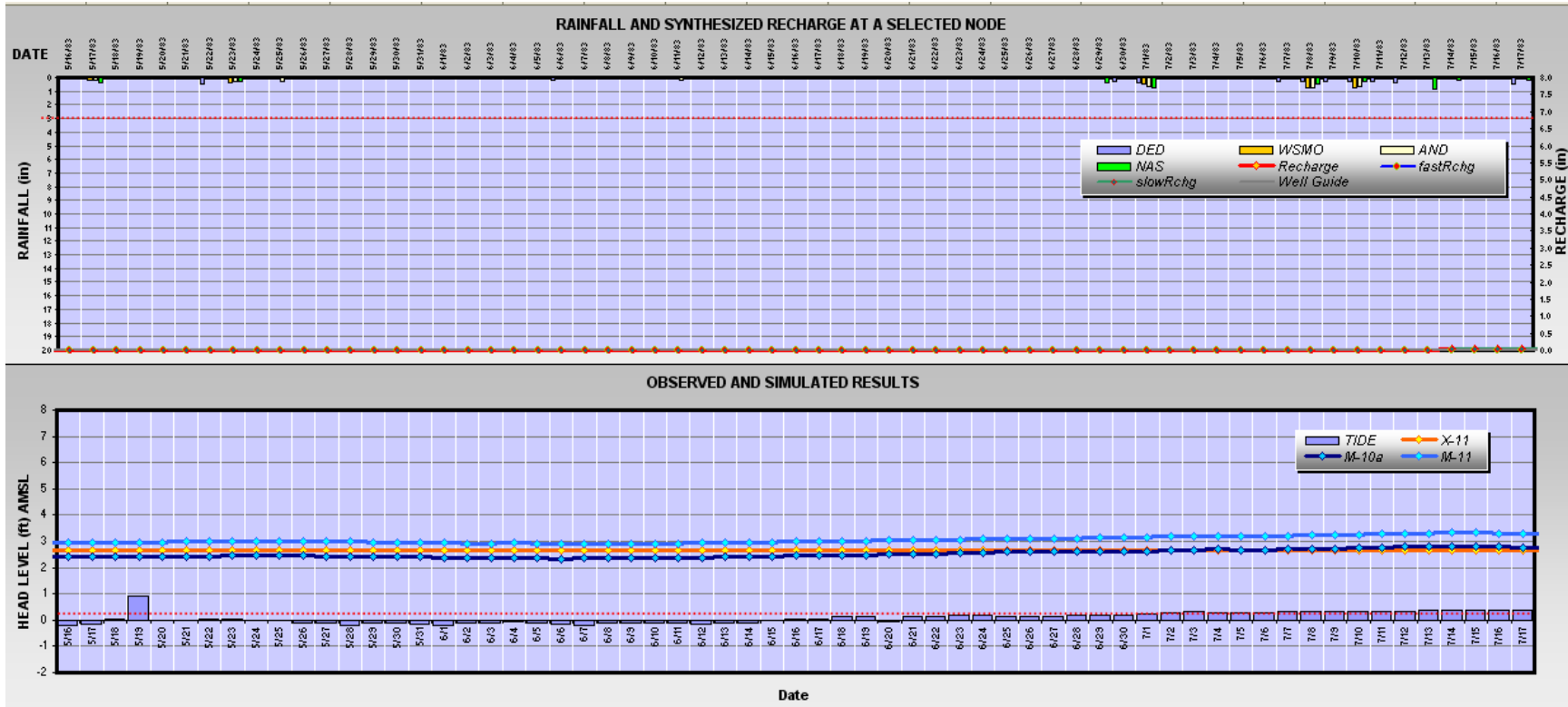


Figure 208. During a post El Niño, having virtually no recharge, shows the tide lifting the hydraulic head at M-10a.

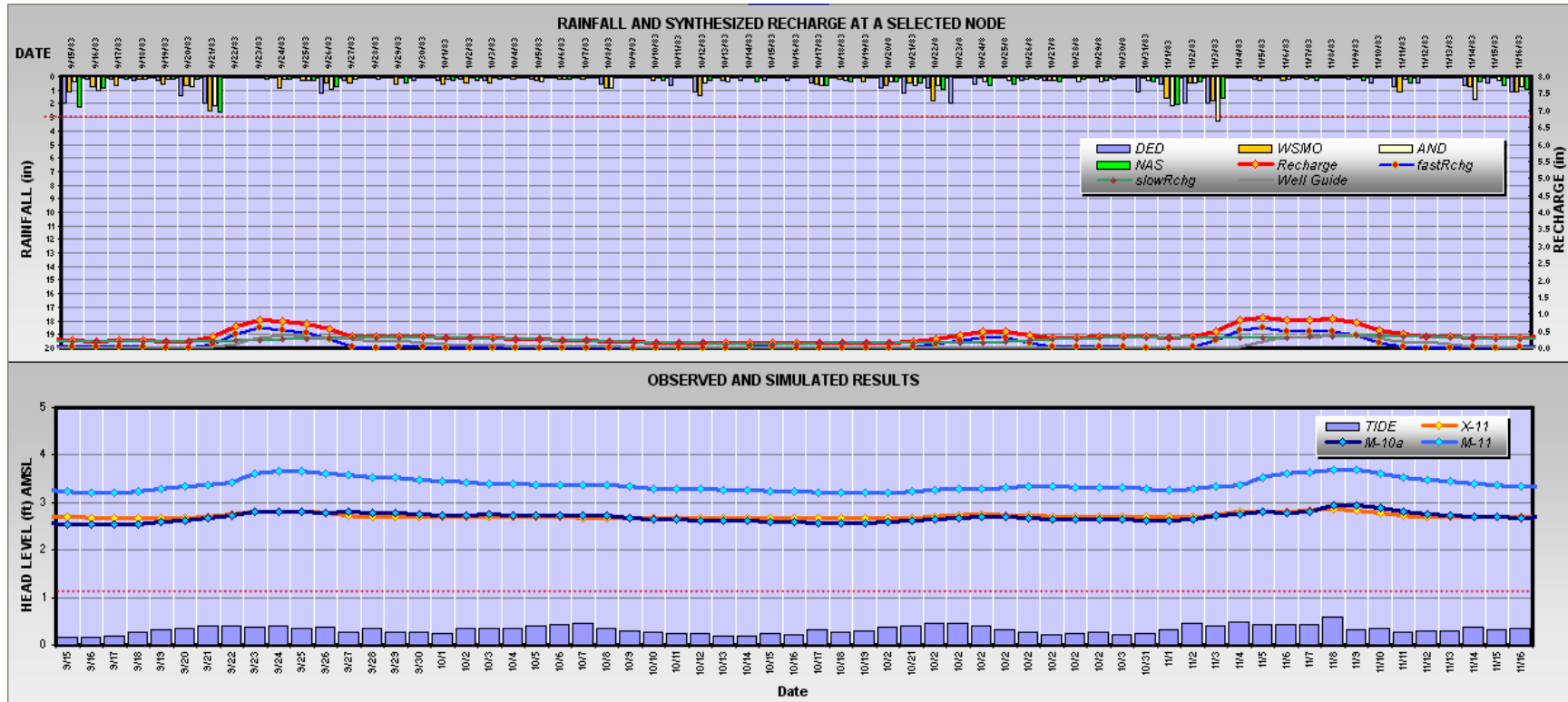


Figure 209. Small synthesized recharge causing GW model simulation to make small responses.

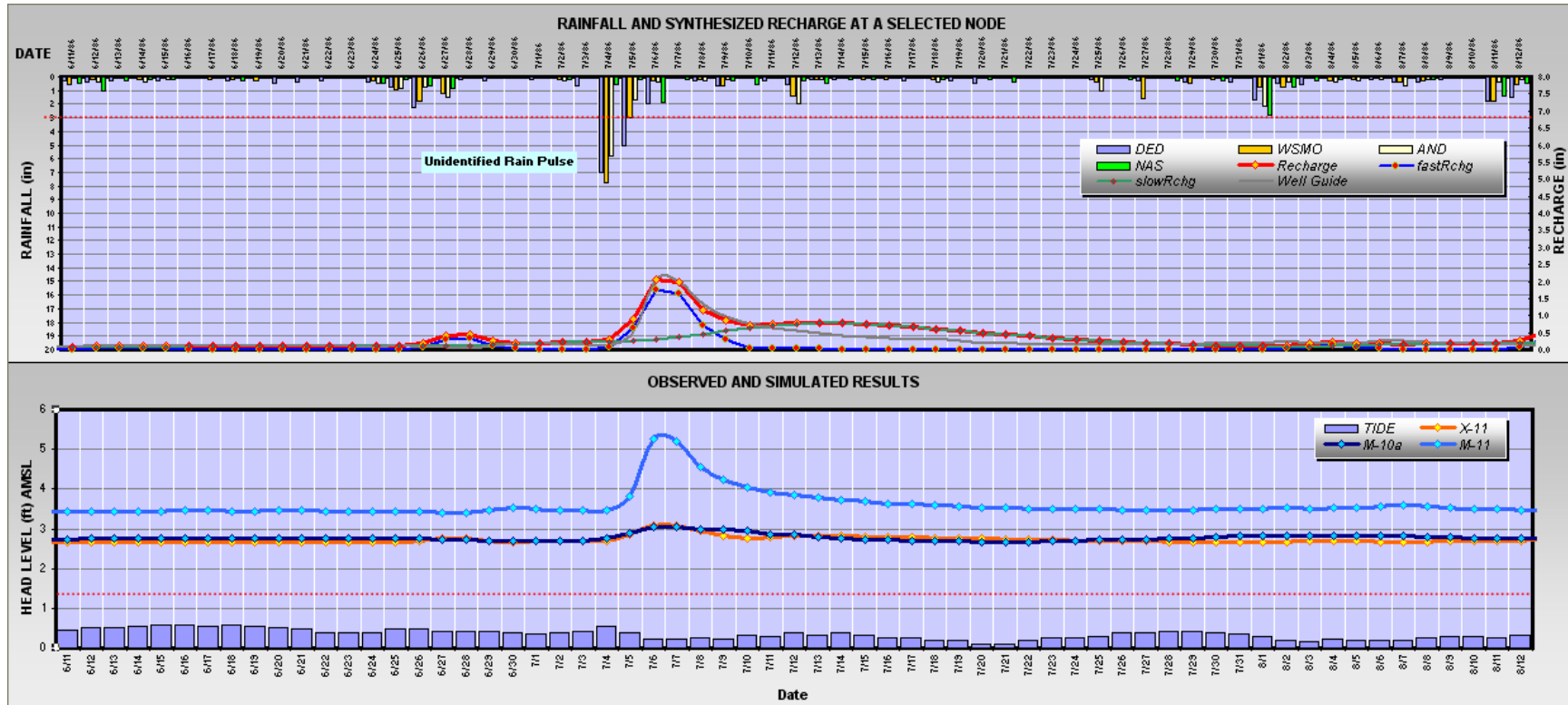


Figure 210. Response for unidentified rain pulse.

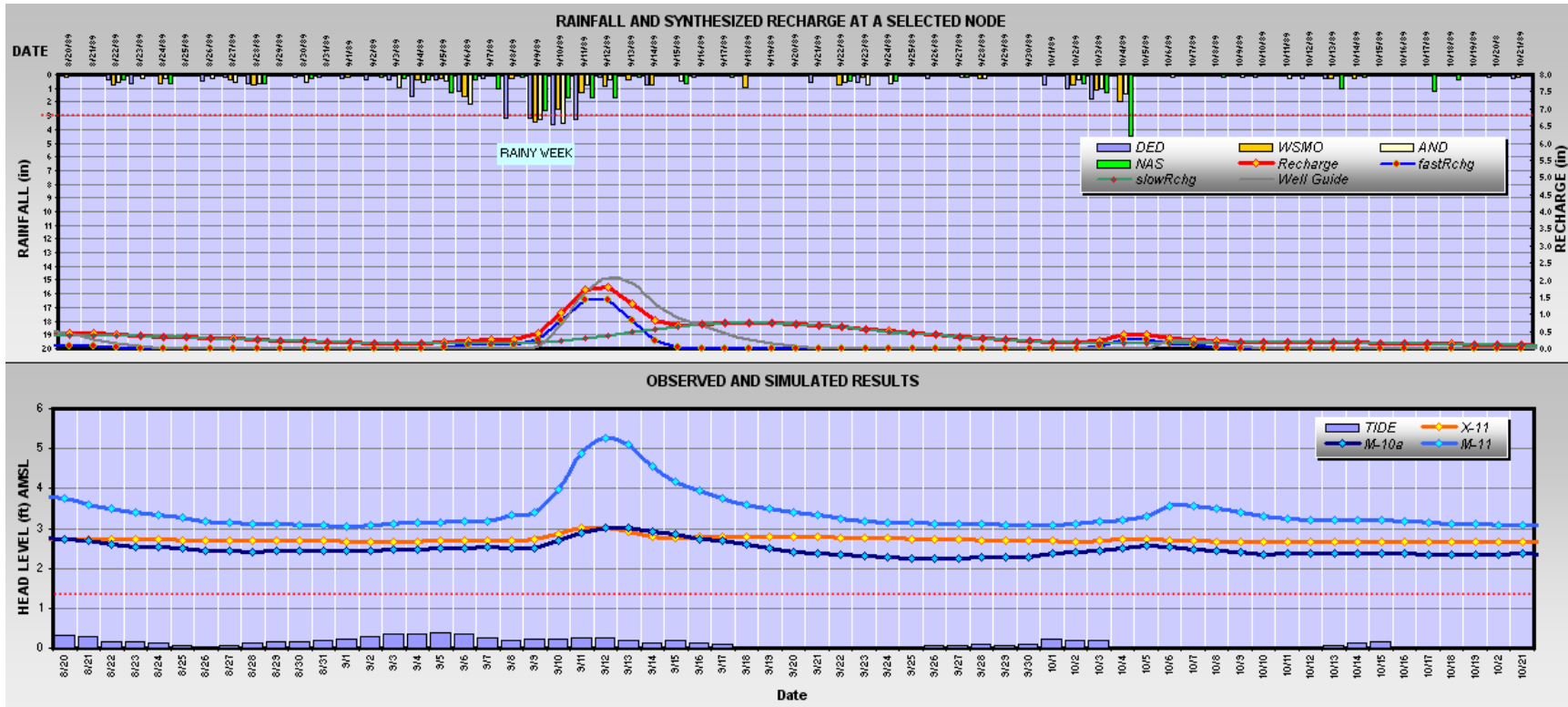


Figure 211. The receding tide draws the water level down.

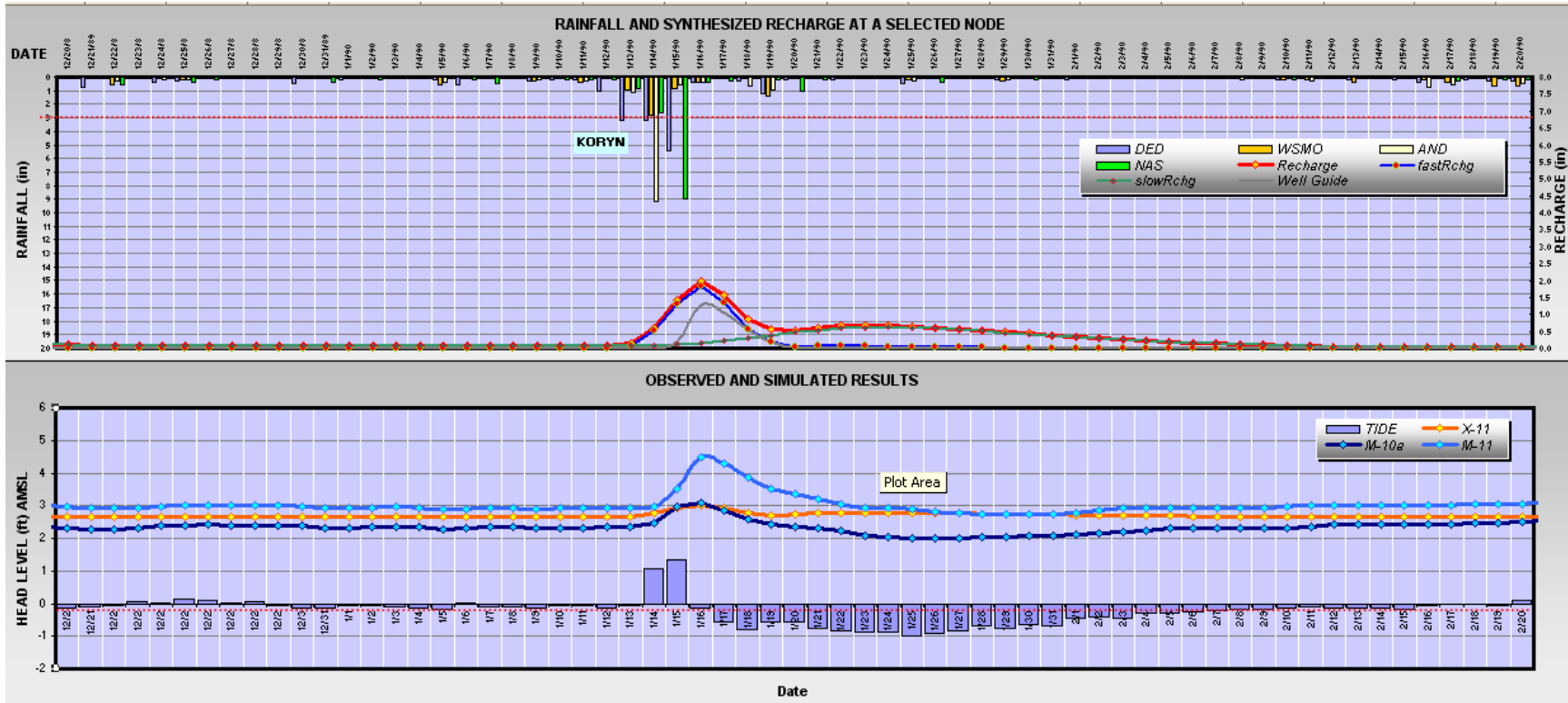


Figure 212. The tide levels going down below mean sea level (bmsl) pulls down the hydraulic head position with it.

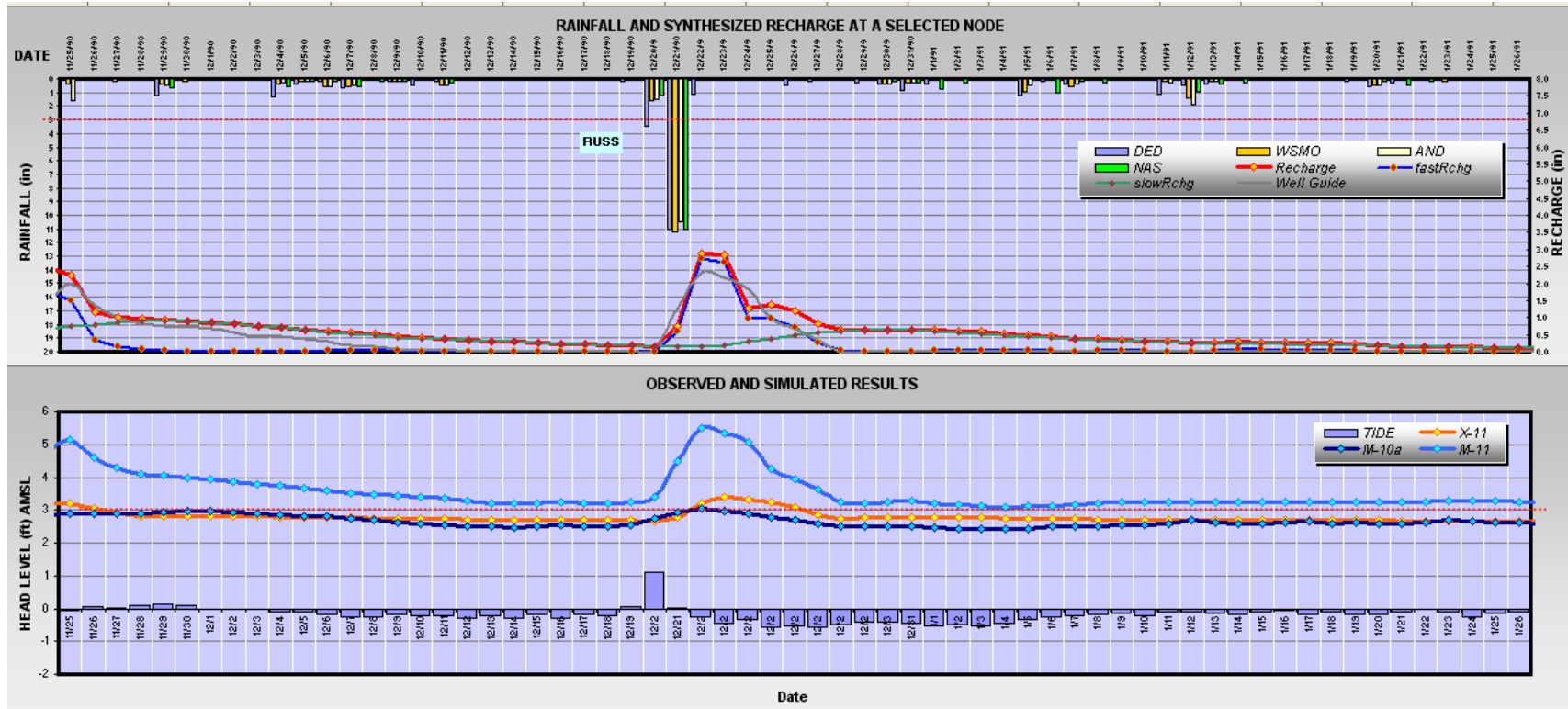


Figure 213. Typhoon Russ, December of 1990.

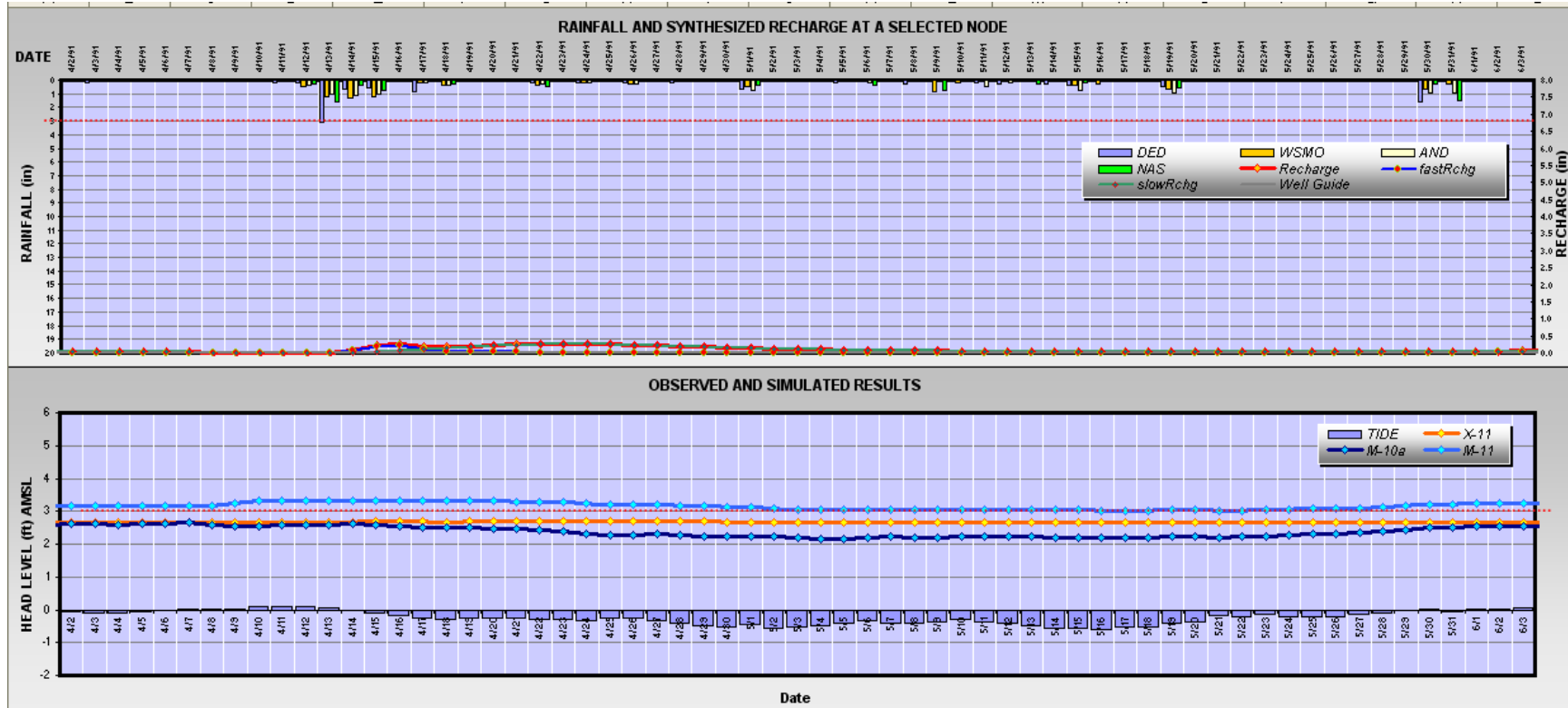


Figure 214. If the tide effect were removed from the observation well data, a good match could be made.

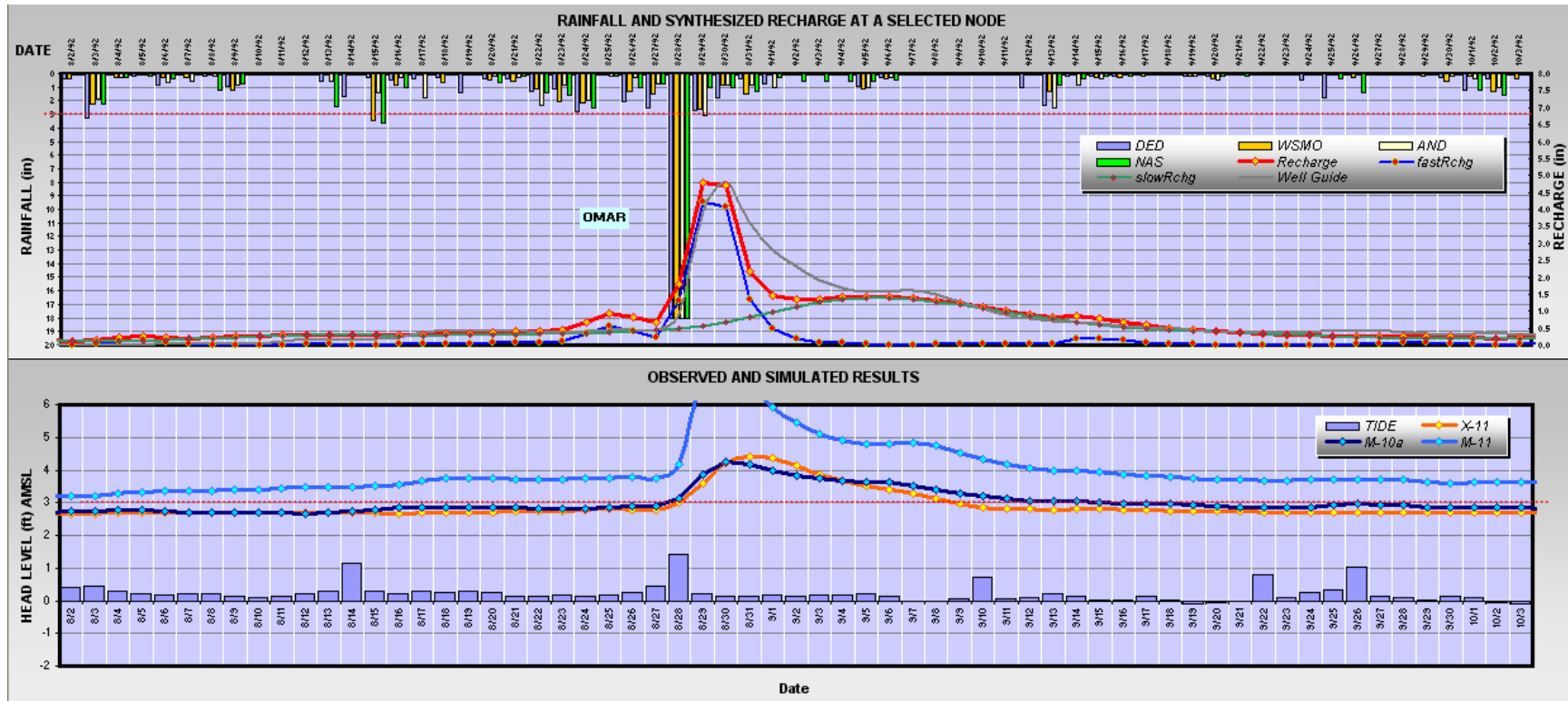


Figure 215. Typhoon Omar’s super sized rain pulse causes M-10a to rise to just about a foot and a half, whereas in M-11, the response raised the water level to 8 feet.

Comparisons with Earlier Models

The AQUA CHARGE results were compared with earlier GW models. In order to do that, the daily values were used to produce monthly average values (Jenson and Jocson, personal communication). The monthly averaged GW simulations and observation wells were superimposed and the graph is shown in Figure 216.

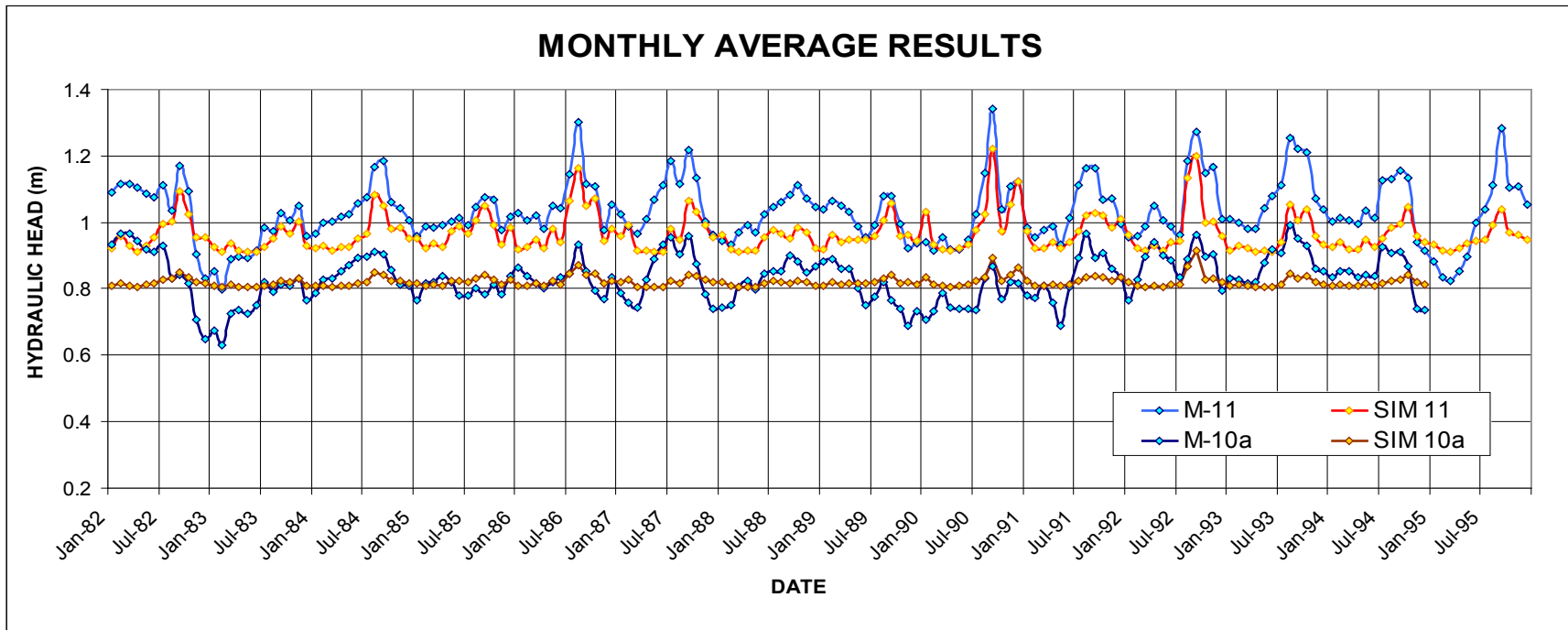


Figure 216. Monthly average simulation chart of observation wells M-10a and M-11, monthly averaged. Simulations for M-11 (SIM 11) and M-10a (SIM 10a).

The monthly averages allowed us to make error analysis comparison with Contractor and Jocson’s models as Contractor did in his last technical report. Contractor used the sum of squared error (SSE) to see the accumulation of squared errors for each model. Then the percent error reduction was calculated. The results are shown in Table 7. The error analysis computations are in Habana, 2008, APPENDIX I.

SSE AND PERCENT ERROR REDUCTION BETWEEN MODELS

Well ID	MODEL'S SSE			PERCENT ERROR REDUCTION		
	SWIG2D	VADOSWIG	AQUA CHARGE	S2D & VS	S2D & AC	VS & AC
M-10a	2.217	0.984	0.723	55.6%	67.4%	26.5%
M-11	4.02	2.237	1.510	44.4%	62.4%	32.5%
TOTAL	6.237	3.221	2.233	48.4%	64.2%	30.7%

Table 7. The Sum Squared Error comparisons to previous models. For the two selected wells and the three models, result in favor of AQUA CHARGE, reducing the percent error to around 30% against VADOSWIG. SWIG2D, VADOSWIG, and AQUA CHARGE are abbreviated S2D, VS, and AC respectively (Contractor et al., 1999).

Discussion

This section discusses the results and comments on the obvious causes of errors in the entire model and its design and covers areas where improvements might be made. It also serves as an explanation of the model’s limitations and how further improvement in the models estimates could be made.

Major Contributors to Error

The obvious inaccuracies mentioned here are identified with the rain and pan evaporation data and tide effects. These errors can be easily noticed in the AQUA CHART and are mentioned in the figures above. The modeling errors can be dramatically reduced and increased accuracy can be achieved if these issues are resolved. Some suggestions are given to reduce prediction errors due to these problems.

Rain and Pan Data: The rainfall data, both temporal and spatial as pulse input and area coverage data to AQUA CHARGE was a major contributor to the errors and inaccuracy found in the modeling results. First, the daily gage reading time was not consistent between stations. The data for one gage station would be read in the morning and dated with that day, but the data would be for the period starting on the previous day’s morning. To correct for this, Dr. Lander suggested that the Dededo gage station rain data should all be adjusted back one day. Another problem with the rain and pan were missing values. The hydrological normal ratio method for accounting for missing data does not necessarily solve accurately the missing rainfall value. Guam experiences the type of tropical weather that is scattered showers regardless of cloud coverage. No averaging method can accurately account for the varied spatial distribution that naturally occurs on this island, but it is better than leaving the data blank for the day. Powerful storms, typhoons, with strong wind gusts, could knock a gage out of operation leaving the meteorologist to make a best estimate from other gage readings near that location. Finally, the

Thiessen Polygon method is not always the best method to handle spatially varied rainfall. Figure 217 shows Thiessen Polygon gage coverage, showing the area of influence Dededo gage covers. The node-sheds with the two selected observation wells covered by the Dededo rain gage are approximately 1.4 miles away for M-11 and 2 miles away for M-10a. In reality, rain can fall at the gage point in Dededo, and none may fall at the observation well areas, or visa versa. Intensities could also vary from point to point but not be revealed in the data or with the Thiessen polygon method. The best way to apply Thiessen Polygons with AQUA CHARGE would be to increase and strategically place the gages near the areas of interest.

An alternative idea is to program AQUA CHARGE to use NEXRAD data for the rainfall. This would reduce the spatial and temporal variation errors, since the grid cell resolution in NEXRAD images can be as small as 1km and updates its images in the internet every six minutes (Lander, personal communication), which the Thiessen polygons for this model cannot accurately account for. The problem with NEXRAD is that no one has collected and archived the bitmap images, except maybe one image at a time for an interesting storm (Lander, personal communication).

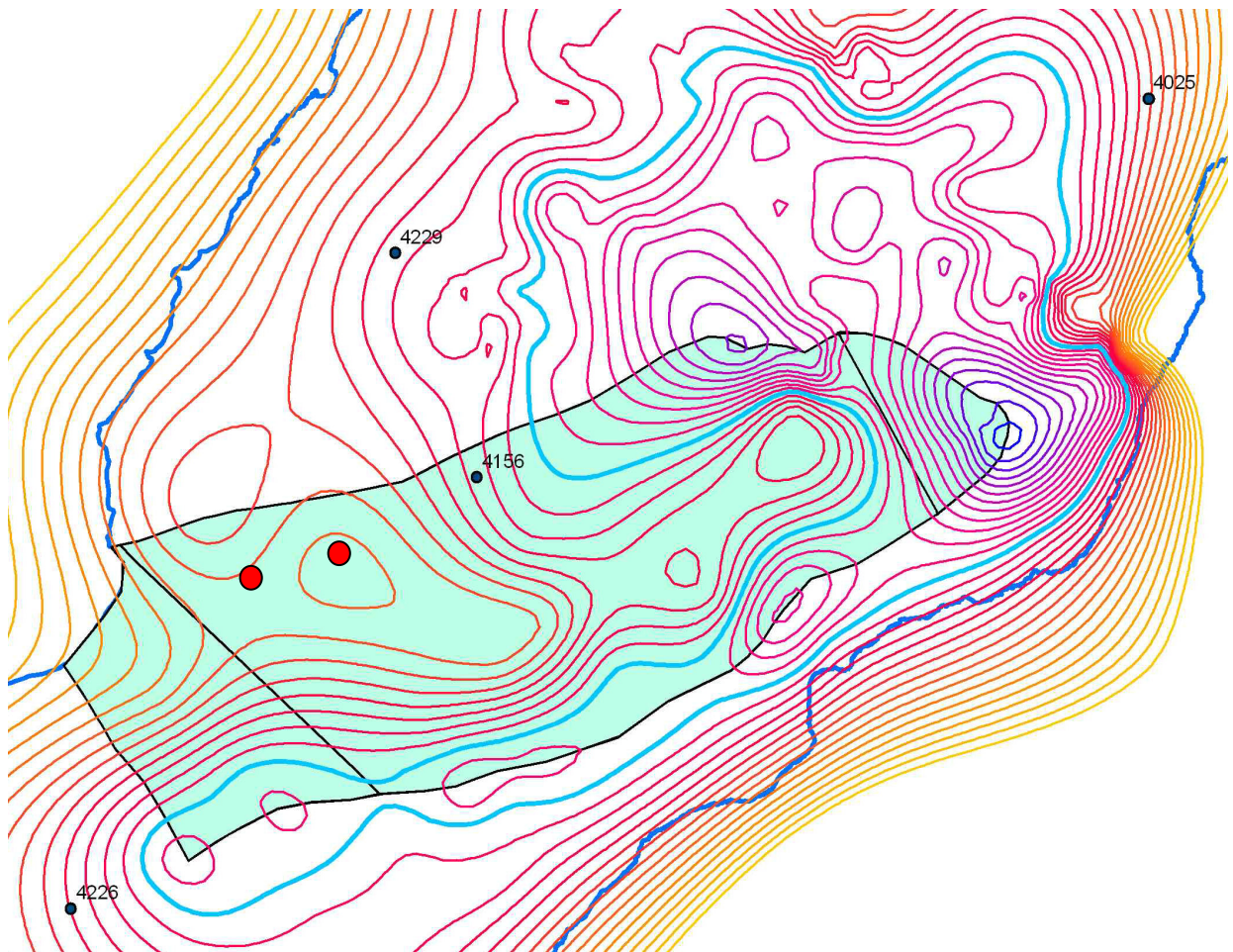


Figure 217. Thiessen polygons, gages, and well location. Thiessen Polygon is not the best method for handling spatially varied rainfall that occurs in Guam. Red points are observation wells and dark blue points are rain gages. Dededo rain gage, gage ID 4156, covers more than 60% of the node-shed model's domain area.

Tide Effect: Tide can influence the fresh water lens position, lifting and lowering the entire freshwater body in the aquifer. The slight lifting increases the error accumulation when computing SSE since tide increase or decrease can raise or drop for an entire month or more. The GW model needs to account for this natural fluctuation in order to refine the match. An alternative is to remove the tide effects lifting and lowering of the lens in the observation well data. This would give the effect of holding the freshwater lens steady as if it were stabilized. With that, we can disregard the need to account for tidal effects in the GW model.

Hydraulic Model Improvement

The hydraulic model designed in AQUA CHARGE is a simple model that could include more details to improve the simulation. A two dimensional model lacks the influential fluid dynamics that occurs in three dimensions (3-D) seen in reality. Now that we have an improved recharge synthesis to provide for the replenishing flux to the GW model, a complex 3-D model should be constructed. The GW modeling could be improved upon by installing all the wells that withdraw from the lens for a defined study domain. With a complete account of the inputs and outputs, we may make accurate determinations of sustainable yield for any place of interest in the domain. A 3-D model can also give us two more insights that the 2-D model lacks: the saltwater interface and possibly the actual recharge also known as specific recharge. Knowing how the salt water interface reacts to recharge, discharge, and pumping would be significant information. One of the most curious questions about the GW is “What is the position of the mixing zone?” These are interesting future research topics and ideas for further improvement and increased usefulness of the model that will be discussed further in the next and final chapter, Recommendations and Conclusion.

RECOMMENDATIONS AND CONCLUSION

The Northern Guam Lens Aquifer (NGLA) water resource, like any natural resource, has its limits and capacity for development. In order to protect it from over development, these measures on limits and capacities must be as accurate as possible for making good management decisions especially when it comes to large scale water supply. Obviously, unlike surface water, groundwater (GW) is invisible which further challenges groundwater utilities management to make optimal decisions. AQUA CHARGE has given us insight into synthesizing recharge in elevated vadose flow systems and GW modeling that has sparked tens of other ideas that will shed light and unearth the mysteries of the NGLA. In this final chapter, we will close with recommendations and conclusions, but not for the purpose of ending. We will close with the intent to inspire the realization of the value of using AQUA CHARGE as a tool for helping agencies make good management choices and achieving optimum development of Guam's main water resource. In recommendations, suggestions and discussions are made for management practice, sustainable yield and optimum development, and advanced GW modeling. Finally, the conclusion will recapitulate and confer the objectives achieved.

Recommendations

Currently, the status of groundwater utility operations is still safe. The NGLA is capable of supplying the Northern Guam population with quality potable water. The questions are of the near future with the expected increase of military and tourist occupants on this island. Will we be able to supply them adequately with the water in the NGLA? Where should we place these new wells to accommodate the increase in demands? Already, the Northwest Field, Andersen Air Force Base military property, is constructing new facilities (Guam PDN, 2008). Just south of the Northwest Field, Naval Computer and Telecommunications Station, Finegayan, is the preferred location where the US Marine training camp and development will occur (JGPO, 2008). Can AQUA CHARGE help agencies make sound decisions and reveal ahead whether these development proposals are going to affect our underground water supply? These are just a few important general questions GWA and GEPA will need to know in order to establish good protective measures in approaching groundwater exploitation.

Management Practice

Groundwater exploitation on Guam, as mentioned earlier, is about to increase in order to supply water to an imminent growth in the island's population. Modeling the aquifer system could be the best way to decide where and how much we can safely pump from the aquifer to meet those demands and feed new areas with quality water without damaging the source.

In the past and maybe still today, GWA managers used simple groundwater principles and rules of thumb to gage against over development. One simple principle of 40 to 1 density difference ratio between the salt water and fresh water was a guide to the depth of the salt water interface. For 1 meter of hydraulic head meant 40 meters bmsl to the salt water interface, a *Ghyben-Herzberg principle*. This was a way to measure the thickness of the lens and monitor for the water budget's balance between input and output. Knowing the thickness of the lens also

meant a practicable place to install a pump in hopes of minimizing the risk of saltwater intrusion. Although we expect the density principles to hold true, the hydraulic head changes did not mean the salt water interface simultaneously moved in concert and in direct response to the fluctuations of the water table (Contractor, 1981). The other limiting guide is simply the average long term pump rates. An overall sustainable yield pump rate was estimated (Mink, 1991) and was not to be exceeded. This sustainable yield value did not take into account that the safe rate for pumping can vary spatially.

Management needs accurate answers fast to respond to the rapid development demands. Many times water managers find modeling inconvenient, complicated, impractical and time consuming, and costly. Modeling can be mistakenly misunderstood and found useful only for academia in making a great research project topic. Just the modeling terminology and the complex mathematics involved can easily leave any listener or reader clueless and intimidated of such a discussion. The complexity can easily cause an agency to look for a simpler and presumably “more practical solution.” Unfortunately, in reality, it is the fact GW modeling is esoteric (Addiscott, 1995) that only people involved in the design and configuration of the models truly understand the mechanism and its usefulness. The translation needs major improvement.

Another discouraging object about modeling the NGLA is its geologic complexity. Most generalization about groundwater flow and hydraulic models comes from gravel or “sandbox” type aquifers making limestone aquifer difficult to accurately model using Darcian equations. The complexity can cause the model to produce inaccurate results making modeling more of a blunt instrument rather than a sharp and useful tool. The AQUA CHARGE conceptual model, employing stream flow synthesis, allowed us to overcome this geologic barrier. The realization that the well responses were stream-like provided an alternative route. The model provides us with the ability to closely examine how a limestone aquifer like Guam’s responds differently and has added much insight into how to manage the resource. Finally, articles such as *Groundwater Models Can Not be Validated* by Konikow and Bredehoeft (1992) and arguments against modelers and their models in terms of *verification*, *validation* and *calibration* give all computer GW models a negative image and its results seem unreliable. Models are not the real world; otherwise it would cease to be a model (Addiscott, 1995). Understand that models are a way of estimating just as the gas gage in a vehicle approximate gasoline level.

The usefulness of modeling becomes more practical as increases in demands on the groundwater system occur. It is true that at the local level, low population density village or small farm size, modeling might be impractical, costly, and unnecessary. In large cities or rapidly growing areas, experts turn to modeling for answers and the model becomes a practical and useful tool (Van Der Heijde et al., 1995). In large scale development, accounting the in-and-out flows for the entire water utility system easily grows into overwhelming proportions. With modern computer technology, modeling has become detailed and sophisticated and its ability to simulate has become more and more reliable. AQUA CHARGE is the most sophisticated, yet user friendly, and detailed vadose flow modeling program ever developed for the NGLA. This model can produce the answers that management needs. With sophisticated fast computer equipment available, those answers can be determined quickly. AQUA CHARGE cycled through 14 years of temporal data over the Yigo-Tumon Trough domain in less than a minute, using a modern laptop.

Sustainable Yield and Optimum Development

It seems that the greatest concern to any GW utility is the question, “What is the sustainable yield?” Van Der Heijde et al. (1995) defines long term sustained yield as “a rate of withdrawal equal to the sum of the changes in recharge and discharge that take place as a result of withdrawals and lowering of water levels by pumping.” They also mention that over a period of time, recharge to a system equals its discharge. In other words, it is the safe withdrawal rate of water from the aquifer without causing any depletion to the lens resulting in salt water intrusion at a particular location for any time. A re-estimation of the sustainable yield with respect to spatial variations and well placement needs to be done for the NGLA. A good GW modeling scenario, employing AQUA CHARGE to provide the synthesized recharge, should be included in determining that value.

In Guam, available budget, politics, and territorial issues challenge optimum development. For example, WERI, in the past, has suggested the optimal placement of underground water pumps are at the parabasal zones. This is where the thickest part of the lens exists, it is the most inland from the shore, and the least vulnerable risk for salt water intrusion since volcanic material lies beneath it. This zone also receives large amounts of allogenic recharge, moving through it like an underground river system in the voids between the volcanic basement and the limestone, maintaining the fresh water thickness in the zone. Still, most pumps are placed beside roads, near power lines, for easy access. It was supposed least costly to build and avoided land owner property issues. Some of these wells are pumping water with detectible salinity and are still in operation. The budget allocation simply seems to out weigh the water quality concern. It would be interesting to show through modeling, optimal placement of wells, simulate operations, and reconfigure the cost and benefits.

Advanced GW Modeling

AQUA CHARGE has now opened new doors for advanced GW modeling. It did that when it was able to produce attenuated and lagged flows of fast and slow recharge synthesis at a daily cycle. It also bypassed the concern of the highly complex limestone bedrock’s triple porosity and changed its focus on time it takes water to get to the water table. With a plausible recharge from rain pulses at a daily time step, we solved the problem of previous GW modeling which was providing a realistic recharge to the hydraulic model. Some ideas are listed and discussed for the future of advanced GW modeling for the NGLA.

In one case, Dr. Leroy Heitz was able to take the AQUA CHARGE data output of the GW modeling for a particular day and using the Darcy Velocity GIS Function, he was able to produce a sample flow direction map for the starting conditions (Figure 218). Using various other GIS functions he was able to produce a map of flow direction and relative magnitudes for the starting conditions (Figure 219). Finally, he sampled the Darcy Function for September 20, 1982, the greatest node point response to recharge for that month. His intent was to gain an understanding of how contaminants introduced at the surface might move through the groundwater system during a stormy period. In Figure 220, as the hydraulic heads vary spatially, depending on the material properties and the node flux as recharge, flow directions change and are different from the initial condition samples. The outcome was a better understanding of which rain gage locations should be compared with well water quality data to determine if Guam’s GW is really under the direct influence of surface water.

YIGO/TUMON AQUIFER

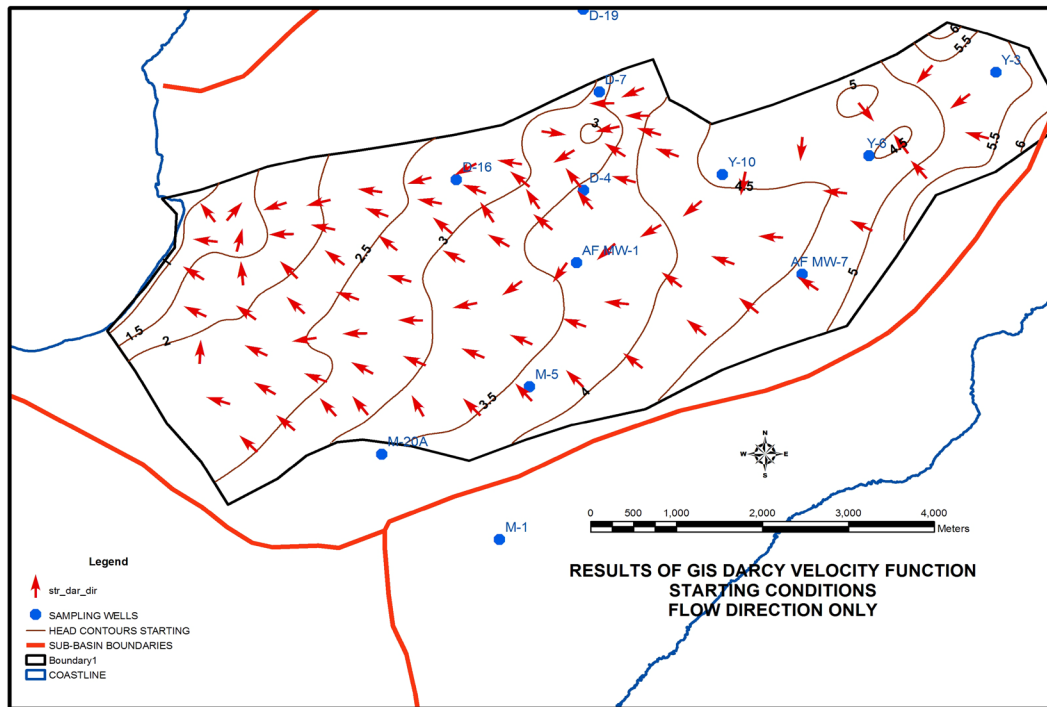


Figure 218. GIS Darcian Function flow direction for initial conditions.

YIGO/TUMON AQUIFER

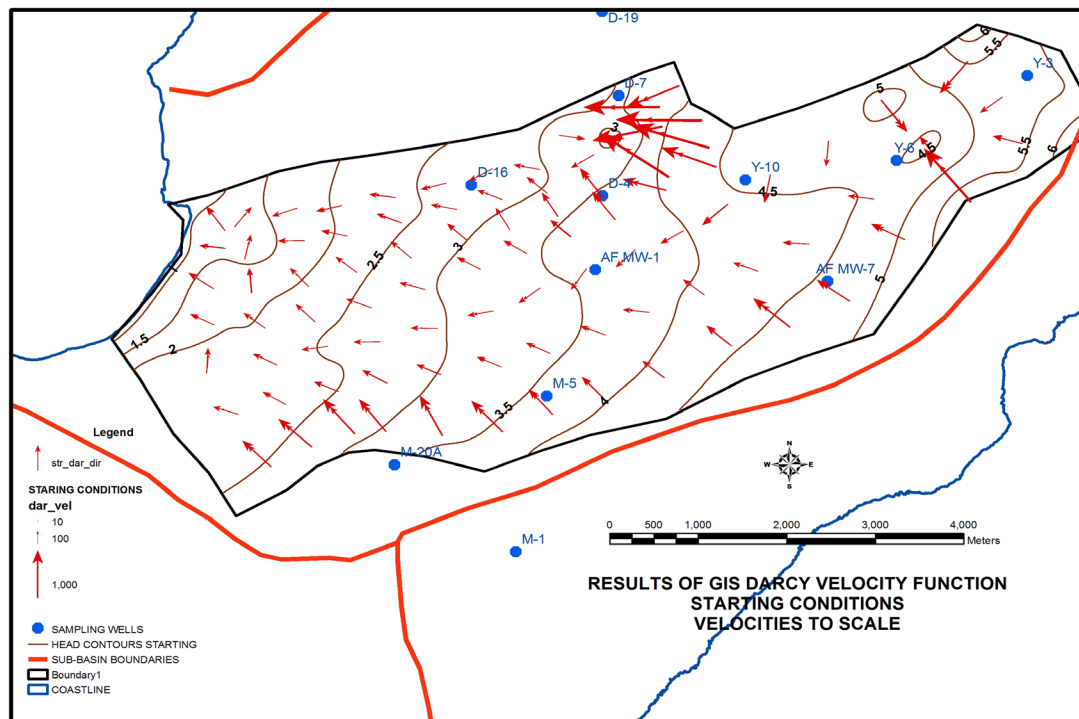


Figure 219. GIS Darcy Velocity Function; starting conditions, flow direction and velocities.

YIGO/TUMON AQUIFER

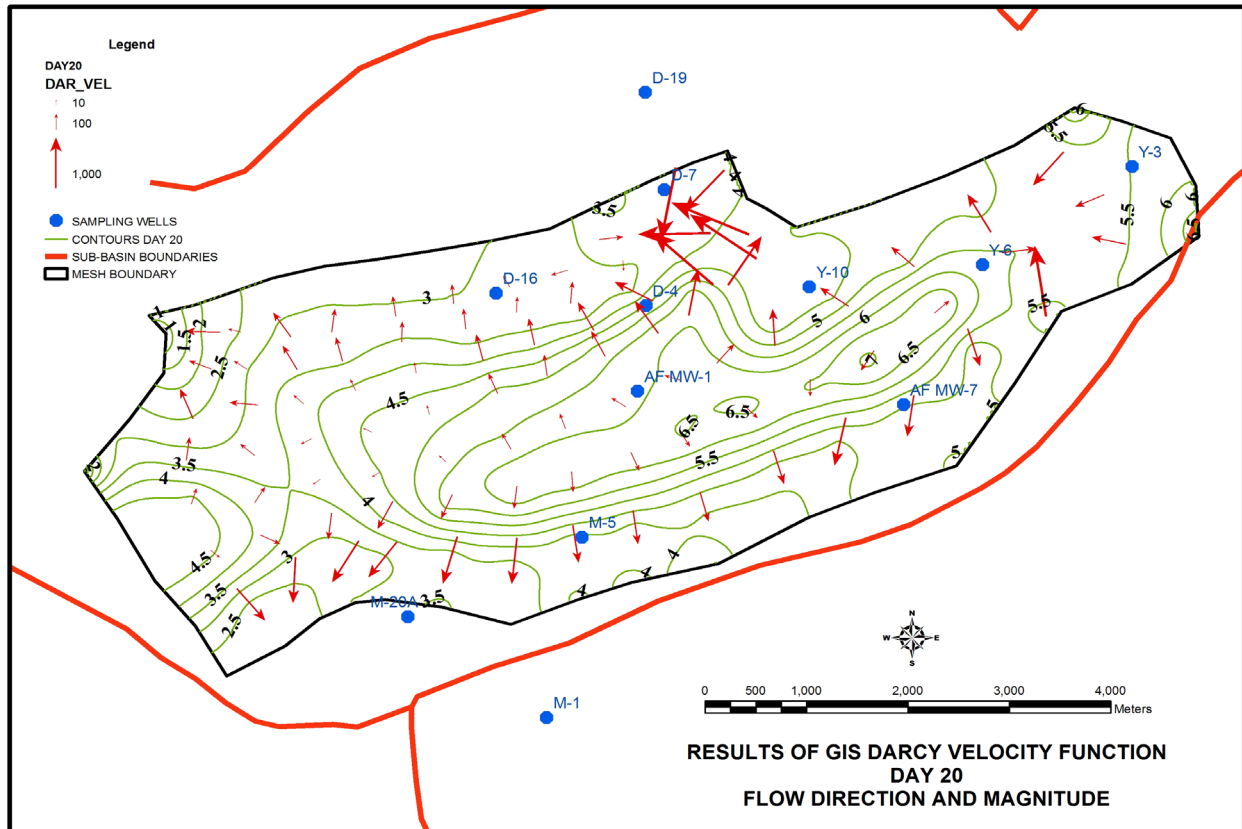


Figure 220. GIS Darcy Velocity Function, flow direction and magnitude. September 20, 1982.

Another advanced GW modeling idea possibility is the development of a full scale, comprehensive hydraulic model for the each existing well and those planned for development in the NGLA. This GW model would be a 3-D mesh with the salt water interface and tide effects included. This GW model would also include at its node points, all of the existing water pump stations in the respective sub-basins. This ground water model could also include the *Theis Equation* for the withdrawal points to simulate the drawdown coning effects. The model could run various pumping and recharge scenarios to determine how different pumping plans could affect the groundwater input and output balance. The model could also show where the vulnerable points are in terms of salt water intrusion. To assist in planning development, prior to installation of the pumps, a well would be installed in the model and simulations would be run. The results will show if the well is optimally placed in the aquifer or if it should be relocated. The development of this complete model will give management a virtual view of the island's water operations in a desktop computer. This will allow agencies to run tests and make adjustments to optimize well placement and meet the supply and demand development balance prior to actual installation. Also, this will minimize costly guess work, guide engineers at Guam's environmental and water development agencies, and maximize our supply's efficiency to meet the island's expectedly increasing population while protecting our valuable water resource.

Conclusion

The conclusion is a summary of the objectives achieved. The objectives from Chapter 1 are reiterated: (a) improve the existing AQUA CHARGE program to simulate the temporal hydrologic processes that influence groundwater recharge, (b) apply 3 sets of soil curves to explore the effects of soil properties on evapotranspiration (ET) and eventual groundwater recharge, (c) use surface water routing techniques to model the effect of vadose zone storage and hydraulics on aquifer recharge, (d) modify AQUA CHARGE to include a 2-D, transient, saturated groundwater flow, finite element model, and (e) make recommendations concerning which modeling parameter values lead to the most realistic recharge estimates.

The AQUA CHARGE program was definitely improved with the inclusion of a modified pulse routing portion as a transfer function and a 2-D transient, saturated flow, finite element method program. This development in the program allowed us to achieve all of the objectives. With the soils layer effect included, increased accuracy in ET determination means better recharge calculation. The accurate measurement of recharge means an accurate measure for sustainable yield. Improved recharge synthesis means more reliable GW modeling. A full scale model of the entire NGLA, with all the wells installed, can give the island the edge for developing plans for optimum groundwater development. The routing for vadose flow synthesis allowed us to examine interesting recharge shapes for various pulses of rain. These recharge synthesis scenarios were named and identified as single pulse recharge, double pulse recharge, multi-pulse recharge, and plateau recharge. By testing various scenarios we were able to control the vadose flow attenuation and lag times to produce a realistic type of recharge. With AQUA CHART connected, we were able to develop a technique called the Well Guide to produce the plausible recharge synthesis.

For part (b) of the objectives, the three sets of soils curve conditions allowed us to examine the influence of the soil layers to ET and recharge. The soil curve adjustment allowed us to examine known models for ET and a linear and curved relationship for recharge. Though the soils were thin, there were differences between the three soil conditions when superimposed, but we found that the differences between models were rather small in a daily cycle. The differences between the models do add up significantly when computing the annual averages. The finite element program lets us control the GW simulation response to the recharge synthesis. It allowed us to connect and calibrate the recharge synthesis through history matching sending the output to AQUA CHART. The program was designed to efficiently explore many parameter settings that led us to the final recommended settings. Using the finite element sub-program, we were able to compute in daily time steps and change the hydraulic conductivity and specific storage for any node. This allowed us to make near matches for two different monitoring well sites with different hydrogeologic parameters. This feat has rendered AQUA CHARGE Deluxe to the forefront of the hydrologic and hydraulic modeling frontier for the NGLA.

REFERENCES

- Ayers, J.F., 1981. Estimate of Recharge to the Freshwater Lens of Northern Guam. Technical Report No. 21, Water Resource Research Center, University of Guam (UOG), Mangilao, Guam.
- Addiscott, T.M., 1992. Simulation Modelling and Soil Behaviour. *Geoderma*, 60 (1993) 15-40, Elsevier Science Publishers B.V., Amsterdam.
- Environmental Systems Research Institute (ESRI), 2007. ArcGIS Desktop Help: Understanding Euclidean Distance Analysis. Web Help, ESRI, <http://webhelp.esri.com/arcgisdesktop/9.2/index.cfm?TopicName=Understanding_Euclidean_distance_analysis>.
- Contractor, D.N., 1980. A Review of Techniques for Studying Freshwater/Seawater Relationships in Coastal and Island Groundwater Flow Systems. Technical Report No. 11, Water Resources Research Center, UOG, Mangilao, Guam.
- Contractor, D.N., 1981, A Two-Dimensional, Finite-Element Model of Salt Water Intrusion in Groundwater Systems. Technical Report No. 26, Water and Energy Research Institute of the Western Pacific, UOG, Mangilao, Guam.
- Contractor, D.N., Ayers, J.F., Winter, S.J., 1981. Numerical Modeling of Salt-Water Intrusion in the Northern Guam Lens. Technical Report No.27, Water and Energy Research Institute of the Western Pacific, UOG, Mangilao, Guam.
- Contractor, D.N., Jenson, J.W., 1999. Simulated Effect of Vadose Infiltration on Water Levels in the Northern Guam Lens Aquifer. Technical Report No. 90, Water and Environmental Research Institute (WERI) of the Western Pacific, UOG, Mangilao, Guam.
- Fetter, C.W., 2001. Applied Hydrogeology. Prentice-Hall, Inc., Upper Saddle River, New Jersey.
- Joint Guam Program Office (JGPO), 2008. Overview of the Draft Guam Joint Military Master Plan. PDF file, JGPO, Guam. <[http://www.ghs.guam.gov/Portals/111/Draft_MP_Overview_FINAL%20\(Color\).pdf](http://www.ghs.guam.gov/Portals/111/Draft_MP_Overview_FINAL%20(Color).pdf)>.
- Guam Pacific Daily News (PDN), Jan 2007. Notice of Issuance Record of Decision Final Environmental Impact Statement for Establishment and Operation of an Intelligence, Surveillance, Reconnaissance, and Strike Capability at Andersen Air Force Base, Guam. Guam PDN, Hagatna, Guam.
- Guam PDN, 2008. Guam Joint Military Master Plan Update. PDF file, Guam PDN, <<http://www.guampdn.com/assets/pdf/M087625105.PDF>>.

Vadose Flow Synthesis for the Northern Guam Lens Aquifer
References

- Guam PDN, Jan 2009. Visa Rules Come Out Today: China, Russia Could Gain Waivers Within 18 Months. Guam PDN,
<<http://www.guampdn.com/article/20090114/NEWS01/901140317/1002/rss>>.
- Guam PDN, Feb 2009. U.S. to Fund \$1 Billion Road Project. Guam PDN,
<<http://www.guampdn.com/article/20090223/NEWS01/902230303/1002/rss>>.
- Guam Visitor's Bureau (GVB), 2006, Guam Visitors Arrivals 2002-2006, Guam PDN,
<http://www.guampdn.com/guampublishing/special-sections/gvb_2006/14-arrivals.htm>.
- Habana, N. C., 2008. Vadose Flow Synthesis for the Northern Guam Lens Aquifer. Masters Thesis, Water and Environmental Research Institute of the Western Pacific, UOG, Mangilao, Guam.
- Istok, J., 1989. Groundwater modeling by the finite element method. American Geophysical Union, Washington, D.C.
- Jenson, J.W., 2006. Ground Water Research, the Groundwater Modeling Project. WERI, UOG,
<<http://www.weriguam.org/projects/ground.htm>>.
- Jocson, J.M.U., 1998. Hydrologic Model for the Yigo-Tumon and Finegayan Sub Basins of the Northern Guam Lens Aquifer. Masters Thesis, Water and Energy Research Institute of the Western Pacific, UOG, Mangilao, Guam.
- Jocson, J.M.U., Jenson, J.W., Contractor, D.N., 1999. Numerical Modeling and Field Investigation of Infiltration, Recharge, and Discharge in the Northern Guam Lens Aquifer. Technical Report No. 88, WERI of the Western Pacific, UOG, Mangilao, Guam.
- Jocson, J.M.U., Jenson, J.W., Contractor, D.N., 2002. Recharge and Aquifer Response: Northern Guam Lens Aquifer, Guam, Mariana Islands. *Journal of Hydrology* 260, 231-254.
- Joint Typhoon Warning Center (JTWC), 1982 – 1995. Annual Tropical Cyclone Report.
<http://metocphinmci.navy.mil/jtwc/atcr/atcr_archive.html>.
- Lander, M. A., 2006-2007. Personal Communications, Water and Environmental Research Institute of the Western Pacific, University of Guam.
- Linsley, R.K., Kohler, M.A., Paulhus, J.L.H., 1982. *Hydrology for Engineers*, Third Edition. McGraw-Hill Book, Inc. printed in the United States of America.
- Mink, J.F., 1976. Groundwater Resources on Guam: Occurrence and Development. Technical Report No. 1, Water and Energy Research Institute of the Western Pacific, UOG, Mangilao, Guam.

- Mink, J.F., 1991. Groundwater in Northern Guam: Sustainable Yield and Groundwater Development. Barrett Consulting Group for Public Utility Agency of Guam, Guam.
- Moore, G.W., Sullivan, N., 1997. Speleology: Caves and the Cave Environment. Cave Books, St. Louis, Missouri.
- Mueller-Dombois, D., Fosberg, F.R., 1998. Vegetation of the Tropical Pacific Islands. Springer-Verlag New York, Inc., New York, New York.
- U.S. Department of Agriculture (USDA), Natural Resource Conservation Service (NRCS; formerly Soil Conservation Service, SCS), 1988. Soil Survey of the Territory of Guam. National Cooperative Soil Survey, USDA, NRCS (SCS), UOG, and Department of Commerce, Guam.
- Taborosi, D., Jenson, J.W., Mylroie, J.E., 2004. Karst Features of Guam Mariana Islands. Technical Report No. 104, WERI of the Western Pacific, UOG, Mangilao, Guam.
- Tracey, J.I., Schlanger, S.O., Stark, J.T., Doan, D.B., May, H.G., 1964. General Geology of Guam, Mariana Islands. United States Government Printing Office, Washington.
- U.S. Army Corps of Engineers (USACE), North Pacific Division (NPD), 1987. User Manual, Microcomputer Version of the Streamflow Synthesis and Reservoir Regulation (SSARR) Model (draft as of 1987). USACE, NPD, Portland, Oregon.
- Van Der Heijde, P., Bachmat, Y., Bredehoeft, J., Andrews, B., Holtz, D., Sebastian, S., 1995. Groundwater Management: the Use of Numerical Models. American Geophysical Union, Washington, D.C.
- Vann, D., 1999. Updated GIS Shapefile of the Basement Volcanic Contour Map of the Northern Guam. Unpublished Masters Thesis, Water and Environmental Research Institute of the Western Pacific, UOG, Mangilao, Guam.
- Ward, A.D., Trimble, S.W., 2004. Environmental Hydrology, Second Edition. CRC Press LLC, Lewis Publishers, Boca Raton, London, New York, Washington, D.C.
- Worthington, S.R.H., 2003. Speleogenesis and Evolution of Karst Aquifers. The Virtual Scientific Journal, Ontario, Canada.

APPENDIX

RECHARGE SYNTHESIS MODEL VB CODES

Recharge Synthesis Codes: Here are the simplified program core codes for both stages of the recharge synthesis model. The code variable connections to the GUI controls have been removed and the notes in green give an explanation for most of the lines.

Stage 1: Zone recharge and area weighted average recharge computation

```

Do      'start the do loop

===== Spatial Data: gets unique zone polygon attributes from the sorted spatial data list. =====

elm = 'shed number, elm is element in the early stages of design, gw model SWIG2D required recharge to elements
stn = 'rain gage station
pstn = 'pan gage station
soid = 'soil id
zar = 'zone area
ear = 'element area or node shed area

===== Initial soil moisture =====

smy = 'initial soil moisture, a GUI text box entry,
dSM(0, elm) = smiy      'set daily soil moisture array at day zero, day before day 1, to initial soil moisture

===== Set month counters =====

monthc = 0      'month count set to zero
thismon = 0    'this month counter set to zero

===== SM Equation Algorithm daily time step for a zone =====

For J = iDys To nDys      'for loop from day 1 to nth day, set with a calendar tool before this Do loop

  If J = iDys Then      'first day If condition
    smy = smiy          'set initial soil moisture, default 0.2 inches
  Else
    smy = SMI           'soil moisture of yesterday, previous day's soil moisture
  End If

  GWR = 0              'ground water recharge variable set to zero
  et = 0               'evapotranspiration set to zero

  smt = smy + RAIN(J, stn)      'soil moisture today, starting soil moisture, is smy + rain(day, gage station)

  If smt > FC(soi) Then      'if soil moisture today > field capacity (soil id), gwr is smt- fc
    GWR = smt - FC(soi)     'a case of super saturated soil, excess goes to recharge, runoff excluded
    smt = FC(soi)          'set smt = fc, setting remaining soil saturation to field capacity
  Else
    'condition when smt <= fc
    Call INTERP1(6, RSoil(), smy, GWRP, soi)      'a public subroutine in a module, solves percent to recharge from charts
                                                    (see Modules: INTERP1)
    GWR = RAIN(J, stn) * (GWRP / 100)      'GWR is rain times decimal % of rain to go to recharge based on smy
    smt = smt - GWR          'this is a recharge reduced initial soil moisture
  End If

  Call INTERP1(6, ESoil(), smt, ETP, soi)      'now to get the ET%, it calls the interpolator, this depends on todays sm
  et = PAN(J, pstn) * (ETP / 100)      'et is pan evaporation(day, station) times the ET decimal percent
  If et >= smt Then      'a case when et is more than the recharge reduced soil moisture
    et = smt            'et is set equal to the remaining available soil moisture that can be evapotranspired
  End If

  SMI = smt - et      'the soil moisture for the end of the day is the recharge reduced soil moisture minus et

  DelSMI = SMI - smy      'change in soil moisture from the previous day

===== Daily area weighted averaging for elements or node-shed =====

dGWR(J, elm) = dGWR(J, elm) + GWR * zar / ear      'daily ground water recharge (day, element or node-shed) AWA recharge
dET(J, elm) = dET(J, elm) + et * zar / ear      'daily AWA et
dSM(J, elm) = dSM(J, elm) + SMI * zar / ear      'daily AWA soil moisture

```

Vadose Flow Synthesis for the Northern Guam Lens Aquifer
Appendix: Recharge Synthesis Model VB Codes

Stage 1 continued...

===== Monthly sums, was generated for SWIG2D in the past, preparation for monthly weighted averaging =====

```
If thismon = Month(dDATE(J)) Then
    monDATE(monthc) = dDATE(J)
    monRAIN(monthc) = RAIN(J, stn) + monRAIN(monthc)
    monPAN(monthc) = PAN(J, pstn) + monPAN(monthc)
    monET(monthc) = et + monET(monthc)
    monGWR(monthc) = monGWR(monthc) + GWR
    monDelSMI(monthc) = DelSMI + monDelSMI(monthc)
Else
    monthc = monthc + 1      'initializing a new month
    thismon = Month(dDATE(J))
    monDATE(monthc) = dDATE(J)
    monRAIN(monthc) = (RAIN(J, stn))
    monPAN(monthc) = (PAN(J, pstn))
    monET(monthc) = et
    monGWR(monthc) = GWR
    monDelSMI(monthc) = DelSMI
End If
```

Next J 'daily next for loop

monthc = 0 'resets month count to zero

===== Monthly area weighted averages as monthly recharge for VADOSWIG =====

For Mo = 1 To nMnths 'from month 1 to the nth month, nMnths was obtained before this Do loop with a calendar tool

```
monRAIN(Mo) = (monRAIN(Mo)) * zar / ear
monPAN(Mo) = (monPAN(Mo)) * zar / ear
monET(Mo) = (monET(Mo)) * zar / ear
monGWR(Mo) = (monGWR(Mo)) * zar / ear
monDelSMI(Mo) = (monDelSMI(Mo)) * zar / ear
elmAr(elm) = ear 'element area array (element) prepared for use in another subroutine
If El = (elm - 1) Then
    monEIRAIN(Mo, elm) = monRAIN(Mo)
    monEIPAN(Mo, elm) = monPAN(Mo)
    monEIET(Mo, elm) = monET(Mo)
    monER(Mo, elm) = monGWR(Mo)
    monEIGWR(Mo, elm) = monER(Mo, elm)
    monEIDelSMI(Mo, elm) = monDelSMI(Mo)
Else
    monEIRAIN(Mo, elm) = monRAIN(Mo) + monEIRAIN(Mo, elm)
    monEIPAN(Mo, elm) = monPAN(Mo) + monEIPAN(Mo, elm)
    monEIET(Mo, elm) = monET(Mo) + monEIET(Mo, elm)
    monER(Mo, elm) = monGWR(Mo) + monER(Mo, elm)
    monEIGWR(Mo, elm) = monER(Mo, elm)
    monEIDelSMI(Mo, elm) = monDelSMI(Mo) + monEIDelSMI(Mo, elm)
End If
```

End If
Next Mo

===== Counters for zones and elements or node-sheds =====

```
If El < elm Then El = elm 'flip flop element or node-shed counter
    czon = czon + 1 'zone count incrementer
If czon < nZones Then Recordset.MoveNext 'if zone count czon < nth zone then move to the next zone recordset row
```

Loop Until czon = nZones 'Do loop until condition

Stage 2: Modified pulse routing subroutine (based on SSARR, 1987)

BedrockCap = 'bedrock capacity, text box entry

```
===== Fast and Slow Splitter =====

For i = iElmnts To nElmnts      'from node-shed 1 to nth node-shed (integer)
  For J = iDys To nDys          'from day 1 to nth day (integer)

    If J = 1 Then
      yGWR = 0                  'initial ground water recharge for day 1 (single precision)
    Else
      yGWR = tGWR              'yGWR set from end of day's recharge
      If yGWR < 0 Then yGWR = 0 'sets negative numbers to zero
    End If

    Call INTERP2(10, PctFast(), yGWR, pctfst, BedrockCap) 'splitter curve interpolator, returns % to fast

    fstRchg(J, i) = dGWR(J, i) * pctfst / 100           'fast recharge split, daily ground water recharge times % to fast (double)
    slwRchg(J, i) = dGWR(J, i) - fstRchg(J, i)         'slow recharge split, dgwr minus fast recharge (double)

    tGWR = yGWR + dGWR(J, i) - fstRchg(J, i) - slwRchg(J - 1, i) 'end of day recharge (single)

  Next J
Next i

===== Routing master algorithm =====

endFast(0) = fiv      'end fast array zero set equal to fast initial value (single)
endSlow(0) = siv     'end slow array zero set equal to slow initial value (single)

For i = 1 To fnps    'fnps is fast number of phases (integer)
  fPH(i) = endFast(0) 'fast phase array set equal to fast initial value (single)
Next i

For i = 1 To snps    'snps is slow number of phases (integer)
  sPH(i) = endSlow(0) 'slow phase array set equal to slow initial value (single)
Next i

For i = iElmnts To nElmnts 'first element to nth element (integer)
  For J = iDys To nDys     'first day to nth day

    Call ROUTE(fnps, fPH(), fstRchg(J, i), xhr, fts) 'module fast router subroutine
                                                (see Modules: modified pulse router subroutine)
    endFast(J) = fPH(fnps) 'endfast array set equal to fast phase array of nth fast number of phases
    fstRtdRchg(J, i) = (endFast(J - 1) + endFast(J)) / 2 'fast routed recharge is average of today and previous day end fast

    Call ROUTE(snps, sPH(), slwRchg(J, i), xhr, sts) 'same router as fast to solve for slow

    endSlow(J) = sPH(snps) 'endslow array set equal to fast phase array of nth slow number of phases
    slwRtdRchg(J, i) = (endSlow(J - 1) + endSlow(J)) / 2 'slow routed recharge is average of today and previous day
    rtdGWR(J, i) = fstRtdRchg(J, i) + slwRtdRchg(J, i) 'sum of slow and fast routed recharge
  Next J
Next i
```

Vadose Flow Synthesis for the Northern Guam Lens Aquifer
Appendix: Recharge Synthesis Model VB Codes

Modules: This is the call sub functions in the master subroutines

Router slave function

```
Public Sub ROUTE(nps, PH(), fli, xhr, ts) 'nps is number of phases, PH() phase array variant, fli is average flow input, xhr time in
                                         hours from a text box entry set to 24 hours, ts is time in storage (single)

    N = 1 'set N to 1 for the loop in 12
    If (nps <= 0) Then GoTo 30 'no solution for nps <= 0, exits sub routine and returns to router master
    If (ts <= 0) Then GoTo 7 'condition for ts <= 0, jumps to 7

    XH2R = xhr / 2 'half of xhr, in this project, xhr = 24, so XH2R = 12

    If XH2R - ts < 0 Then 'if ts is greater than XH2R, the difference resulting in a negative number, go to 10
        GoTo 10 'goes to 10 to set TSR, time storage ratio, keeps N = 1
    Else: GoTo 2
    End If

    7  TSR = 0.5 'sets TSR to 0.5
       N = 6 'sets N to 6
       GoTo 12 'goes to 12 with N = 6 and TSR = 0.5

    2  N = (XH2R / ts) + 1
       If (N > 48) Then GoTo 7
       XH2R = XH2R / N

    10 TSR = XH2R / (ts + XH2R) 'sets TSR to this ratio if ts > XH2R, TSR = 12/(ts+12), moves to 12 with N = 1

    12 For i = 1 to N 'N is the number of times the for loop rolls depending on the conditions above
        QI = fli 'average flow input
        For J = 1 to nps 'phase for loop
            DQ = QI - PH(J) 'flow difference of QI - phase flow
            If (Abs(DQ) - 0.0001 <= 0) Then GoTo 20 'when |DQ| <= 0.0001, exits for j loop, runs next i, DQ is too small
        17  DQ = DQ * TSR 'new DQ is DQ times TSR
            QI = PH(J) + DQ 'new QI is the phase flow + new DQ
            PH(J) = QI + DQ 'new phase flow is new QI + new DQ
        Next J
    20 Next i

    30 End Sub
```

Soil curve interpolator function

```
Public Sub INTERP1(NUMVALS, y(), xval, yval, soiRow) 'NUMVALS = 6, y() is percent array, xval is previous day soil
                                                    moisture, yval is percent yield return, row in the table for soil type

Dim x(NUMVALS), fctr As Single 'dimensions the x() arrays, fctr is a multiplying factor

fctr = 0 'factor starts at zero

For i = 1 To NUMVALS 'for loop 1 to 6, creates the x array percent of field capacity in inches
    x(i) = fctr * FC(soiRow) 'creates the x array as decimal percent of the soils field capacity, incrementing by a factor of 0.2
    fctr = fctr + 0.2 'incrementing the factor by 0.2
Next i

For i = 1 To NUMVALS 'for loop 1 to 6
    If x(i) > xval Then 'condition when x array is greater than previous day soil moisture value
        yval = y(i - 1) + (y(i) - y(i - 1)) * (xval - x(i - 1)) / (x(i) - x(i - 1)) 'interpolation equation
    Exit Sub
    End If
Next i

End Sub
```


Fast/slow splitter curve interpolator function

```
Public Sub INTERP2(NUMVALS, y(), xval, yval, BC)      'NUMVALS = 10, y() is percent array to fast flow, yval is return
                                                    'percent to fast flow, BC is bedrock capacity

Dim pctBC          'dimension percent of BC

If BC <= 0 Then    'condition if BC was set <= 0
    pctBC = 0      'pctFC is set to
Else
    pctBC = xval / BC * 100    'else pctBC is xval's percent of BC
End If

If xval >= BC Then    'if condition when the xval is greater than BC
    yval = y(NUMVALS)    'return yval to the maximum percent to fast at BC
    Exit Sub            'condition met, exit the subroutine
End If

For i = 0 To NUMVALS    'interpolation loop if xval is within 0 and BC
    If splitX(i) > pctFC Then    'splitX(i) array of 0.1 increment percent of BC
        yval = y(i - 1) + (y(i) - y(i - 1)) * (pctFC - splitX(i - 1)) / (splitX(i) - splitX(i - 1))    'interpolation equation
        Exit Sub    'exits the sub routine and returns yval solution
    End If
Next i

End Sub
```

TERMINOLOGIES, ABBREVIATIONS, ACRONYMS, AND BLENDS

1-D – One dimensional

2-D – Two dimensional

3-D – Three dimensional

amsl – Above mean sea level

ARGUS ONE – ARGUS® Open Numerical Environment

AQUA CHARGE – A vadose recharge flow synthesis modeling program designed for the Northern Guam Lens Aquifer (NGLA), using surface hydrology techniques as an alternative for dealing with the complex island karst system. Designed and programmed by Habana with guidance from Heitz.

AWA – Area weighted average

AWC – Available water content

BASIC – Beginner's All-purpose Symbolic Instruction Code (a high level programming language)

bmsl – Below mean sea level

ESRI - Environmental Systems Research Institute®

ET – Evapotranspiration

FEM – Finite element method

FC – Field Capacity

FORTRAN – The IBM Mathematical **F**ormula **T**ranslating System (a general-purpose, procedural, and imperative programming language)

GEPA – Guam Environmental Protection Agency

GIS – Geographic Information Systems

GW – Groundwater

GWA – Guam Waterworks Authority

GUI – Graphical User Interface

K_{x/y} – Hydraulic conductivity in the x and y 2-D plane, plan view

mgd – Unit, million gallons per day

MS – MICROSOFT®

msl – Mean sea level

NCDC – National Climatic Data Center

NGLA – Northern Guam Lens Aquifer

NRCS – Natural Resource Conservation Service (formerly known as SCS)

nps – Number of phases

PAT – Polygon attribute table

PAW – Plant available Water

RRSM – Recharge reduced soil moisture

SCS – Soil Conservation Service

S-SS – Surfaces sub-surface

SBW – Semi-bandwidth

SM – Soil moisture

SMI – Soil Moisture Index

SMY – Soil moisture of yesterday

SSARR – Streamflow Synthesis and Reservoir
Regulation

SSM – Starting soil moisture

SWIG2D – Salt Water Intrusion Groundwater
flow model 2-D (Contractor)

T_s – Time in storage

USACE – United States Army Corps of
Engineers

UNSAT1D – **Un**saturated model **1D**imensional
(Contractor)

USDA – United States Department of
Agriculture

VADOSWIG – A combined program of
UNSAT1D and SWIG2D (Contractor)

VB – Visual BASIC

WERI – Water and Environmental Research
Institute of the Western Pacific

WP – Wilting Point

